Fluorine Gas as a Selective Difluorinating Reagent

ALEXANDER STUART HAMPTON

FLUORINE GAS AS A SELECTIVE DIFLUORINATING REAGENT

ALEXANDER S. HAMPTON

A thesis submitted for the degree of Doctor of Philosophy

Department of Chemistry
Durham University

April 2020

Abstract

The development of organofluorine chemistry has revolutionised the way many agrochemical and pharmaceutical companies design and screen potential new active ingredients. As part of these advances, several methods of selectively introducing C−F, $>CF_2$ or $-CF_3$ groups into a range of organic compounds has been developed.

In this thesis, we describe the selective syntheses of $>CF_2$ groups using fluorine gas (F_2) by transformation of CH_2 groups α- to carbonyl systems. Our fluorination methodology was applied to a range of 1,3-diketone, 1,3-diester, 1,3-ketoester and ester substrates to produce the corresponding $CF_2C{=}O$ derivatives. The reactivity of F_2 was mediated by the addition of various nitrogen bases, with the addition of quinuclidine appearing to afford the best selectivity for the selective synthesis of $>CF_2$ containing compounds which could, in principle, be scaled up to manufacturing quantities.

Further reactions of some of the difluoroesters synthesised during this project were investigated. The $ArCF_2X$ moiety is of particular interest currently to the life science industries due to the beneficial physicochemical and pharmacokinetic properties that the incorporation of fluorine provides. In particular, amidation reactions were successfully performed to generate a new synthetic route to difluoroamides.

Finally, selective fluorinations of aromatic systems using F_2 in basic media was attempted to complement previous literature on the fluorination of these systems in acidic media.

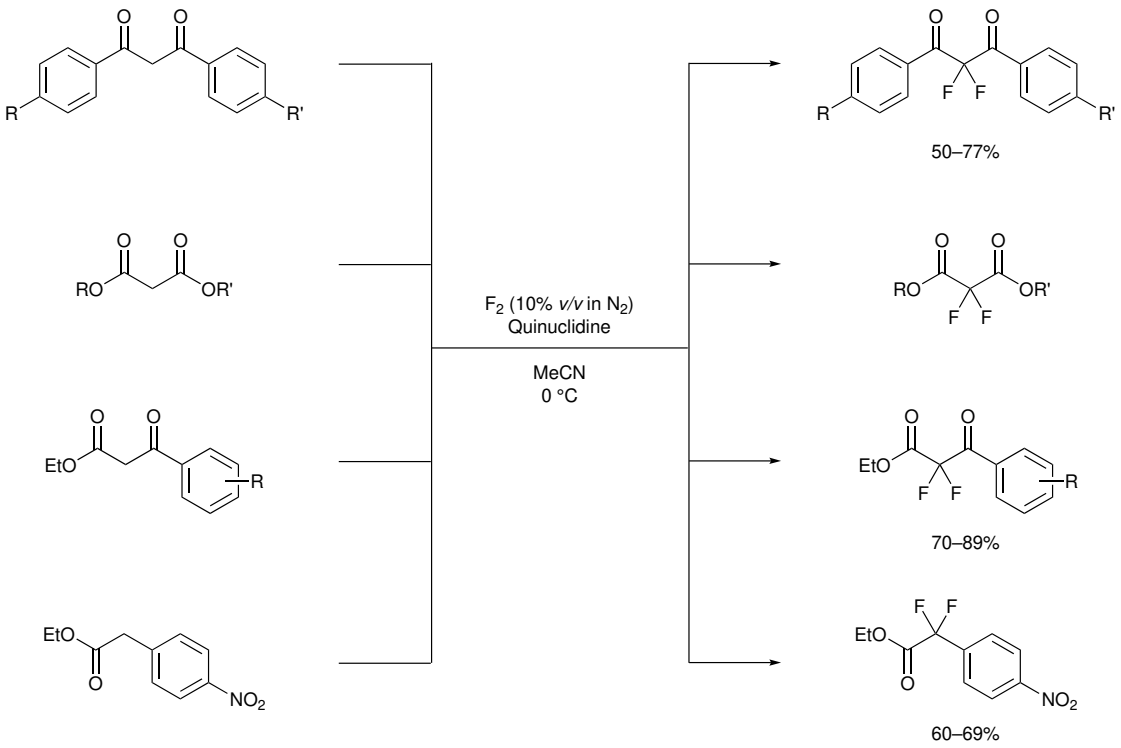

Scheme 1: Selective difluorination reactions performed using F_2 described in this thesis

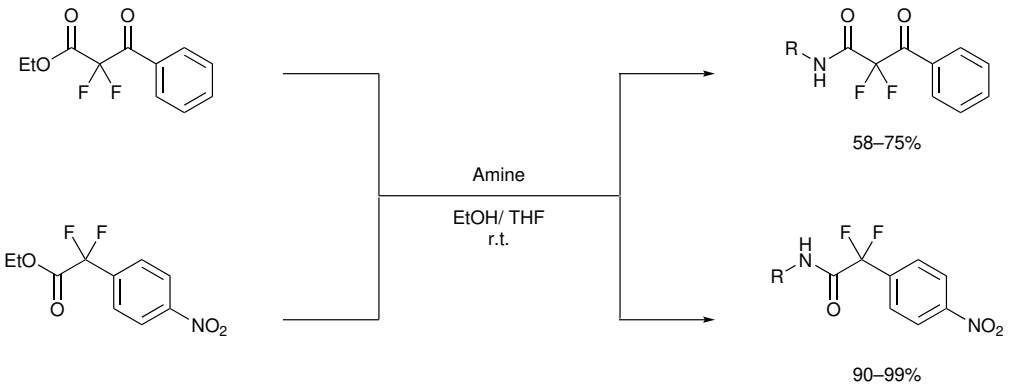

Scheme 2: Amidation reactions involving difluoroesters synthesised using F_2

Acknowledgements

I would firstly like to acknowledge all of the support that Professor Graham Sandford has given me throughout my time at Durham; both as my PhD supervisor, and as my academic advisor during my undergraduate degree. I'm thankful for the introduction into organofluorine chemistry, the constant encouragement, advice —– both in and out of the lab, and more recently — patience reading this thesis.

I would also like to thank Syngenta for funding this project, and Dr. Graham McDougald for his support over the years. Dr. Martin Bowden, Dr. Peter Burland and Dr. Rachel Donkor were extremely helpful during my placement at Syngenta Jealott's Hill.

This research would not have been possible without the support of the experienced analytical and support staff in Durham's Chemistry Department. I would like to thank Alan, Juan and Catherine in NMR, Dima for his incredible work in crystallography, Dave and Pete in mass spectrometry, Malcolm and Aaron in the glassbowing workshop and Annette for her tireless work in ensuring the efficient running of this Department.

I have greatly enjoyed the past few years with various members of the Sandford research group; Tony, Craig, Etienne, Darren, my fellow Musketeers Josh and Marcus, Neshat, Ben and Mark. I would also like to thank the many 4^{th} year and exchange students that we have been lucky to have spend time with us; Alex, Anne, Bobbi, Zahide, Rob, Sophie, Lawrence, Kiera, Johnny, Ellis and Tom. I would especially like to thank Etienne for teaching me how to use the fluorination rig, and Johnny for continuing parts of this work.

While not in the lab, I have greatly enjoyed the last few years spending time with some wonderful people at Ustinov, in particular those that I spend time with on the Exec; Alex, Jamie, Thom, Alastair, Tom, Diana, Connor, Vera, Bryony and

Rebecca. I will also miss the lazy afternoons and late nights spent at both Howlands and Sheraton with Ed, Yan, Matt and James.

I would like to thank my parents for their continual love and support, despite spending twice as long in Durham as I originally planned to! I am eternally grateful for all the opportunities and inspiration that they have provided me with.

Finally I would like to thank my wonderful partner Hayley for keeping my sane, and more importantly fed throughout the past few years. I would not have been able to finish this thesis without being able to run ideas by you, and hope that some of them made sense.

Memorandum

The work described in this thesis was carried out at Durham University between September 2016 and September 2019, or at Syngenta's Jealott's Hill International Research Centre during October 2018. This thesis is the work of the author, except where acknowledged by reference, and has not been submitted for any other degree. The copyright of this thesis rests with the author. No quotation from it should be published without the author's prior written consent and information derived from it should be acknowledged.

This work has been presented, in part, at:

1. Syngenta Collaborative Research Conference, Jealott's Hill, UK, 19–20$^{\text{th}}$ September 2019, *oral presentation, 1st place talk prize*
2. 19$^{\text{th}}$ European Symposium on Fluorine Chemistry, Warsaw, Poland, 25–31$^{\text{st}}$ August 2019, *poster presentation, 2nd place prize of the organic stream*
3. Postgraduate Gala Symposium, Durham, UK, 20$^{\text{th}}$ June 2019, *oral presentation*
4. 18$^{\text{th}}$ RSC Postgraduate Symposium in Fluorine Chemistry, Southampton, 11–12$^{\text{th}}$ April 2019, *poster presentation*
5. Syngenta Collaborative Research Conference, Jealott's Hill, UK, 13–14$^{\text{th}}$ September 2018, *poster presentation*
6. 22$^{\text{nd}}$ International Symposium on Fluorine Chemistry, Oxford, UK, 22–27$^{\text{th}}$ July 2018, *poster presentation*
7. Postgraduate Gala Symposium, Durham, UK, 21$^{\text{st}}$ June 2018, *poster presentation*

Abbreviations

18-crown-6	1,4,7,10,13,16-hexaoxacyclooctadecane
a	anhydrous
Å	angström
AcOF	acetyl hypofluorite
$AgBF_4$	silver tetrafluoroborate
AgF	silver fluoride
AI	active ingredient
Ar	aryl
ASAP	atmospheric solid analysis probe
BIOMe	methoxybenziodoxole
BKE	β-ketoester
BPU	benzoyl phenyl urea
Bu	butyl
CaF_2	fluorspar
CCDC	Cambridge Crystallographic Data Centre
$(CD_3)_2CO$	deuterated acetone
CD_3CN	deuterated acetonitrile
$CFCl_3$	trichlorofluoromethane

$CHCl_3$	chloroform
CNS	central nervous system
conc.	concentrated
COSY	correlation spectroscopy
Cs_2CO_3	caesium carbonate
CsF	caesium fluoride
$Cu(NO_3)_2 \cdot 2.5\,(H_2O)$	hydrated copper (II) nitrate
$Cu(OTf)_2$	copper (II) triflate
d	day
D_2O	deuterium oxide
DABCO	1,4-diazabicyclo[2.2.2]octane
DAST	diethylaminosulfur trifluoride
dba	dibenzylideneacetone
DBH	1,3-dibromo-5,5-dimethylhydantoin
DBM	1,3-diphenylpropane-1,3-dione
DBU	1,8-diazabicyclo[5.4.0]undec-7-ene
DCM	dichloromethane
difluoro-BKE	α,α-difluoro-β-ketoesters
DMF	dimethylformamide
DMI	1,3-dimethyl-2-imidazolidinone
DPPF	1,1'-bis(diphenylphosphino)ferrocene
DT_{50}	half life
dq	doublet of quartets
E	electrophilicity parameter

EDG	electron-donating group
EI	Electronic ionisation
equiv.	equivalents
ESI	Electrospray ionisation
Et	ethyl
EWG	electron-withdrawing group
F_2	fluorine gas
FBB	fluorinated building block
g	gram
GC	Gas Chromatography
GC-MS	Gas chromatography—Mass spectrometry coupling
h	hour
H_2	hydrogen gas
hν	photochemical
Hz	Hertz
H_2O	water
halex	halogen exchange
HCOOH	formic acid
HgF_2	mercury(II) fluoride
HSQC	heteronuclear single quantum coherence
HMBC	heteronuclear multiple bond correlation
HF	hydrogen fluoride
IR	infrared
J	coupling constant, Hz

K	Kelvin
K_2CO_3	potassium carbonate
KF	potassium fluoride
KHMDS	potassium bis(trimethylsilyl)amide
LiHMDS	lithium bis(trimethylsilyl)amide
LiOTf	lithium trifluoromethanesulfonate
Lit.	literature
LiTMP	lithium tetramethylpiperidide
m-	meta
M	molar
m/z	relationship mass/charge
Me	methyl
mL	mililliter
MeOH	methanol
MeCN	acetonitrile
$MgCl_2$	magnesium chloride
$MgSO_4$	magnesium sulfate
MHz	Megahurtz
min	minutes
Mp	melting point
M.S.	Mass spectrometry
N	nucleophilicity parameter
N_2	nitrogen gas
n-$Bu_4NH_2F_3$	tetrabutylammonium dihydrogentrifluoride

Na_3AlF_6	cryolite
$NaBF_4$	sodium tetrafluoroborate
$NaBH_4$	sodium borohydride
NaCl	sodium chloride
$NaCO_3$	sodium carbonate
NaF	sodium fluoride
NaH	sodium hydride
$NaHCO_3$	sodium bicarbonate
NaOEt	sodium ethoxide
NaOtBu	sodium tert-butoxide
NaOTf	sodium trifluoromethanesulfonate
NBS	*N*-bromosuccinimide
NH_3	ammonia
NMP	*N*-methyl-2-pyrrolidone
NMR	nuclear magnetic resonance
o-	ortho
p-	para
P_4O_{10}	phosphorous pentoxide
Pd/C	palladium on carbon
Ph	phenyl
pK_a	acid dissociation constant
ppm	parts per million
Pt/C	platinum on carbon
PTFE	poly(tetrafluoroethylene)

R	alkyl
Rf	retention factor
Rh/C	rhodium on carbon
r.t.	room temperature
s	nucleophilic-specific slope parameter
S_EAr	aromatic electrophilic substitution
Selectfluor™	1-chloromethyl-4-fluoro-diazonia[2.2.2]bicyclooctane bis(tetrafluoroborate)
SET	single electron transfer
SF_4	sulfur tetrafluoride
SiF_4	silicon tetrafluoride
SIPr	1,3-bis-(2,6-diisopropyl phenyl)imidazoline-2-ylidene
S_NAr	aromatic nucleophilic substitution
temp.	temperature
THF	tetrahydrofuran
TLC	thin layer chromatography
TMEDA	tetramethylethylenediamine
$TMSCF_2H$	(difluoromethyl)trimethylsilane
Ts	tosyl
X	halogen
XeF_2	xenon difluoride
XRC	X-ray crystallography
δ	chemical shift/ ppm
Δ	heat

Contents

Chapter 1

Selective Fluorination Strategies

1.1 Introduction

The world's population is growing at a steady pace and is expected to reach 9.7 billion by the year 2050.[1] At the same time, the amount of land available for the growth of arable crops is decreasing due to climate change making some areas no longer available for crop production. This is compounded by the increase in meat-based diets as global populations move to cities. Meat-based diets require more water, land and energy than a vegetarian diet, and so it is likely that global food shortages will increase, and begin to affect the developed world.[2] As such, there is growing pressure on agrochemical companies to develop new methods of increasing global food production; either by increasing crop yields by the development of new herbicides and insecticides or by the development of new crop strains that themselves are more resistant to disease or have a wider tolerance of growing conditions.

Fluorine is incorporated into bioactive molecules due to a wide range of favourable physiochemical properties such as enhanced bioavailability as well as increased metabolic permeability and stability.[3–5] Agrochemical companies are following the trend set by pharmaceutical companies of regularly introducing fluorine atoms into potential active ingredients (AI)s. One discovery strategy involves systematically incorporating fluorine into every synthetically available position of a potential agrochemical to determine if this will increase beneficial physiochemical properties of the AI. In 2018, 30% of the new Food and Drug Administration (FDA) approved drugs contained at least one fluorine atom, with an average of 2.7 fluorine atoms per fluorinated drug, and fluorine is found in 50% of marketed agrochemicals.[6]

In general, fluorine atoms have seen growing use in applications in everything from household applications, such as non-stick frying pans and waterproof phones, to industrial applications, such as refrigerants and fluoropolymers. Its unique properties have led to the development of new areas of synthetic chemistry focusing on the selective incorporation of fluorine into molecules. Despite being the 13$^{\text{th}}$ most abundant element in the earth's crust, fluorine is usually found naturally in the insoluble salts fluorspar (CaF_2) or cryolite (Na_3AlF_6) which give rise to the limited examples of fluorinated highly toxic natural products. Since the discovery of the first fluorinated natural product potassium fluoroacetate and its metabolites, there have only been a handful of other fluorinated natural products discovered, such as 4-fluorothreonine, nucleocidin, several ω-fluorinated fatty acids and recently (2*R*3*S*4*S*)-5-fluoro-2,3,4-trihydroxypentanoic acid.[7–13] Despite the other halogens having a lower natural abundance than fluorine, there are around 3000 natural products containing other halogens which highlights the difficulties organisms have incorporating fluorine.[14] Fluorine has been used to increase bioactivity since fludrocortisone (**1**, Florinef), was approved in 1955 in which fluorine replaces hydrogen at the 9- position (Figure 1.1).

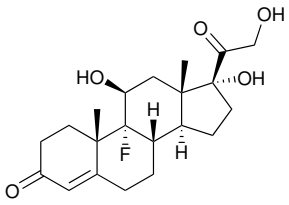

1

Figure 1.1: Fludrocortionse, tradename Florinef

Agrochemical companies incorporate fluorine into AIs to utilise its unique biochemical and physiochemical properties. This thesis is concerned with the development of inexpensive fluorination methodologies that could, in principle, be used for the manufacture of new fluorinated agrochemicals.

Consequently, this introduction discusses organofluorine chemistry in general, and its applications in agrochemicals. It will also discuss reactions concerning the formation of CF_2 groups, which are of particular relevance to the results discussed.

1.2 Properties of Fluorine

Fluorine is slightly larger than hydrogen, but with completely different electronic properties due to fluorines high electronegativity and three lone pairs of electrons. It is this difference in electronegativity that leads to a range of physiochemical and biochemical properties that are beneficial in AIs.

1.2.1 Size of Fluorine

While the van der Waals radius of fluorine is only 20% larger than hydrogen, the C−F bond displays characteristics such as size and length that are more similar to a C=O bond than a C−H bond (Table 1.1).[15–17] Fluorine is often used as a bioisostere for the C−OH group. For example, fluorine has been successfully used to replace a tertiary hydroxyl group in the Syngenta triazole fungicide flutriafol **2**. While the fluorinated analogue is still able to bind to its target site and display some biological activity, the overall fungicidal effect is reduced due to the lack of a hydroxyl functionality to act as a hydrogen bond donor.[18]

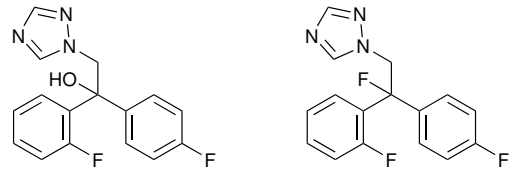

2 **3**

Figure 1.2: Flutriafol and its trifluorinated analogue

The high electronegativity of fluorine leads to a highly polarised C−F bond (1.41 D) that leads to a bond with more electrostatic and less covalent character (Table 1.2).

Table 1.1: Bond length and volumes of the C−F bond compared to the C−H, C=O, C−OH and S=O bonds[15–17]

Bond	Bond length/$\mathring{A}$	van der Waals radius/$\mathring{A}$	van der Waals volume of atom/$\mathring{A}^3$	Total size /$\mathring{A}$
C−H	1.09	1.20	7.24	2.29
C−F	1.35	1.47	13.31	2.82
C−Cl	1.77	1.75	22.45	
C=O	1.23	1.52	14.71	2.73
C−OH	1.43	1.52	14.71	
S=O	1.44	1.52	14.71	

Table 1.2: Electronic properties of the C−F bond compared to the C−H, C=0, C−OH and S=O bonds

Bond	Electronegativity of the element	Dipole moment (μ)/D
C−H	2.20	~ -0.4
C−F	3.98	1.41
C−Cl	3.16	1.87 (CH_3Cl)
C=O	3.44	2.33 ($H_2C{=}O$)
C−OH	3.44	2.87 (CH_3OH)
S=O	3.44	4.44 ($CH_3SO_2CH_3$)

1.2.2 Bond Strengths

The C−F bond (105.4 kcal mol^{-1}) is the strongest single bond to carbon in organic chemistry due to its increased electrostatic nature. Ionic contributions between $F^{\delta-}$ and $C^{\delta+}$contributes to the standard covalent bond increasing overall bond strength. The strength of a C−F bond depends on the number of fluorine atoms attached to the carbon. As more fluorines are added to carbon, the *p*-character of the C-F increases, leading to more polarization and, hence, stronger bonds as observed for the bond strengths of fluoromethane to tetrafluoromethane (Table 1.3).[19] The negative charge density on each additional fluorine remains constant, and so successive fluorines are attached to an increasingly positive carbon, therefore, increasing the electrostatic contributions to bond strength.

Table 1.3: Effect of fluorine substitution on the strength of the C-F bond

Entry	Compound	C-F Bond energies/ kcal mol^{-1}
1	CH_3F	107
2	CH_2F_2	110
3	CHF_3	115
4	CF_4	116

Increasing the number of hydrogens replaced by fluorine can have significant effects on the overall polarity of the molecule. Whereas 1,4,7,10,13,16-hexaoxacyclooctadecane (18-crown-6, **4**) shows good selectivity for binding cations, the corresponding perfluorinated crown ether **5** has reversed polarity at the centre and thus binds to anions such as fluoride or superoxide anions (Figure 1.3).

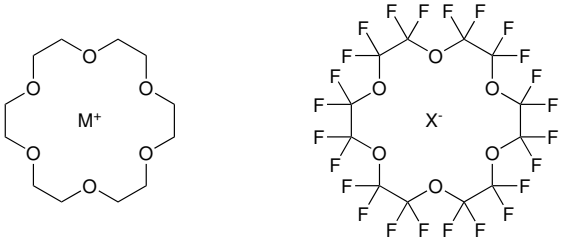

4
M^+ = e.g., Na^+, K^+

5
X^- = e.g., F^-, O_2^-

Figure 1.3: Comparison of the ion complexes of 18-crown-6 and its perfluorinated analogue

A further effect of the C-F bond polarization is its effect on hybridisation. The non-polarized C-H bond prefers to be attached to sp^2 hybridised carbons whereas fluorine prefers to be attached to sp^3 hybridised carbon atoms. The fluorine attracts *p*-electron density from the sp^3 carbon into its low lying 2p orbital. The preference for fluorine to be attached to an sp^3 carbon can be shown in the Cope 3,3-sigmatropic rearrangement of 1,1-difluoro-1,5-hexadiene **6** to 3,3-difluoro-1,5-hexadiene **7** which is favoured by 5 kcal mol^{-1} (Figure 1.4).[20]

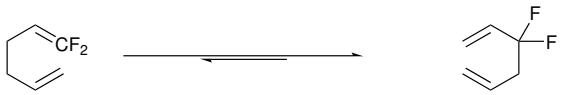

6 **7**

Figure 1.4: Isodemic Cope rearrangement of **6** illustrating the preference for fluorine to bond to an sp^3 carbon

1.2.3 pK_a

Fluorine is the most electronegative element and as such, can have a significant electronic effect on nearby functional groups. Incorporating fluorine into organic molecules can lower the pK_a of functional groups, even several carbons away (Table 1.3) and this effect increases with the incorporation of subsequent fluorine atoms.[21] Changes in pK_a can have many positive effects on physiochemical properties such as solubility and binding affinities, and pharmacokinetic properties such as bioavailability and metabolism. The lowering of the pK_a of nearby amines, alcohols, carboxylic acids and phosphonic acids can increase bioavailability and efficacy by increasing membrane penetration at physiological pH.[22]

Table 1.4: Effect of fluorine substitution on pK_a and pK_b

Carboxylic acid	pK_a	Alcohol	pK_a	Amine	pK_b
CH_3CO_2H	4.76	CH_3CH_2OH	15.9	$CH_3CH_2NH_2$	10.6
CH_2FCO_2H	2.59	CF_3CH_2OH	12.4	$CF_3CH_2NH_2$	5.7
CHF_2CO_2H	1.34	$(CH_3)_3CH_2OH$	19.2	$C_6H_5NH_2$	4.6
CF_3CO_2H	0.52	$(CF_3)_3CH_2OH$	5.1	$C_6F_5NH_2$	−0.36

1.2.4 Lipophilicity

The lipophilicity of an AI is important in agrochemicals for two main reasons; membrane permeability and soil leaching. Lipophilicity is expressed as log$P$ where P is the partition coefficent between octanol and water.

$$\log P_{\mathrm{oct/wat}} = \log\left(\frac{[\mathrm{substrate}]_{\mathrm{octanol}}}{[\mathrm{substrate}]_{\mathrm{water}}}\right) \tag{1.1}$$

Lipophilicity increases the amount of the AI that is transported *in vivo* around the target organism and raises the rate of passive diffusion across membranes. More

lipophilic molecules often have higher binding efficiencies at the active site regions of enzymes as these have a lower polarity than the rest of the cellular environment.

Increased lipophilicity is commonly exploited in insecticides such as diflubenzuron **8** which has an increased penetration into the central nervous system (CNS) of insects that is correlated to their log$P$.[23] This strategy effects the CNS of insects, thus not harming treated crops.

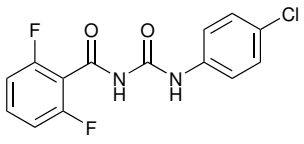

8

Figure 1.5: Diflubenzuron

If a molecule is too lipophilic then the increase in solubility causes formulation and stability issues. While the incorporation of an AI across a membrane by passive diffusion is desired, if the AI is too lipophilic, it is possible for the compound to remain trapped in the lipid core and not be transported to the desired site. Above a log$P$ value of approximately 3.5, the mobility of the compound through the plants xylem starts to become very limited.[24] Lipophilicity of an AI requires a balance though; if the AI is not lipophilic enough then it will not be taken up by the plant or insect or transported around the organism.

The incorporation of fluorine can modulate lipophilicity, either raising or lowering it, depending on the location of the fluorine atom. In the case of aliphatic systems, terminal mono-, di-, and tri-fluorinated systems tend to decrease lipophilicity due to the polar effects of the strong C-F and C$-$CF$_3$ bond dipoles created by the electronegative fluorine.[25]

Perfluoroalkyl groups are added to organic molecules to increase lipophilicity such as in the broad spectrum insecticide flubendiamide **9**.[26] Incorporation of fluorine into aryl and heteroaryl systems such as PhF, PhCF$_3$ and PhOCF$_3$ also increases lipophilicity due to interactions of fluorine with π-bonds. AIs are often made more lipophilic by incorporating a fluorophenyl moiety such as in meperfluthrin **10**. While α-fluorinated carbonyl derivatives are more lipophilic in octanol, the standard organic solvent used to determine partition coefficients, they are less lipophilic in hydrocarbon-water systems such as hexane or benzene. α-Fluoro and α,α-difluoro carbonyl derivatives undergo an increased rate of hydration compared to the non-

fluorinated carbonyl system. In an octanol-water mixture, fluorine substitution increases the rate of acetalization with the alcohol, and hence lipophilicity increases.

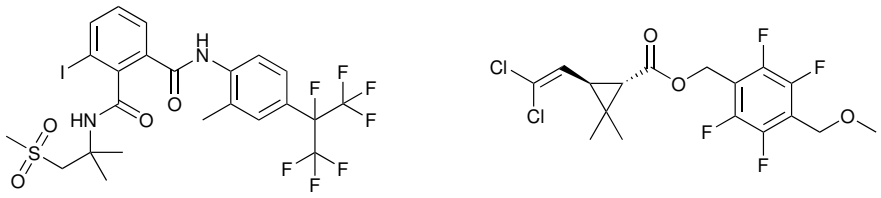

9 **10**

Figure 1.6: Flubendiamide and meperfluthrin

A log$P$ value of around 3 is the trigger for potential leaching of an AI through the soil, which can have significant environmental concerns unless half-life in the soil (DT_{50}) is short. Aquatic organisms uptake organic compounds at a rate that is roughly in proportion to their log$P$ value and, with limited means of excretion, AIs can build up to toxic amounts.

1.2.5 Degradation of Active Ingredients in Soil

The DT_{50} is essential to consider in the development of new agrochemicals due to environmental and economic considerations. There is a beneficial steric halogen effect of introducing fluorine into the 2- and 6- positions of phenyl rings on environmental stability. The introduction of fluorine can cause different metabolic pathways to decompose the AI as discovered by comparing the benzyl phenyl urea insecticide diflubenzuron **8** with its N-2,6-dichlorobenzoyl analogue **11**.

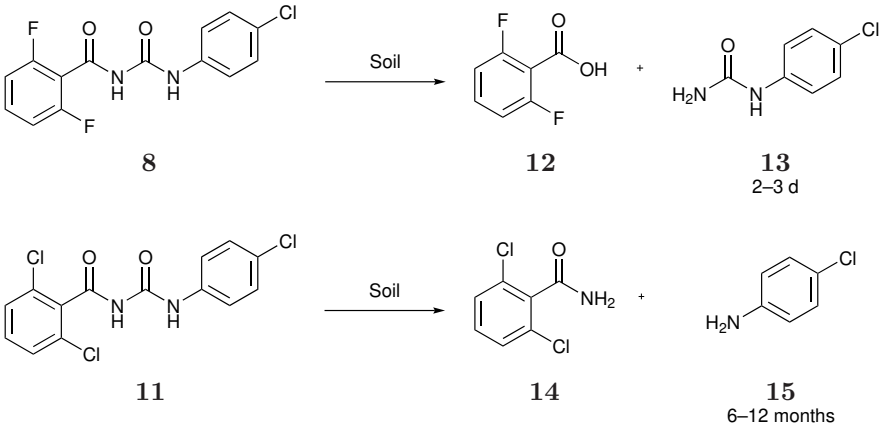

8 **12** **13**

11 **14** **15**

Scheme 1.1: Metabolism of diflubenzuron and its dichlorinated analogue under soil conditions

Both diflubenzuron **8** and the chlorinated analogue **11** are stable at acidic pH but hydrolysed in the soil (pH 9-10) with a DT_{50} of 2-3 days (d) and 6-12 months respectively.[27] At higher pH values, they undergo different amide hydrolysis reactions. The different reactions can be explained by comparing the bond angles between the -CO(NH)- moiety and the aromatic ring. Due to the larger size of chlorine, the 2,6-dichlorobenzoyl moiety is at 90° to the benzoyl phenyl urea (BPU) frame, whereas the smaller fluorine results in the 2,6-difluorobenzoyl moiety lying in the same plane as the BPU frame.[23] Without this rotation, the amide adjacent to the difluorophenyl ring in **8** is susceptible to hydrolysis, and so is metabolised at a much faster rate. Interestingly, **8** has a larvicidal activity against *Pieris brassicae* 20 times that of the chlorinated analogue **11** despite having a lower log$P$ value due to the more hydrophilic nature of fluorine than chlorine. Usually, the larvicidal activity is proportional to a higher log$P$ value.

1.2.6 Oxidative Metabolism

AIs are rarely excreted from an organism without some modification performed to aid excretion. In mammals, this is usually performed by Cytochrome P450 monooxygenases found in the liver. This family of heme-thiolate proteins selectively oxidise compounds at specific, metabolically labile sites. Once oxidised, lipophilicity is decreased, and, hence, the metabolites are excreted more readily. This is a significant issue for the pharmaceutical industry, as the body attempts to detoxify and excrete drugs before they reach their desired target site. The C-F bond is the strongest single bond in organic chemistry, and introduction of fluorine effectively blocks oxidative metabolism at that position.[28] This effect was used in the lead optimisation of the cholesterol inhibitor Ezetimib **16**.[29,30] Introduction of fluorine onto the aromatic rings in the *para* position prevents ring oxidation by Cytochrome P450 enzymes. Additionally dealkylation of the C**4** methoxy group and stereoselective benzylic oxidation, resulted in a compound that was 400 times more potent than the lead compound **17**.

In particular, 4-fluorophenyl groups are often used in AIs to increase bioavailability.[31] However, while electron-withdrawing fluorine atoms stabilise aromatics against oxidative and electrophilic attack, polyfluorination can increase susceptibility to nucleophilic attack. It is for this reason that usually only a few fluorine atoms, in specific locations, are incorporated into agrochemicals, in general.

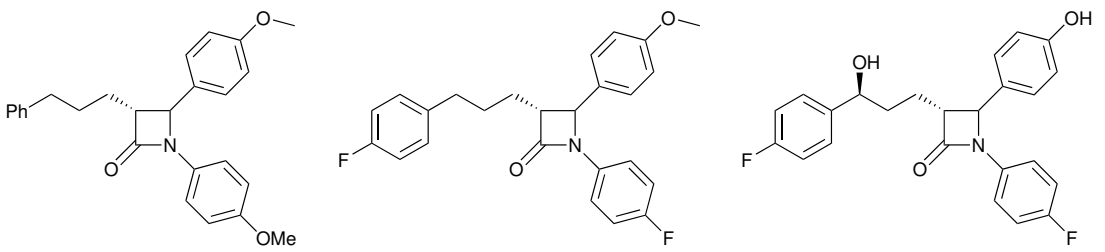

17
SCH 48461
ED_{50} = 2.2 mg/ kg

18
ED_{50} = 0.7 mg/ kg

16
SCH 58235
ED_{50} = 0.04 mg/ kg

Figure 1.7: Ezetimibe and its precursor clinical candidates with their effective doses (ED_{50})

The metabolic pathways that an AI can undergo are very crop-specific. By careful selection of the fluorination site, the applicable crop selection can be broadened or narrowed and, in some cases, can be drastically altered. By moving the location of a $-CF_3$ group and a few other minor structural changes, picoxystrobin **19** (Syngenta) is now no longer a fungicide, but the acaricide fluacryprim **20** with a completely different mode of action as it now fits the active site of a different enzyme.

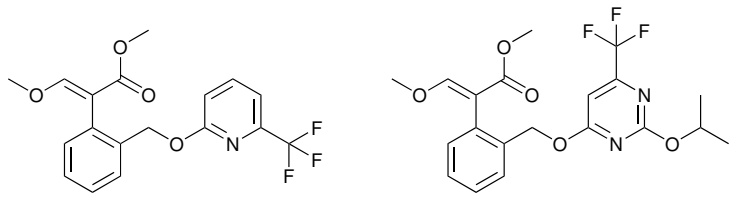

19 **20**

Figure 1.8: Picoxystrobin and fluacryprim

The importance of fluorine in the agrochemical industries can not be overstated due to the range of beneficial physicochemical properties it can imbue as discussed above. As fluorine is generally not present in naturally occurring molecules, there has been much focus on developing methods of introducing fluorine into organic systems. Importantly, the specific location of fluorine in a molecule is important as it relates to pK_a and metabolic stability and, therefore, regioselective fluorination strategies are desired. There are many excellent reviews on selective electrophilic and nucleophilic fluorination strategies to introduce C-F, CF_3 and $-OCF_3$ into molecules, and, of particular relevance to the research in this thesis, Pattison has recently written a review on synthetic strategies to generate α,α-difluorodiketones.[5,32–38] In the following sections, a brief overview of the fluorination methodology of particular relevance to the research in this thesis is described.

1.3 Selective Difluorination Strategies

Fluorine increases the electrophilicity of carbonyl carbons when it is introduced α-to the moiety. Incorporation of two fluorine atoms can often drastically increase the rate of hydration of the carbonyl group due to fluorines electronegativity that activates the C=O group to nucleophilic attack. While hydration is often not desired for synthetic applications, it can have beneficial biophysical properties. Several enzymes are inhibited by hydrated ketones, and hydrated difluoroketones have been used as highly effective inhibitors by replacing amide moieties that are susceptible to hydrolysis (Scheme 1.2).[39,40]

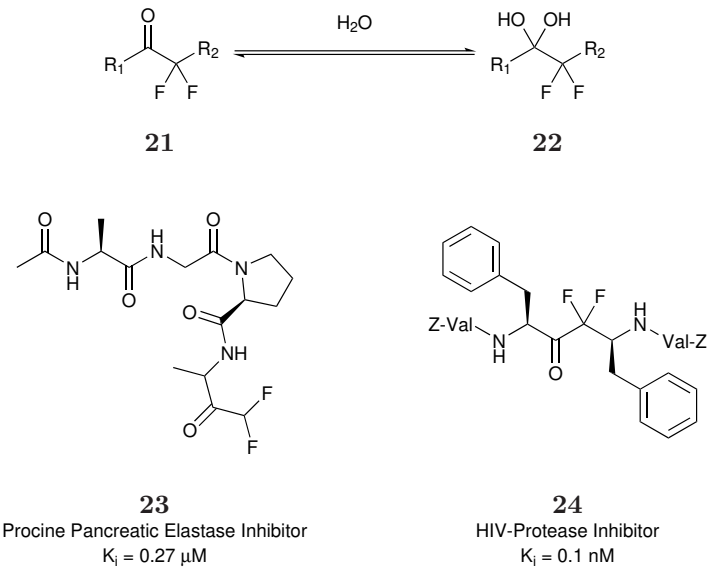

Scheme 1.2: Hydrate formation of an α,α-difluoroketone and examples of enzyme inhibitors containing this functionality

Of particular interest to the agrochemical and pharmaceutical industries are the synthesis of $ArCF_2H$ containing compounds due to unique biochemical properties that allow these systems to act as a bioisostere of both hydroxyl and thiol as wells as acting as a lipophilic hydrogen bond donor.[41,42] For example, the fluorinated pyrazole carboxamide **30** has increased fungicidal activity against *Alternia solani* when a difluoromethyl group (**30a**, X = H) is present compared to the trifluoromethyl derivative (**30b**, X = F) (Figure 1.10).[43] The difluoromethyl group acts as a weak hydrogen bond donor to the amide carbonyl, and appears to have a significant role in the enzyme-inhibitor interaction. Incorporation of an $ArCF_2H$ moiety into an organic molecule also increases the metabolic stability, solubility and oral bioavailability compared to the phenyl derivative. Consequently, this thesis will focus on the

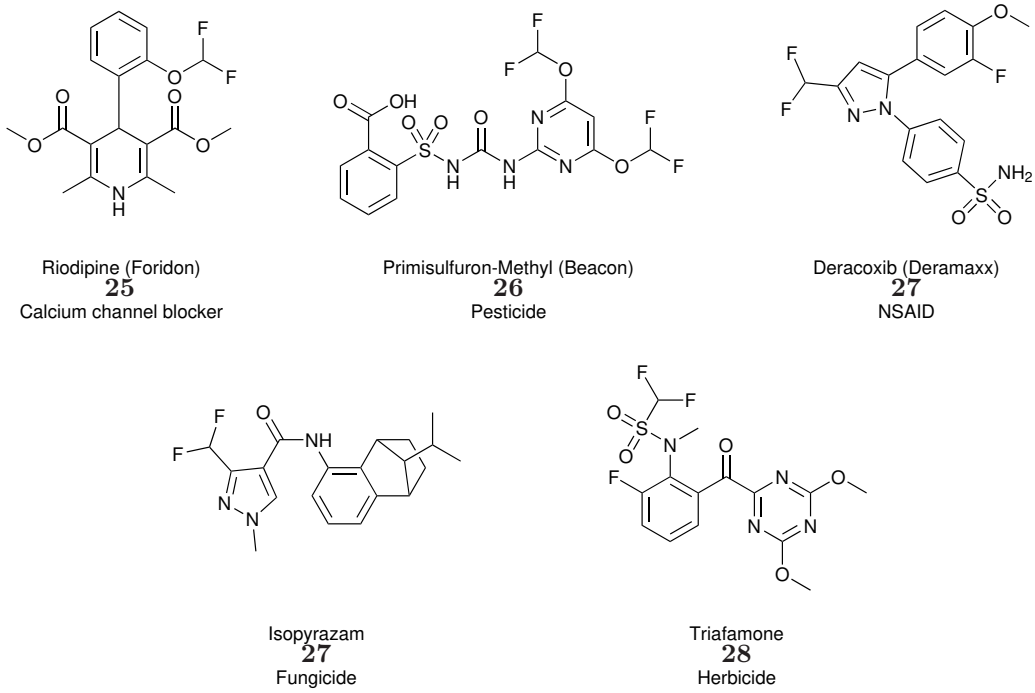

Figure 1.9: Example CF_2 containing pharmaceuticals and agrochemicals

growing field of selective formation of CF_2 by fluorination strategies; in particular the synthesis of α,α-difluorodiketones, the use of difluoromethyl fluorinated building blocks and direct fluorinations using relatively inexpensive fluorine gas.

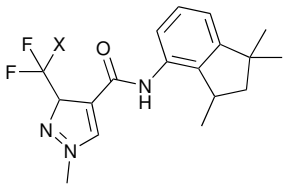

Figure 1.10: Fluorinated pyrazole carboxamide

1.3.1 Nucleophilic Fluorinations for $RCOCF_2R$ Synthesis

Most nucleophilic fluorination reactions using fluoride occur through halogen exchange (halex) reactions utilising existing synthetic strategies for incorporating other halogens into molecules. Hydrogen fluoride (HF) is often used on an industrial scale due to its low cost (Scheme 1.3). Mixing HF with a nitrogen base such as triethylamine or pyridine gives a less volatile fluorinating reagent with a pH near neutral which lowers the corrosive nature of the HF reagent.[44]

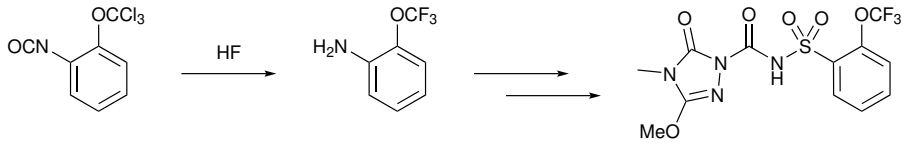

31 **32** **33**

Scheme 1.3: Part of the synthesis of flucarbazone highlighting nucleophilic fluorination by HF to form an $-OCF_3$ group[44]

While these halex strategies are useful to introduce C-F, $C-CF_3$ or $O-CF_3$ groups, the formation of *gem*-difluoro groups is more difficult due to the formation of monofluorinated products or unwanted by-products. Some success at transforming *gem*-dichloro and *gem*-diiodo groups to the desired CF_2 is achieved using silver salts such as silver tetrafluoroborate ($AgBF_4$).[45] An advantage of using this methodology is that different halogens in a molecule can be replaced by fluorine, such as in the synthesis of a *gem*-difluorinated glucopyranosyl using silver fluoride (AgF) (Scheme 1.4).[46]

34
X = Cl, I

35
35–84%

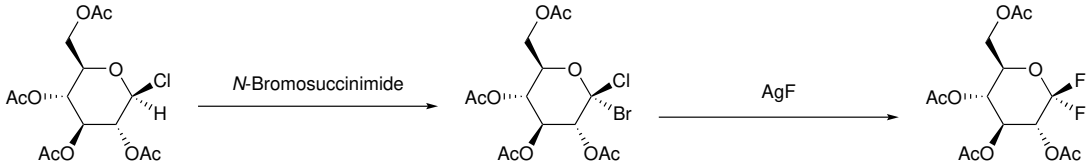

36

37
62%

38
70%

Scheme 1.4: Nucleophilic substitutions of halogens by fluoride

The CF_2 functionality can be readily introduced using deoxyfluorination agents such as sulfur tetrafluoride SF_4, diethylaminosulfur trifluoride (DAST) **39**, Deoxo-Fluor **40**, Xtalfluor-E and Xtalfluor-M **41a**,**b** (Figure 1.11).

These reagents convert carbonyls to CF_2 groups in usually good yields and are often functional group tolerant. DAST **39** has been used to successfully difluorinate potentially biologically active compounds, as well as a wide range of carbonyl-containing molecules (Scheme 1.5).[47,48] Unfortunately **39** is moisture sensitive, and upon heating can convert to the highly explosive $(NEt_2)_2SF_2$ after eliminating SF_4.

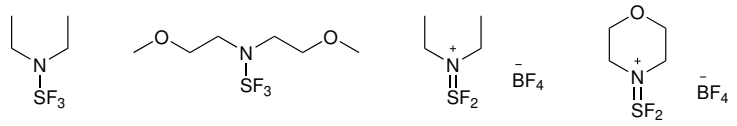

39 **40** **41a** **41b**

Figure 1.11: Nucleophilic fluorinating agents DAST, Deoxo-Fluor, Xtalfluor-E, Xtalfluor-M

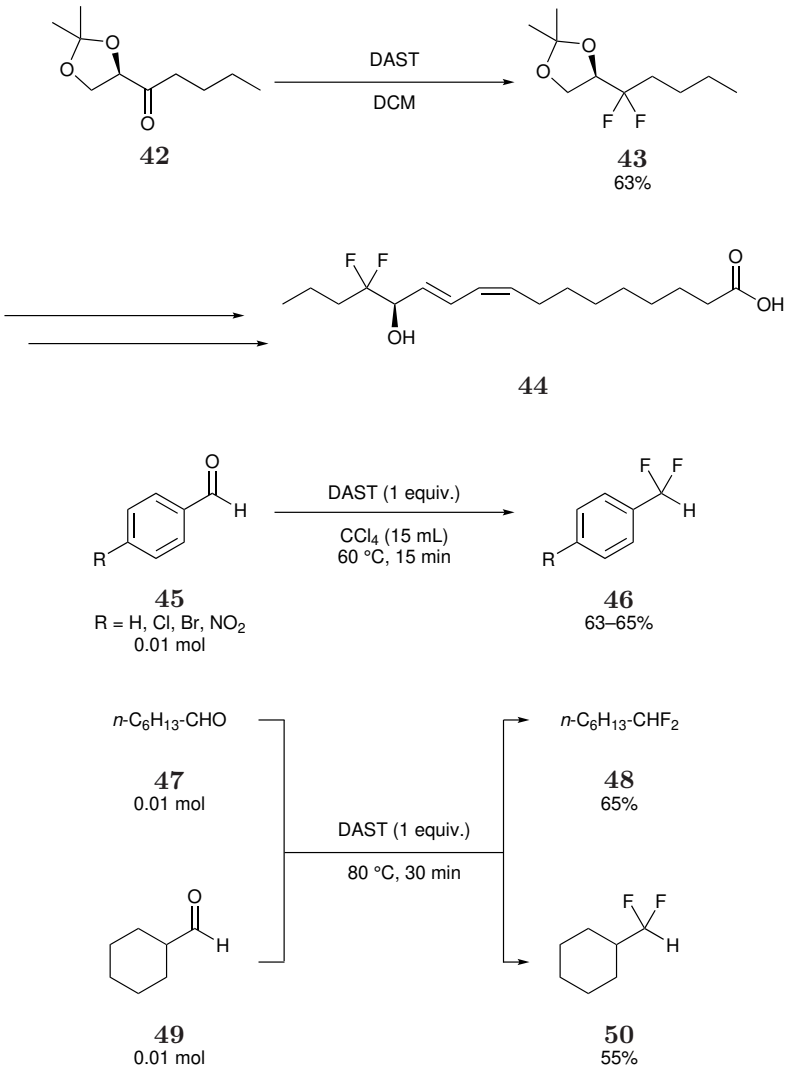

42 **43** **44** **45** **46** **47** **48** **49** **50**

Scheme 1.5: Examples of nucleophilic fluorinations using DAST including part of the synthesis of (R)-14,14-difluoro-13-hydroxy-9(Z),11(E)-octanedienoic acid

Deoxofluor **40** now has more widespread use than DAST **39** as it is more thermally stable, but is also moisture-sensitive, and decomposes to produce HF. **41a** is also commonly used as it is non-explosive, crystalline, less moisture sensitive and results in fluorodeoxygenation with fewer by-products such as corrosive HF. While these

nucleophilic fluorinating agents offer more control than HF, in general, they are too expensive to use on the scales required for the agrochemical industry.[49]

These general reagents for CF_2 formation have been used to synthesise difluorocarbonyl derivatives ($CF_2C{=}O$ groups). It is possible to selectively replace bromine instead of chlorine with fluorine α- to carbonyls by using mercury (II) fluoride (HgF_2).[50] While this strategy of bromination using *N*-bromosuccinimide (NBS) followed by fluorination using HgF_2 proceeds with excellent conversion and selectivity to form α,α-difluorocarbonyls (Scheme 1.6), HgF_2 is highly toxic, and so not practical on larger scales.

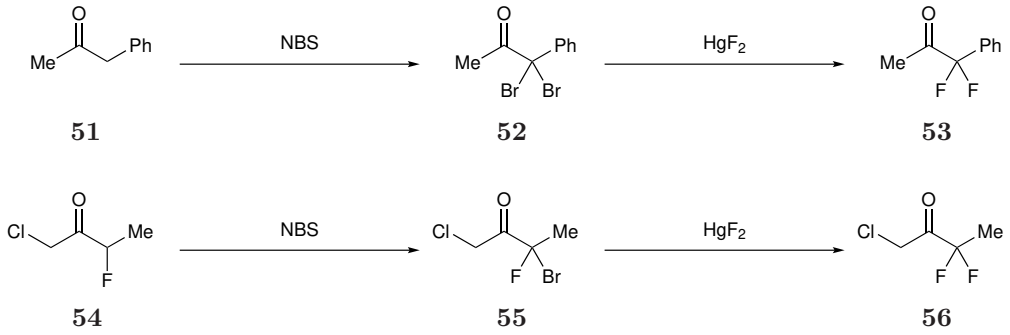

Scheme 1.6: Halogen exchange of *gem*-dihalodicarbonyl compounds

Some examples of α,α-difluorocarbonyl compounds synthesised by the deoxyfluorination of 1,2-dicarbonyl compounds using DAST and related fluorinating agents are shown in Scheme 1.7.[37,51–53] These reagents show selectivity for deoxyfluorination of benzylic carbonyl in 1,2-ketoesters, though extreme care must be taken when heating reactions using **39** as it is potentially explosive at temperatures above 50 °C. Reactions with 1,2-diketones showed a similar selectivity, with difluorination preferentially replacing the benzylic carbonyl. Fluorination of 1,2-ketoaldehydes leads in general to the polyfluorinated ethers due to increased reactivity of the aldehyde carbonyl, though the difluoro acid can be obtained by reacting the aldehyde in low concentration in the presence of moisture to form the hydrated adduct which blocks dimerisation.

α,α-Difluorocarbonyl derivatives have also been synthesised by oxidative fluorodesulfurization of an α-hydroxyorthothioester **64** with tetrabutylammonium dihydrogentrifluoride (n-$Bu_4NH_2F_3$) and 1,3-dibromo-5,5-dimethylhydantoin (DBH) (Scheme 1.8). DBH acts as a source of electrophilic bromine which activates the thioethers as leaving groups. Fluoride from n-$Bu_4NH_2F_3$ then displaces the thioether and, after oxidation, the resulting difluoro(methylthio)methyl ketone **65** is produced.[54,55]

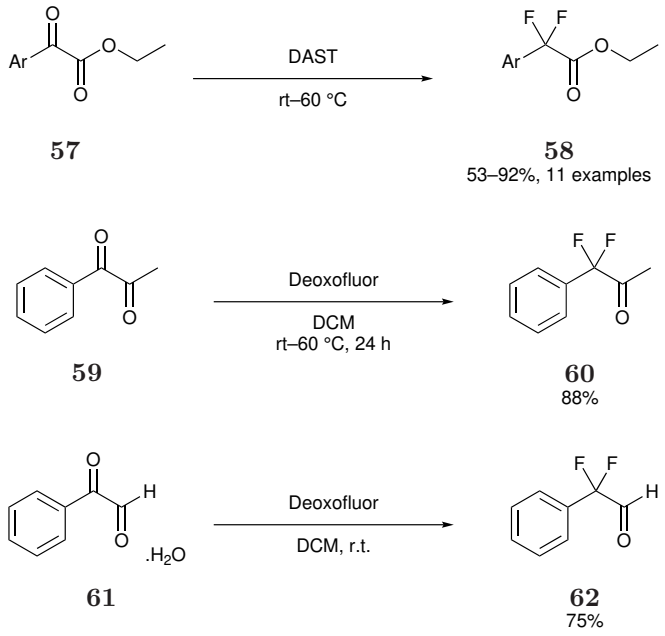

Scheme 1.7: Examples of nucleophilic fluorinations of dicarbonyls to give α,α-difluorocarbonyl compounds[37,51–53]

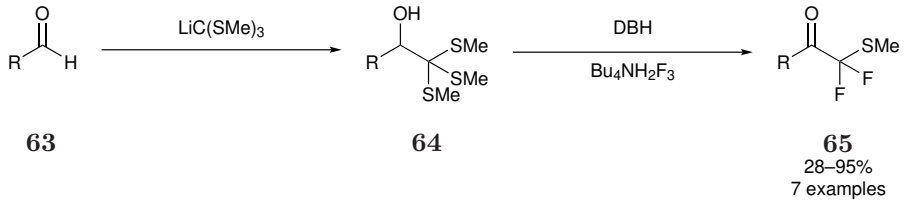

Scheme 1.8: Oxidative fluorodesulfurization to give α,α-difluorocarbonyl compounds[54,55]

1.3.2 Electrophilic Fluorination for CF_2 Synthesis

While many nucleophilic fluorinating reagents give good conversion to the desired $>CF_2$ containing products, they are often hazardous. Electrophilic fluorinating agents were designed to be easier to use on a discovery scale using general laboratory equipment and many successful synthetic strategies have been widely reported.[56–59] The majority of currently used electrophilic fluorinating agents contain a labile N-F bond that is used to deliver "F^+", often from a quaternary ($R_3N^+FX^-$) nitrogen salt. Selectfluor™ **66** is a bench stable, non-hygroscopic white solid that is commonly used on a discovery scale to regioselectively introduce a single fluorine atom. The synthesis of the most common electrophilic fluorinating agents are well reported in the literature, and there is continual development of related chiral electrophilic fluorinating agents (Scheme 1.9).[60,61]

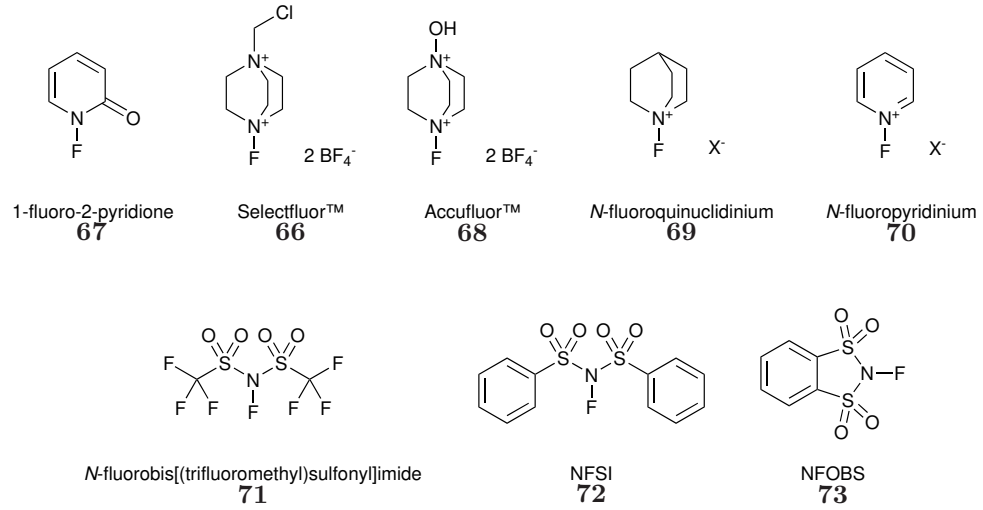

Scheme 1.9: Commonly used electrophilic fluorinating agents

The development of electrophilic fluorinating agents has greatly pushed the boundaries of synthetic organofluorine chemistry but it is worth noting that there are two significant limitations to these reagents that are often overlooked. Many electrophilic fluorinating agents have a very low atom economy due to the low molecular weight of fluorine relative to the fluorinating agent—Selectfluor™ **66** is only 5% fluorine by weight. Due to the low atom economy relatively large amounts of the reagent are required, which can often cost significantly more than nucleophilic reagents. Due to these cost issues, electrophilic fluorinating agents are rarely used on an industrial scale with the noticeable exception of the high value fluorinated steroid fluticasone propionate **75** (Flovent, Flonase) (Scheme 1.10).[62]

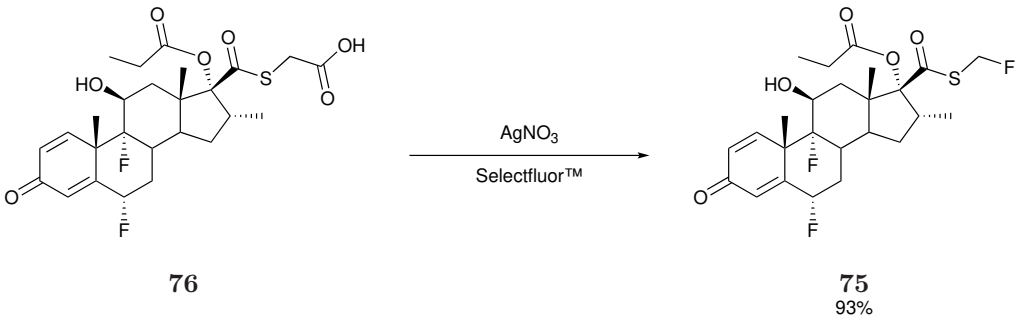

Scheme 1.10: Synthesis of fluticasone propionate highlighting the fluorination using Selectfluor™[62]

Electrophilic fluorinating agents are easy to use in regular glassware, and they allow for the avoidance of corrosive or hazardous sources of fluorine. However, it is worth mentioning that all electrophilic fluorinating agents are synthesised by dir-

ect fluorination using fluorine gas followed by a counterion exchange. Electrophilic fluorinating agents do not remove the issues created by using fluorine gas in the synthesis of Selectfluor™ **66**, as frequently stated in the literature.

Electrophilic fluorinating agents give the highest conversion when there are enolizable protons present in a compound, usually α- to a carbonyl group. Selective difluorination of cytidine **77** to give the 5,5-difluoro-6-methoxy adduct **78** is achieved using both Selectfluor™ **66** and acetyl hypofluorite (AcOF) (Scheme 1.11).[63,64] The 5-fluoro adduct is not detected under these conditions.

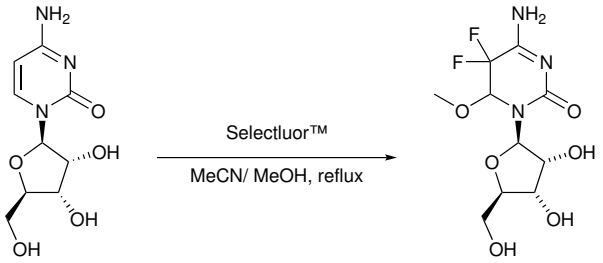

77 **78** 82%

Scheme 1.11: Difluorination of cytidine by Selectfluor™ to give the 5,5-difluoro-6-methoxy adduct[63]

1.3.2.1 Synthesis of α,α-Difluorocarbonyl Derivatives

Electrophilic fluorinating agents introduce fluorine with good selectivity at enolisable positions by reacting with the enol tautomer, and so are often used to introduce fluorine α- to carbonyl groups; monofluorination of α- and β-dicarbonyl derivatives is well reported.[56,65–68] Difluorination is often seen as an unwanted side reaction in these fluorinations, and, in many cases, conditions are optimised to limit the formation of difluorinated by-products.

Banks found that while monofluorination of positions α- to C=O groups can occur relatively quickly, difluorination occurs much slower, and depends on the proportion of the monofluorinated intermediate existing in the enol form (Scheme 1.12).[56] The rate of difluorination appears to decrease in the order diketone > ketoester > ketoamide. Intermediates that have a high proportion of the keto form can eventually achieve complete conversion to the difluoro product, but can this take over 20 days. The rate of difluorination can be dramatically increased by forming the sodium enolate of the monofluorinated intermediate before the addition of a second equivalent of the electrophilic fluorinating agents. Difluorination of the less reactive

substrates was only achieved by fluorinating the monofluoro enolate in a stepwise reaction. These results indicate that the keto form of the monofluoro intermediate is resistant to subsequent fluorination but the enol, and especially the enolate form, can undergo additional fluorination to give the *gem*-difluoro product.

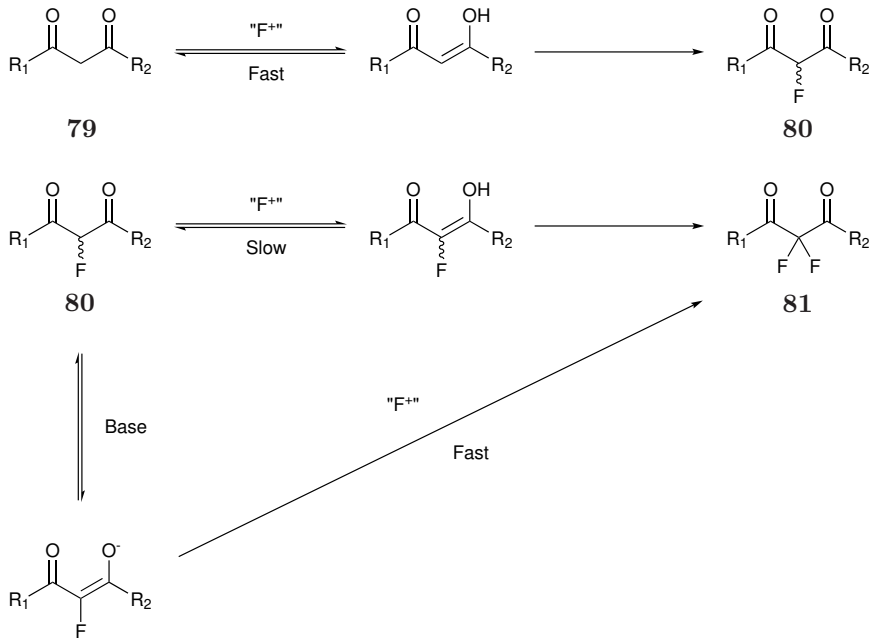

Scheme 1.12: General mechanism of electrophilic difluorination of β-dicarbonyl derivatives[56]

However, a one-pot difluorination of propiophenone **82** was achieved with good selectivity (95:5 diF:mF) using the *N*-F sultam **83** as a source of electrophilic fluorine, and potassium bis(trimethylsilyl)amide (KHMDS) as a strong organometallic base to form the metal enolate (Scheme 1.13).[69] Interestingly the choice of base is important, as using lithium bis(trimethylsilyl)amide (LiHMS) to generate the lithium enolate and one less equivalent of **83** gives the monofluorinated product with a 95:5 selectivity compared to the difluoro product.

A commonly used strategy to synthesise an α,α-difluoroketo compound by C–F bond formation is to difluorinate the related enamine or imine and then hydrolysis to give the desired ketone. As imines tautomerize to the corresponding enamines faster than ketones to enols, fluorinations with electrophilic fluorinating agents often given greater conversion to the difluoro product than their ketone equivalent. During the difluorination of the *N*-butylimine **85** with **71**, the addition of a weak base such as sodium carbonate (Na_2CO_3) is required to remove the super acid by-product bis[(trifluoromethane)sulfonyl]azane ($HN(SO_2CF_3)_2$) produced after **71** has trans-

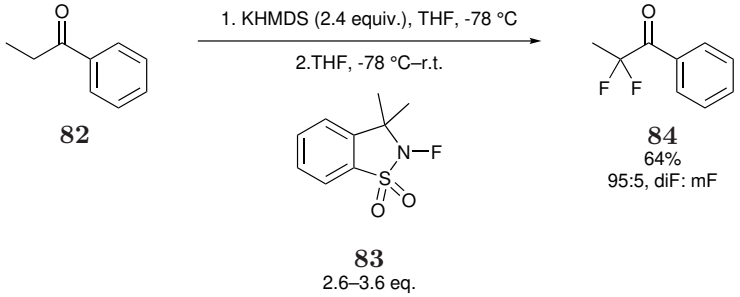

Scheme 1.13: *gem*-Difluorination of propiophenone[69]

ferred its fluorine atom (Table 1.5).[58] Stavber expanded the results of DesMarteau to compare the observed selectivity when different electrophilic fluorinating agents are used to fluorinate **85**.[70] While most give the difluoro compound as the major product, the *N*-fluoro pyridinium salt (Table 1.5, Entry 4) shows complete selectivity for the monofluorinated product **86**.

Table 1.5: Selectivity of fluorination of an *N*-buimine[37]

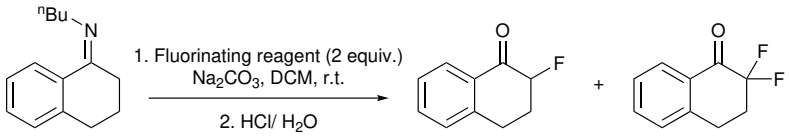

85 **86** **87**

Entry	Fluorinating reagent	Ratio **86**:**87**	Yield[a]/%
1	**71**[b]	0:100	65[c]
2	**66**	0:100	95
3	**72**	12:88	65
4	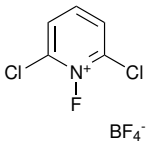	100:0	65

[a] Total yield of both **87a** and **87b** as determined by ^{19}F NMR spectroscopy

b Na_2CO_3 added

c Isolated yield

Alkynes can be difluorinated in an acetonitrile (MeCN)/ H_2O solvent mixture to produce α,α-difluoroketones (Scheme 1.14). The two solvent system plays a key

role, the MeCN solvates the alkyne, and the water traps the carbocation formed during fluorination. The reaction proceeds selectively when a phenylacetlyene is used as the substrate, with complete Markovnikov regioselectivity observed due to formation of the more stable carbocation at the benzylic position. This selectivity is observed when a range of electrophilic fluorinating reagents are used.[71–73]

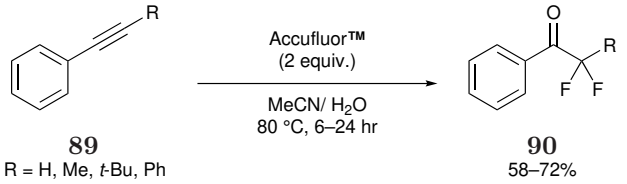

Scheme 1.14: Fluorination of phenylalkynes with electrophilic fluorinating agents such as Accufluor™[71–73]

Browne *et al.* developed successful *gem*-difluorination by grinding β-diketones and β-ketoesters in a mixture mill with an electrophilic fluorination agent (Scheme 1.15).[74,75] While high conversion of starting material to the 2-fluoro and 2,2-difluoro was achieved, selectivity for the difluoro product is low. Benefits of this method include reactions not requiring solvent or heat, and requiring significantly shorter reaction times (2 h compared to up to 5 d) for similar reactions using conventional methods. Interestingly, the selectivity for the monofluoro product can be increased to 50:1 from 3:2 to the difluoro product by the addition of a small amount of MeCN. This selectivity is similar to that observed when these substrates are fluorinated with electrophilic fluorinating agents under various conditions.[67,68] The addition of sodium chloride (NaCl) as a grinding auxiliary is required to achieve any conversion to the difluoro product when a liquid ketoester is used as a starting material. Addition of sodium carbonate increases conversion to the difluoro product, but from these experiments, it cannot be determined if this improvement is due to the Na_2CO_3 acting as a base, as an additional grinding auxiliary agent, or a combination of these two factors.

Gem-difluorination is most successful when there is only one preferred enolizable carbon atom. The desired 2,2-difluoro-1,3-keto product was isolated as the major product by Bertozzi despite the presence of alternative enolisable sites by the addition of an excess of cesium carbonate (Cs_2CO_3) (Scheme 1.16).[76] By premixing the diketone and base, the central $>CH_2$ is deprotonated forming the enolate as these protons are more acidic than the enolisable protons adjacent to each carbonyl. Excess base ensures that the monofluorinated intermediate remains as the enolate, allowing for subsequent fluorination.

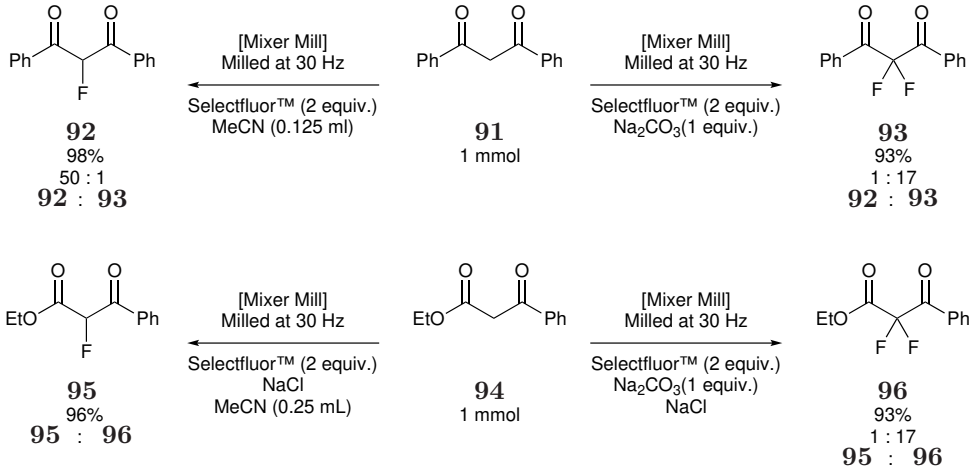

Scheme 1.15: Mechanochemical grinding difluorinations of 1,3-diphenylpropane-1,3-dione and ethyl benzoylacetate with Selectfluor™[74,75]

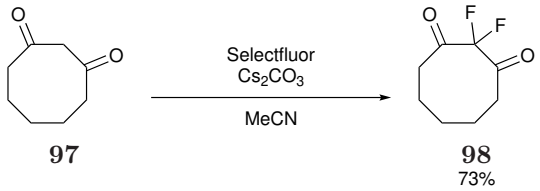

Scheme 1.16: Synthesis of 2,2-difluoro-1,3-cyclooctanedione[76]

Pattison developed a hybrid electrophilic fluorination/ fragment based building block methodology to potentially fix the issue of non-regioselective difluorination in compounds with multiple enolisable protons (Scheme 1.17).[77] A geminal bis(boron) compound **99** is deprotonated using lithium tetramethylpiperidide (LiTMP) then coupled with an ester to form an α-diboryl ketone **101** which readily tautomerises to a boron enolate. This enolate is selectively formed, even if there are other enolisable protons present because boronates can stabilise α-carbanions through hyperconjugation with the empty p-orbital of boron. The enolate can then be trapped with an electrophile such as **72** twice to yield the desired *gem*-difluoro compounds **102**. This difluoro-coupling has a vast potential scope by simple variations of the starting materials.

1.3.3 CF_2 Containing Building Blocks

While it is certainly possible to make *gem*-difluoro products using nucleophilic or electrophilic fluorinating agents, there are often issues associated with using these such as selectivity and toxicity of some reagents. There is a large amount of liter-

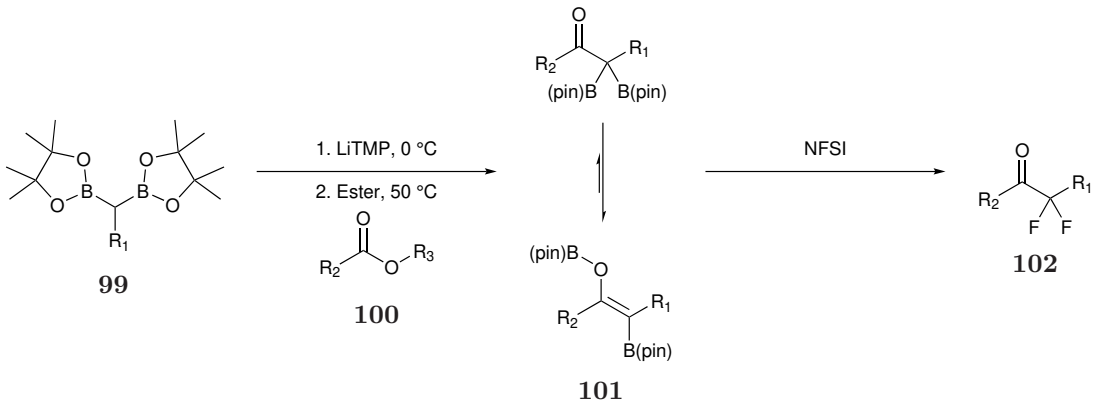

Scheme 1.17: Synthesis of α,α-difluoroketones via an α,α-bis(enolate) equivalent[77]

ature on the introduction of a trifluoromethyl ($-CF_3$) group into a molecule. Key examples of $-CF_3$ reagents include the Ruppert-Prakash (trifluoromethyltrimethylsilane, $TMSCF_3$, **103**), Togni I **104** and II **105** and Umemoto reagents I **106** and II **105**.

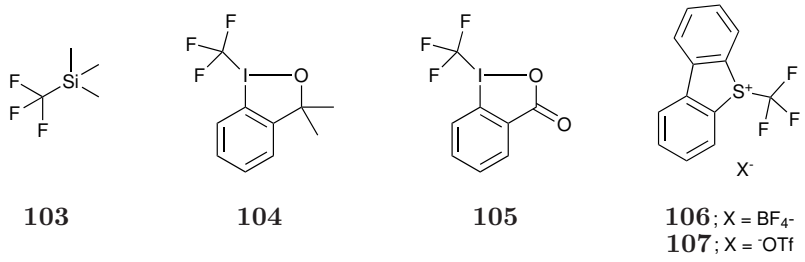

Figure 1.12: Several commonly used reagents used to incorporate the $-CF_3$ group

By adapting the reagents and strategies used to incorporate $-CF_3$ into molecules, there has been a recent growth in the number of papers published that can introduce $>CF_2$ into organic systems in the form of $-CF_2H$, $-CF_2CO_2R$, $-OCF_2H$ and $-SCF_2H$ using adapted reagents. For example, (difluoromethyl)trimethylsilane ($TMSCF_2H$, **108**) is often used in an analogous fashion to the CF_3 variant **103**. While fluoride-activated addition reactions to aldehydes using **103** proceed with excellent yields at r.t., the use of $TMSCF_2H$ gives low yields using these conditions, even at 100 °C, due to the stronger C–Si bond in $TMSCF_2H$.[78] Further studies have shown that room temperature additions can proceed using $TMSCF_2H$ by performing the reaction in polar aprotic solvents such as dimethylformamide (DMF) (Scheme 1.18).[79] While this provides a simple route for introducing a CF_2H moiety into organic systems, the high cost of **108** prohibits the use of this reagent on a manufacturing scale.

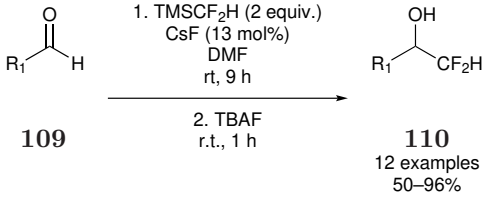

Scheme 1.18: Direct nucleophilic difluoromethylation of various aldehydes with (difluoromethyl)trimethylsilane[79]

Alternatively, difluoromethyl phenyl sulfoxide ($PhSOCF_2H$, **111**) and difluoromethyl phenyl sulfone ($PhSO_2CF_2H$, **112**) have been used as simple, one-step reagents to introduce the $>CF_2$ functionality (Scheme 1.19).[80,81] Reactions occur with good conversion, but poor diastereoselectivity, yet the additional PhSO or $PhSO_2$ handle allows for additional processes to expand the range of CF_2 containing compounds.[82]

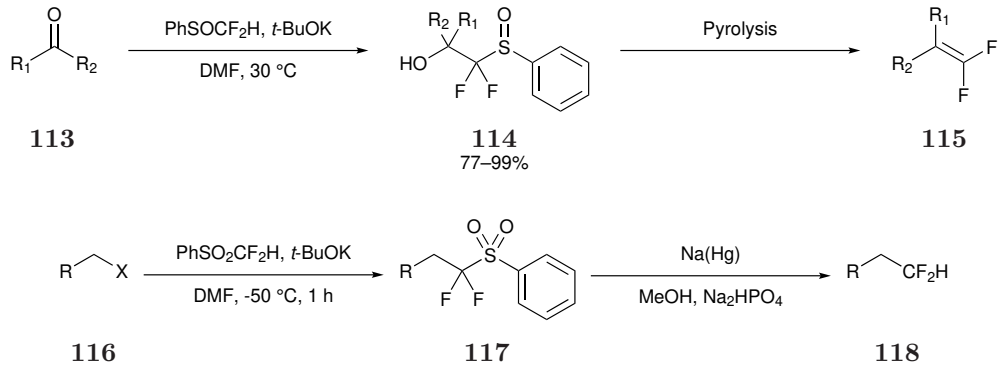

Scheme 1.19: Additions of $PhSOCF_2H$ and $PhSO_2CF_2H$ and further functionalisation[80–82]

The ethyl halodifluoroacetates, in particular commercially available ethyl bromodifluoroacetate **119**, have been used as fluorinated building blocks (FBB) through various synthetic strategies such as Reformatsky and aldol reactions.[83–86] Successes have been achieved with good yields, but often require multiple equivalents of zinc (Scheme 1.20).

Ethyl aryldifluoroacetates **124** can be synthesised by coupling **119** with arylboronic acids **129**, aryl halides **130** or arylzinc compounds **131**.[87–90] Yields for these reactions are moderate to good, but often require the use of expensive palladium, ruthenium or cobalt catalysts for radical reactions via a difluorocarbene like intermediate, or stoichiometric quantities of copper or zinc (Scheme 1.21).

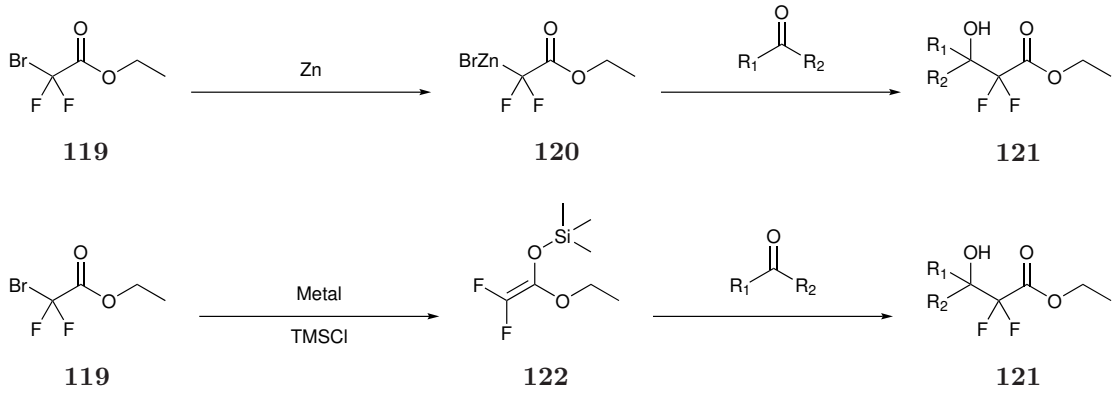

Scheme 1.20: Reformatsky reaction (top) and aldol reaction (bottom) using ethyl bromodifluoroacetate

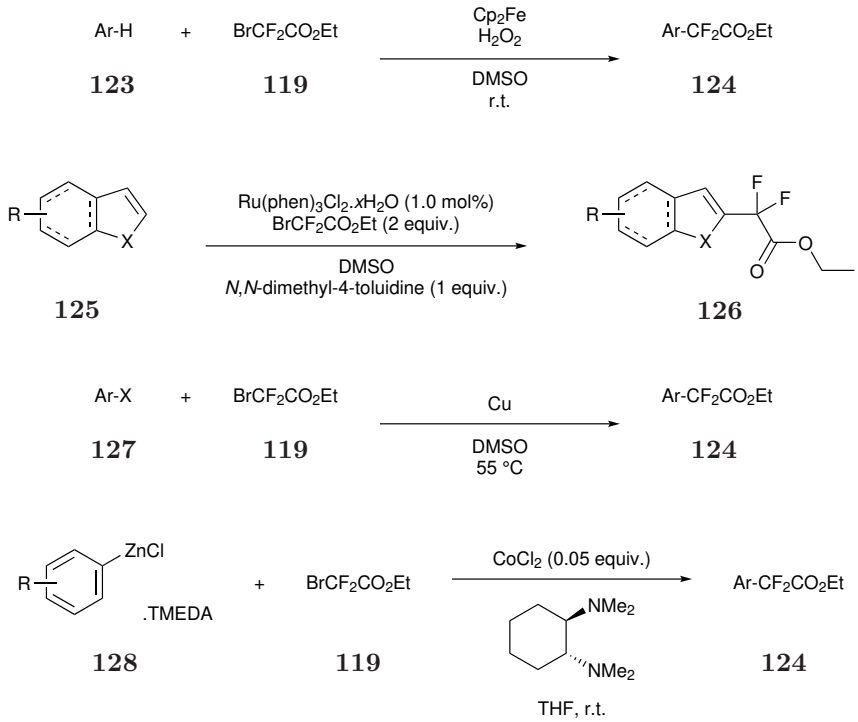

Scheme 1.21: Synthesis of $ArCF_2CO_2Et$ compounds using ethyl bromodifluoroacetate[87–90]

Notably, the difluoro ester can be hydrolysed to the difluoroacid, and then decarboxylated to produce the $-CF_2H$ containing substrate such as in the case of benzofuran derivatives (Scheme 1.22).[91]

Additionally, there is growing interest in one pot difluoromethylations to produce $ArCF_2H$ using the readily available FBB **119** (Scheme 1.23).[92,93] While these meth-

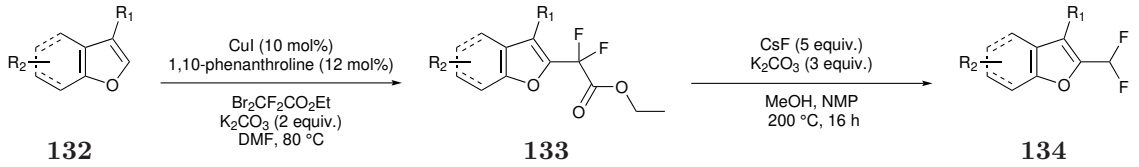

Scheme 1.22: Stepwise synthetic strategies to generate $ArCF_2H$ compounds using $>CF_2$ containing FBBs[91]

ods use a cheap source of $>CF_2$, they usually require large amounts of expensive metal catalysts.

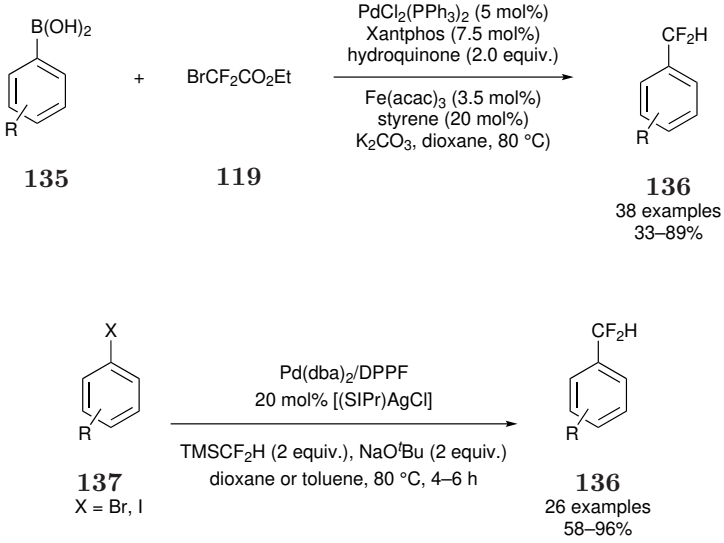

Scheme 1.23: One-pot synthetic strategies to generate $ArCF_2H$ compounds using CF_2 containing FBBs[92,93]

Iseki *et al.* showed that 2,2-difluoro-β-ketoesters can be synthesised by reaction of an acid chloride and difluoroketene silyl acetal **122** using mild conditions developed by Hosomi (Scheme 1.24).[94,95]

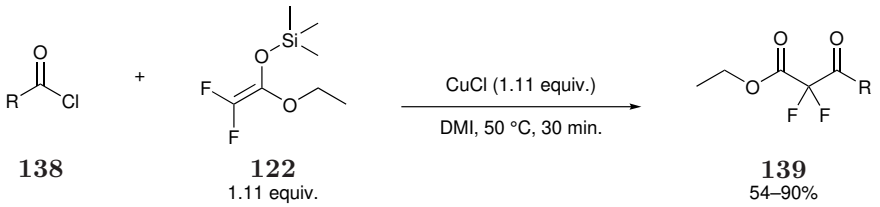

Scheme 1.24: Synthesis of 2,2-β-ketoesters from an acid chloride and silyl enol ether[95]

While *gem*-difluoroalkene building blocks usually react with nucleophiles at the difluoro substituted carbon by addition-elimination or S_N2 type additions, the introduction of a siloxy group causes the difluoroalkene to react with electrophiles to give α,α-difluoroketones.[96] Addition of copper (II) triflate ($Cu(OTf)_2$) in MeCN causes oxidation of the difluoroenol silyl ether **140** which homocouples to form the tetrafluoro dimer **141** in excellent yields. Addition of a heteroaromatic and slight modification of the reaction conditions allowed for oxidative cross-coupling between the difluoroenol silyl ether and the heteroaromatic giving a more complex FBB (Scheme 1.25).

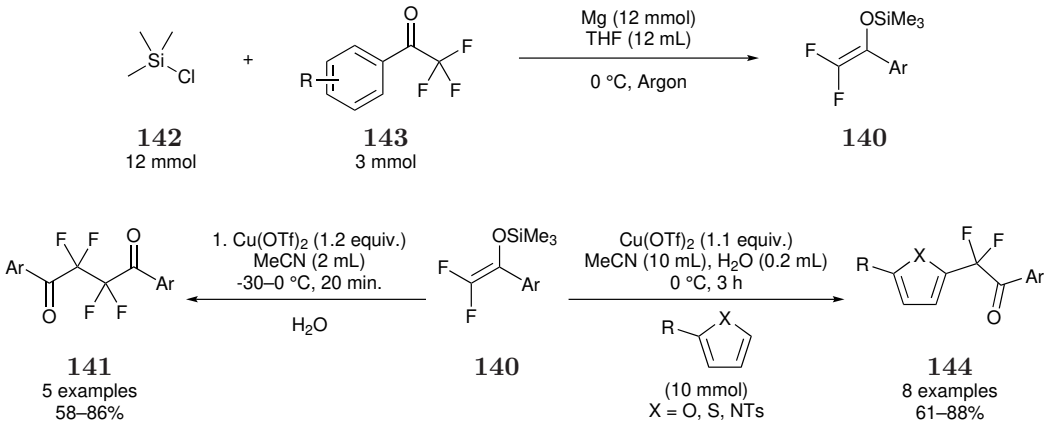

Scheme 1.25: Oxidative cross-coupling of difluoroenol silyl ethers **140** with heteroaromatics or itself to give the homocouple product **141**[96]

These are only a selection of the ever growing field of CF_2 containing FBBs. This thesis will focus on strategies of C–F bond formation, particularly industrially viable routes to fluorinate organic compounds for the synthesise of CF_2–C=O containing organic systems.

1.3.4 Direct Fluorinations

We discussed above the synthesis of difluoro containing compounds, in particular difluoroketones and $ArCF_2H$ derivatives. While many of these strategies give the desired products with good conversions, they often require reagents that may be impractical on an industrial scale due to cost. Fluorine gas (F_2) is a potentially useful fluorinating reagent due to its low cost and high reactivity. It is synthesised from the electrolysis of potassium bifluoride in anhydrous hydrogen fluoride (aHF).[97] This molten fluoride salt is used as the electrolyte due to the very low electrical conductivity of aHF. F_2 is an attractive reagent for industrial fluorinations as it can

be generated *in situ* which helps alleviate safety concerns with storing large amounts of pressurised F_2 on site. Despite the use of F_2 as a selective fluorinating agent on an industrial scale for several decades in the synthesis of 5-fluorouracil, many proponents of electrophilic fluorinating agent still maintain that it is too dangerous to use, despite the recent ongoing development of direct fluorination apparatus at various sites in the UK. The choice of solvent is important and a high dielectric medium, such as MeCN or formic acid (HCOOH), is used to promote electrophilic fluorinations over radical fluorination.

1.3.4.1 Selective Monofluorination Reactions

Despite fluorine's high reactivity, there are several examples of selective monofluorination using F_2 and many of the strategies used to selectively monofluorinate compounds were developed at Durham.[98–102] The most successful selective direct fluorinations have been achieved using carbonyl containing substrates with enolisable protons. In these cases, F_2 acts as an electrophilic source of fluorine, with conversion to the desired fluorinated product dependent on the degree of enolisation. The observed reactivity (cyclic 1,3-diketones > 1,3-diketones > 1,3-ketoesters) is similar to that observed using electrophilic fluorinating agents, which is indicative of a similar electrophilic mechanism.

The first successful direct fluorination of 1,3-dicarbonyls to give a 2-fluoro-1,3-dicarbonyl product was the fluorination of sodium diethyl nitromalonate **145** by Adolph *et al.* (Scheme 1.26).[103] The desired 2-fluoro product **146** was isolated in excellent yield without formation of the 2,2-difluoro product that had previously been formed when perchloryl fluoride was used as the fluorinating agent. While an efficient synthesis of **146**, this methodology has very limited substrate scope as only highly acidic dialkyl malonates are deprotonated by the aqueous sodium bicarbonate and then soluble in the water solvent. Additionally, a 50% mixture of F_2 and N_2 was used which is now avoided due to safety concerns.

Purrington developed methodology to directly fluorinate trimethylsilyl enol ethers to give α-fluoro ketones using dilute fluorine in trichlorofluoromethane ($CFCl_3$).[104] Attempts in other solvents and temperatures give no α-fluoroketone product. This methodology was then applied to the fluorination of β-diketones and β-ketoesters to give average yields (Scheme 1.26). The best results are achieved when the only enolisable proton was in the desired 2-position, but when there were several possible enolisable protons, a mix of products is produced that can not be separated.[105]

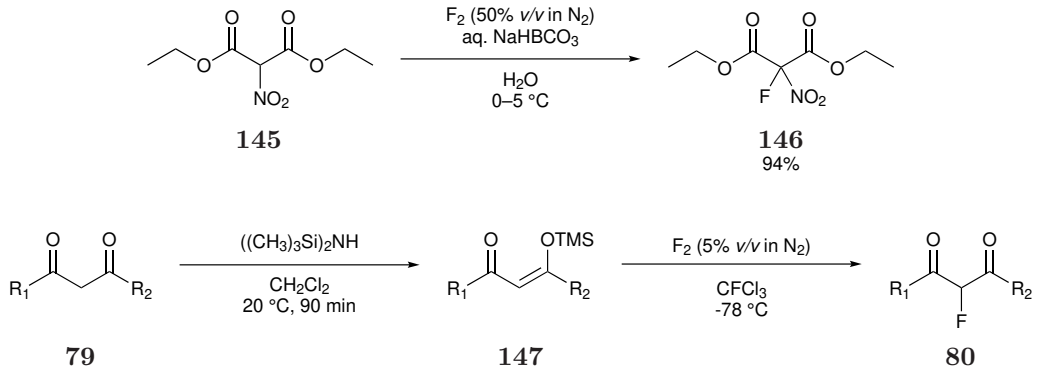

Scheme 1.26: Direct fluorination with F_2 to give 2-fluoro-1,3-dicarbonyl compounds[103,105]

Greenhall investigated the direct fluorination of various 1,3-dicarbonyl compounds in HCOOH and determined that diketones and ketoesters form the 2-fluoro product with high selectivity.[106] It is worth noting that little tar was formed, even at the relatively high temperature (10–15 °C), and that there is no reaction with diesters under the same conditions. Isolation of products with multiple enolisable protons was possible using this methodology allowing for the selective fluorination of diketones with alkyl substituents (Table 1.6, Entry 1). Small amounts of the 2,2-difluoro product is formed, but the rate of difluorination is significantly lower than the rate of monofluorination under the conditions employed. Fluorination of ethyl 2-chloroacetoacetate **148** using these conditions gave a conversion of 15% to the mono-fluoro product. Analysis of the tautomerism of **148** in HCOOH determined that the enol content is approximately 15%, with a ketone enolisation half life of 18 h. This indicates that no **149-keto** converts to **149-enol** during the reaction conditions, and that only **149-enol** is fluorinated during the reaction.

Table 1.6: Direct fluorination of 1,3-dicarbonyl compounds[103,105]

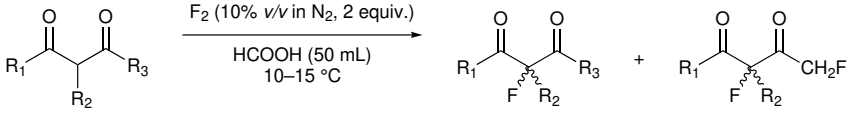

79 25 mmol — **80** — **150**

Entry	R_1	R_2	R_3	Conversion/%	Yield%	
					80	**150**
1	CH_3	H	CH_3	90	70	11
2	OCH_2CH_3	H	CH_3	60	80	10
3	OCH_2CH_3	Cl	CH_3	15	85	5

Chambers investigated the synthesis of α-fluoroketones by reacting enol acetates and silyl enol ethers in MeCN and HCOOH.[107] The enol acetates gave good yields in general (56–66%) when MeCN is used as the solvent. Reactions were slower in 98% HCOOH but tended to give higher conversion (61–71%) to the α-fluoroketones when the esters were stable to acid hydrolysis. The silyl enol ethers have a noticeably lower stability in acidic medium, which explains why the desired products were isolated in a lower yield (23–35%) than in MeCN, and reactions in HCOOH give the parent ketone as the major product instead of any fluorinated products.

While ketones and ketoesters can be directly fluorinated in MeCN or acidic solvents, diesters have very low reactivity under these conditions and show no signs of fluorination. Fluorinations in MeCN or HCOOH are very slow with low conversion of starting material, with fluorination occurring on alkyl groups preferentially to fluorinations at the 2- position.

Dialkyl fluoromalonate esters, in particular, diethyl 2-fluoromalonate **152** have shown potential use as FBB, and have been used to synthesise several biologically important molecules (Scheme 1.27).[108–110]

These compounds can be synthesised via halex reactions or reactions with electrophilic fluorinating agents, and so it was recognised that a route using F_2 would be desired for an industrial scale. Based on previous work by Adolph, Hutchinson investigated the direct fluorination of sodium salts of dialkyl malonates and noticed high conversion to the desired 2-fluoro product.[114] The overall conversion to the 2-fluoro product is dependent on the conversion to the sodium salt, with the fluorination step occurring with complete conversion (Table 1.7). While NMR conversion

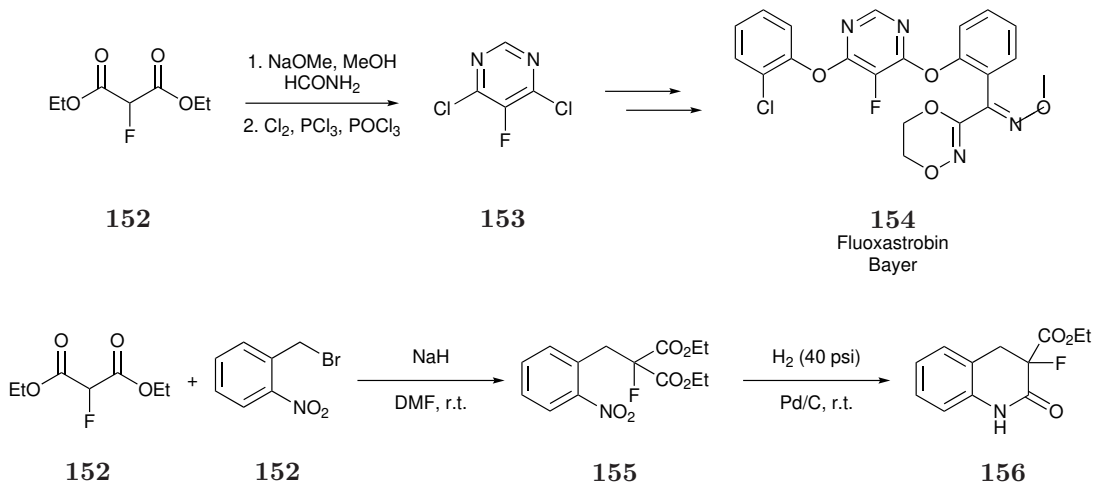

152 **153** **154** Fluoxastrobin Bayer

152 **152** **155** **156**

Scheme 1.27: Example uses of diethyl 2-fluoromalonate as a FBB[111–113]

is high, there is limited selectivity between the 2-fluoro and 2,2-difluoro products when R_2 = H (Table 1.7, Entries 1 and 2). Conversions appear to be lower when sodium ethoxide (NaOEt) is used instead of NaH highlighting the importance of forming the carbanion before fluorination.

Table 1.7: Direct fluorination of dialkyl malonate salts[114]

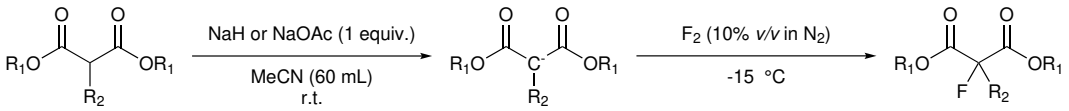

151 12.5 mmol — **158** — **159**

Entry	R_1	R_2	Equiv.		NMR	NMR
			NaH	F_2	Conversion%	Yield%
1	Et	H	1	2	71	37[a] + 23[b]
2	Et	H	2.25	3	94	14[a] + 37[b]
3	Et	Me	1	2	74	59
4	Et	Me	1[c]	2	42	59
5	Et	*n*-Bu	1.25	2.3	66	69
6	Me	OMe	1.25	2.9	75	51
7	Et	NO_2	1.25	2	100	73
8	Et	NO_2	1[c]	2	77	89
9	Et	Cl	1.25	2	97	40
10	Et	Ph	1.25	1.2	72	41

[a] Diethyl fluoromalonate

[b] Diethyl difluoromalonate

c NaOEt used as the base

Chambers investigated using transistion metal salts to promote selective fluorination at the 2-position.[115] While the addition of transition metal salts does not effect the conversion or selectivity detected when **160** is fluorinated with F_2 in HCOOH, there is an increase in conversion to the 2-fluoro product when MeCN is the solvent. In particular, hydrated copper (II) nitrate ($Cu(NO_3)_2 \cdot 2.5\,(H_2O)$) gives high selectivity for the 2-fluoro product when a range of malonates was trialled and give very little of the 2,2-difluorinated products (Scheme 1.28). Copper nitrate allows for the selective fluorination of β-ketoesters, but the conversion is noticeably lower than for malonates ($\sim$40%). Chambers proposes that the increase in selectivity for the 2-fluoro position is due to the metal increasing the rate of enolisation, the rate-determining step of fluorination in which the malonate chelates the Cu^{2+} in the enol form. Direct fluorination of **160** to **152** was further optimised by Harsanyi (Scheme 1.28).[116]

The most industrially important FBB synthesised using F_2 is methyl 2-fluoro-3-oxopentanoate **162** by F2 Chemicals Ltd based in Preston, UK. Methyl 3-

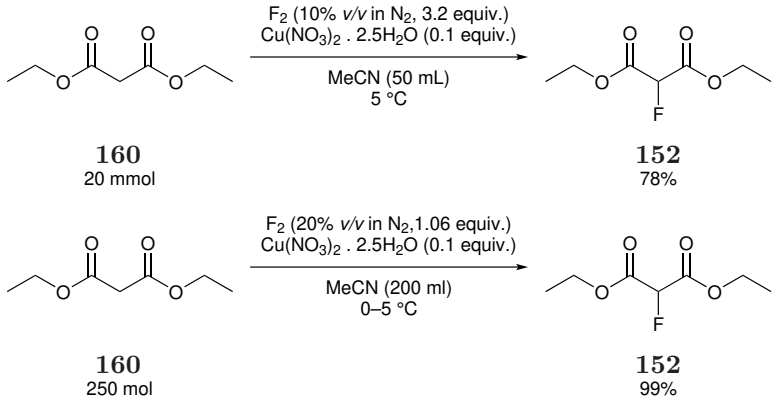

Scheme 1.28: Copper catalysed direct fluorination of malonates and optimisiation of reaction conditions by Harsanyi[115,116]

engoxopentanoate **161** is fluorinated on a multi tonne scale to give **162** with excellent selectivity. This is then cyclised by the addition of formadine acetate and sodium methoxide (NaOMe) to give 6-ethyl-5-fluoro-4(3*H*)-pyrimidone **163** (Scheme 1.29).[106,117,118] This is used in the synthesis of voriconazole (**164**, Vfend, Pfizer), a triazole auntifungal that previously had annual sales of over a billion USD.

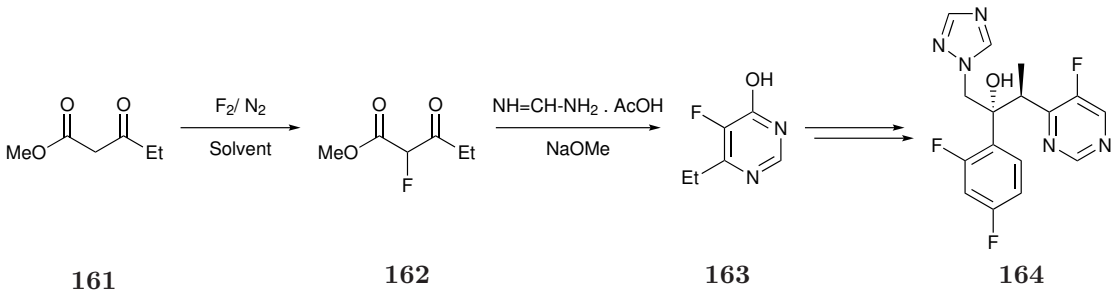

Scheme 1.29: Part of the synthesis of voriconazole highlighting the selective direct fluorination step using F_2[106,117,118]

1.3.4.2 Selective Difluorination Reactions

The previous section highlights examples of selective direct mono-fluorination strategies using F_2. In contrast, there are very few examples in the literature of $>CF_2$ compounds made selectively using F_2; usually difluorinated derivatives are recorded as by-products during attempts to selectively introduce a single fluorine atom at a specific site.

While diazoketones were first fluorinated using F_2 in 1976 by Leroy and Wakselman to give a mixture of products, it was not until Patrick investigated the fluorination

of diazo compounds with F_2 that the corresponding $>CF_2$ containing products were isolated in excellent yields (65–94%, Scheme 1.30).[119,120] While this gives a route to making a range of difluoro compounds selectively due to the favourable enthalpy change upon transformation of a $>CN_2$ to a $>CF_2$ group, it requires the use of $CFCl_3$ as a solvent. This has been banned since the Montreal Protocol in 1987 after it was discovered that it is an ozone-depleting chemical.

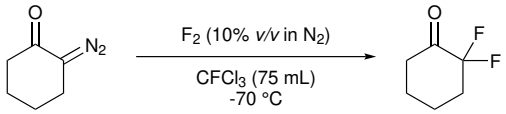

165
0.01 mol

166
65%

Scheme 1.30: Synthesis of an α-difluoro compound by the direct fluorination of the corresponding diazo compound with F_2[120]

Linear 1,3-diketones such as pentane-2,4-dione **167** form the monofluorinated product **168** rapidly in acidic solvents such as HCOOH when fluorinated with F_2. The 3,3-difluoro product **169** is formed very slowly due to **168** existing in the keto form in HCOOH and tautomerizing to the reactive enol form very slowly. Chambers *et al.* discovered that cyclic diketones produce the corresponding *gem*-difluoro product when fluorinated using similar conditions.[121] The exact ratio of the monofluorinated products **171a** or **171b** and difluoro **172a** or **172b** compared to unreacted starting material depends on the amount of F_2 added, and the duration of the reaction (Table 1.8).

Table 1.8: Direct fluorination of cyclic ketones using F_2[121]

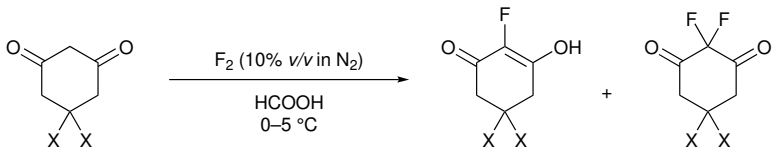

X = H **170a** **171a** **172a**
X = Me **170b** **171b** **172b**

Entry	Substrate	Molar ratio F_2:Substrate	Conversion/%	Yield/%	
				171	**172**
1	**170a**	2.2:1	100	-	75[a]
2	**170a**	1.1:1	70	40[b]	33[b]
3	**170b**	2.6:1	100	-	80[a]
4	**170b**	1.0:1	85	27[b]	38[b]

[a] Isolated yield

[b] Yield calculated by GC-MS

While monofluorination decreases the rate of enolization to the enol form in acyclic 1,3-diketones, cyclic 1,3-diketones such as **171a** and **171b** exist in the enol form as determined by NMR spectroscopy and crystallography. Christe's investigation into proton acceptors determined that although fluorine can act as a proton acceptor in a bifurcated bond, the OH···O interactions are stronger and so the enol H is hydrogen-bonded to the carbonyl.[122] Purrington theorised that while introducing a filled p orbital from the fluorine into the 1,3-diketone pentadienyl anion system results in a destabilising primary HOMO-HOMO interaction, there are two favourable secondary orbital interactions between the fluorine and carbonyl groups.[105] As such, the enol form is more stable than the ketone. As the rate of fluorination depends on the proportion of the enol form present, this suggests why **171a** and **171b** can readily fluorinate again forming **172a** or **172b** under the reaction conditions.

The difluoro product is formed as the major product when an excess of fluorine is used; however, a further hydration reaction appears to occur as shown by the appearance of a second peak in the ^{19}F NMR spectra. In (Table 1.8, Entries 1 and 3) there was full conversion of starting material and none of the monofluoro present, but 20–25% of the hydrated products **173a**,**b** as determined by comparing the ^{19}F NMR shifts to a sample of the hydrated product formed by recrystallisation of pure samples of the difluoro products from aqueous acetone (Figure 1.13). These systems

can be dehydrated using strong dehydrating agents such as phosphorous pentoxide (P_4O_{10}).

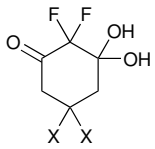

X = H **173a**
X = Me **173b**

Figure 1.13: Hydrated difluoro product[121]

When roughly equivalent amounts of F_2 to starting material were used (Table 1.8, Entries 2 and 4) the ratio of **174** to **175** was roughly equal, with a slight excess of **172**. This indicates that the rate of fluorination of **171** is only slightly higher than that of **170** and appears to be based purely on the proportion of material in the enol conformer.

1.4 Conclusion

Fluorine plays a highly important role in the design of new biologically active compounds as AIs in agrochemistry. Introduction of fluorine into specific sites of biologically active molecules can drastically improve various desired properties for the agrochemical industries. Even a minor improvement can have a noticeable effect given the large amounts of herbicides and insecticides that are applied to crops globally each year. As profit margins in the agrochemical industry are significantly lower than in the pharmaceutical industry, methods of introducing fluorine selectively into AIs for manufacture on an industrial scale as cheaply as possible are required.

The $>CF_2$ group is of growing interest in FBBs due to many beneficial physiochemical properties. This introduction has reviewed some of the current methods of introducing $>CF_2$ groups, specifically α- to carbonyl derivatives, as possible routes to develop potential new AIs. Unfortunately some difluoromethylating reagents are often expensive or require stoichiometric amounts of metal.

There are limited examples of introducing fluorine via C–F bond formation to form desired $>CF_2$ functionalities. Current methods often involve thermally unstable deoxyfluorinating agents such as DAST **39**, or large excesses of expensive electro-

philic fluorinating agents. There appears to be no general route to synthesising $>CF_2$ functionalities using F_2 as a cheap and readily available fluorinating agent.

Chapter 2

Synthesis of 2,2-Difluoro-1,3-diketones

2.1 Aims and Approach

Fluorine gas is a relatively inexpensive fluorinating agent that has successfully been used to selectively monofluorinate dicarbonyl compounds on an industrial scale to manufacture pharmaceutical products. However, although F_2 has been used to introduce a CF_2 group α- to a carbonyl in a limited number of cyclic β-diketones, a general methodology for the selective introduction of a CF_2 α- to a carbonyl moiety using fluorine gas has not been achieved.

Previous fluorinations of carbonyl systems in acidic conditions have given the >CHF product almost exclusively, and the incorporation of a second fluorine atom at these sites appears to be inhibited. The aim of this thesis is to develop a synthetic methodology to selectively convert $>CH_2$ groups α- to carbonyls to $>CF_2$ groups with the possibility that this could be used on the industrial scale. To do this, the effect of bases as mediating agents for selective fluorinations using F_2 shall be investigated with the aim at increasing selectivity for the difluoro product by increasing the concentration of fluoro enol intermediates in solution that reacts readily with F_2 (Scheme 2.1).

A final issue with the synthesis of *gem*-difluoro products appears to be isolation of the products. Given the significantly lower reactivity of monofluorinated intermediates with fluorinating reagents compared to the non-fluorinated starting material, there is often not insignificant amounts of monofluorinated products present in the product

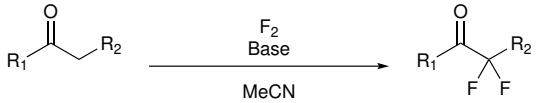

176 **102**

Scheme 2.1: Proposed synthetic strategy for the selective introduction of CF_2 groups α- to carbonyls by base mediated selective direct fluorination

mixture. In most reported cases in the literature, either no attempt is made to fully remove this unwanted by-product, or isolation has been unsuccessful. As so few groups have successfully managed this, it is possible that this separation is difficult, and so synthetic strategies with very high selectivity for the difluoro product are required.

At Durham we have shown that DBM **91** and its derivatives react via the enol tautomer with electrophilic fluorinating agents and that bases catalyse the tautomerism to the enol form.[123,124] While we can not conclusively state that F_2 reacts in a bimolecular S_N2 reaction with **91** in a similar manner to Selectfluor™ it is likely that any *in situ* N−F intermediates formed with a similar structure to Selectfluor™ may react similarly, with the enol tautomer.[125]

Selectfluor™ **66** is currently synthesised from 1,4-diazabicyclo[2.2.2]octane (DABCO, **177**) on an industrial scale in a three step synthesis including fluorination using F_2 (Scheme 2.2).[126]

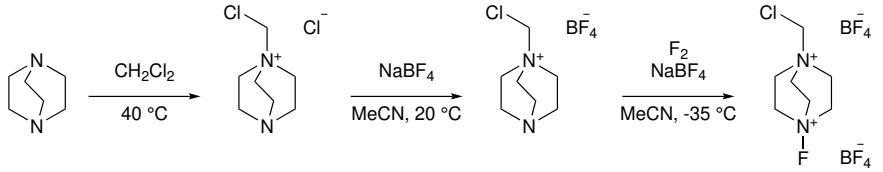

177 **178a** **178b** **66**

Scheme 2.2: Industrial synthesis of Selectfluor™

The *in situ* generation of a fluorinating agent would significantly lower the costs of electrophilic fluorinating agents, as well as allowing for the more widespread use of F_2 on a laboratory scale if reactivity could be controlled (Scheme 2.3).

Various different bases will be trialled as potential mediating agents to try and replicate the high selectivity obtained using pre-formed electrophilic fluorinating agents (Scheme 2.4).

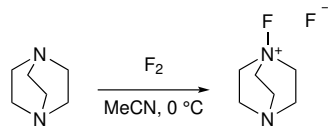

177 **179**

Scheme 2.3: Proposed in situ N-F^+ fluorinating agent produced by DABCO and F_2

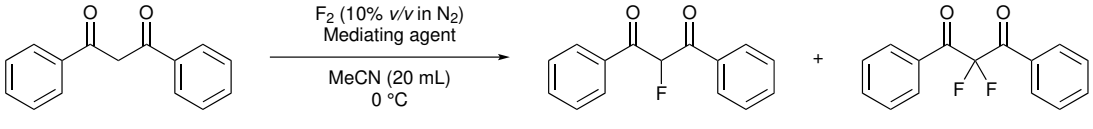

91
2 mmol

92 **93**

Scheme 2.4: Screening conditions for the fluorination of 1,3-diketones

There are two main safety considerations with using F_2; the highly corrosive nature of fluorine, and the highly exothermic nature of C–F bond formation using F_2. All apparatus connected to the fluorination apparatus must be formed out of a highly fluorinated material such as polytetrafluoroethylene (PTFE), and any metal parts must be sufficiently passivated. This is achieved by slowly passing small amounts of F_2 through the experimental rig system and selectively coating the inner metal layer of any components to form a metal fluoride layer lining the inside of the fluorination apparatus. Pressurised F_2 should be diluted with an inert gas such as nitrogen (usually to a 10% or 20% mixture v/v with N_2) or helium. The apparatus is described in Figure 8.1 in the General Experimental. Reaction vessels must be appropriately cooled to prevent decomposition of the C–C bonds with a bond dissociation energy of 348 kJ mol^{-1}.[16] Dilution of F_2 with nitrogen helps slow down the reaction allowing time for cooling to occur.

2.2 Mediating the Direct Fluorination of DBM

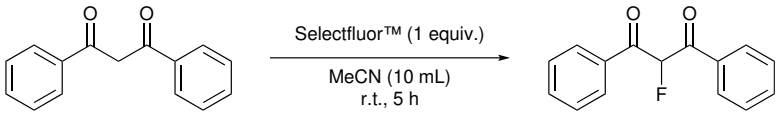

91
1 mmol

92
100% (84% isolated)

Scheme 2.5: Fluorination of 1,3-diphenylpropane-1,3-dione with Selectfluor™[56]

While fluorinations with Selectfluor™ **66** or other electrophilic fluorinating agents give good conversions of diketones to the monofluorinated products with high se-

lectivity (Scheme 2.5), our attempts to fluorinate 1,3-diphenylpropane-1,3-dione (DBM, **91**) at the $>CH_2$ site with one equiv. of F_2 in acetonitrile (MeCN) gave no noticeable conversion by NMR spectroscopy. Isolation of the 2-fluoro product **92** in a good yield has been reported when a large excess (16 equiv.) of F_2 in acetic acid was used, confirming the very low reactivity of diketones under these reaction conditions.[127] However, in the polar aprotic solvent MeCN, a polyfluorinated tar was formed when a large excess (20 equiv.) of F_2 was used (Table 2.1, Entries 1 and 2). These control experiments show that DBM would make an ideal model system to use to develop selective fluorinations at the $>CH_2$ site, as direct fluorinations in MeCN doesn't give fluorinated products to any extent compared to existing electrophilic fluorinating agents.

2.2.1 Effect of Bases on the Fluorination of DBM

Chambers investigated the effect of adding potassium fluoride (KF) as a base to promote the selective fluorination of carbonyl compounds with acidic protons.[115] While the addition of excess KF promoted converison of the starting material, selectivity for the monofluoro product was detected over the difluoro product in an 8:1 ratio on average. With this in mind, we decided to look at soluble nitrogen bases to mediate the selectivity of direct fluorinations of DBM using F_2.

2.2.1.1 Bases

DABCO **177** was trialled as the first mediating agent due to its structural similarity to Selectfluor™ **66** . A solution of DBM with one equivalent of DABCO was made in MeCN. After cooling to 0 °C and purging the reaction vessel with N_2, one equivalent of F_2 diluted to a 10% *v/v* mixture in N_2 was added at a prescribed flow rate of 15 mL min^{-1}. The addition of F_2 was kept relatively slow to ensure good mixing. NMR yields were calculated by comparisons of the integrals (CF dp at −189.9 ppm, CF_2 s at −102.7 ppm) to a known amount of α,α,α,-trifluorotoluene.

Table 2.1: Screening conditions for the fluorination of 1,3-diphenylpropane-1,3-dione

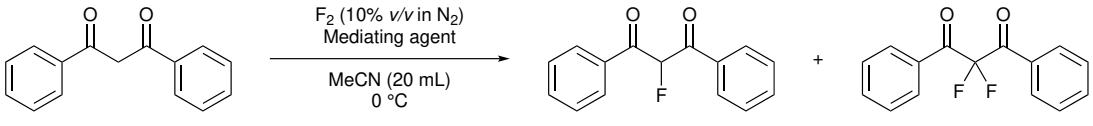

91 2 mmol **92** **93**

Entry	Base	Equiv. of base	Equiv. of F_2	Yield by NMR/%		
				91	**92**	**93**
1	-	-	1	100	0	0
2	-	-	20	Polyfluorinated tar		
3	DABCO	1	1	32	4	20(7)[a]
4	DABCO	1	1[b]	30	3	19
5	DABCO	1	2	1	1	37
6	DABCO	1	3	Polyfluorinated tar		
7	DABCO	2	2	Many fluorinated products		
8	DABCO	0.1	1	22	28	8
9	Quinuclidine	1	1	42(41)[a]	10(8)[a]	43(33)[a]
10	Quinuclidine	1.2	1[b]	54	1	43
11	Et_3N	1	1	56	25	6
12	Cs_2CO_3	1	1	0	4	14
13	NaCl	1	1	0	33	12(6)[a]
14	NaCl, DBU	1	1	7	19	16

[a] Isolated yield

b F_2 (20% *v/v* in N_2) used

When equivalent amounts of DBM, F_2 and DABCO were used (Table 2.1, Entry 3), the 2,2-difluoro product **93** was the main product formed as determined by ^{19}F NMR. The formation of **93** contrasts with results seen when equivalent amounts of Selectfluor™ and substrate are reacted, in which the monofluorinated product **92** is formed rather than the difluoro product **93** (Scheme 2.5).[56,66,67]

After workup and purification by column chromatography on silica gel with hexane and dichloromethane (DCM) (1:1) as the eluent, the major difluorinated product

was isolated in 7% yield and confirmed as the difluorinated product by NMR spectroscopy and X-ray crystallography (XRC).

Increasing amounts of F_2 to 2–3 equivalents (Table 2.1, Entries 6 and 7) caused the formation of a polyfluorinated tar making it very difficult to identify or separate any fluorinated compounds present. With the amount of DABCO limited to 0.1 equiv. (Table 2.1, Entry 8), the monofluorinated product **92** was the main product detected by ^{19}F NMR spectroscopy. The noticeable drop in the conversion of **91** to **92** and **93** when DABCO is less than stoichiometric indicates that the fluorination is dependent on the concentration of DABCO.

Other organic bases were used to try and increase the chemoselectivity of the fluorination of DBM. Addition of other bases showed varying effects on the conversions to **92** and **93** (Table 2.1). Quinuclidine (Table 2.1, Entries 9 and 10) provided the highest conversion to the difluorinated product **93** according to ^{19}F NMR spectroscopy, with very little unwanted aromatic fluorination competing.

Several potential mediating agents that do not contain nitrogen were trialled and selective direct fluorination was detected when both cesium carbonate (Cs_2CO_3) (Table 2.1, Entry 12) and sodium chloride (NaCl) (Table 2.1, Entry 13) were used. While there was conversion to the desired fluorinated products with Cs_2CO_3 and NaCl (Table 2.1, Entries 12 and 13), there was also significant amounts of unwanted aromatic fluorination making it difficult to isolate desired products. The reaction was repeated with an equivalent of the strong base 1,8-diazabicyclo[5.4.0]undec-7-ene (DBU), (Table 2.1, Entry 14) to see if this addition aided conversion to **93**. Analysis of the ^{19}F NMR spectra after an aqueous workup showed the formation of several new unwanted fluorinated products.

2.2.2 Optimisation of the Synthesis of 2,2-Difluoro-1,3-diphenylpropane-1,3-dione

Given the results discussed in Table 2.1, quinuclidine appears to be the best mediating agent of the bases screened at maximising conversion to the desired difluoro product. Therefore, fluorination of **91** was repeated with varying amounts of quinuclidine and F_2 and conversion to **92** and **93** monitored by NMR spectroscopy to optimise conditions to provide the highest yield of difluoro-DBM **93**.

Table 2.2: Screening conditions for the quinuclidine mediated fluorination of 1,3-diphenylpropane-1,3-dione

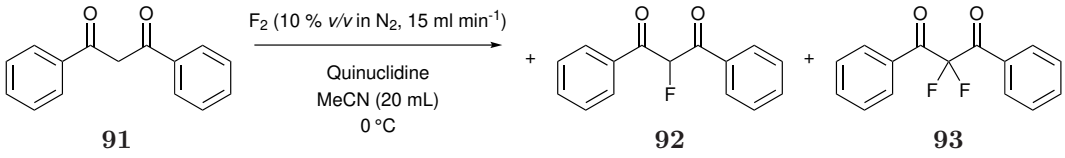

91 **92** **93**

Entry	Equiv. of quinuclidine	Equiv. of F_2	Conversion	Ratio of products by NMR		
				91	**92**	**93**
1	1	1	81	3	2	4
2	1.1	2.1	99	1	5	47
3	1.1	2.3	99	1	16	120

Only a small excess of both quinuclidine and F_2 were required to obtain high conversions (nearly 90% by NMR spectroscopy) of **91** to **93** with minimal traces of remaining **91** or other products observed. While increasing the equivalents of F_2 gave ever increasing amounts of the desired product **93** as observed by ^{1}H and ^{19}F NMR spectroscopy, an increase in aromatic fluorination (Figure 2.1) was seen. Thus the optimised conditions were adjusted to limit the formation of these undesired fluoroaromatic products.

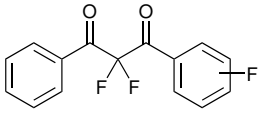

180

Figure 2.1: Unwanted fluoroaromatic by-product

After purging the reaction vessel with N_2, the reaction mixture was partitioned between H_2O and DCM in order to remove any HF or protonated quinuclidine produced as by-products during the fluorination. Initial attempts at isolating **93** by column chromatography on silica gel with 15% EtOAc *v/v* in hexane mixture as the eluent were unsuccessful, with many fractions containing both the desired **93** and **92**. Replacing EtOAc with DCM helped increase the separation between **92** and **93**, but there was still some overlap of **93** and unreacted starting material when hexane and DCM (1:1) was used as the eluent. Complete separation was achieved using a hexane and $CHCl_3$ (1:1) mixture as the eluent and **93** was isolated as a white solid (57%). The product was fully characterised by high resolution NMR spectroscopy, accurate mass spectrometry and XRC. Individual carbon atoms were assigned using

heteronuclear single quantum correlation (HSQC) and heteronuclear multiple bond correlation (HMBC) 2D NMR spectroscopy.

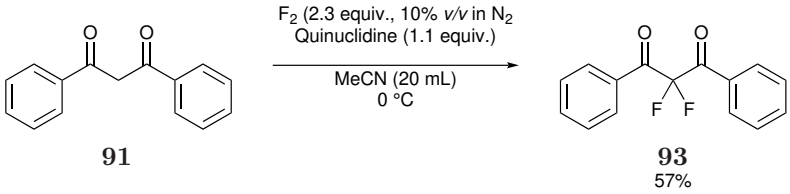

Scheme 2.6: Synthesis of 2,2-difluoro-1,3-diphenylpropane-1,3-dione

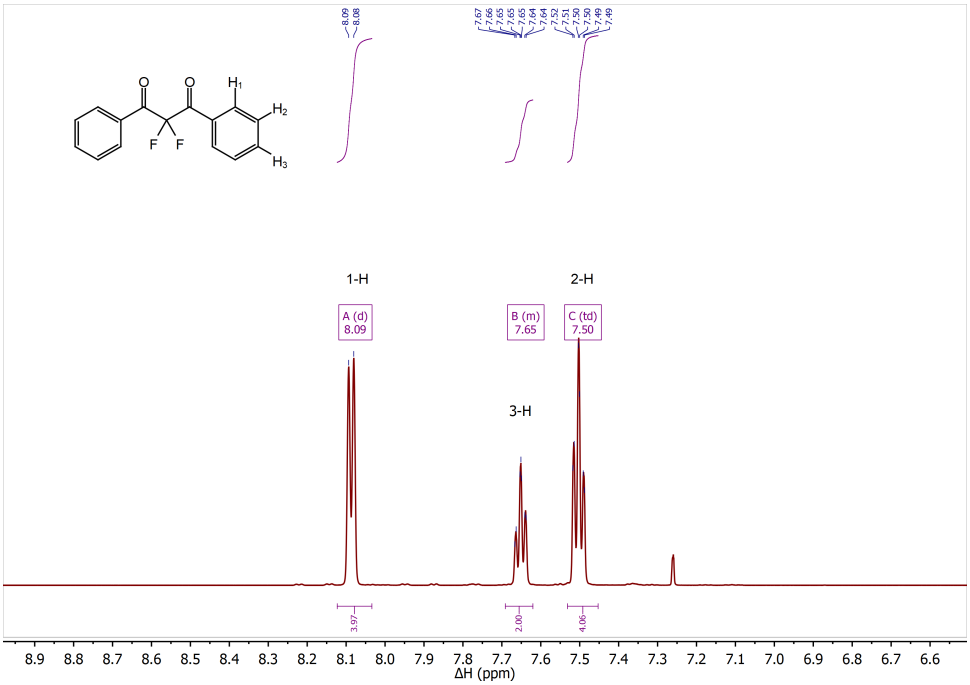

Figure 2.2: ^{1}H NMR spectrum of 2,2-difluoro-1,3-diphenylpropane-1,3-dione

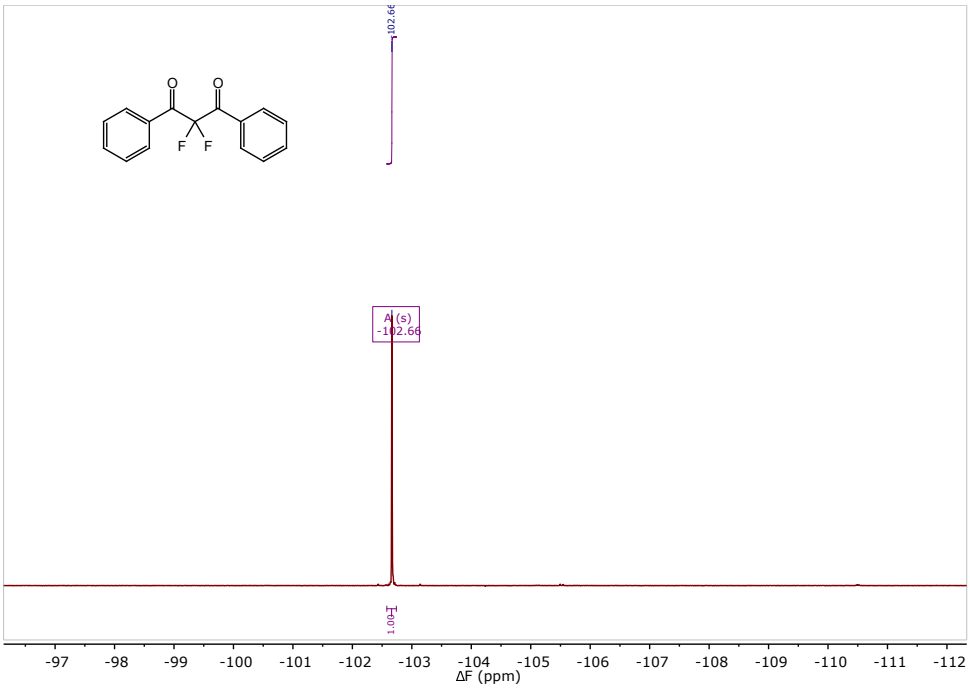

Figure 2.3: ^{19}F NMR spectrum of 2,2-difluoro-1,3-diphenylpropane-1,3-dione

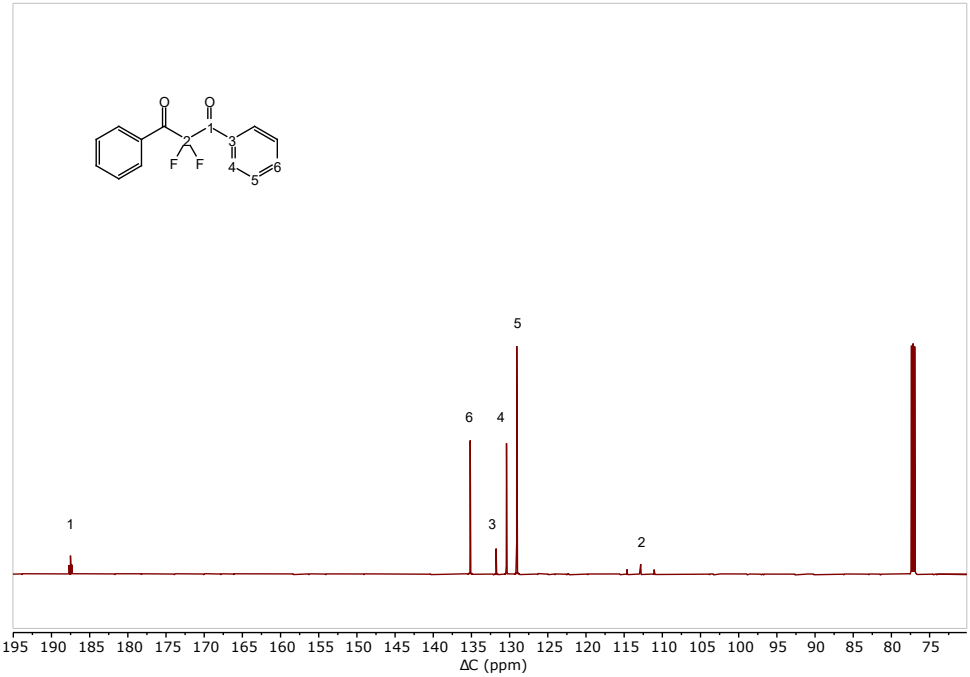

Figure 2.4: ^{13}C NMR spectrum of 2,2-difluoro-1,3-diphenylpropane-1,3-dione

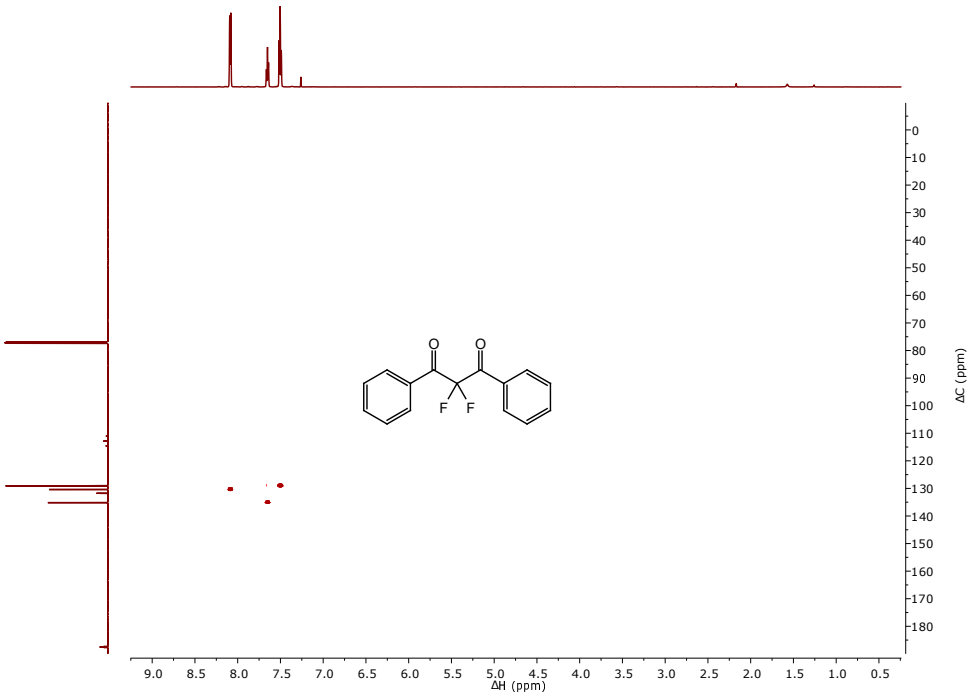

Figure 2.5: HSQC NMR spectrum of 2,2-difluoro-1,3-diphenylpropane-1,3-dione

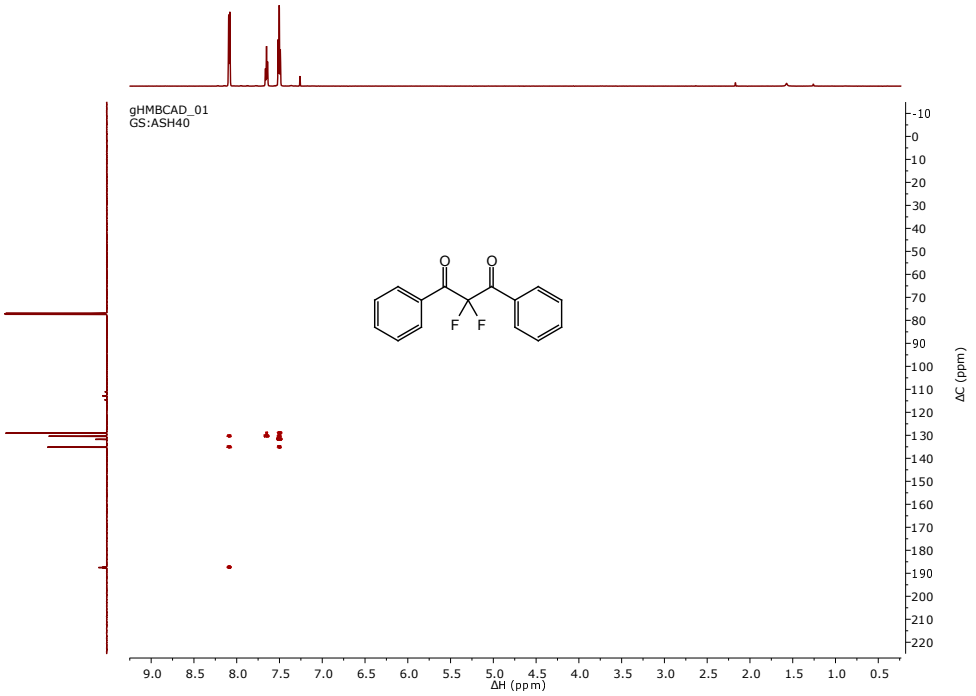

Figure 2.6: HMBC NMR spectrum of 2,2-difluoro-1,3-diphenylpropane-1,3-dione)

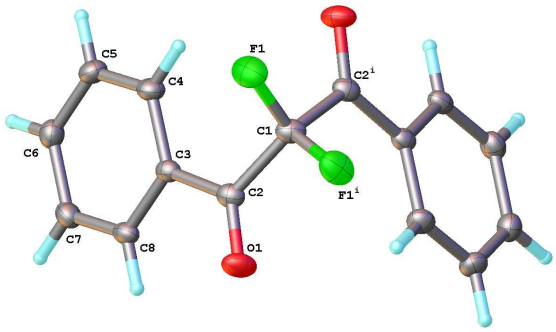

Figure 2.7: Molecular structure of 2,2-difluoro-1,3-diphenylpropane-1,3-dione as confirmed by X-ray crystallography

2.2.3 Recycling Quinuclidine

Quinuclidine is an expensive and toxic base, and so a method for reusing it would make successive reactions more cost efficient. In an attempt to determine if the reaction could be repeated with the same high selectivity for **93**, another equivalent of **91** was added to the reaction mixture after the initial fluorination was completed, and then a second fluorination was undertaken.

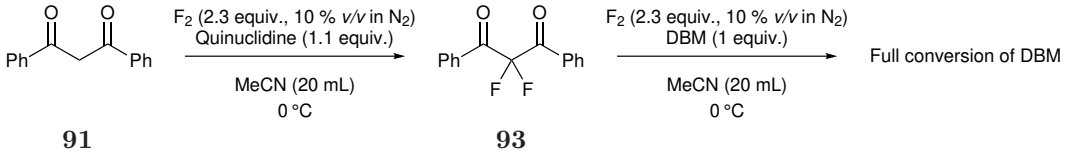

91 **93**

Scheme 2.7: Attempt at recycling the quinuclidine for a base mediated direct fluorination of **91**

The lack of peak at 6.87 ppm in the ^{1}H NMR spectrum after the second fluorination corresponding to the C**2**-H in **91-enol** indicated that the reaction had successfully gone to full conversion with an increase in the total amount of the desired **93** formed. Unfortunately, large amounts of aromatic ring fluorination had occured as detected by ^{1}H and ^{19}F NMR spectroscopy. It appears that approximately 22% of the total amount of **93** formed has undergone an additional ring fluorination to form **180**. Given the difficulty of removing trace amounts of **180**, no attempts were made to isolate the desired product **93**. Unfortunately this appears to be a non-viable method for reducing the amount of quinuclidine required due to the significant amounts of unwanted extra fluorination of **91** that occurs in the longer reaction conditions.

2.3 Synthesis of 1,3-Diphenylpropane-1,3-dione Derivatives

Given the success in synthesising and isolating difluoro product **93**, various DBM derivatives were synthesised as starting materials to develop the scope of the subsequent fluorination reaction. As would be expected, DBM derivatives with electron-donating substituents have shown an increased reactivity to monofluorination with existing electrophilic fluorinating agents such as Selectfluor™ over those with electron-withdrawing substituents.[123]

Various acetophenone and benzoyl chloride derivatives were coupled using lithium bis(trimethylsilyl)amide (LiHMDS) in THF based on an established literature pro-

cedure.[128] Incomplete conversion to the desired product was detected if the reaction was left overnight. Stirring for 48 hrs at r.t. led to complete conversion as observed by ^{1}H NMR, and the products were isolated as solids in excellent yields after purification by recrystallization or column chromatography.

Table 2.3: Synthesis of DBM derivatives

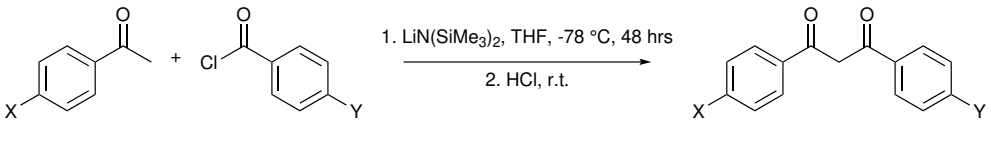

181 **182** **91**

DBM Derivative	X	Y	Isolated Yield/%
91a	H	Me	95
91b	H	OMe	94
91c	H	Cl	98
91d	F	H	100
91e	H	NO_2	99
91f	Cl	Cl	98
91g	F	F	81
91h	NO_2	NO_2	99

The isolated yield for **91g** is noticeably lower than that of the other derivatives. Analysis by GC-MS of the crude product showed two products, the desired product and a minor product with an M^+ of 382 *m/z*. This mass corresponds to the formation of the tribenzoyl product (**183** formed by the subsequent further reaction of **91g**), which was removed during purification (Scheme 2.8).

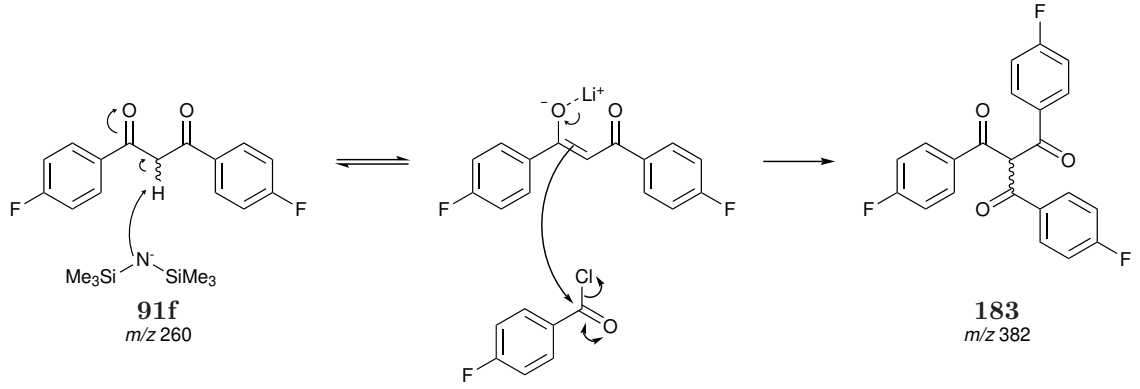

Scheme 2.8: Mechanism for the synthesis of the unwanted product with *m/z* 382

Analysis of the ^{1}H NMR spectra of **91**-**91h** in $CDCl_3$ indicated that the products exist in solution in a high enol ratio (>90%) (Figure 2.8). The high enol ratio was calculated by comparing the integrals of the peak at approximately 6.8 ppm due to the enol C-H and the peak at approximately 4.6 ppm corresponding to the ketone CH_2. The enol -OH proton was not visible in $CDCl_3$ due to the low concentration of the keto form. The structure of several derivatives of **91** were confirmed by XRC (Figure 2.9).

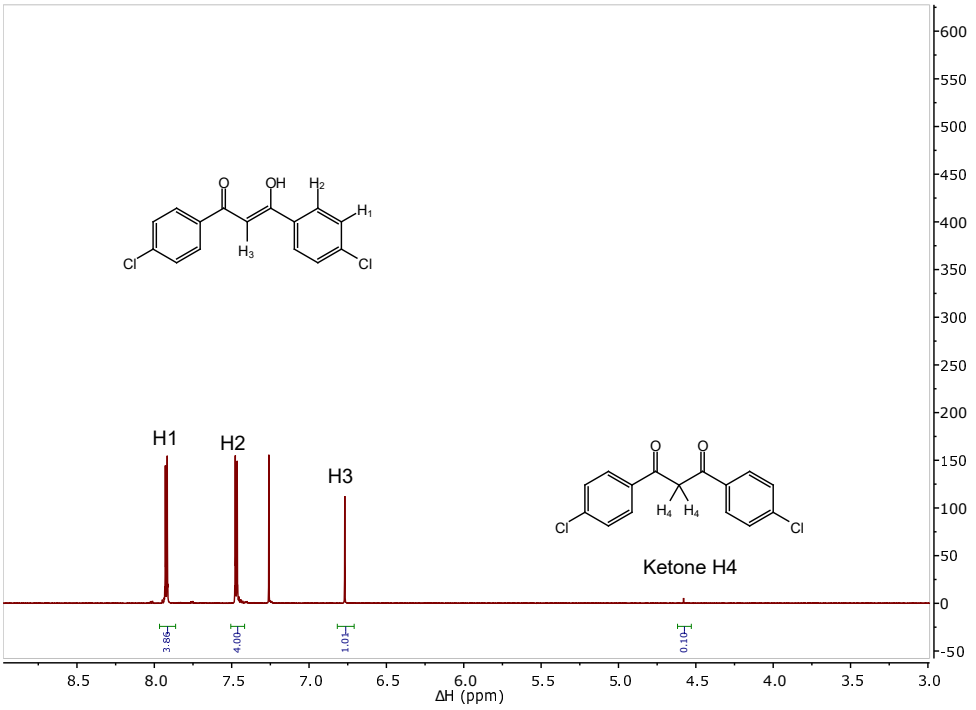

Figure 2.8: ^{1}H NMR spectrum of 1,3-bis(4-chlorophenyl)propane-1,3-dione with the enol and keto forms highlighted

Removal of solvent under reduced pressure can result in the product precipitating out as two differently coloured solids which we believe are the keto and enol forms. We believe the whiter coloured solid is the enol form of the product, and appeared to be less soluble in organic solvents then the darker keto forms.[124]

For most examples, both aromatic rings are in the same plane, however for **91b** the non-substituted ring is at a 26° angle relative to the carbonyl plane. While half the examples are orthorhombic (**91a**,**b**,**f**) and the other monoclinic (**91d**,**e**,**g**), all exist in the *enol* form. For the bis-substituted compounds **91f**,**g** the alcoholic hydrogen is found to lie in the middle of the two oxygen atoms as shown by the same C**2**-CO bond lengths. For the other derivatives, the O-H and C**2**-CO bond lengths are

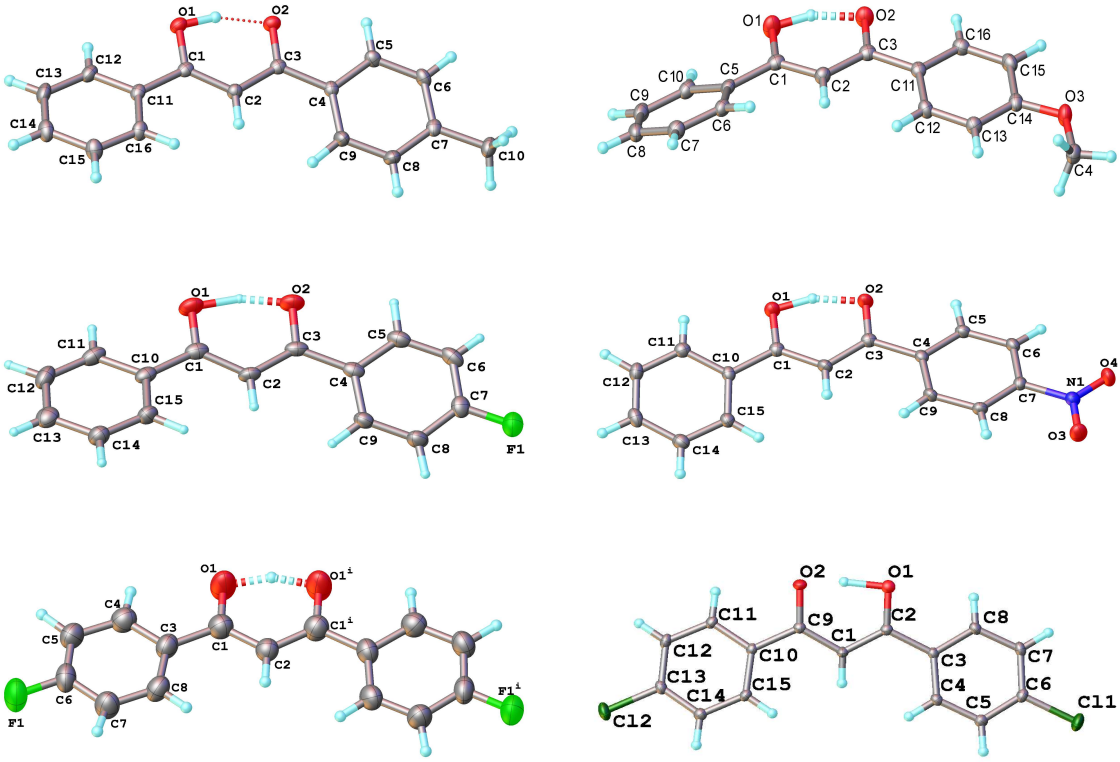

Figure 2.9: Molecular structure of **91a**,**b**,**d**–**g** as determined by XRC

shorter on the non-substituted ring side, which indicates that these derivatives are enolised on the left side (C**1**) as viewed.

2.4 Synthesis of 2,2-Difluoro-diketone Derivatives

2.4.1 Isolation of Products 93c–h

With reaction conditions and a purification method optimised for the fluorination of DBM **91**, fluorination of the 1,3-diketone substrates were performed. There are reports on the monofluorination of **91** and its derivatives, but very little literature on the synthesis of the corresponding difluorinated product **93** and its derivatives.[74,129] Most literature methods involve using large amounts of an electrophilic fluorinating agent in an attempt to achieve full conversion to the difluorinated product. Further reading into the supporting information of the published papers show that isolation of the difluorinated products were either not attempted or performed unsuccessfully; indeed, most reported preparations of difluorinated diketones contain significant amounts of the monofluorinated product.

Table 2.4: Synthesis of 2,2-difluro-1,3-diketones

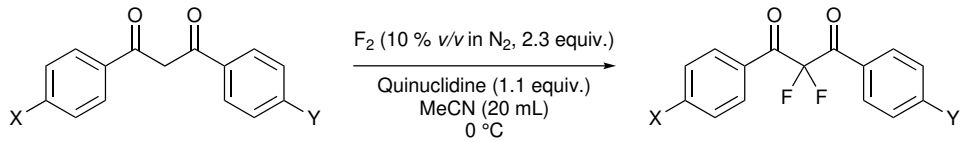

91 **93**

1,3-diketone	Product	Structure	Isolated yield/%
91	**93**	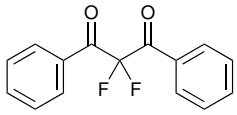	57
91a	**93a**	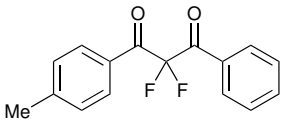	41[a] 10[a](mono-F) 12[a](Ar-F)
91b	**93b**	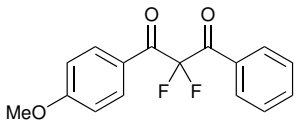	31[a] 16[a](Ar-F)
91c	**93c**	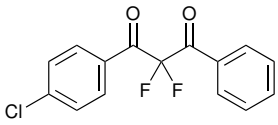	60
91d	**93d**	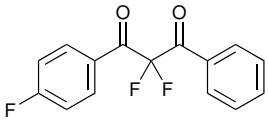	60
91e	**93e**	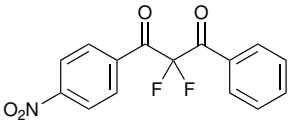	50
91f	**93f**	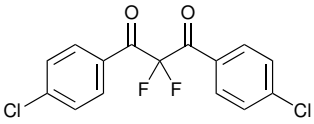	72
91g	**93g**	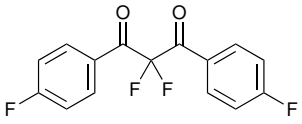	76
91h	**93h**	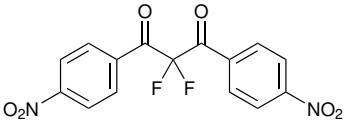	77

[a] NMR yield

Using the optimised fluorination conditions described in Scheme 2.6, the desired difluoro products **93c**–**h** were synthesised and isolated in good yields and purity (Table 2.4), with their structures confirmed by XRC in many cases (Figure 2.11).

Attempts to isolate the desired products via column chromatography on silica gel with hexane and EtOAC or DCM as the eluent were unsuccessful, and gave the products as an oil. However, purification via column chromatography on silica gel using hexane and chloroform (1:1) as the eluent allowed isolation of the desired products as solids.

The two derivatives with electron donating groups on the rings, **91a** (-Me) and **91b** (-OMe), were not isolated due to the formation of significant amounts of ring fluorinated impurities (Figure 2.1). Large amounts of polyfluorinated tar was formed and removed during the purification previously mentioned. The desired difluoro products that had undergone a single additional ring fluorination appeared to have identical retention factors on silica gel thin layer chromatography (TLC) to the desired products in every solvent system trialled. Due to their viscous nature, these impurities could not be separated from the difluoro products by recrystallization or distillation. Unfortunately, these polyfluorinated by-products could not be removed thus highlighting the need to prevent over-fluorination.

In the case of **93b** the isolated product contained the desired product and a further fluorinated product in a 2:1 ratio. This higher ratio of aromatic fluorination matches the better electron donating ability of the methoxy group compared to the methyl derivative. GC-MS of this product gave two peaks with masses corresponding to the desired product, and one that had undergone further fluorination on the aromatic ring. Analysis of the Mass spectrometry peaks show a fragment with an *m/z* of 105.1 corresponding to a $[C_8H_6FO_2]^+$ fragment (Figure 2.10). The fluorine is located on the aromatic ring bearing the -OMe substituent which confirmed that the addition of an electron donating group increases aromatic fluorination. Electron donating groups are activating and *ortho* and *para* directing, and NMR spectroscopy confirmed that the fluorine is located *ortho* to the -OMe group of **93b**.

Analysis of the crude products by ^{19}F NMR and GC-MS showed that none of the diketones underwent aromatic fluorination prior to enol fluorination as no aryl-F was formed before CF_2. The reactive nature of F_2 means that even though fluorination at C**2** is favoured, aromatic fluorination will still occur if the aryl rings are sufficiently activated.

Products **91c-91h** containing electron withdrawing groups were isolated in moderate to good yields because these substituents helped prevent unwanted aromatic fluorination by deactivating the phenyl rings. Products **91f-91h** containing two electron withdrawing groups lowered the nucleophilicity at C**2** to such an extent that

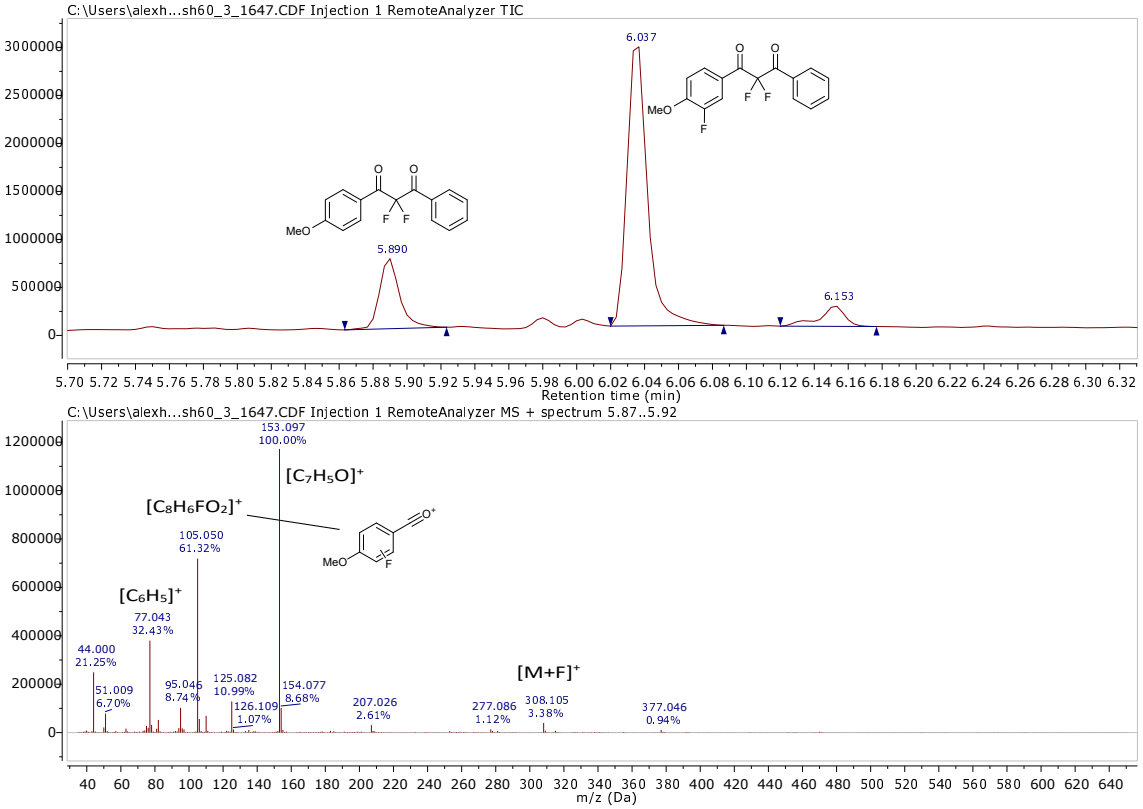

Figure 2.10: GC-MS of the product mixture after fluorination of 1-(4-methoxyphenyl)-3-phenylpropane-1,3-dione

the reaction was slowed enough that almost no aromatic fluorination occurred. The crude products were isolated as solids in over 90% conversion before purification by recrystallisation. This sharply contrasts with products **93** and **93c**–**e** which were initially isolated as oils requiring column chromatography to fully purify.

All of the products decomposed slightly on silica as the addition of two fluorine atoms α- to a carbonyl increase the electrophilicity of C**1**.[37] Product **91e** decomposed significantly on silica, with the formation of signals in the ^{19}F NMR spectra consistent with a CF_2H moiety indicating that debenzoylation has occurred. These signals were not present in the crude product mixture. In the presence of a base, nearly all products **91**-**91h** are susceptible to undergo a debenzoylation reaction.[130] It is currently unknown why this side reaction has occurred significantly more in the case of **91e** compared to the isolation of other difluoro products, in particular the isolation of **184** which contains two $-NO_2$ groups.

The molecular structures of **93c**,**e**–**h** as determined by XRC are noticeably different to the non-fluorinated starting materials (Figure 2.11). While the non-fluorinated

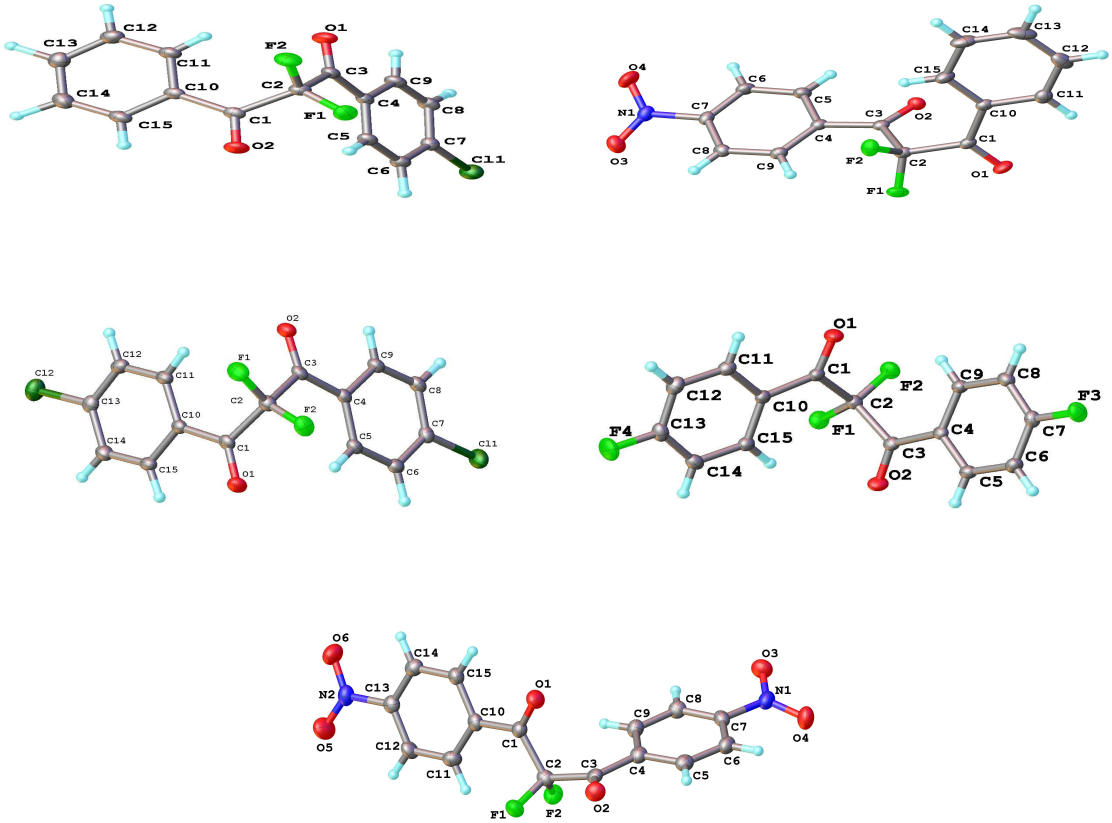

Figure 2.11: Molecular structure of **93c**, **184**, **185**, **186** and **187** as determined by XRC

derivatives exist in the *enol* form with the two aryl rings and dicarbonyl moiety mostly in the same plane due to stabilising intra molecular hydrogen bonding, there is significant rotation seen in the difluorinated derivatives. These all exist in the keto form, with the dicarbonyl moiety rotated to maximise the distances between the lone pairs of the electron-rich fluorine and oxygen atoms. Usually one of the fluorine atoms lies in a *syn* orientation to one of the oxygens (eg. **93e** has a F-C-C-O dihedral angle of 15.6°) creating a dipole. This dipole appears to aid in crystal packing by forming weak intermolecular interactions with an aryl ring in an adjacent molecule (Figure 2.12). The two aryl rings are rotated so that they are no longer in the same plane to create an additional orthogonal π-stacking interaction. Similar π-stacking interactions were seen in the non fluorinated derivatives, but as compounds were mostly planar, formed repeating layers of overlapping molecules.

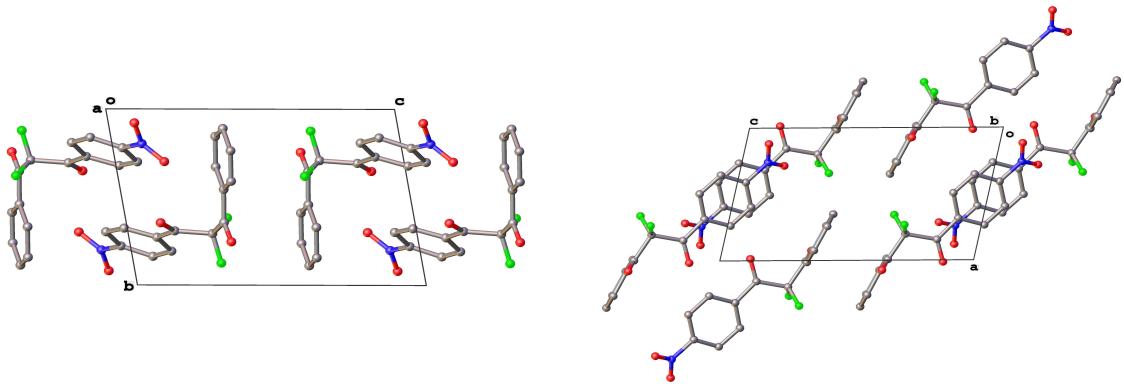

Figure 2.12: Crystal packing structures of **93e** as determined by XRC

2.5 Mechanism of Fluorination

The exact mechanism of direct fluorination, either electrophilic or radical, has been a subject of debate and depends on both the substrate and solvent. Many of the earliest reported direct fluorinations are proposed to occur via a free radical mechanism using $F^{\bullet}$, though due to the low dissociation of F_2 (<1% at rt and atmospheric pressure) Miller theorised an initiation step utilising a C−H containing molecule to generate $F^{\bullet}$ and $R^{\bullet}$.[131–134] In general, radical fluorinations require higher temperatures and usually result in perfluorination.

An electrophilic mechanism was suggested in previous attempts at direct fluorinations of 1,3-dicarbonyl substrates.[106] Formic acid was used as the solvent which would increase the susceptibility of F_2 towards nucleophilic attack. The rate of fluorination is dependant on the rate of enolisation, with fluorination occuring at either the C**1**- or C**3**- position depending on which enol is formed. Further fluorination at the **3**- position to yield the difluoro product is possible, but occurs much slower due to the lower rate of enolisation compared to the non fluorinated parent compound (Scheme 2.9). Chambers *et al.* hypothesised that a comparison of the product profiles produced by fluorination of a substrate with electrophilic fluorinating agents and by direct fluorination could provide further insight into the mechanism.[100] The similar products seen when F_2 and Selectfluor™ were used help support our conclusion that our base mediated direct fluorinations of 1,3-dicarbonyl substrates described above are occurring via an electrophilic mechanism, rather than a single electron transfer (SET) reaction.

Previous work by Rozatian *et al.* have shown that DBM and its derivatives react via the *enol* tautomer with electrophilic fluorinating agents, and that bases cata-

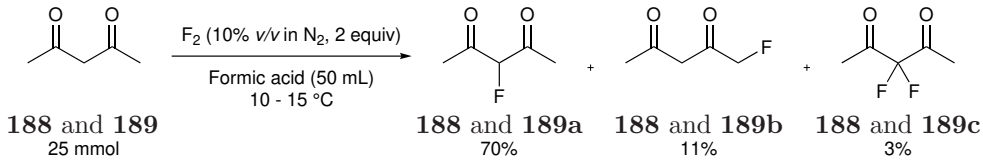

Scheme 2.9: Previous work on the direct fluorination of 1,3-dicarbonyls[106]

lyse tautomerism to the enol form.[123] A quantitive reactivity scale for commercially available electrophilic fluorinating agents based on kinetics studies of the monofluorination of **91** and several derivatives was developed. Importantly, it was confirmed that electrophilic fluorinating agents react in a similar mechanism to an S_N2 reaction utilising "F^+". Consequently, we presume that the base mediated direct fluorination occurs in an electrophilic process with the *enol* tautomer in a similar method to Selectfluor™ .

Keto–enol tautomer studies have shown that DBM exists nearly entirely (92%) in the enol form in MeCN.[135] The two tautomers can be identified by characteristic shifts in the ^{1}H NMR spectrum, with a peak at 4.6 ppm relating to the keto and at 6.9 ppm relating to the enol form. The enol form is strongly favoured due to the formation of an intramolecular hydrogen bond between the two carbonyls. Unlike the starting material, the monofluorinated intermediate exits in the ketone form as fluorine prefers to be sp^3 hybridised compared to sp^2, as shown by a doublet in the ^{1}H NMR spectrum at 6.5 ppm, and confirmed by XRC (Figure 2.13).

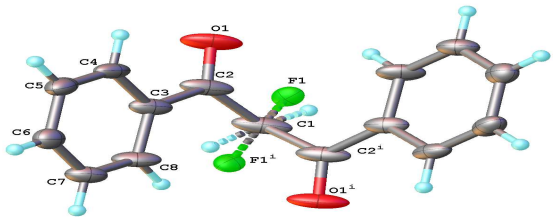

Figure 2.13: Molecular structure of 2-fluoro-1,3-diphenylpropane-1,3-dione (**92**) as confirmed by X-ray crystallography

Thus, fluorination of diketones by F_2, *N*–F or any other electrophilic fluorinating agent occurs by reaction with the enol form only. Similarly, reaction of 2-fluoro diketones occurs via the fluorination of the enol form and the rate determining step for the second difluorination is the tautomerisation of the mono-fluoro ketone form to the enol.[124] Monofluoro diketones exist predominantly in the keto form.

Dolbier determined that a single fluorine is thermodynamically more stable at an sp^2 carbon compared to an sp^3 carbon in monofluoropropenes. Purrington *et al.* investigated the position of keto–enol equilibria in α-fluoro-β-diketones and found that in general, acylic variants display the keto form while cyclic variants display the enol form.[105,136] However, it was determined that **92** has a pK_a two units less than **91** in absolute ethanol. This implies that the fluorine increases the stability of **92-enolate**, which conflicts with their conclusion that fluorine destabilises **92-enol** relative to **92-keto**.

Purrington proposes that as the enolate cannot form the intramolecular hydrogen bonded enol, the molecule rotates around the C**1**-C**3** bond to maximise the distance between the two partially charged oxygen atoms (Scheme 2.10). In this orientation there is a favourable secondary orbital interaction between one of the oxygen atoms and the fluorine that helps to reduce the unfavourable HOMO-HOMO interaction between the fluorine and the extended β-diketone framework that is isoelectronic with a pentadienyl anion. This favourable interaction, along with the inductive effect of fluorine, explains why the **92-enolate** is more acidic than **91-enolate**.

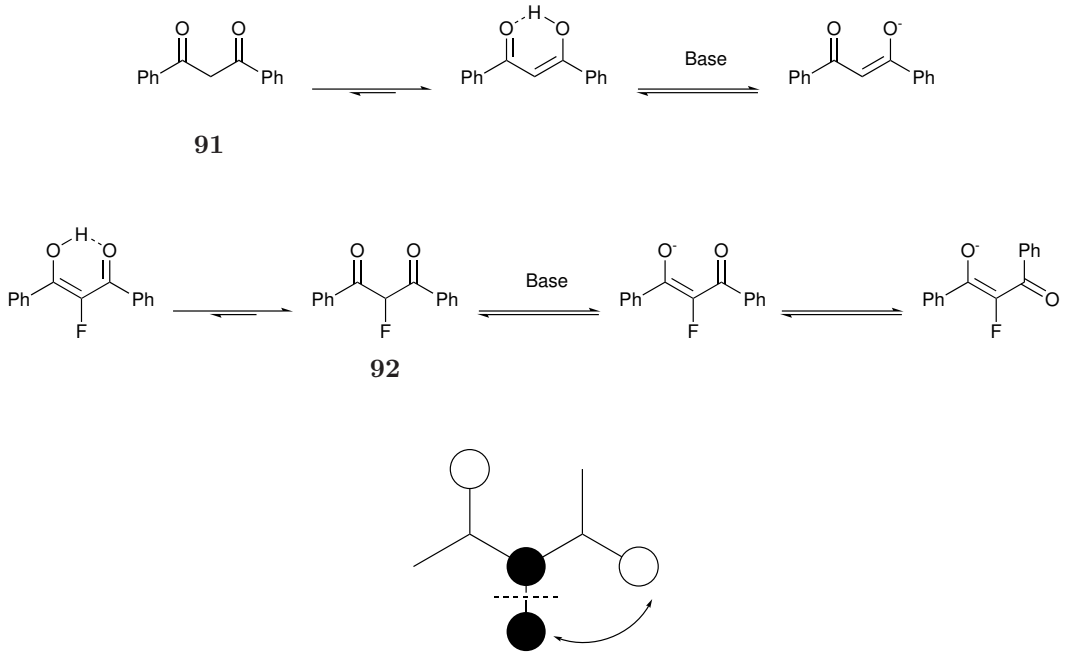

Scheme 2.10: Proposed conformation of the enolate form of 2-fluoro-1,3-diphenylpropane-1,3-dione in solution[105]

When a sample of **92** was isolated by column chromatography, recrystallisation from hexane and analysis by XRC confirmed that **92** exists in the rotated keto conformer in the solid state originally proposed by Purrington (Figure 2.13). It is unknown

whether upon protonation there is a significant barrier to rotation to reform the original orientation in the solution phase, or if this form is only thermodynamically stable in the solid phase.

Consequently, we could propose that the role of the quinuclidine is to catalyse the tautomerism of the keto form of the monofluoro diketone intermediate to the corresponding enol form.

At first glance, we may expect a base such as quinuclidine to deprotonate the **keto-92** to give the enolate (Scheme 2.11). However, neither DABCO (pK_{aH}(MeCN) = 18.29), quinuclidine (pK_{aH}(MeCN) = 19.5) or Et_3N (pK_{aH}(MeCN) = 18.46) are strong enough bases to deprotonate **91-keto** (estimated pK_{aH}(MeCN) = pK_{aH}(DMSO) + 12.9 = 13.4 + 12.9 = 26.3).[137–139] Consequently, the simple mechanism of quinuclidine acting as a base for deprotonation is unlikely (Scheme 2.11).

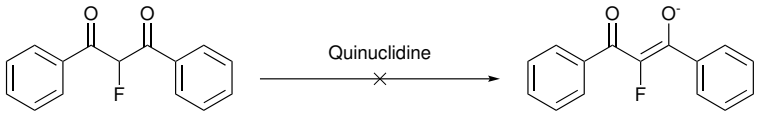

92

Scheme 2.11: Proposed deprotonation of 2-fluoro-1,3-diphenylpropane-1,3-dione by quinuclidine

Quinuclidine gave the best conversion of **91** to **93** upon fluorination with F_2, and so it is clear that it plays an important role in the mechanism. Alternatively, an *in situ* *N*–F electrophilic fluorinating agent might be formed between quinuclidine and fluorine, which is then selectively fluorinating **91** (Scheme 2.12).

Since Selectfluor™ is synthesised by directly fluorinating **178b** in the presence of sodium tetrafluoroborate ($NaBF_4$) (Scheme 2.2), a similar reaction was attempted with DABCO to see if a stable N–F reagent similar to Selectfluor™ could be formed *in situ*.

A solution of DABCO in MeCN reacted with 1 equiv. of F_2 in order to determine if a stable *in situ* intermediate between DABCO and F_2 was formed. After purging, 1 equiv. of DBM was added, but after 30 min stirring, no fluorination of DBM was identified by ^{19}F NMR spectroscopy.

To test the possibility that *N*-fluoroquinuclidinium fluoride (**191**) is formed *in situ*, *N*-fluoroquinuclidinium triflate (**192**) was synthesised following a literature procedure (Scheme 2.14) and then reacted with **91**. These *N*-fluoroquinuclidinium salts

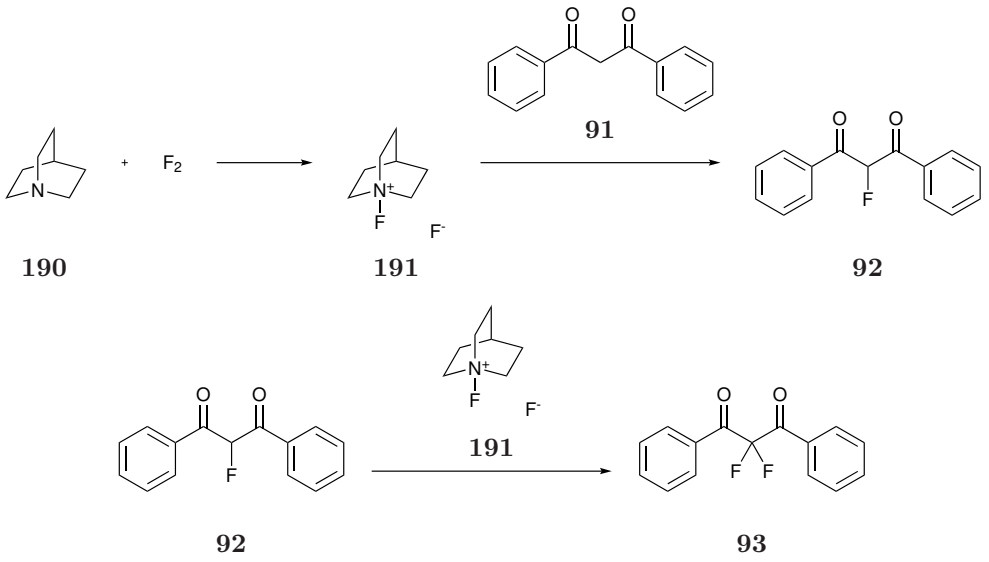

Scheme 2.12: Quinuclidine forming an *in situ* fluorinating agent that fluorinates 1,3-diphenylpropane-1,3-dione

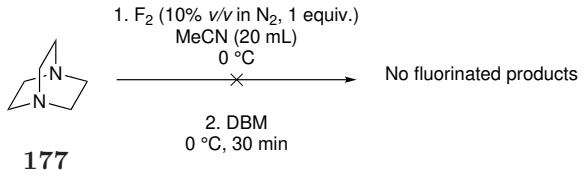

Scheme 2.13: Attempts to fluorinate DABCO to develop an *in situ* fluorinating agent

appear to be milder fluorinating agents than Selectfluor™ (**66**) as shown by their lower reactivity with similar substrates, and the reported quantitative "F^+" transfer from **66** to quinuclidine upon mixing at r.t.[140–145] **192** appears to have the same reactivity as **191**, but is more soluble in a range of solvents including MeCN, and is not nearly as hygroscopic—**191** requires handling in a glovebox. Sharif gave no prediction on whether the N-fluoroquinuclidinium salts fluorinate via an S_N2 or SET pathway, but the similar N^+-F bond lengths in **192** (1.407(6) Å) to **66** (1.37(2) Å) indicate a similar bond strength which could result in a transfer of F^+ by the same mechanism.[146]

DBM was reacted with an equivalent of **192** in CD_3CN in an NMR tube kept at 25 °C to monitor the rate of conversion. After 144 h there was 12% conversion to the monofluorinated product by ^1H NMR spectroscopy but none of the difluorinated product. This is a lower conversion than that seen with **66** as expected. The reaction was repeated on a larger scale with varying amounts of **192** and quinuclidine

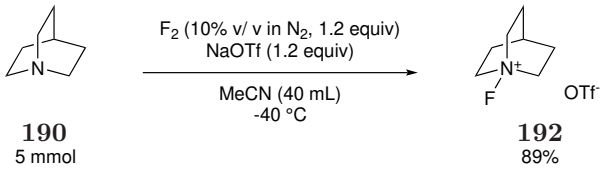

190
5 mmol

192
89%

Scheme 2.14: Synthesis of *N*-fluoroquinuclidinium triflate (**192**) based on a literature procedure

(Table 2.5). After stirring for 72 h at 60°C, the solvent was removed, and yields calculated by comparison of the integral values against a known amount of α,α,α,-trifluorotoluene (Table 2.5).

Table 2.5: Fluorination of DBM with *N*-fluoroquinuclidinium triflate

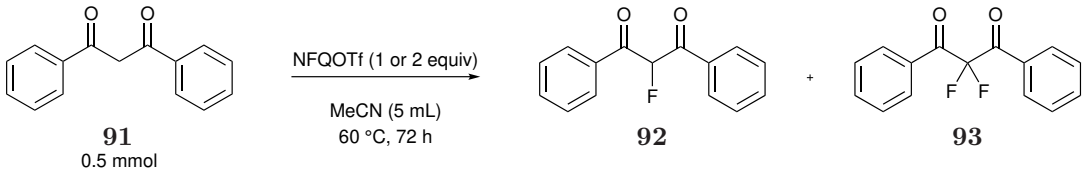

91
0.5 mmol

92

93

Entry	Equiv of NFQOTf	Conversion by NMR/%		
		91	**92**	**93**
1	1	43	21	4
1	2	45	33	6

2.5.0.1 PK_a Analysis

Unfortunately, a comparison of the pK_as in MeCN of the mediating agents shows no real correlation between basicity and conversion to the difluoro product. Conversion to the monofluorinated product was higher when Et_3N was used despite having a similar pK_a to DABCO (Table 2.1, Entry 11). DABCO and quinuclidine are more nucleophilic than Et_3N due to steric reasons which may help interactions with DBM or F_2, increasing the observed rate constant.

Table 2.6: pK_a of the mediating agents in H_2O and MeCN with their effect on the fluorination of DBM

Base	pKa		NMR yield/%	
	H_2O	MeCN	**92**	**93**
DABCO-H_2^{+2}	3.0, 8.8	18.3	4	20(7)
Quinuclidine-H^+	11.0	19.5	10(8)*	43(33)*
Et_3N-H^+	10.8	18.5	25	6
Cs_2CO_3	6.4, 10.3		4	14
NaCl	-7	10.3	33	12(6)*

* Isolated yield

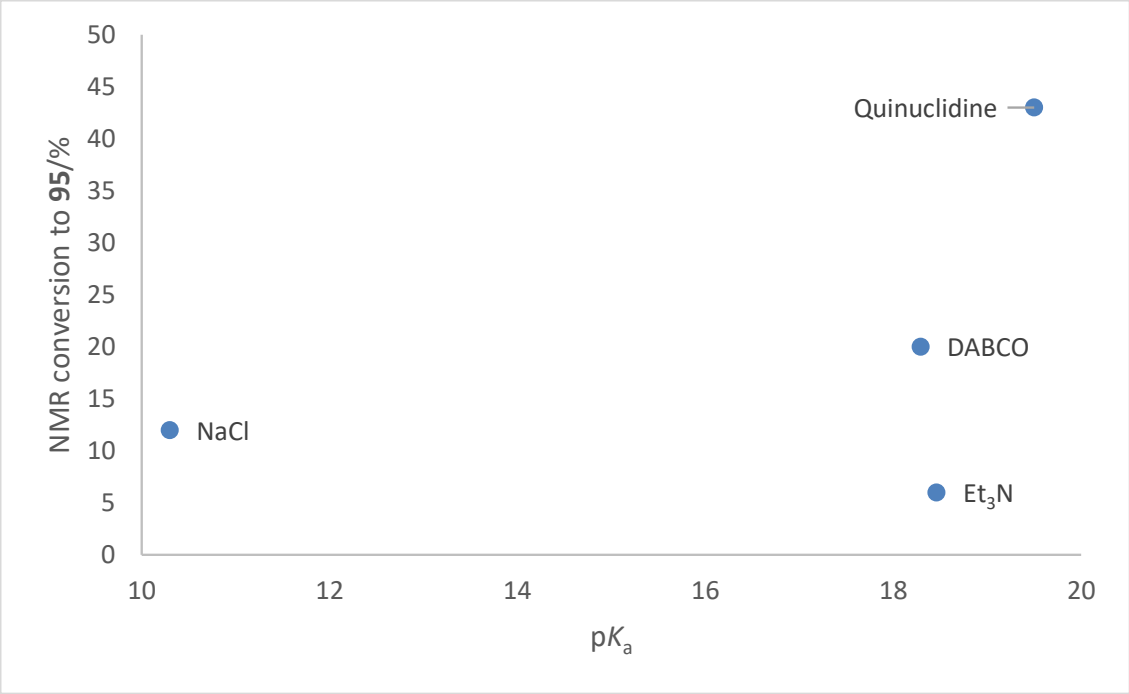

In the case of Cs_2CO_3 (Table 2.1, Entry 12), the lower pK_a is unlikely to deprotonate **92**, and so we propose that the carbonate reacts with any HF present that is produced as a by-product from fluorination.

In (Table 2.6, Entry 5) NaCl is not nearly basic enough to deprotonate the enol form of the starting material. Instead, it is hypothesised that the salt is interacting with F_2 to generate small amounts of ClF and F^- which is then reacting with the enol forms of **91** and **92**.

The lower conversion when Et_3N is used compared to DABCO, despite their similar pK_as in MeCN, indicates that the selectivity is not entirely due to the base strength. Deprotonation of either the starting material or the monofluorinated product gives the corresponding enolate which then reacts with F_2. Quinuclidine gave an NMR yield of the difluoro product **93** that was 7 times higher than when Et_3N was used, far more than expected given the pK_a difference of 1, and thus implies that quinuclidine is also interacting with fluorine.

2.5.0.2 N-F Compound

The nitrogen of quinuclidine could, in principle, interact with fluorine to form either a discrete N-F^+ bond or some form of associated amine-fluorine compound. Alternatively, the nitrogen could be protonated and fluorine interacting with this quinuclidinium-H^+. (Figure 2.14).

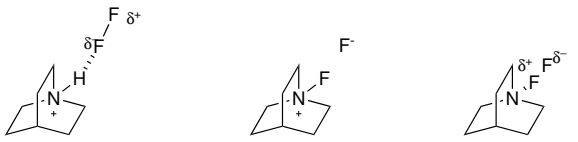

193 **191** **194**

Figure 2.14: Possible N-F fluorinating reagents generated *in situ* in a quinuclidine mediated direct fluorination

2.5.0.3 Reactions of 2-Fluoro-1,3-diphenylpropane-1,3-dione with Quinuclidine

To investigate potential interactions between **92** and quinuclidine, equivalent amounts were dissolved in CD_3CN in an NMR tube kept at 25 °C. This proton integral initially rapidly decreased, but then slowly increased over the next several days (Figure 2.15).

As soon as the quinuclidine was added to **92** in the CD_3CN the solution turned more yellow. Analysis by ^{19}F NMR immediately after this addition showed a significant number of peaks corresponding to aromatic fluorination. A new doublet at −190 ppm had appeared indicating that some of **92** has undergone an unwanted fluorination on the aromatic ring (Figure 2.16).

It appears that **92** is unstable in the presence of quinuclidine, and so it is possible that some of the aromatically fluorinated products may not be entirely due to an unselective direct fluorination of **91**, but are products of a competing unwanted

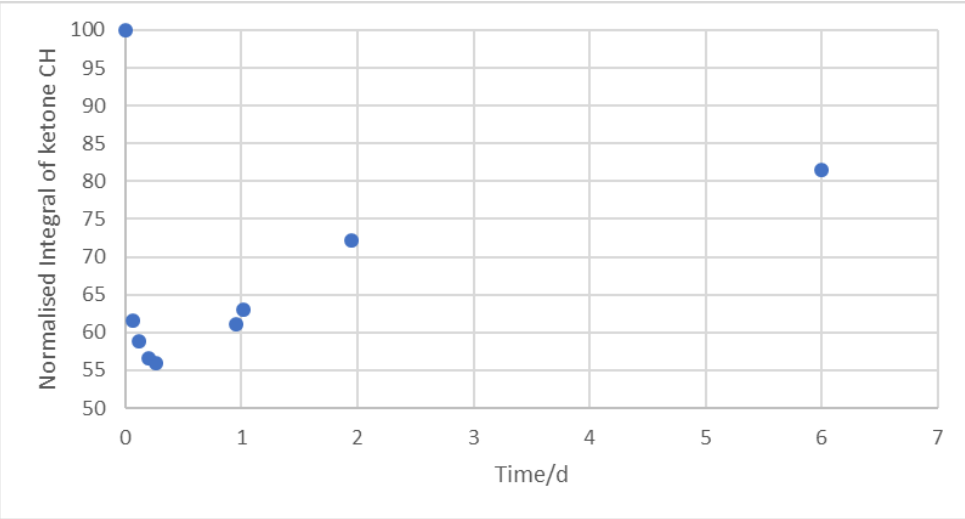

Figure 2.15: Change in intensity of the C**2**H peak in the keto form of 2-fluoro-1,3-diphenylpropane-1,3-dione in the ^{1}H NMR spectrum after an equivalent of quinuclidine was added

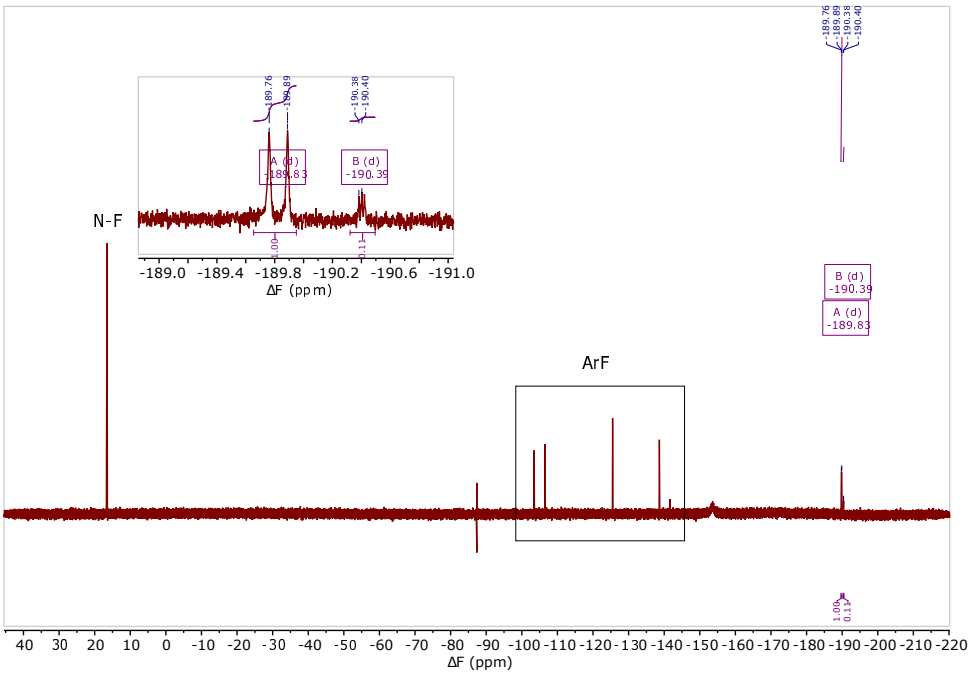

Figure 2.16: ^{19}F NMR spectrum of 2-fluoro-1,3-diphenylpropane-1,3-dione in CD_3CN minutes after the addition of an equivalent of quinuclidine

reaction pathway (Scheme 2.15). This is supported by the relatively minimal amount of ring fluorinated products detected by ^{19}F NMR spectroscopy when quinuclidine was initially screened as a base.

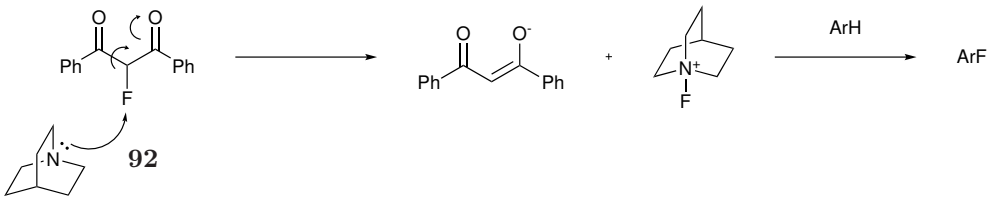

Scheme 2.15: Unwanted defluorination of 2-fluoro-1,3-diphenylpropane-1,3-dione by quinuclidine leading to the *in situ* generation of an N–F^+ reagent that performed unselective ring fluorination

2.5.1 Quinuclidinium–F_2 Interaction

Due to the experimental setup requiring purging the apparatus with nitrogen before the introduction of fluorine, quinuclidine is added to a solution of DBM in MeCN at r.t. Upon mixing, the solution appears to turn slightly more yellow coloured, which could be indicative of a deprotonation occuring. It is likely that a significant proportion of the **91-enol** is deprotonated prior to fluorination which would allow for the formation of **193** as a potential fluorinating agent.

Given the observations above, a mechanism for the quinuclidine mediated direct fluorination of DBM with F_2 is proposed in Scheme 2.17. **91** is deprotonated by quinuclidine prior to the addition of fluorine, and it is proposed that the fluorinating agent is generated *in situ* by the interaction of fluorine with this protonated base **193**. This will act as an electrophilic fluorinating agent and fluorinate **91-enol** to give **92**. A rotation and deprotonation will occur to give **92-enolate** in the orientation proposed by by Purrington with the two oxygen atoms far apart.

Since reaction between *N*-fluoroquinuclidinium triflate **192** and diketones such as DBM only proceed at elevated temperatures (Table 2.5), fluorination of DBM with **192** in a similar mechanism to Selectfluor™ is probably not occuring.

It is well established that in the reaction of fluorine with nitrogen bases such as DABCO derivatives, that a $R_3N^+F\cdots F^-$ salt is formed which can be transformed to $R_3N^+F\cdots BF_4^-$ upon addition of sodium tetrafluoroborate.[126] Consequentially, the reaction of quinuclidine with F_2 is most likely to form *N*-fluoroquinuclidinium fluoride **191** *in situ*.[142,147]

Fluoride ion is a very strong base, especially when formed *in situ* in anhydrous conditions. Since the pK_a(MeCN) of HF is ∼25.2 and the pK_a(MeCN) of DBM-keto **91** is ∼26.3, F^- could be sufficiently basic to deprotonate the enol form of DBM as this would have a slightly lower pK_a(MeCN). Additionally, F^- would be strong

enough to deprotonate the keto form of 2-fluoro-1,3-diphenylpropane-1,3-dione to give the enolate. The enolate is highly reactive towards electrophiles and can be fluorinated by R_3N^+-F or $[R_3NH-F_2]^+$ in solution. A proposed mechanism is as follows (Scheme 2.16).

Clearly, there is an unusually beneficial effect of quinuclidine compared to other bases. The reaction with fluorine to give a $R_3N^+F\cdots F^-$ intermediate, transfer of fluoride to deprotonate the keto form and any subsequent reaction of enolates with R_3N^+-F or $[R_3NH-F_2]^+$ all contribute to the efficient difluorination process.

The increased acidity of the **92** compared to **91** will ensure that in the presence of F^- or other bases, **92** is preferentially deprotonated to **91**, and hence reacts with fluorine preferentially. This explains the observed preferential selectivity for **93** as the major product. While the introduction of fluorine usually inhibits further fluorination at the same site due to electronegativity, in this case the increased acidity due to the introduction of a single fluorine leads to increased conversion to the difluoro product.

Additionally, quinuclidine appears to be able to react with **92** and possibly **93** (Scheme 2.18). As the reaction proceeds the ratio of C**2**H to C**2**F decreases, and so it becomes increasingly likely that quinuclidine could come into contact with a C**2**F. In this case, a side reaction appears to occur that leads to unwanted ring fluorination reactions.

When electron withdrawing groups are added to the aromatic ring, limited amounts of unwanted ring fluorinated products are produced. These groups appear to lower the electron density in the ring, deactivating them to ring fluorination by any *in situ* generated fluorinating agents. The similar isolated yields of **93** with an electron-withdrawing group (EWG) present on both rings (**91f**, **184** and **187**) show that it is not dependent on which EWG is added.

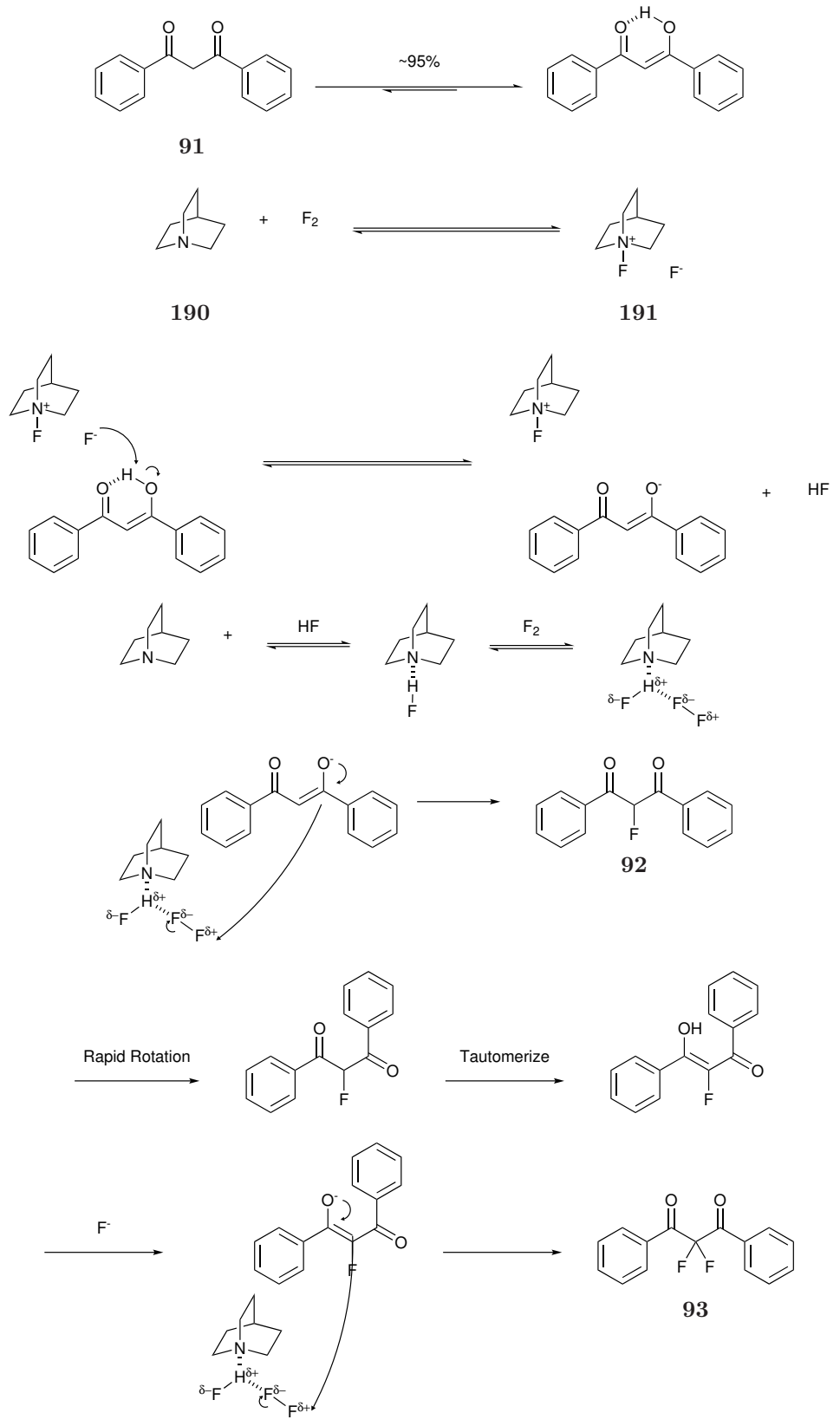

Scheme 2.16: Proposed mechanism of the quinuclidine mediated direct fluorination of DBM

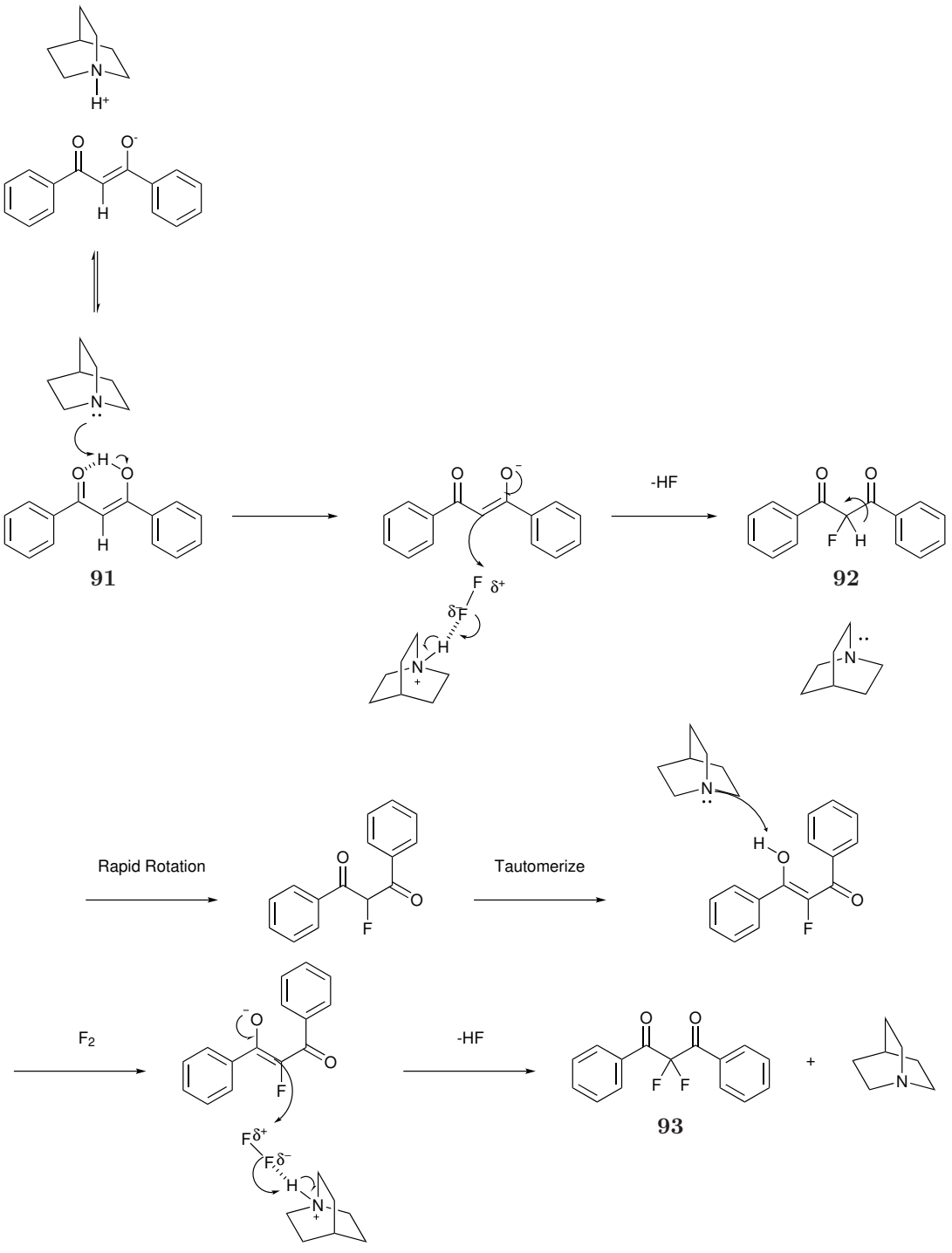

Scheme 2.17: Proposed mechanism of the quinuclidine mediated direct fluorination of DBM

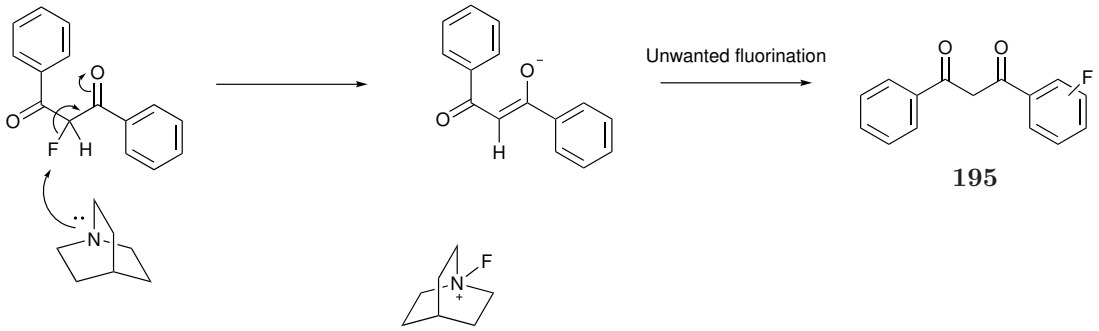

Scheme 2.18: Proposed side reaction between 2-fluoro-1,3-diphenylpropane-1,3-dione and quinuclidine to give unwanted ring fluorinated products

2.6 Difluorination of 1,3-Diester Derivatives

2.6.1 Introduction

Given previous Durham research synthesising diethyl 2-fluoromalonate **152** using F_2, we attempted to develop a route to difluorinated malonates from dimethyl malonate **196**. Dibenzoyl malonate **199** was also trialled as a model diester system as it has structural similarities to **91**, and so may be difluorinated with similar reactivity and selectivity.

2.6.2 Fluorination of Dimethyl Malonate

Quinuclidine mediated direct fluorination of dimethyl malonate **196** was trialled using conditions optimised for the difluorination of **91** (Scheme 2.19).

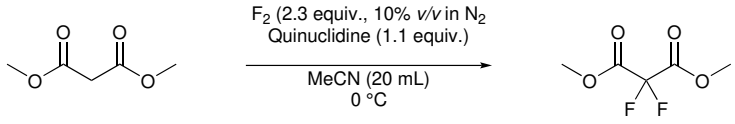

196 **198**

Scheme 2.19: Quinuclidine mediated direct fluorination of dimethyl malonate using conditions optimised for DBM

A sample of the reaction mixture was added to a mixture of 1 mL $CDCl_3$ and 1 mL H_2O and shaken. The organic phase was extracted for NMR analysis, and showed a 23:1 ratio of the difluoro product **198** to the monofluoro product **197** (Figure 2.17). The reaction mixture was concentrated, diluted with H_2O and the organic products extracted with EtOAc. It appears that significant amounts of defluorination and hydrolysis has occurred during the aqueous workup as shown by the significant increase in the proportion of **197**, and the presence of two CF_2 containing products—the desired **198** and an acid produced by hydrolysis of **198**. The two ester groups become highly activated to nucleophilic attack after difluorination has occurred, which can lead to this unwanted hydrolysis and the possible formation of hydrate products.

2.6.3 Fluorination of Dibenzoyl Malonate

Upon fluorination of dibenzoyl malonate **199**, good selectivity (5:1) for the difluoro product **201** over the monofluoro product **200** was detected in the ^{19}F NMR spectra

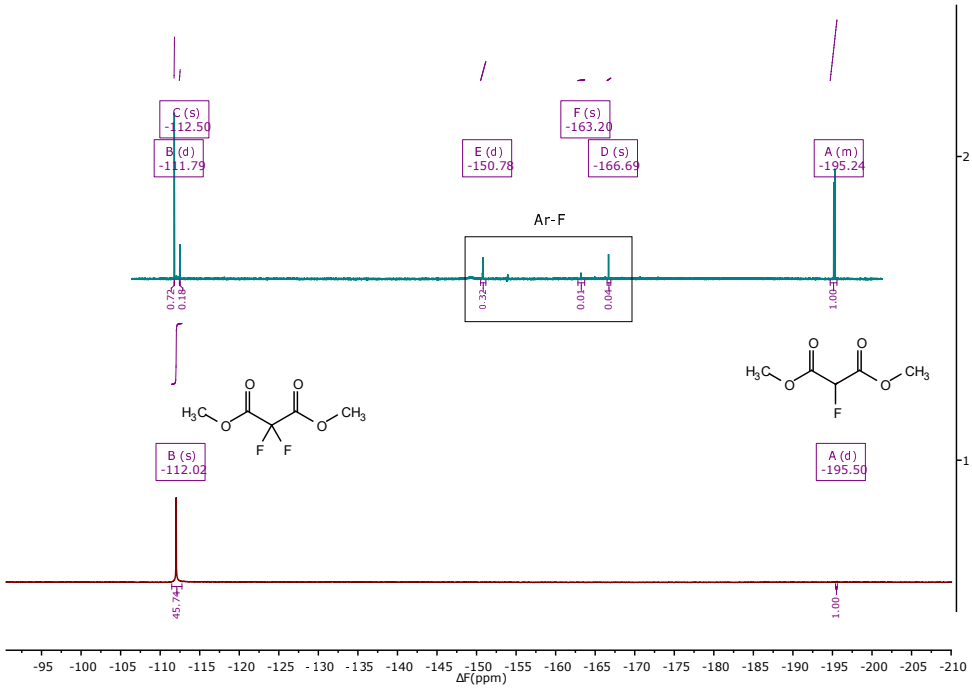

Figure 2.17: ^{19}F NMR spectra of the reaction mixture (bottom) and the crude product after an aqueous workup (top)

of the crude product after filtering through a short silica plug to remove any excess HF or protonated quinuclidine. (Figure 2.18). Significant amounts of ring fluorination appears to have occurred as can be determined by the peaks around −113–−117 ppm. This can be rationalised as the –CH_2OCOR is more electron donating than the –COR found in **91** and, hence, activates the ring towards ring fluorination.

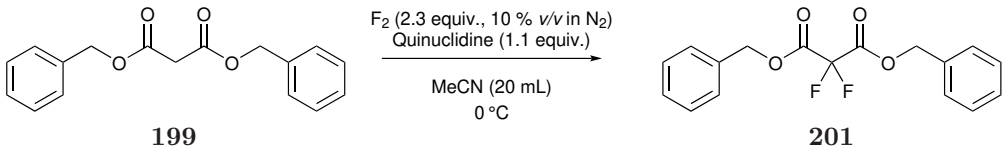

199 **201**

Scheme 2.20: Quinuclidine mediated direct fluorination of dibenzyl malonate using conditions optimised for DBM

The fluorination was repeated using 1.5 equiv. of quinuclidine and 4.0 equiv. of 10% *v/v* F_2 in N_2 at an increased flow rate of 30 mL min^{-1} in 40 mL MeCN. We proposed that increasing the equivalents of reactants would increase the conversion to **201**, and the increased flow rate would limit the reaction time and thus help prevent unwanted further ring fluorinations from occurring. After fluorination, the majority of the solvent was removed under reduced pressure, and the resulting orange solution passed through a silica plug with $CHCl_3$ as the eluent to remove any protonated

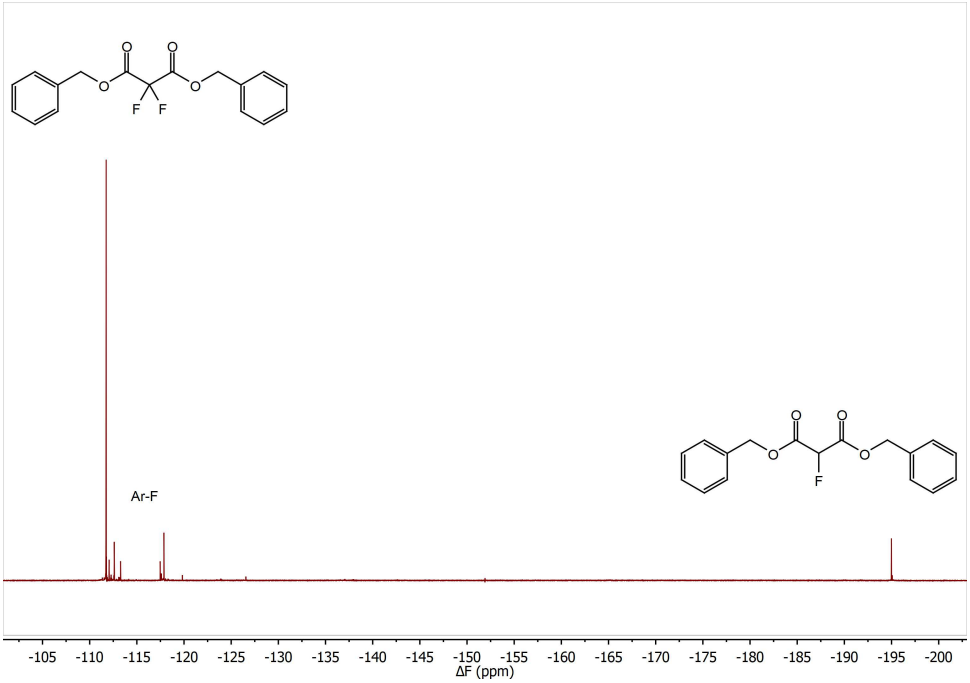

Figure 2.18: ^{19}F NMR spectrum of the crude product mixture of the quinuclidine mediated direct fluorination of dibenzoyl malonate

quinuclidine or polyfluorinated tar. Removal of the solvent gave a clear yellow oil that contained a mixture of **201** and **200** in a 3:1 ratio.

Attempts to isolate the desired product **201** by Kugelröhr distillation, column chromatography with both hexane and DCM (1:1), and 15% EtOAc *v/v* in hexane mixtures as the eluents, all proved unsuccessful at removing the unwanted ring fluorinated products. It was theorised that an acid-base extraction at various pH would allow for the selective separation of any unreacted starting material **199** and any of the monofluorinated intermediate **200** by utilising the effect of fluorine substitution on the pK_{a}. This also proved unsuccessful.

While these experiments have shown that 2,2-difluoro-1,3-diesters can be synthesised using base mediated direct fluorination strategies with high selectivity over the 2-fluoro product, the increased reactivity of the carbonyl groups adjacent to the CF_2 group caused significant problems with isolating the desired product and no further attempts to isolate **198** or **201** were made at this stage of the project.

2.7 Conclusion

Selective difluorinations using F_2 was investigated. While F_2 does not react significantly with the 1,3-diketone DBM in MeCN, fluorination to give the 2,2-difluoro product could be achieved by mediation with one of several nitrogen bases. Of these, quinuclidine performed the best, giving high selectivity for the 2,2-difluoro product over the 2-fluoro product and minimising unwanted aromatic fluorinations. A range of DBM derivatives were synthesised following a literature procedure and fluorinated using optimised conditions to develop several new 2,2-difluoro-1,3-diketone products.

This appears to be the first general case of F_2 being used to selectively introduce a *gem*-difluoro group, and a mechanism for this has been proposed. We believe that quinuclidine reacts with F_2 producing F^- which deprotonates **91-enol** and **92**. These reactive enolates then react with an electrophilic sources of fluorine, either R_3N^+-F, or $[R_3NH-F_2]^+$ that are formed *in situ*.

Chapter 3

Synthesis of 2,2-Difluoro-β-ketoesters

3.1 Aim and Approach

In the previous chapter 1,3-diketones and 1,3-diesters were successfully selectively fluorinated with F_2 to give the corresponding α,α-difluoro products. While monofluorination of 1,3-ketoesters in acidic solvents has been used to create products that have seen use industrially, such as in the synthesis of the antifungal Voriconazole **164**, there appears to be very little literature on the fluorination of 1,3-ketoesters in non-acidic solvents, or the synthesises of the corresponding difluoro products. It has been determined experimentally that BKEs are much less reactive to difluorination using a range of electrophilic fluorinating agents or F_2 than related 1,3-diketones, and selective difluorination using F_2 has not been previously reported. Previous attempts at fluorinating ethyl acetoacetate with F_2 gave less than 1% of the desired difluoro product by ^{19}F NMR spectroscopy.[106]

There are very few AIs that are synthesised using α,α-difluoro-β-ketoesters (difluoro-BKEs). We propose that the current limitations in synthesising this class of compounds has resulted in a lack of available FBBs for agrochemical and pharmaceutical companies to use to develop new AIs. It would, therefore, be of significant interest to develop cheap and scalable synthetic strategies to difluoro-BKEs, as these could potentially be highly desired FBBs for the synthesis of more complex fluorinated systems.

3.2 Fluorination of β-Ketoesters

While 1,3-diesters have previously successfully been fluorinated with F_2 to give the chemoselective α,α-difluoro product, the introduction of a $>CF_2$ group activates the carbonyl groups leading to hydrolysis and decomposition during aqueous workups and purification by column chromatography on silica gel. We theorised that the replacement of one of the ester groups with a ketone group would increase the stability of the corresponding difluoro compound and allow for isolation of the desired product.

3.2.1 Base Mediated Direct Fluorination of Ethyl Benzoylacetate

Readily available ethyl benzoylacetate **94** was used as a model system for the development of conditions for selective 2,2-difluorinations. In an initial experiment to isolate a pure sample for reference purposes, **94** was fluorinated using similar conditions that were developed for the difluorination of **91** and its derivatives (Scheme 3.1) and we hoped that quinuclidine would show a similar selectivity for the difluoro product **96** over the monofluoro product **95**.

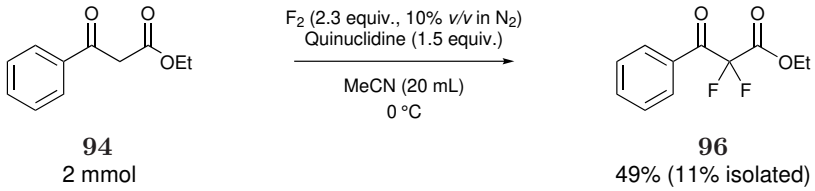

94
2 mmol

96
49% (11% isolated)

Scheme 3.1: Quinuclidine mediated direct fluorination of ethyl benzoylacetate using conditions optimised for DBM

In an attempt to limit decomposition by purification via column chromatography using silica gel, the product was isolated by vacuum distillation using Kugelröhr distillation. The introduction of the two fluorine atoms is predicted to lower the boiling point significantly, which could allow for the easy separation from any unreacted starting material. A significant amount of material thermally decomposed resulting in the low (11%) isolated yield by mass recovery.

While the reaction did not produce significant amounts of tar, the low crude yield (49%) was explained by significant amounts of hydrolysis occurring during the aqueous work-up prior to distillation. Reextraction of the aqueous phase several times with $CHCl_3$ gave 0.119 g of a beige coloured solid. Analysis by ^{19}F NMR

spectroscopy showed a second peak at −106.9 ppm corresponding to a different CF_2-containing compound **202**. We suggest that this is the difluoro acid produced by hydrolysis of **96** — the lack of signals corresponding to the ethyl ester group in the ^{1}H NMR spectrum support this. There are also signals corresponding to a product containing a CF_2H group(**203**) which highlights the increased reactivity of carbonyl groups α- to a CF_2 group.[37] There is a 2:1 ratio of resonances between **202** and **203**.

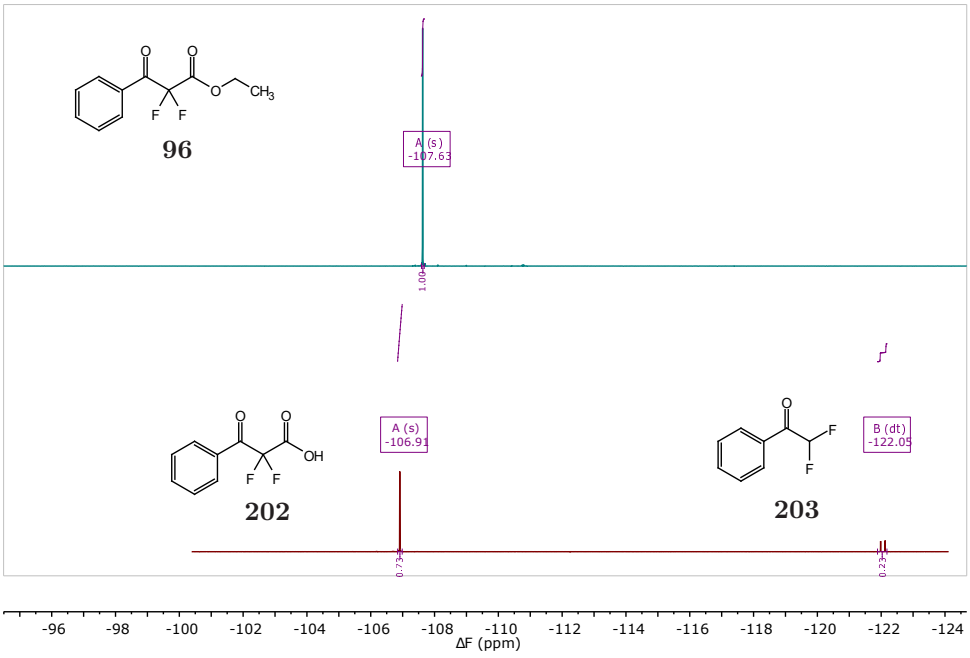

Figure 3.1: Top: ^{19}F NMR spectrum of **96**, Bottom: ^{19}F NMR spectrum of the beige coloured solid isolated after reextraction of the aqueous phase with $CHCl_3$ with proposed assignments

This initial experiment demonstrated the possibilities of using F_2 for the synthesis of difluoro-BKEs but the difficult purification stage requires some development.

3.2.1.1 Base Screening

Successful fluorination with quinuclidine indicated that selectivity for the difluoro product could be mediated with bases, but that aqueous workup and purification by distillation would not be appropriate methods of purifying the desired product. The fluorination was repeated with varying equivalents of several potential nitrogen bases. After purging the reaction vessel, the MeCN was removed under reduced pressure, and the crude tarry mixture was washed through a large silica plug with $CHCl_3$ as the eluent. No aqueous work-up was performed in order to limit the

amount of unwanted hydrolysis. We proposed that any remaining HF would react with the silica gel, possibly to form hexafluorosilicic acid $(H_3O)_2[SiF_6]$ which would be absorbed onto the silica (3.1). $CHCl_3$ was chosen as the eluent as its relatively high eluting power should limit the time organic material is exposed to silica while not dissolving any tar or amine residues.

$$SiO_2 + 6\,HF \longrightarrow (H_3O)_2[SiF_6] \tag{3.1}$$

After washing through the small scale silica plug, the products were analysed by ^{19}F NMR and yields of the fluorinated products **95** and **96** calculated by comparison of peak integrals to a α,α,α-trifluorotoluene reference.

As expected, the lack of mediating agent (Table 3.1, Entry 1) led to unselective fluorination, with the formation of several undesired fluorinated products including fluoroatomatic derivatives as observed by the ^{19}F spectrum. Comparisons of the ^{19}F NMR spectra of the base screenings are available in the Experimental section. DABCO was subsequently trialled as a mediating agent (Table 3.1, Entry 2). Conversion to the fluorinated products **95** and **96** was considerably lower with 1.1 equiv. of DABCO than conversion to the corresponding fluorinated diketones when DBM (**91**) was used as a starting material, and matches the differences in reactivity of diketones and BKEs.[106] The volume of solvent was increased to 40 mL from 20 mL (Table 3.1, Entry 3) to effectively double the path length that fluorine passes through before it leaves the solution but the conversion was significantly lower than when 20 mL of MeCN was used. To ensure that this was not due to the concentration of base and starting material decreasing by half, the experiment was repeated with double the equiv. of **94** and F_2 (Table 3.1, Entry 4) to maintain the same concentration of reactants as Entry 2. In both of these cases trace amounts of **95** and **96** were detected by ^{19}F NMR spectroscopy. Instead significant amounts of dark brown tar were formed. Increasing the amount of DABCO added (Table 3.1, Entries 4 and 5) also resulted in the formation of a large amount of tarry products, and so we concluded that while small amounts of DABCO and F_2 gave relative selectivity but low conversion, attempts to increase the conversion result in the formation of tar.

Table 3.1: Screening conditions for the base mediated difluorination of ethyl benzoylacetate

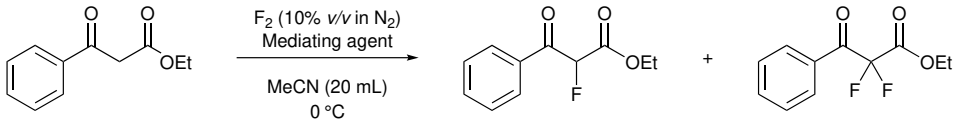

94 2 mmol | **95** | **96**

Entry	Base	Equiv. of Base	Equiv. of F_2	NMR yield/%	
				95	**96**
1	None	-	2.3	8	2
2	DABCO	1.1	2.3	16	10
3	DABCO[a]	1.1	2.3	1	1
4	DABCO[b]	1.1	2.3	0	0
5	DABCO	1.5	2.3	0	3
6	DABCO	1.5	4.0	0	1
7	DBU	0.5	2.3	12	6
8	DBU	1.5	2.3	18	3
9	Et_3N	1.1	2.3	11	1
10	3-Quinuclidinol[a]	1.1	2.3	0	1
11	Quinuclidine	1.1	2.3	0	42
12	Quinuclidine	1.1	3.5	6	41
13	Quinuclidine	1.1	3.0[c]	6	51
14	Quinuclidine	1.5	3.0[c]	0	73
15	Quinuclidine	1.5	3.0[c]	0	85[d]

[a] 40 mL MeCN used

[b] 40 mL MeCN, 4.0 mmol **94**, 2.3 equiv. F_2 and 1.1 equiv. DABCO used

[c] 30 mL min^{-1} flow rate of 10% *v/v* F_2 in N_2 used

[d] Isolated yield after 20 mL column

Attempts to mediate the selectivity with the strong base DBU (Table 3.1, Entries 7 and 8) showed limited conversion to products **95** and **96**. Increasing the equiv. of DBU decreased the amount of **96** produced as detected by NMR but resulted in the formation of large amounts of tarry by-products. Similar results were seen when Et_3N was used to mediate the selectivity, with **95** detected as the major desired

fluorinated product (Table 3.1, Entry 9). 3-Quinuclidinol has a similar structure to quinuclidine, but is significantly cheaper and less toxic. Fluorinations with 3-quinuclidinol as a mediating agent showed very limited conversion to desired fluorinated products (Table 3.1, Entry 10). Due to the low solubility of 3-quinuclidinol in MeCN, 40 mL of MeCN was used. A similar conversion to **96** was seen when 40 mL of MeCN was used with both DABCO and 3-quinuclidinol.

Similarly to the base mediated fluorination of DBM observed in Chapter 2, quinuclidine appeared to be the most effective base at increasing selectivity for the difluoro product **96**. Increasing the equivalents of F_2 to 3.0 equiv. with an increased flow rate of 30 mL min^{-1} and 1.5 equiv. of quinuclidine were found to be the optimum conditions for conversion to **96** (Table 3.1, Entry 14). Filtering the concentrated reaction mixture through a small column made out of silica in a 20 mL syringe with $CHCl_3$ as the eluent afforded the desired product **96** as a pale yellow oil in 85% isolated yield (Table 3.1, Entry 15). No further purification was required as the desired products were isolated in excellent purity (>95%). These fluorination conditions and method of purification was used to isolate products **96** and **96b–f** in good to excellent yields.

Figure 3.2: Small scale silia plug used to remove tar and HF without an aqueous workup to isolate compounds **96** and **96b–f**

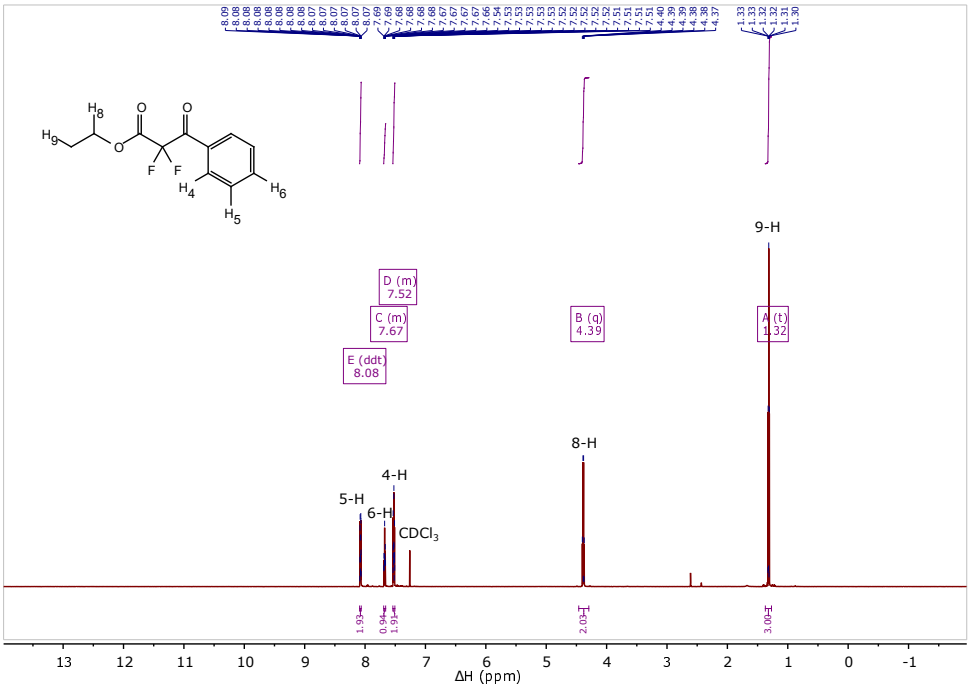

Figure 3.3: ^{1}H NMR spectrum of 2,2-difluoro-3-oxo-3-phenylpropanoate

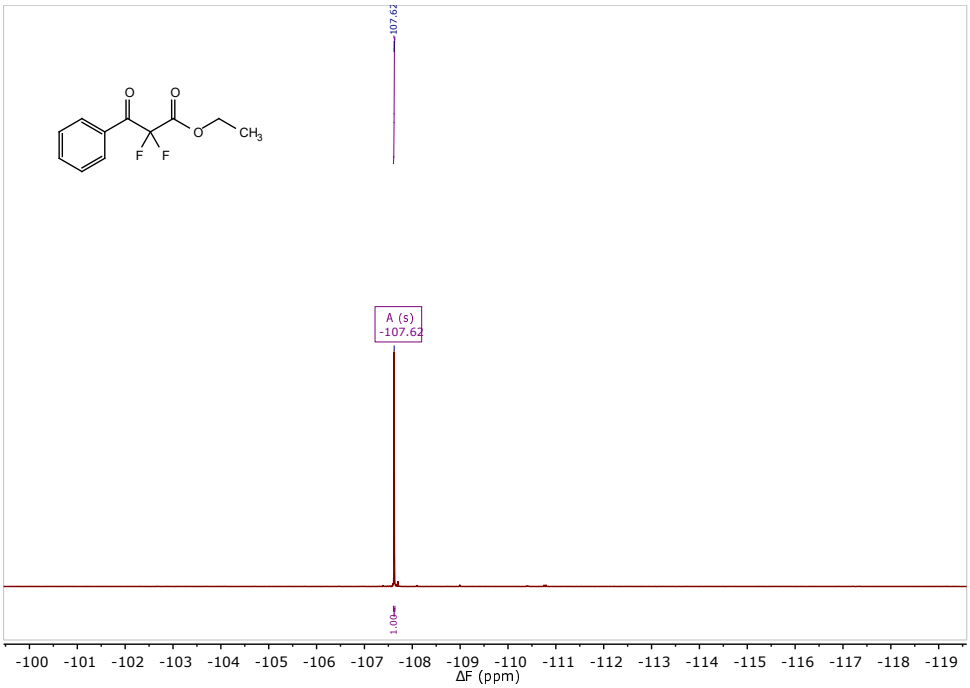

Figure 3.4: ^{19}F NMR spectrum of 2,2-difluoro-3-oxo-3-phenylpropanoate

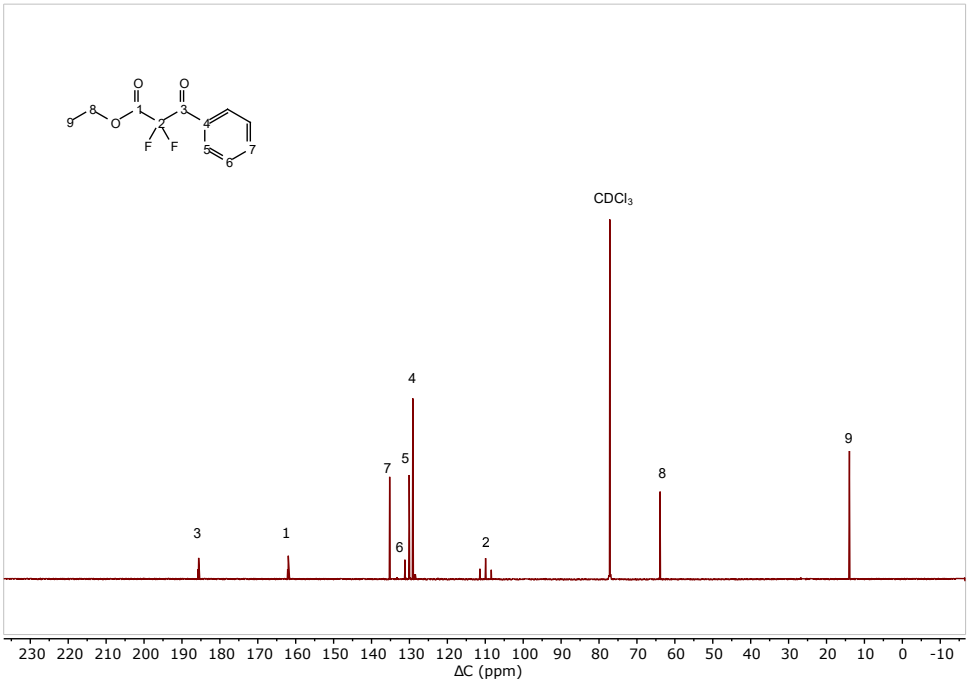

Figure 3.5: ^{13}C NMR spectrum of 2,2-difluoro-3-oxo-3-phenylpropanoate

3.2.2 Synthesis of Ethyl Benzoylacetate Derivatives

Derivatives of **94** with various substituents on the phenyl ring are not commercially available, but there are various synthetic routes to prepare these substrates in the literature.[148–152] While many of these require the use of sodium hydride (NaH), work by *Clay et al.* developed a method using milder reagents, magnesium chloride ($MgCl_2$) and Et_3N, that achieved excellent yields (up to 99%) with a methodology that has been scaled up to a multi kilogram scale.[153] In an attempt to further increase the substrate scope, a derivative replacing the phenyl ring with a pyridine moiety was synthesised following a literature procedure (Table 3.2).[154]

The derivatives were synthesised in excellent yields, with purity higher than the reported literature in some cases as shown by the isolation of the desired products as solids and not as the reported oils. We propose that the large range of values reported in the literature for the NMR shifts and melting point values is due to different keto–enol ratios. The keto:enol ratio in $CDCl_3$ were calculated by comparison of the integrals of the keto and enol forms of the C**2**H. In all cases, the major enol tautomer is formed using the ketone carbonyl, with **94a**,**b** and **94e** displaying an additional enol form based on the ester carbonyl. It appears that the keto–enol ratio has no effect on whether the product is a solid or oil as shown by the range in keto proportions (16–75%) detected in the NMR spectrum of the isolated products (Table 3.3).

Table 3.2: Synthesis of ethyl benzoylacetate derivatives synthesises following a literature preparation[153]

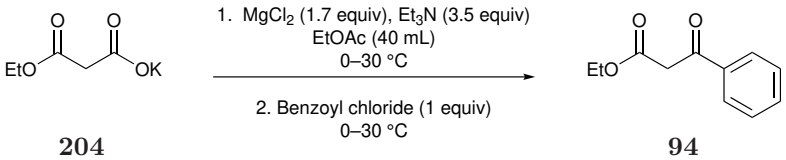

204
10 mmol

94

Entry	Compound	Structure	Yield/%
1	**94a**	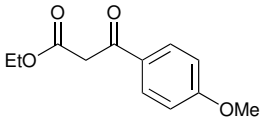	76
2	**94b**	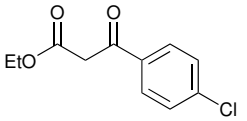	91
3	**94c**	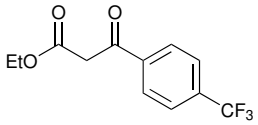	95
4	**94d**	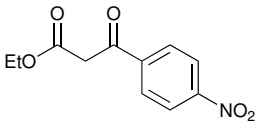	98
5	**94e**	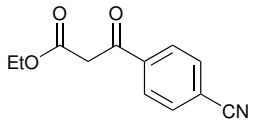	95
6	**94f**	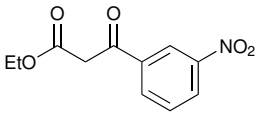	75
7	**94g**	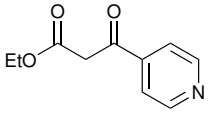	72*

* Synthesised following the literature procedure reported by Ragavan *et al.*[154]

The different keto–enol ratios are only present in solution, and so are probably solvent dependent. Crystals of the solid products were grown by slow evaporation of a supersaturated solvent and were analysed by single crystal XRC. These were all found to form as the enol tautomer which indicates that the enol form is thermodynamically stable more often than not under these conditions (Figure 3.6).

Table 3.3: Comparison of the keto–enol ratios in $CDCl_3$ of the benzoylacetate derivatives synthesised

Entry	Compound	Ketone/%	Enol/%	State
1	**94a**	75	17, 8	Oil
2	**94b**	73	20, 7	Solid
3	**94c**	60	40	Oil
4	**94d**	26	74	Solid
5	**94e**	75	17, 8	Solid
6	**94f**	58	42	Solid
7	**94g**	16	84	Solid

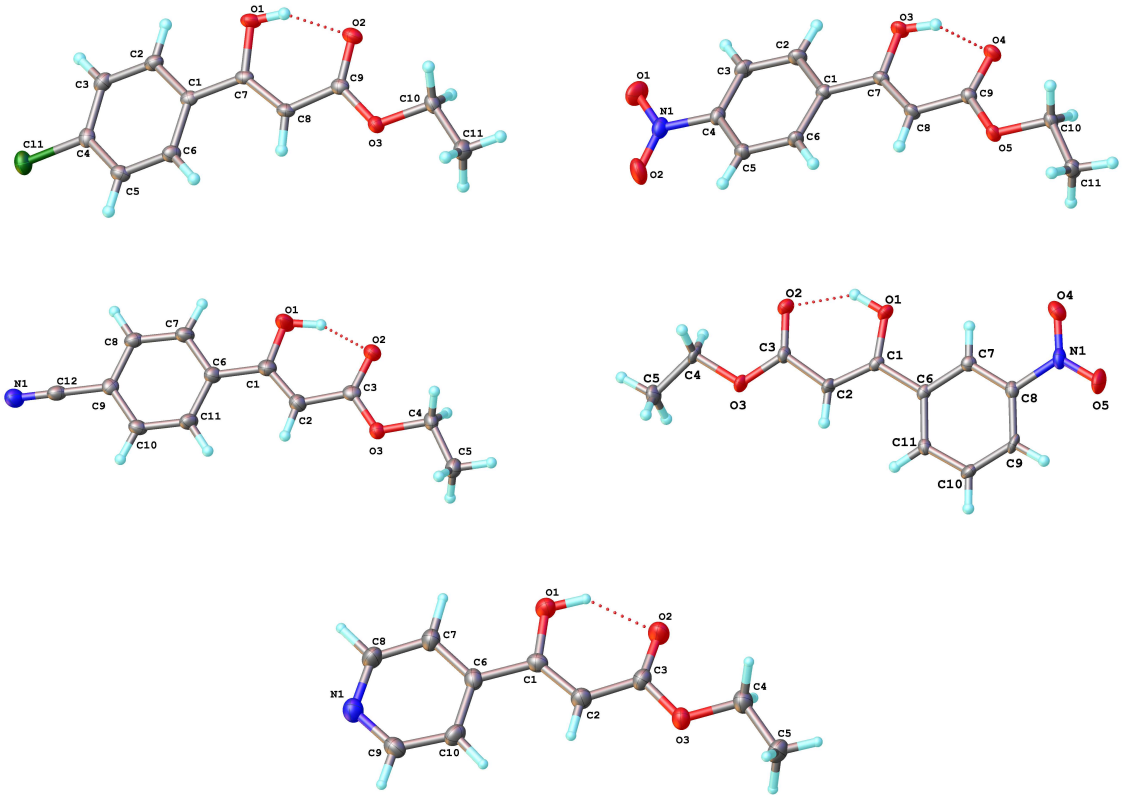

Figure 3.6: Molecular structure of several synthesised ethyl benzoylacetates as determined by XRC

3.2.3 Synthesis of Ethyl 2,2-Difluoro-3-oxo-3-propanoate Derivatives

Derivatives **94a**–**g** were fluorinated using the conditions optimised for **94** (Table 3.4). Purification by column chromatography using the small scale silica column with

$CHCl_3$ as the eluent yielded **96b–f** in high yields with no further purification needed. The methoxy derivative (**96a**) gave substantial amounts of product that had undergone further aromatic ring fluorination in a similar fashion as to when 1-(4-methoxy)-3-phenylpropane-1,3-dione (**91b**) was fluorinated. This reaction was repeated with 2.5 equiv. of F_2, however a significant amount (20%) of this unwanted aryl fluoride product was detected by ^{19}F NMR spectroscopy. The methoxy group increases the rate of fluorination at C**2** but additionally, activates the aromatic ring towards fluorination. Given the difficulties with removing the unwanted fluorinated products in the DBM based reactions, no further attempts at isolating **205a** was attempted. The lack of success with this compound compared to the others highlighted the beneficial effect of electron withdrawing groups on decreasing the reactivity of the aromatic ring of starting materials towards competing fluorination.

Compound **96d** contained some unwanted aryl fluoride material, but repeating with 2.8 equiv. of F_2 gave the desired product after purification.

Compound **96g** was not isolated as a pure product as several fluorinated products were detected in the ^{19}F NMR spectrum after attempts at purification by column chromatography using a silica gel support. Reaction of F_2 with the nitrogen of the pyridine ring to give an *N*-fluoropyridinium salt is suggested to be the cause of low yields in this case.

Table 3.4: Quinuclidine mediated direct fluorination of ethyl benzoylacetate derivatives (**94a**–**g**)

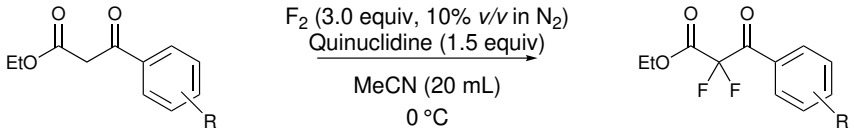

94
2 mmol

96
70–89%

Entry	Starting Material	Product	Structure	Yield/%
1	**94a**	**96a**	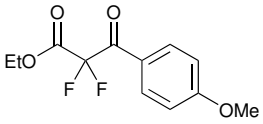	Not isolated
2	**94b**	**96b**	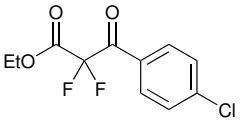	89
3	**94c**	**96c**	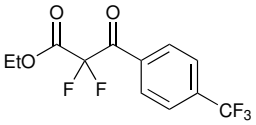	87
4	**94d**	**96d**	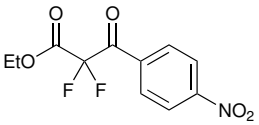	77
5	**94e**	**96e**	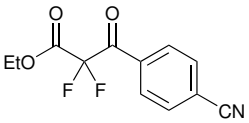	70
6	**94f**	**96f**	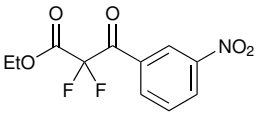	78
7	**94g**	**96g**	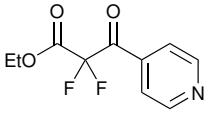	Not isolated

A suitable crystal of **96d** for XRC was grown by slow evaporation from an EtOH and water mixture. Interstingly the molecular structure identified was that of the *gem*-diol hydrate of the ketone carbonyl group (Figure 3.7). The molecules in the crystal are linked by hydrogen bonds to form corrugated layers. α,α-Difluoroketones can readily form hydrates in aqueous solution, but there are very few examples of organic structures containing a $C(OH)_2-CF_2-C$ fragment in the Cambridge Crystallographic Data Centre (CCDC), and only one of these is acyclic.

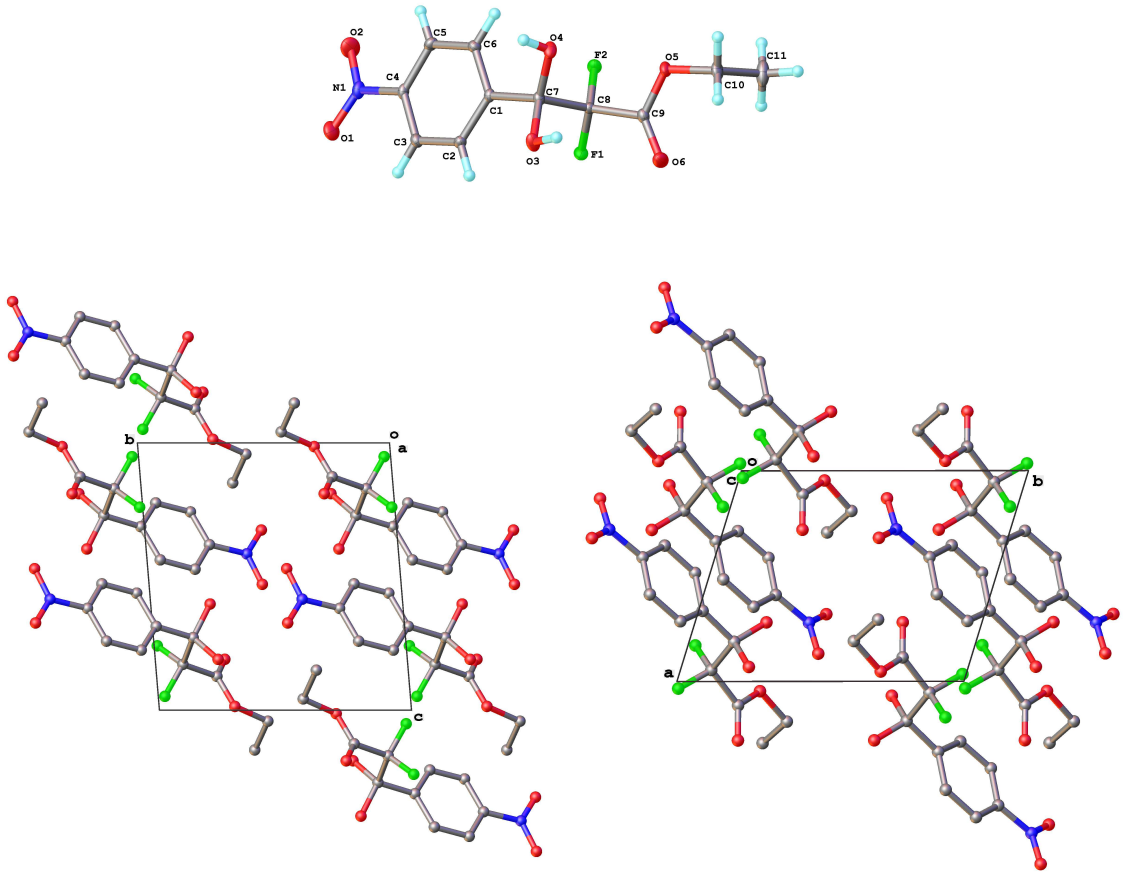

Figure 3.7: Molecular structure and crystal packing structure of **96d** as determined by XRC and crystallography

Given the success of selectively difluorinating **94** and its derivatives using a quinuclidine optimised direct fluorination, attempts were made to difluorinate other BKEs of potentially industrial relevance.

3.2.4 Difluorination of Alkyl β-Ketoesters

The ethyl and methyl 3-oxopentanoate esters were trialled as simple aliphatic BKE that could lead to potentially useful CF_2 containing FBBs.

Table 3.5: Screening conditions for the base mediated difluorination of methyl 3-oxopentanoate

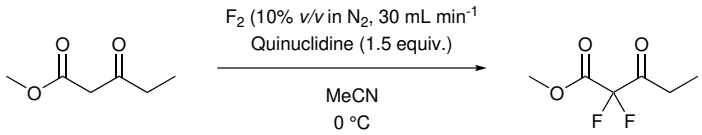

161
2 mmol
0.251 mL

206

Entry	Volume of MeCN/ mL	Equiv of F_2	NMR conversion to **206**%	Recovered Mass/ g
1	20	3.0		0.001[a]
2	20	4.5	84	0.203[b]
3	40	5.5	89	0.237[c]
4	40	5.5[d]	90	0.311[e]

[a] Silica plug used instead of 20 mL column

[b] Further purification by vaccuum distillation attempted

[c] Further purification by column chromatography attempted

[d] 1.7 equiv. of quinuclidine added

[e] Further purification by distillation using a Kugelröhr

The recovered yield of the crude product when a silica plug was used instead of a mini column is significantly lower despite washing through with a much larger volume of solvent (Table 3.5, Entry 1). While conversions to **206** were good when a large amount of F_2 was added, full conversion was never achieved. Increasing the volume and F_2 (Table 3.5, Entries 3 and 4) did not significantly increase conversion to **206** as measured by NMR, though trace amounts of unwanted fluorinated by-products were detected in the ^{19}F NMR spectra.

Despite being predicted to have different boiling points, with the introduction of fluorine lowering the boiling point, isolation of **206** by vaccuum distillation was unsuccessful (Table 3.5, Entry 2). Distillation using a Kugelröhr was also attempted as these are better at separating small volumes of material that has multiple different boiling points (Table 3.5, Entry 4). A colourless oil (0.146 g) was obtained, but unfortunately analysis by NMR spectroscopy indicated that this oil contained 12% of unreacted **161** by weight. Purification was also attempted by column chroma-

tography using silica gel with a 15% EtOAc *v/v* in hexane mixture as the eluent (Table 3.5, Entry 3). No desired product was detected in any fractions obtained, and thus it appears that **206** has hydrolysed on the column similarly to 2,2-difluoro-1,3-diesters (**198**, **207**) that were synthesised previously but not isolated.

Fluorination attempts with ethyl 3-oxopentanoate **208** also showed good selectivity for the desired difluoro product **209** (Table 3.6). However, full conversion could not be achieved, and isolation of **209** was not successful due to hydrolysis during an aqueous work-up. Increasing the equivalents of F_2 to 4.0 and purification by column chromatography using silica gel in a 20 mL syringe as the column afforded 0.264 g of a pale yellow oil that was 73% **209** and 27% unreacted **208** by NMR. Use of the mini column drastically increased the mass recovered compared to using a silica plug. No further attempts to isolate **209** were attempted but, on a larger scale, distillation of the pure difluoro ketoester **209** should be possible.

Table 3.6: Screening conditions for the base mediated difluorination of ethyl 3-oxopentanoate

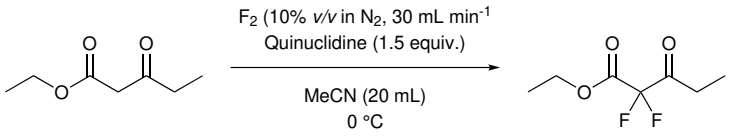

208
2 mmol
0.285 mL

209

Entry	Equiv of F_2	NMR ratio **209** : **208**	Recovered Mass/ g
1	3.0	1 : 2.4	0.010[a]
2	4.0	4.5 : 1	0.264

[a] Aqueous work-up performed before washing through a silica plug used instead of 20 mL column

Quinuclidine appears to dramatically increase selectivity for the 2,2-difluoro product during direct fluorinations of β-ketoesters with F_2. Selectivity of >95% was detected, but full conversion was not achieved despite the addition of a large excess of F_2. Isolation of these 2,2-difluoro-β-ketoesters is inherently difficult due to their tendency to hydrolyse in aqueous conditions and during purification via column chromatography. The success at isolating **96** and its derivatives indicated that an aromatic ring helps to prevent rapid hydrolysis and aid isolation.

3.3 Reactions of 2,2-Difluoro-β-ketoesters with Amines

We previously noted that **96** appears to hydrolyse and also potentially decarboxylate during the aqueous workup. While this could potentially be used to expand the range of FBBs that **96** can be used to make, no further investigations into this were attempted as part of this thesis. Instead, **96** was reacted with several amines to develop a new route to difluoroamide derivatives (Scheme 3.2).

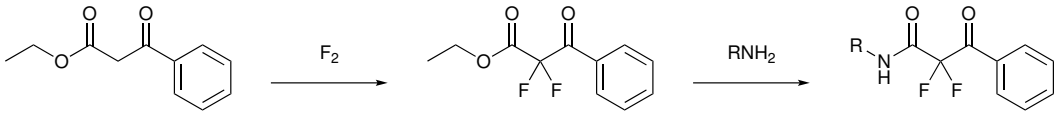

94 **96** **210**

Scheme 3.2: Route to difluoroamides using F_2 as a fluorinating agent

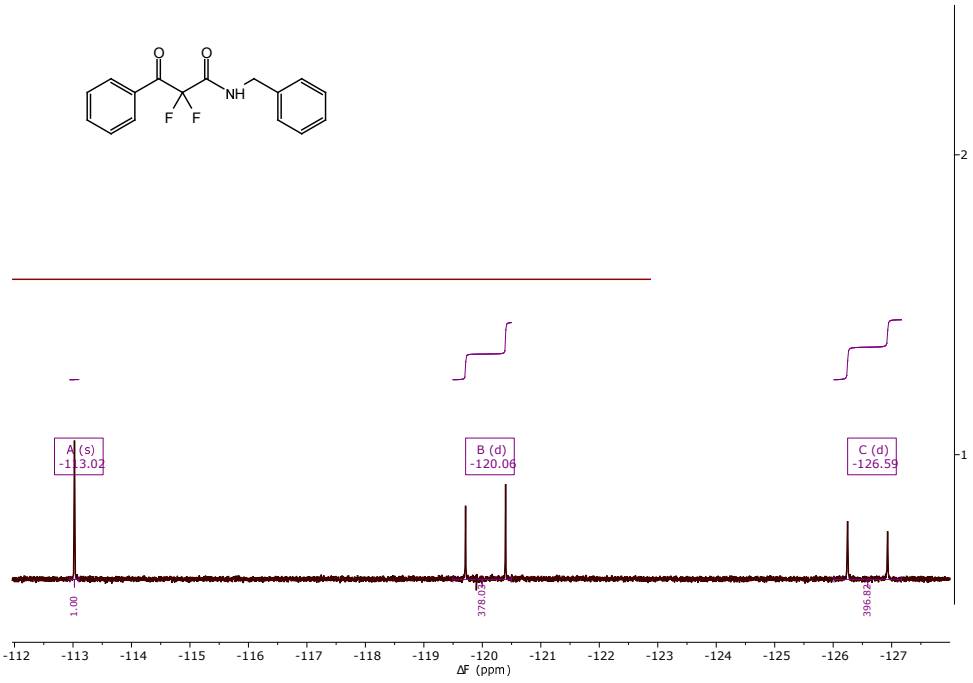

Figure 3.8: ^{19}F NMR spectra of the starting material (top) and crude product from the reaction in EtOH (bottom)

The synthesis of a few difluoroamides with a similar structure to **96** have previously been reported. These can be either be made by fluorinating the corresponding amide with an excess of an electrophilic fluorinating agent such as Selectfluor™ or by palladium-catalyzed carbonylation of aryl boronic acid derivatives.[155,156] Both of

these methods are much less viable on a manufacturing scale due to the cost of the reagents.

Middleton reported the synthesis of several α,α-difluoroarylacetamides by mixing the corresponding amine and ethyl α,α-difluoroarylacetate in EtOH and stirring overnight. Consequently, reacting **96** with varying amounts of benzylamine in EtOH led to complete conversion of starting material after stirring overnight at 40 °C. Investigation of the ^{19}F spectrum showed the presence of an unidentified product as shown by the presence of CF_AF_B systems with $^2J_{FF}$ coupling constants of 257 Hz **210c** (Figure 3.8).

It is likely that several possible diastereomers were formed, but could not be identified. However, changing the reaction solvent to tetrahydrofuran (THF), increasing the equivalents of base to ten and the reaction time to 3 d gave conversion to the desired products.

The amides were isolated in good yields with the exception of **210a** (Table 3.7, Entry 5). Incomplete conversion by ^{19}F NMR was detected even after leaving the reaction to stir for a week. The desired product could not be isolated from unreacted **96**, even appearing to co-crystalise with it. The lower reactivity of morpholine reflects its lower nucleophilicity.

Table 3.7: Synthesis of difluoroamides from 2,2-difluoro-3-oxo-3-phenylpropanamide in THF

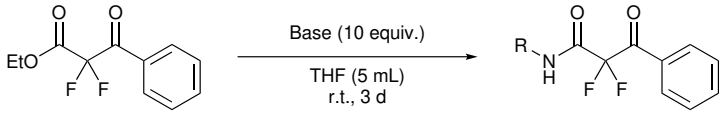

96
0.5 mmol

210

Entry	Amine	Product	Structure	Isolated Yield/%
1	Ammonia[a]	**210b**	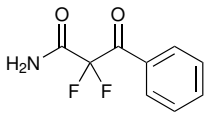	58
2	Benzylamine[b]	**210c**	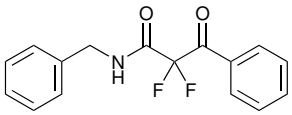	75
3	Allylamine	**210d**	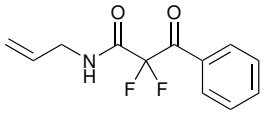	70
4	Propargylamine	**210e**	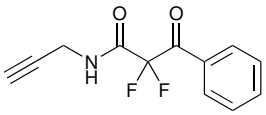	62
5	Morpholine	**210a**	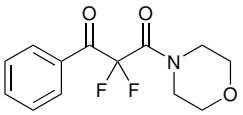	Not isolated

[a] 4 M ammonia (NH_3) in MeOH used

[b] 2 equiv. of amine used

3.4 Proposed Fluorination Mechanism

We propose a similar mechanism for the quinuclidine mediated direct fluorination of BKEs as we proposed previously for 1,3-diketones. BKEs react with electrophilic sources of fluorine in the enol conformer, with the corresponding enolate reacting faster. The pK_a of the **95** is predicted to be slightly lower (by ∼1.6) than the non fluorinated **94**, thus is deprotonated preferentially, which explain why selectivity for the difluoro product **211** is achieved (Scheme 3.3).

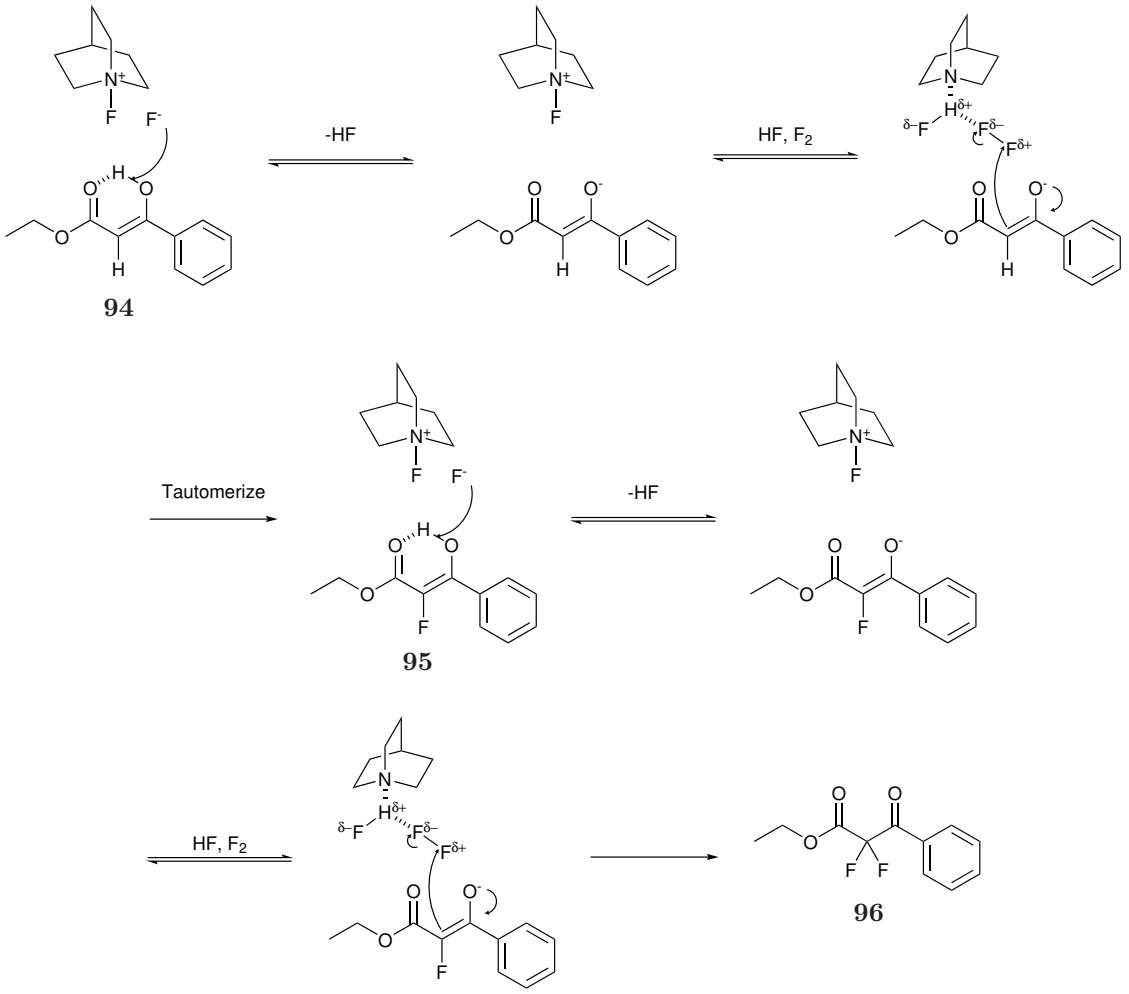

Scheme 3.3: Proposed mechanism of the quinuclidine mediated direct fluorination of **94** to give **96**

Derivatives of **94** with an electron donating group on the aromatic ring **94a** underwent additional unwanted aromatic fluorination. Similar to when **91b** was fluorinated, the –OMe group activates the aromatic rings to unwanted fluorination *ortho* to the substituent. These unwanted products could not be separated from the desired product. Derivatives with electron withdrawing substituents **94b**–**f** had their aromatic rings deactivated towards unwanted fluorination, and so were isolated easily.

3.5 Conclusion

Several nitrogen bases were trialled to increase the selectivity of fluorination with F_2 to give desired 2,2-difluoro-1,3-ketoester products. Similarly to the fluorination

of 1,3-diketones, quinuclidine was found to most effectively mediate fluorination to give desired *gem*-difluoro products. More forcing conditions were required to achieve conversion to the desired difluoroketoester product which matches the literature assessment that BKEs are less reactive to 2,2-difluorination than 1,3-diketones. There appeared to be less unwanted fluorinated by-products as these BKEs contained only one aromatic ring, and no fluorination was detected on the ethoxide group. Isolated yields were higher due to the formation of less unwanted products, and the modified workup to use a smaller 20 mL column with $CHCl_3$ as the eluent. Shortening the time that products were on the column from several hours to 20–30 min. limited the amount of hydrolysis that occurred on exposure to silica. This is important for the 2,2-difluoro BKEs which readily hydrolyse during an aqueous workup, or while eluting down a regular sized column.

Chapter 4

Synthesis of $ArCF_2X$ Compounds

4.1 Introduction to $ArCF_2X$ chemistry

Difluoromethylene, $>CF_2$, compounds are of increasing interest to the life sciences due to potentially potent biophysicochemical properties as mentioned previously in this thesis. The $-CF_2H$ group is isosteric and isopolar to the $-OH$ and $-SH$ groups, and can act as a lipophilic hydrogen bond donor. Examples of $ArCF_2H$ containing agrochemicals are the pre-emergence herbicides dithiopyr **212** and thiazopyr **213** (Figure 4.1).

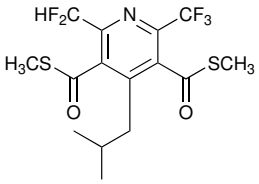

212

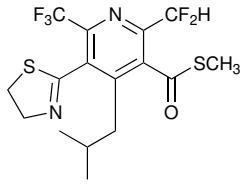

213

Figure 4.1: Example $ArCF_2H$ containing agrochemicals

There are currently limited industrially viable methods for the synthesis of $ArCF_2H$ systems, though new methods are being developed on a discovery scale. For example, the *gem*-difluoro group can be introduced by deoxyfluorination using hazardous nuceleophilic fluorinating agents such as DAST **39**.[51]

Alternatively, a difluoromethylating reagent can be incorporated into target compounds to generate $ArCF_2H$ **46** derivatives.[157–160] This often requires stoichiometric amounts of metals to couple an aryl system with the CF_2H reagent. Hartwig developed coupling conditions of iodoarenes **214** with $TMSCF_2H$ **108** as a route

to **46**, but this method requires a large excess of the expensive $-CF_2H$ fluorinating agent **108** and was limited to electron-rich and electron-neutral iodoarenes (Scheme 4.1).[161] This reaction was later modified to encompass electron-poor iodoarene and heteroaryl iodide **215** substrates by Xu *et al.* (Scheme 4.1).[162] However, aldehydes and ketones functionalities are not tolerated using this methodology as the CF_2H anion adds directly to the carbonyl group.

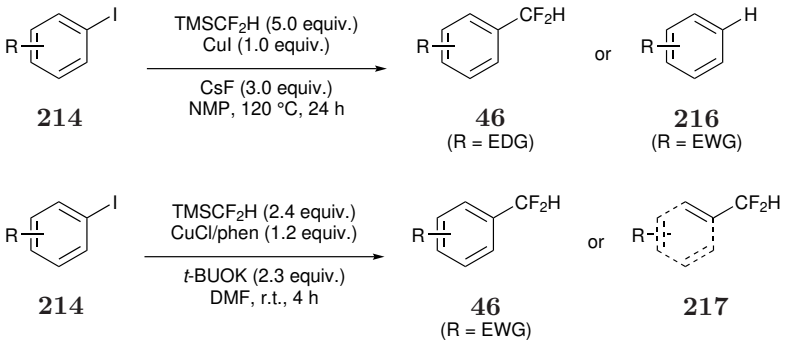

Scheme 4.1: Synthesis of $ArCF_2H$ from iodoarenes and heteroaryl iodides[161,162]

Given the strength of the C–F bond, it is difficult to selectively reduce readily available $ArCF_3$ containing compounds made using $TMSCF_3$ to the corresponding $ArCF_2H$. It requires the presence of a second $-CF_3$ group on the ring, and a large excess (30 equiv.) of magnesium.[163]

Sato developed coupling conditions between the readily available ethyl bromodifluoroacetate **119** and several vinyl or aryl iodides in the presence of copper powder (Scheme 4.2).[87] Yields are varied (21–69%), and only three examples using aryl iodides were reported.

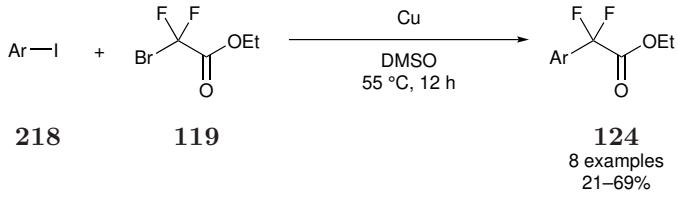

Scheme 4.2: Synthesis of ethyl 2,2-difluoro-2-arylacetates[87]

Amii expanded on this work by developing a route to a range of ring-substituted $ArCF_2CO_2Et$ **124** systems in good yield by coupling ethyl 2,2-difluoro-2-(trimethylsilyl)acetate **219a** with iodoarenes **220** (Scheme 4.3).[164] While the reaction requires stoichiometric copper, substrates include iodoarenes with either electron-donating or withdrawing groups or heteroaryl iodides. While a large range

of difluoroesters were synthesised, the overall yield of this two-step process is highly varied.

The reaction was further modified to use a catalytic amount of copper in the coupling process and using the related ethyl 2,2-difluoro-2-(triethylsilyl)acetate **219b** as the $>CF_2$ containing reagent. Yields are significantly lower for this reaction, and the substrate scope is more limited.

More recently, Uneyama developed a similar route to **219a** using ethyl trifluoroacetate **221** as starting material (Scheme 4.3).[165] While the $>CF_2$ containing reagent **221** is much cheaper than $TMSCF_2H$ **108**, these routes still require large excesses of metal reagents to ensure conversion to the desired product.

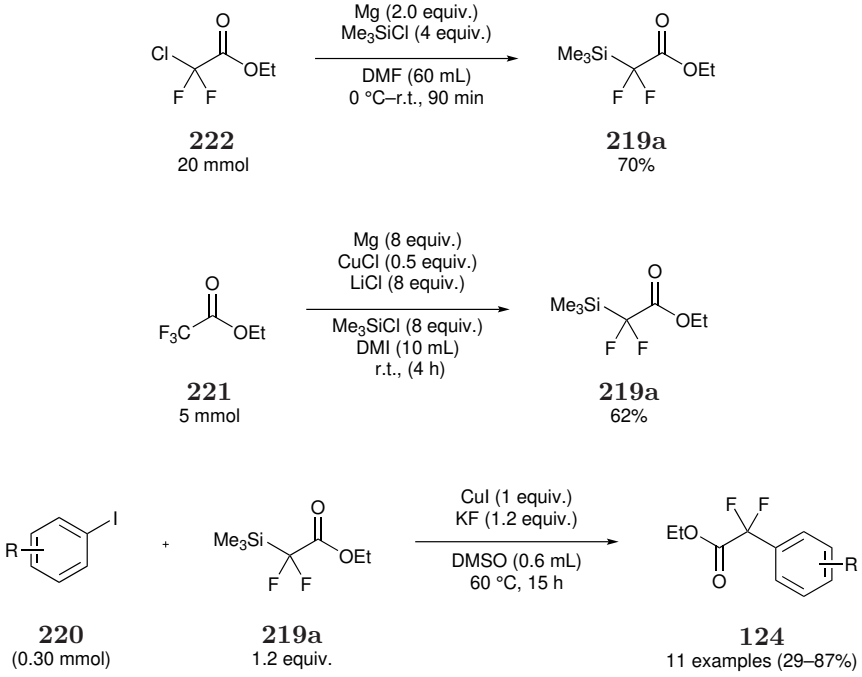

Scheme 4.3: Literature synthesis of ethyl 2,2-difluoro-2-arylacetates from iodoarenes and ethyl 2,2-difluoro-2-(trimethylsilyl)acetate[164,165]

As part of their work into coupling iodoarenes with $>CF_2$ reagents, Amii *et al.* developed conditions to obtain $ArCF_2H$ compounds by hydrolysing **124** to the difluoro acid **223**, and then decarboxylating to the target **46** (Scheme 4.4).[164] The presence of the $>CF_2$ group in **124** increases the reactivity of nucleophilic substrates at the carbonyl, and hence **124** is readily hydolysed to **223** using the mild base pottasium carbonate (K_2CO_3). This difluoroacid can be used as a FBB in a range of reactions including the synthesis of a pyridine derived $>CF_2$ containing pharmacophore **225** (Scheme 4.4).[166–170]

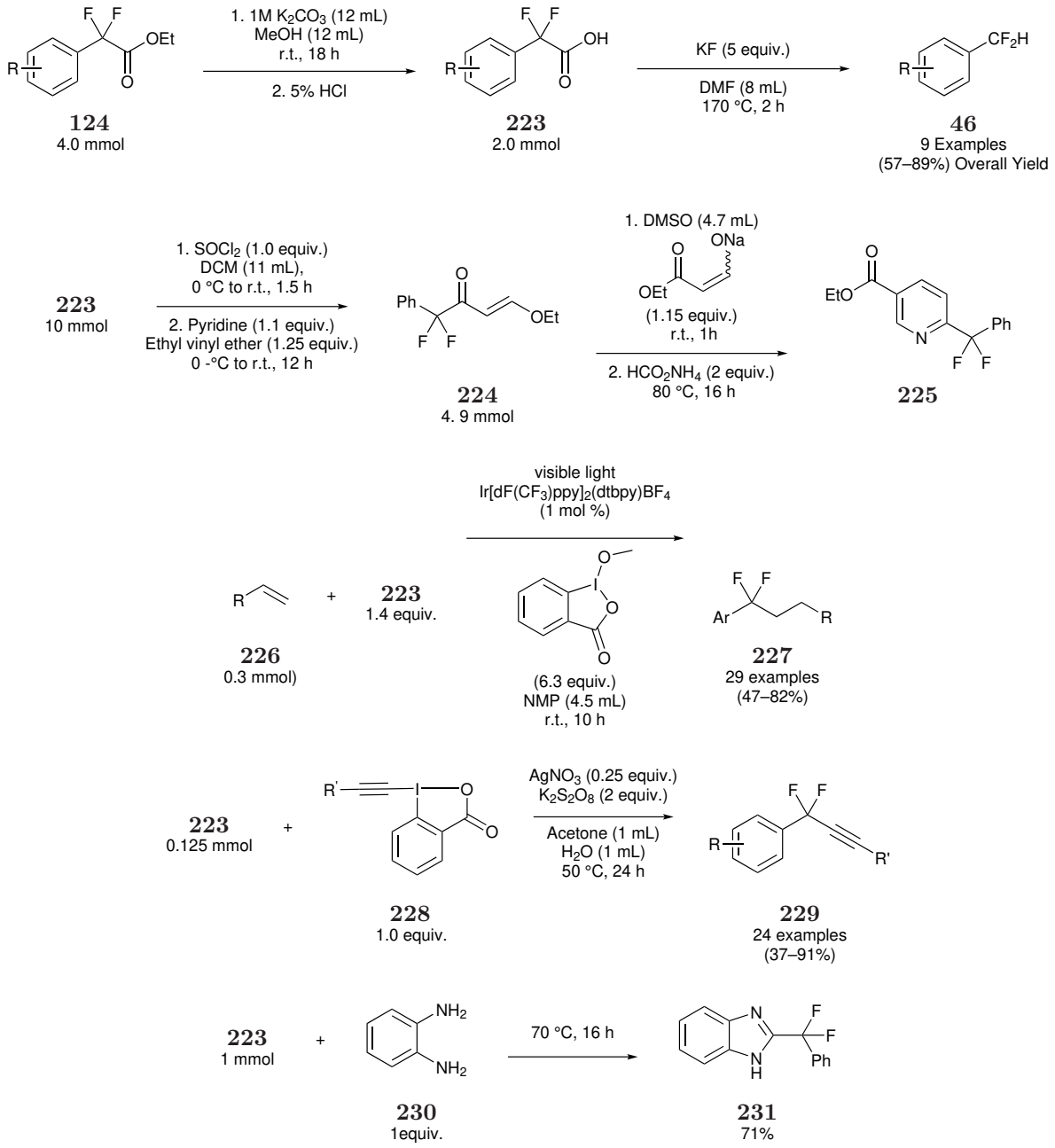

Scheme 4.4: Syntheses and uses of $ArCF_2CO_2H$ as a $>CF_2$ containing FBB[164,166–170]

There are limited methods of generating $ArCF_2X$ compounds on an industrial scale, despite their potential usage as FBBs. Previously in this thesis the selective difluorination of 1,3-dicarbonyl products was successfully developed and this chapter will focus on the selective direct difluorination of carbonyl compounds as a potential route to $ArCF_2X$ containing FBBs.

4.2 Aims

Amii *et al.* developed a route to ArCF$_2$H containing compounds from the related difluoro ester **124** in excellent yields. These esters were made in a two step reaction with a varied, and often low, overall yield. This chapter will investigate attempts at synthesising ArCF$_2$CO$_2$Et derivatives in a one-step selective difluorination of the non-fluorinated starting material. Further reactions shall be investigated to expand the potential uses of ArCF$_2$CO$_2$Et derivatives as ArCF$_2$X containing FBBs.

4.3 Fluorination of Ethyl 2-(4-Nitrophenyl)acetate

The 4-nitrophenyl derivative **234a** was chosen as a target to develop fluorination conditions. This product has previously been reported, but in a low isolated yield of 29% (20% over the two steps).[164] The non-fluorinated ester ethyl 2-(4-nitrophenyl)acetate **232a** is commercially available for a low cost, and we believe the presence of the electron withdrawing $-NO_2$ group should limit unwanted ring fluorination. These factors make **232a** an ideal test substrate for developing conditions to selectively difluorinate α- to the ester. Selective direct fluorinations of this compound will be investigated to try and synthesise **234a** in a one step reaction (Scheme 4.5).

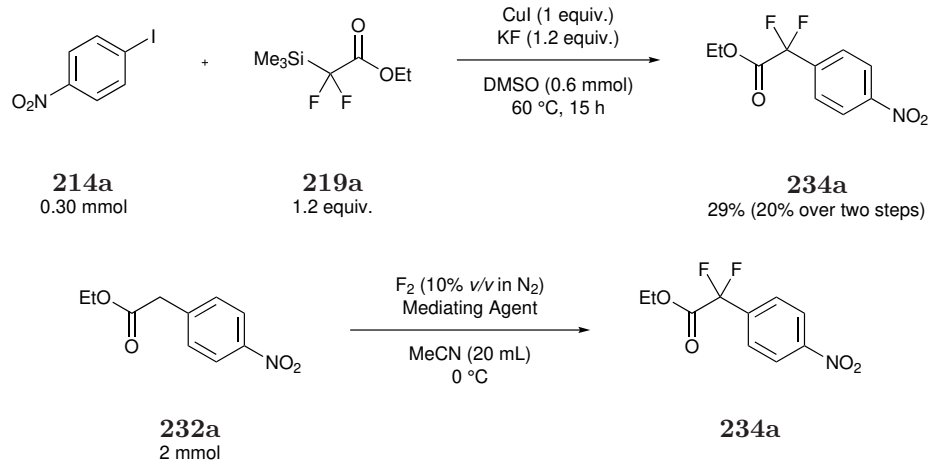

Scheme 4.5: Literature synthesis of ethyl 2,2-difluoro-2-(4-nitrophenyl)acetate (top),[164] and proposed one step synthesis using F_2 (bottom)

An initial test fluorination of **232a** was attempted with quinuclidine as a mediating agent to see if selective difluorination α- to the carbonyl is feasible following the succesful use of quinuclidine in previous chapters. The number of equiv. of quinuclidine was reduced to try and limit the overall degree of fluorination, and especially

prevent any unwanted aromatic fluorination so that a pure sample of **234a** could be isolated. Following successful small scale experiments, the reaction was scaled up to provide a suitable mass of **234a** for these studies (Scheme 4.6).

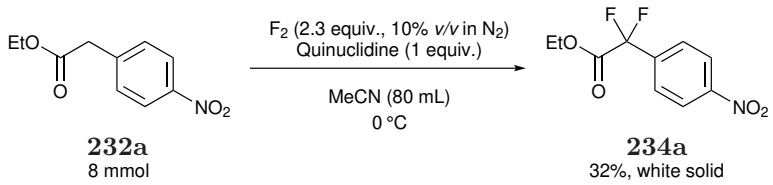

232a
8 mmol

234a
32%, white solid

Scheme 4.6: Trial synthesis of ethyl 2,2-difluoro-2-(4-nitrophenyl)acetate using F_2

Following reaction with F_2 in MeCN in the presence of quinuclidine, the reaction solvent was removed under reduced pressure and the yellow oil residue partitioned between DCM and H_2O. The aqueous phase was then washed with DCM. The combined organic phases were dried over $MgSO_4$, and the solvent removed under reduced pressure to give a crude product that was purified by column chromatography on silica gel with ethyl acetate 15% *v/v* in hexane solvent mixture as the eluent to give the desired product **234a** as a white solid in 32% yield. A sample was dissolved in hexane, and gave crystals by slow evaporation of the solvent which were analysed by single crystal XRC (Figure 4.7).

The aromatic protons in a 1,4-disubstitued aromatic would usually be detected as a dq in the ^{1}H NMR spectra as they show an AA'XX' pattern. The C**4**H protons in **234a** are detected as a multiplet due to $^4J_{HF}$ coupling with the fluorine atoms on the CF_2 group (Figure 4.2). Several of the carbon atoms in **234a** are split by the CF_2 group as shown by the four triplets seen in the ^{13}C NMR spectrum (Figure 4.4).

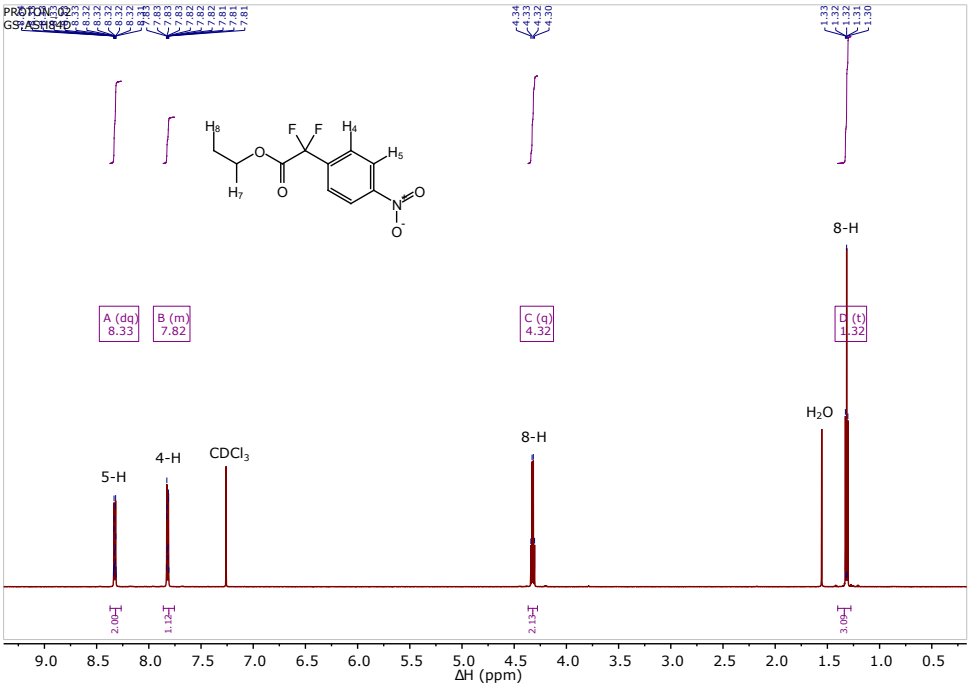

Figure 4.2: ^{1}H NMR spectrum of ethyl 2,2-difluoro-2-(4-nitrophenyl)acetate

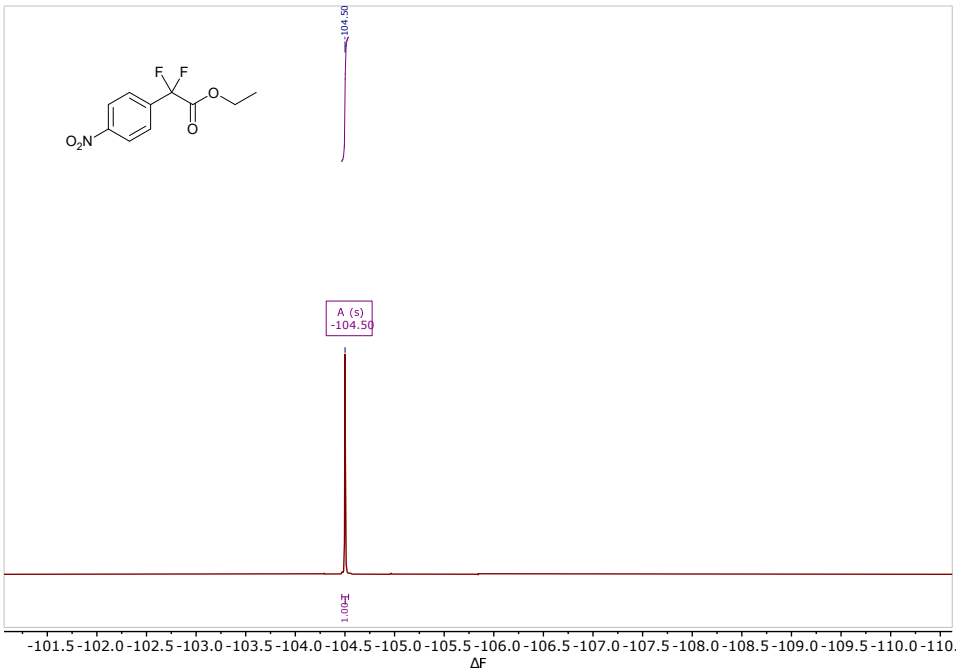

Figure 4.3: ^{19}F NMR spectrum of ethyl 2,2-difluoro-2-(4-nitrophenyl)acetate

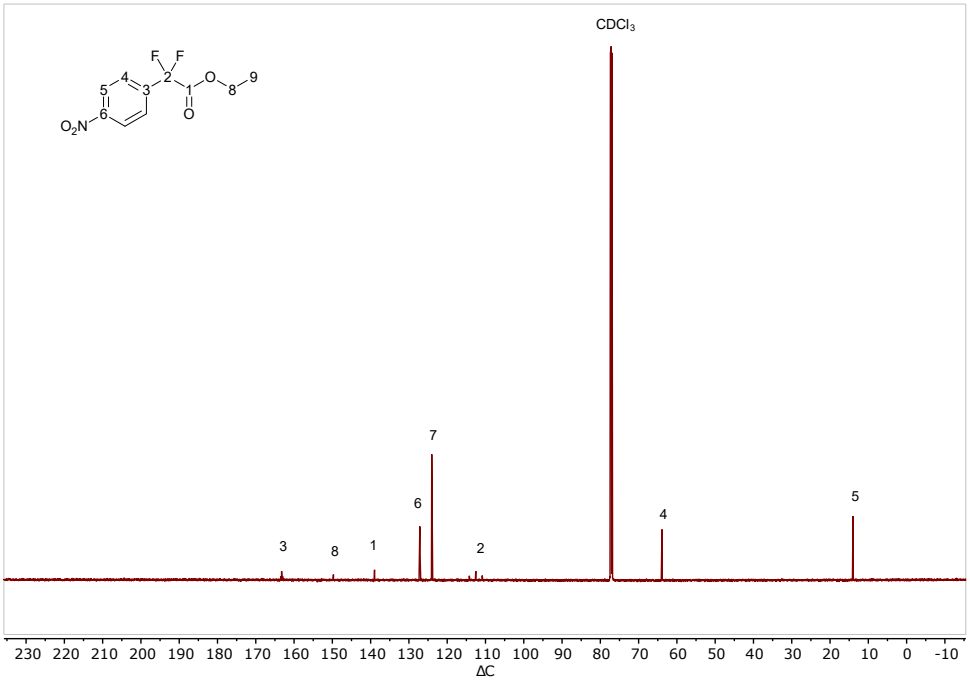

Figure 4.4: ^{13}C NMR spectrum of ethyl 2,2-difluoro-2-(4-nitrophenyl)acetate

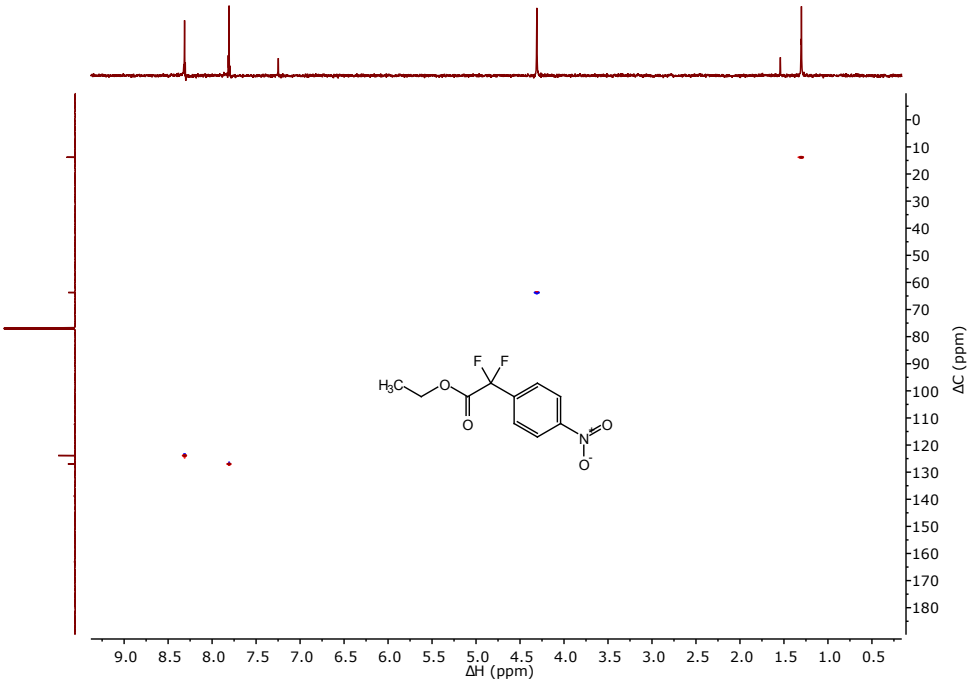

Figure 4.5: HSQC NMR spectrum of ethyl 2,2-difluoro-2-(4-nitrophenyl)acetate

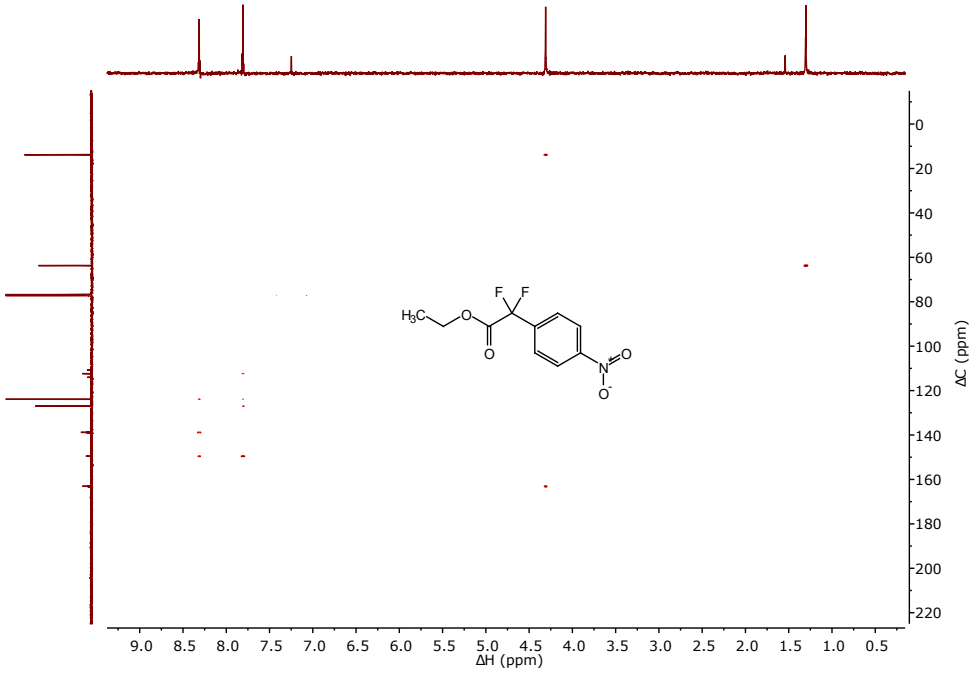

Figure 4.6: HMBC NMR spectrum of ethyl 2,2-difluoro-2-(4-nitrophenyl)acetate

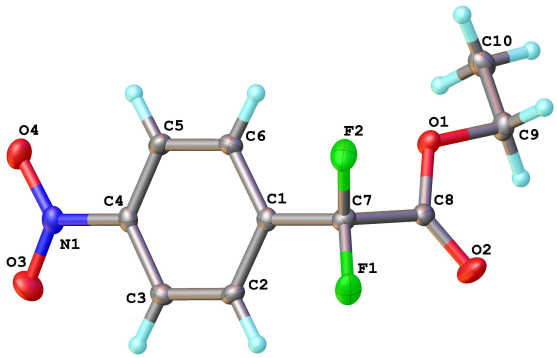

Figure 4.7: Molecular structure of ethyl 2,2-difluoro-2-(4-nitrophenyl)acetate as confirmed by X-ray crystallography

4.3.1 Base Mediations

The conditions to promote formation of the desired *gem*-difluoro product were optimised using a similar strategy as described in the previous chapters. The conversion of **232a** to the monofluoro product **233a** and the difluoro product **234a** by fluorination with F_2 were investigated and analysed by ^{19}F NMR spectroscopy. Various possible mediating agents were used to try and optimise conversion to the target product **234a**.

The $>CH_2$ group in **232a** is predicted to have a significantly higher pK_a than the $>CH_2$ group of the 1,3-diketones fluorinated previously due to the presence of only one electron withdrawing carbonyl group. Non substituted phenylacetate **232** has a pK_a(DMSO) calculated to be 22.7.[171] The pK_a(DMSO) can be converted to the pK_a(MeCN) value by the following equation to give the pK_a(MeCN) of **232** as 33.3 (Equation 4.1).[138]

$$\mathrm{p}K_\mathrm{a}(\mathrm{MeCN}) = 1.00\mathrm{p}K_\mathrm{a}(\mathrm{DMSO}) + 12.9 \tag{4.1}$$

By comparison, the pK_a(MeCN) of quinuclidine is 19.5, a difference of roughly 14 units from the pK_a(MeCN) of **232**. This difference should be too large for quinuclidine to deprotonate any of **232** by acting as a specific base. It is possible that the fluoride anion F^- could act as a base as its pK_a(MeCN) of 26 is significantly closer to the pK_a(MeCN) of **232** as discussed in previous chapters. Consequently, mediating agents that would increase the concentration of F^- such as potassium fluoride and urea were trialled, as well as the nitrogen bases used previously.

After each fluorination, the reaction mixture was purged with N_2 before the reaction solvent was removed under reduced pressure. The crude product mixture was washed through a silica plug on a sinter with several volumes of DCM as the eluent to remove any remaining HF. To determine the relative conversion to the desired product **234a** compared to other fluorinated products, the integrals of all signals in the ^{19}F NMR spectra were summated and the proportion of integrals due to **233a** (−190.9 ppm) and **234a** (−104.5 ppm) were then calculated.

Table 4.1: Comparison of selectivity for the desired ethyl 2-(4-nitrophenyl)acetate over other fluorinated products

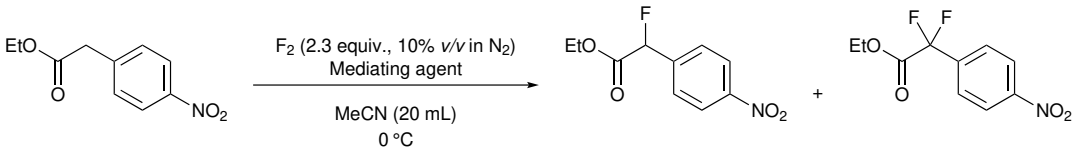

232a 2 mmol — **233a** — **234a**

Entry	Base	Equiv. of base	Proportion of signals in the ^{19}F NMR spectrum/%		
			233a	**234a**	Polyfluorinated products
1	None	-	14	0	86
2	KF	2.0	8	0	92
3	KF 18-crown-6	2.0 2.0	6	1	93
4	KF 18-crown-6	2.0 0.1	8	0	92
5	Urea	1.0	0	0	100
6	Tetramethylurea	1.0	0	0	0
7	DABCO	2.0	27	2	73
8	Et_3N	2.0	0	0	0
9	Quinuclidine	1.1	7	85	8
10	DBU	0.1	9	0	91
11	DBU	2.0	22	5	73
12	Tri-*n*-butylamine	1.0	0	0	100
13	Pyridine	1.0	0	0	100
14	*N*-methyl pyrrolidone	0.5	4	0	96

The conversion to the desired product **234a** with 2.0 equiv. of KF was not significantly different to the base fluorination with no mediating agent present (Table 4.1, Entries 1 and 2). However, significant amounts of KF were present as an undissolved solid prior to the fluorination due to its low solubility in MeCN and so there was no significant increase in the amount of fluoride ion present in solution. Upon addition of the KF, the pale yellow-coloured solution of **232a** in MeCN changed to a pale lilac/purple.

An equiv. of 18-crown-6 ether was added due to its affinity for the potassium cation K^+ to increase the solubility of the F^- in MeCN (Table 4.1, Entry 3). Instantly, the reaction solution turned from the clear pale yellow coloured solution to a clear dark purple coloured solution. While trace amounts (1%) of the desired difluoro product **234a** were now detected, the major product with 57% of the relative fluorinated signals in the ^{19}F NMR spectrum of the crude product is a peak at −132.88 ppm (dt). Comparison with the literature indicates that this is due to formation of monofluoro-18-crown-6 **235** (Figure 4.8).[172] Repeating with 0.1 equiv. of 18-c-6 (Table 4.1 Entry 4) gave no conversion to the unwanted by-product **235**, but also no conversion to the desired product **234a**.

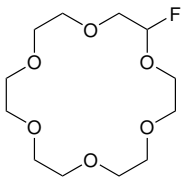

235

Figure 4.8: Monofluoro-18-crown-6

Urea was also trialled as a mediating agent (Table 4.1, Entry 5) but the lack of conversion to the desired products may be due to the apparant low solubility of urea in MeCN. Tetramethylurea was then trialled as the addition of four methyl groups to the two nitrogens dramatically increases the solubility of tetramethylurea in MeCN compared to urea (Table 4.1, Entry 6). However, no fluorination of **232a** was detected by NMR spectroscopy. A weak singlet at −23.1 ppm was detected in the ^{19}F NMR spectrum which may be due to the formation of an *N*-F associated product, but no further attempts to identify this product were made.

Several amines previously trialled as mediating agents for the selective 2,2-difluorination of 1,3-dicarbonyls were then used (Table 4.1, Entries 7–11). Similar selectivities for the monofluoro and difluoro product were obtained compared to reactions with dicarbonyl compounds as reported previously. The fluorination with Et_3N as the mediating agent was noticably different, with no fluorination of starting material Et_3N occuring (Table 4.1, Entry 8). A singlet at −163.5 ppm was present before the aqueous work-up. We believe this to be silicon tetrafluoride (SiF_4), produced by reaction of HF with the glassware used to store the concentrated reaction mixture, which is hydrolysed upon the addition of H_2O.

Two additional nitrogen bases were trialled as mediating agents. Tri-*n*-butylamine (pK_a(MeCN) 18.1) was used to determine the effect of increasing the alkyl chain length compared to Et_3N (Table 4.1, Entry 12). Upon addition of this base, a slow change in the solution colour to a pinkish hue occured over approximately 10 min. While small amounts of fluorination of the starting material does occur using **236**, none of the desired products, and only unwanted ring fluorinated products were detected.

Pyridine was trialled as a mediating agent as its lone pairs should be unhindered by the alkyl groups attached as these are locked in the planar aromatic ring structure (Table 4.1, Entry 13). It is also possible that the electrophilic fluorinating agent *N*-fluoro pyridinium fluoride **70a** could be made *in situ*, which would likely react with **232a** to give the monofluoro product **233a**. However, after aqueous workup, neither of the desired products **237a** or **234a** were detected by ^{19}F NMR spectroscopy.

Conversions to **234a** when either DABCO, Et_3N, quinuclidine or DBU were used as mediating agents appear to be unrelated to the pK_a(MeCN) of the protonated amines (18.3, 18.5, 19.5 and 24.3 respectively). DBU has a higher pK_a(MeCN) than quinuclidine, but significantly lower selectivity for **234a**. DABCO and Et_3N have very similar pK_as(MeCN), but the addition of Et_3N appeared to prevent all fluorination of **232a** from occuring. A colour change similar to that seen previously was detected, with the intensity dependent on the base added. The addition of DABCO afforded no noticeable change in colour, Et_3N turned the solution very, very pale purple, and quinuclidine and DBU producing an intense purple solution, requiring only 0.1 equiv. of DBU to achieve this colour. Quinuclidine has repeatedly mediated regiselectivity for the desired *gem*-difluoro product for a range of substrates far more successfully than should be expected purely from its pK_a(MeCN). To investigate the nucleophilicity of quinuclidine, *N*-methyl pyrrolidine was trialled as a mediating agent. It has the same pK_a(MeCN) as DABCO (18.3), but a similar nucleophilicity parameter (N) and nucleophilic-specific slope parameter (s) for a given electrophilicity parameter (E) to quinuclidine (4.4).[173,174]

$$\log(k)_{20^\circ\mathrm{C}} = s(\mathrm{N} + \mathrm{E}) \tag{4.2}$$

$$\text{Quinuclidine: } s = 0.60, \mathrm{N} = 20.54 \tag{4.3}$$

$$N\text{-Methyl pyrrolidine: } s = 0.52, \mathrm{N} = 20.59 \tag{4.4}$$

Interestingly, a highly unselective fluorination occured when *N*-methyl pyrrolidine was trialled as the mediating agent (Table 4.1, Entry 14). None of the desired difluoro product **234a** was formed, and the monofluoro product **233a** made up a very small proportion (<5%) of all the fluorinated material.

Given the results discussed in Table 4.1, quinuclidine again appears to be the most effective mediating agent of the bases screened. Therefore, fluorination of **232a** was repeated with varying amounts of quinuclidine and F_2 and conversion to **233a** and **234a** monitored by NMR spectroscopy to optimise this process.

Table 4.2: Screening conditions for the quinuclidine mediated fluorination of ethyl 2-(4-nitrophenyl)acetate

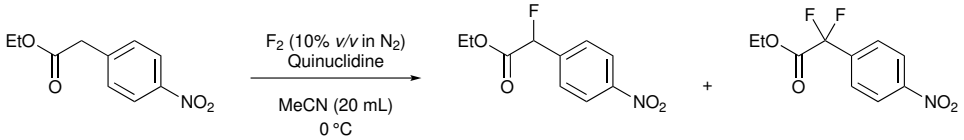

232a 2 mmol | **233a** | **234a**

Entry	Equiv. of quinuclidine	Equiv. of F_2	Ratio of products by a combination of ^1H and ^{19}F NMR		
			232a	**233a**	**234a**
1	0.1	2.3[a]	50	4	1
2	1.0	2.3	3	1	5
3	1.1	2.3	3	1	5
4	1.5	2.3	2	1	7
5	1.1	3.0	1	1	7
6	1.5	2.5	3	1	10
7	1.5	3.0	2	11	11
8	1.5	3.5	1	Trace	7
9	1.5	4.0	1	Trace	6
10	1.5	4.5	1	Trace	11
11[b]	1.5	4.1	2	1	12
12[b]	1.5	4.5	1	1	13
13[b]	1.3	4.6	1	1	11

[a] 5 mmol **232a**, 5 ml min^{-1} flow rate of 10% *v/v* F_2 in N_2 and 50 mL MeCN used

[b] 20 mmol of **232a** and 200 mL MeCN used

A limiting amount of quinuclidine was added to investigate whether quinuclidine acts catalytically in increasing the selectivity to **234a** (Table 4.2, Entry 1). The low conversion to **234a** shows that this is not the case, and that stoichiometric amounts of quinuclidine are required. Increasing the amount of quinuclidine added promoted conversion to the desired difluoro product (Table 4.2 Entries 2–4), but a more noticeable effect was seen when the amount of F_2 was increased (Table 4.2, Entry 5).

The reaction was repeated with 1.5 equiv. of quinuclidine, and samples of the reaction mixture periodically taken after increasing equivalents of F_2 had been added (Table 4.2 Entries 6–11). Unreacted starting material remained even after a large excess of F_2 had been added, but further attempts to increase conversion by adding yet more F_2 resulted in the formation of unwanted ring fluorinated products.

The reaction was scaled up to a 20 mmol scale using a a 500 mL glass reactor fitted with an overhead stirrer with details in Figure 8.2 in the Experimental General (Table 4.2 Entries 11–13). This setup allows for more efficient mixing of the reaction mixture with an increased path length for the fluorine to pass through the solvent. A higher conversion to the desired product **234a** was detected by NMR spectroscopy using this setup as expected.

With fluorination conditions developed, different workups to isolate **234a** without causing unwanted hydrolysis were investigated. Recrystallisation of crude **234a** using $CHCl_3$, acetone and a mixture of EtOH/ and H_2O as solvent systems resulted in significant amounts of hydrolysis to the difluoroacid **223a** (Figure 4.9).

Purification of crude reaction mixtures by column chromatography on silica gel was then attempted and various solvent systems were assessed to limit decomposition of **234a** during purification. A 10% EtOAc *v/v* in hexane solvent mixture solvent mixture as the eluent afforded **234a** which was isolated as a pale yellow solid in a 60–69% yield depending on the scale used (Scheme 4.7). More forcing conditions were needed than previously used to fluorinate 1,3-diketones and BKEs. This highlights the lower reactivity and selectivity of *gem*-difluorination α- to carbonyls compared to 1,3-dicarbonyl substrates. Isolated yields were lower than the related 4-nitrophenyl containing difluoro-BKE product **96d** (Table 3.4) highlighting the tendency of **234a** to decompose or hydrolyse during workup and purification.

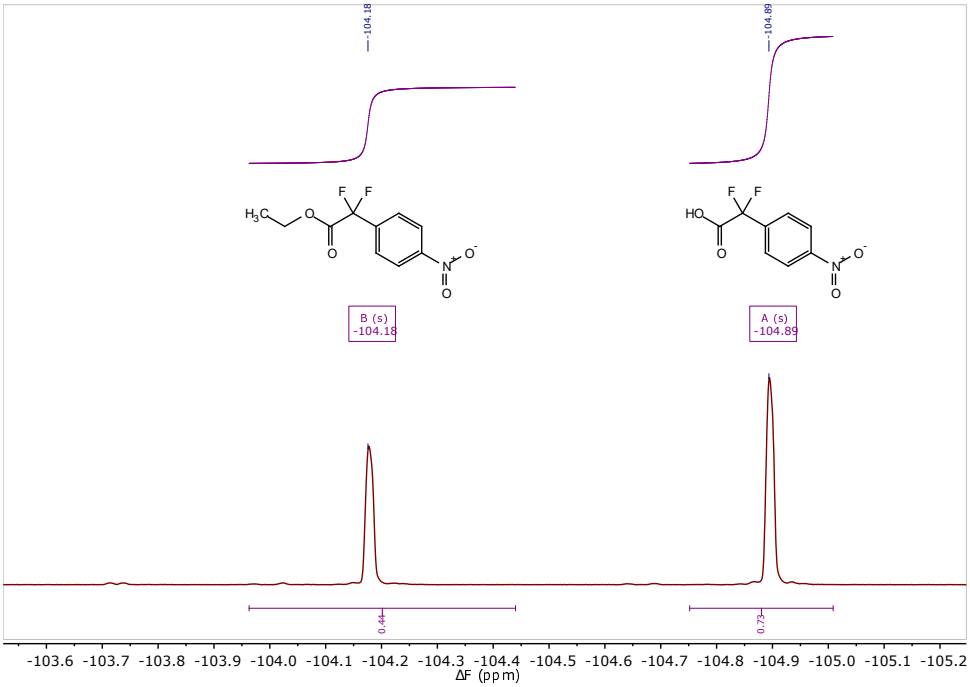

Figure 4.9: ^{19}F NMR spectrum after attempts at purifying ethyl 2,2-difluoro-2-(4-nitrophenyl)acetate by recrystallisation

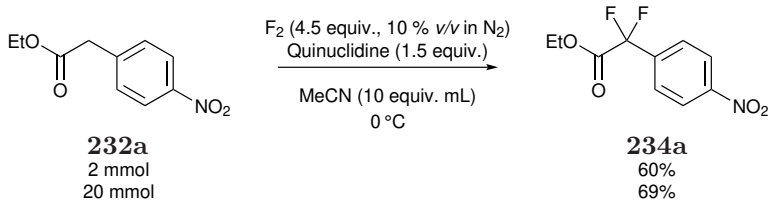

232a
2 mmol
20 mmol

234a
60%
69%

Scheme 4.7: Synthesis of ethyl 2,2-difluoro-2-(4-nitrophenyl)acetatee using F_2

4.4 Fluorination of Ethyl Phenylacetate Derivatives

The conditions in Scheme 4.7 were then used to fluorinate a range of ethyl phenylacetate derivatives with EWGs attached to the ring. No derivatives with EDGs were trialled as we predicted these would form significant amounts of ring fluorinated by-products.

Ethyl 2-(4-fluorophenyl)acetate **232b** was fluorinated using 4.0 equiv. of F_2 (Scheme 4.8). No singlet was detected in the ^{19}F NMR spectrum of the concentrated reaction mixture in a similar region to the $>CF_2$ group in **234a** (-104.5 ppm). Several peaks were detected in the ^{19}F NMR spectrum, but these all disappeared after a $D_2O/CDCl_3$ shake. We propose that these signals are due to polyfluorinated

tar by-products. A small amount (∼5% of total peak signals) of unreacted **232b** remained in the crude product mixture. The fluorination was repeated with 3.0 equiv. of F_2, but again, no desired difluoro-product was detected by NMR.

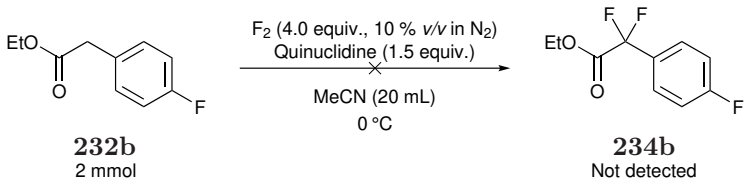

232b
2 mmol

234b
Not detected

Scheme 4.8: Attempted synthesis of ethyl 2,2-difluoro-2-(4-fluorophenyl)acetate using F_2

The 4-fluoro moiety is less of an EWG than the 4-nitro, and so it is possible that the aromatic ring in **234b** was not sufficiently deactivated to prevent unwanted ring fluorination. Ethyl 2-(4-(trifluoromethyl)phenyl)acetate **232c** was trialled as the $-CF_3$ group has similar inductive properties to the $-NO_2$ group (Scheme 4.9).

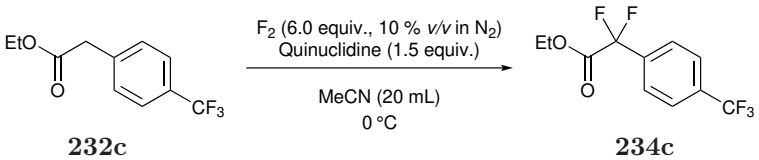

232c
2 mmol

234c

Scheme 4.9: Attempted synthesis of ethyl 2,2-difluoro-2-(4-(trifluoromethyl)phenyl)acetate using F_2

Analysis by ^{19}F NMR spectoscopy of a sample of the reaction mixture taken after the addition of 3.0 equiv. of F_2 low conversion to a singlet peak at −104.5 ppm believed to be the desired difluoro product **234c**, as well as trace amounts of the monofluoro product (doublet at −184.2 ppm). An additional 3.0 equiv. of F_2 were then added. While conversion to **234c** increased, several peaks were present at around −63.0 ppm corresponding to unwanted products containing a $-CF_3$ moiety (Figure 4.10). The reaction mixture was purified by column chromatography on silica gel with a 5% EtOAc *v/v* in hexane solvent mixture as the eluent to try and isolate desired products, but the product mixture largely decomposed on silica, and **234c** could not be isolated.

The 4-CN derivative **232d** could similarly activate the CH_2 group by inductive and by resonance effects to the 4-NO_2 system and the fluorination of the 4-CN derivative was studied (Scheme 4.10).

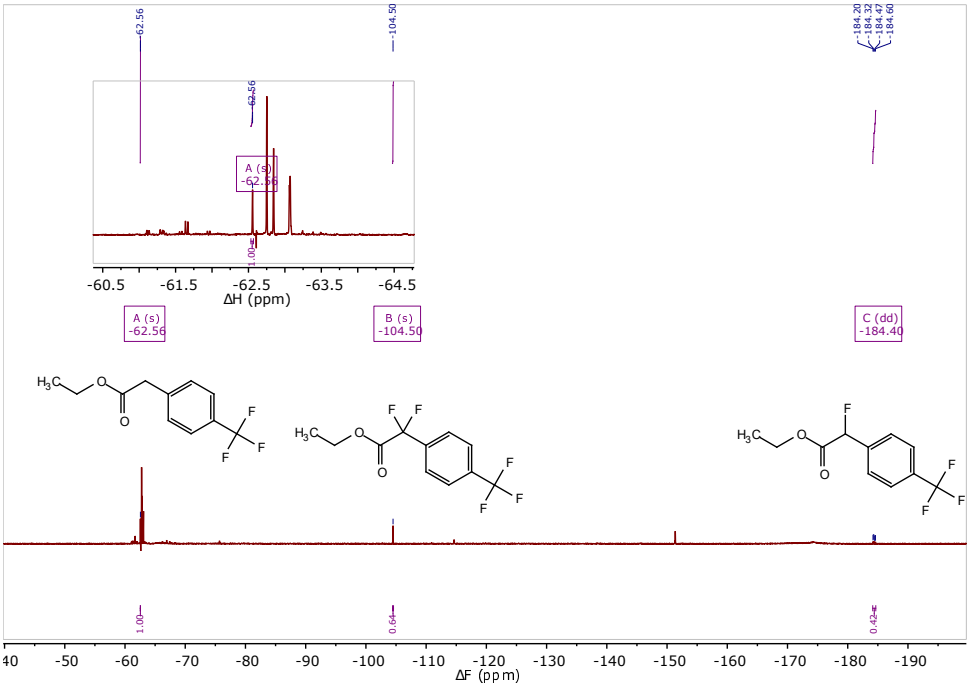

Figure 4.10: Reaction mixture after fluorination of ethyl 2-(4-(trifluoromethyl)phenyl)acetate with 6.0 equiv. of F_2

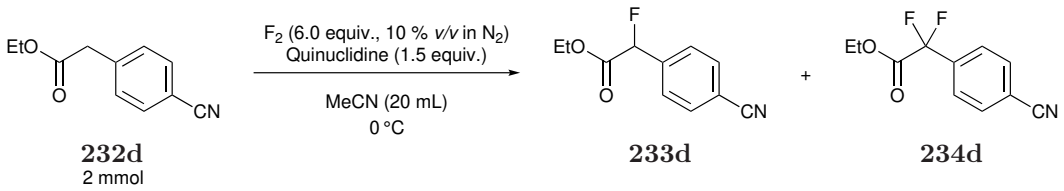

Scheme 4.10: Attempted synthesis of ethyl 2,2-difluoro-2-(4-cyanophenyl)acetate using F_2

Good selectivities for the desired difluoro product **234d** and the monofluoro product **233d** were observed, though the reaction did not go to completion after 6.0 equiv. of F_2 were added. The ratio of **234d**:**233d** decreased by roughly a half (3.3:1 to 1.8:1) during the aqueous workup, and a singlet was seen in the aqueous phase at −122.3 ppm (Figure 4.11). We believe that some of the desired product **234d** hydrolyses to the corresponding difluoro acid **223b**.

The crude product was then purified by column chromatography on silica gel with a 5% EtOAc *v/v* in hexane solvent mixture as the eluent, but the desired product **234d** could not be isolated due to hydrolysis problems.

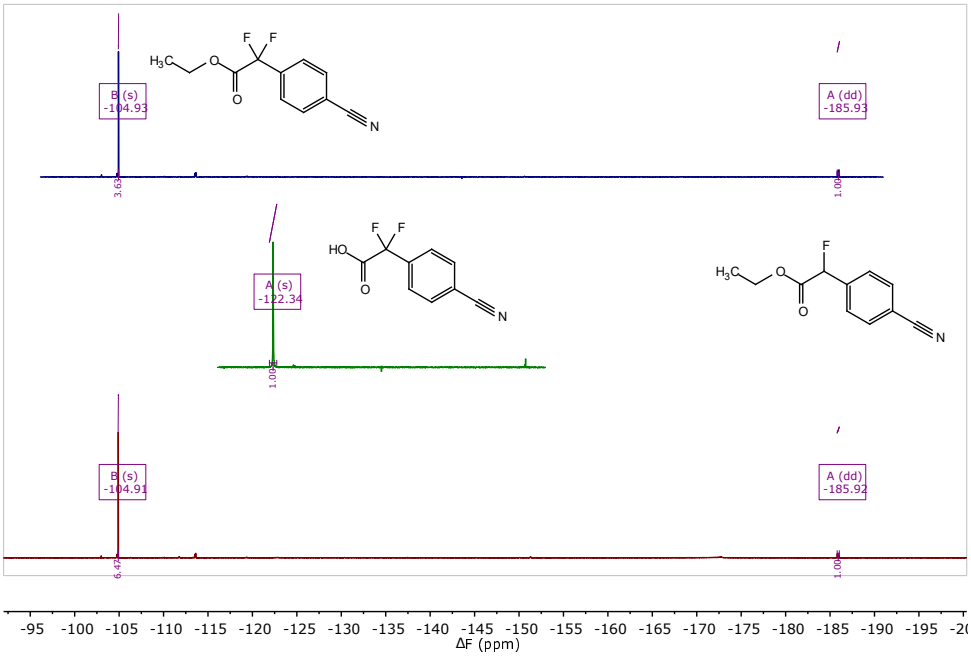

Figure 4.11: ^{19}F NMR of the concentrated reaction mixture (top), the aqueous phase (middle) and the organic phase after an aqueous workup (bottom)

The 2-NO_2 and 3-NO_2 derivatives **232e** and **232f** respectively were fluorinated to see if the position of the $-NO_2$ EWG on the ring effects the selectivity of difluorination α- to the carbonyl.

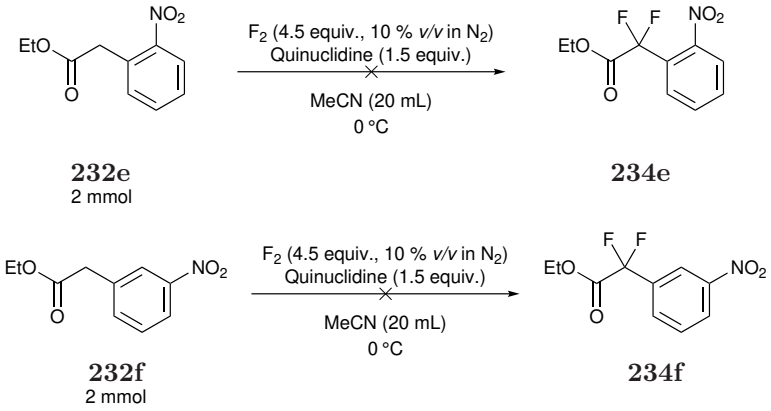

Scheme 4.11: Attempted synthesis of ethyl 2,2-difluoro-2-(2-nitrophenyl)acetate (top) and ethyl 2,2-difluoro-2-(3-nitrophenyl)acetate (bottom) using F_2

Both **232e** and **232f** showed better conversion to the corresponding monofluoro and difluoro products than **232b–d**, even with less equivalents of F_2. However, many signals (>10) were seen in the ^{19}F NMR spectra of each crude crude product. At-

tempts at isolating the difluoro products **234e** and **234f** by column chromatography proved unsuccessful.

4.5 Proposed Fluorination Mechanism

A mechanism has been proposed in the previous chapters for the quinuclidine mediated direct fluorination of dicarbonyl systems in which quinuclidine forms a $R_3N^+F\cdots F^-$ salt whyich allows deprotonation of keto forms by fluoride.

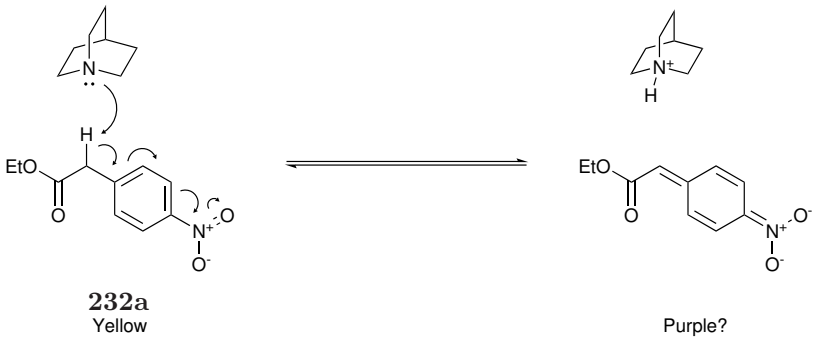

Scheme 4.12: Proposed $-NO_2$ stabilised resonance forms

Alternatively, if selectivity is increased due to the inductive effect of the electron withdrawing $-NO_2$ group in the *para* position, then a similar selectivity should be seen with **232c** and **232d** as the $-CF_3$ and $-CN$ groups have similar inductive effects to the $-NO_2$ group. Additionally, selectivity in the cases of **232e** and **232f** should be higher due to their location closer to the $-CH_2$ protons. The results found indicate that selectivity does not appear to be due to inductive effects.

A proposed mechanism for the quinuclidine mediated selective difluorination of **232a** is provided in Scheme 4.13. This mechanism is primarily based off the assumed mechanism for the difluorination of related dicarbonyl systems. Further mechanistic studies are needed to determine why fluorination of substrates where the $-NO_2$ group is in the *para* position are more efficient.

More forcing conditions are required for difluorination compared to those used to difluorinate dicarbonyl containing substrates. The CH_2 protons in **232a** are less acidic than the corresponding protons in related dicarbonyl compounds due to the lack of the second electron withdrawing carbonyl moiety. As such, fluorination of **232a** is predicted to be significantly slower than fluorination of dicarbonyls. To test this hypothesis, an equal mix of **232a** and the dicarbonyl DBM **91** were fluorinated in the presence of a limiting amount of F_2 (Scheme 4.14).

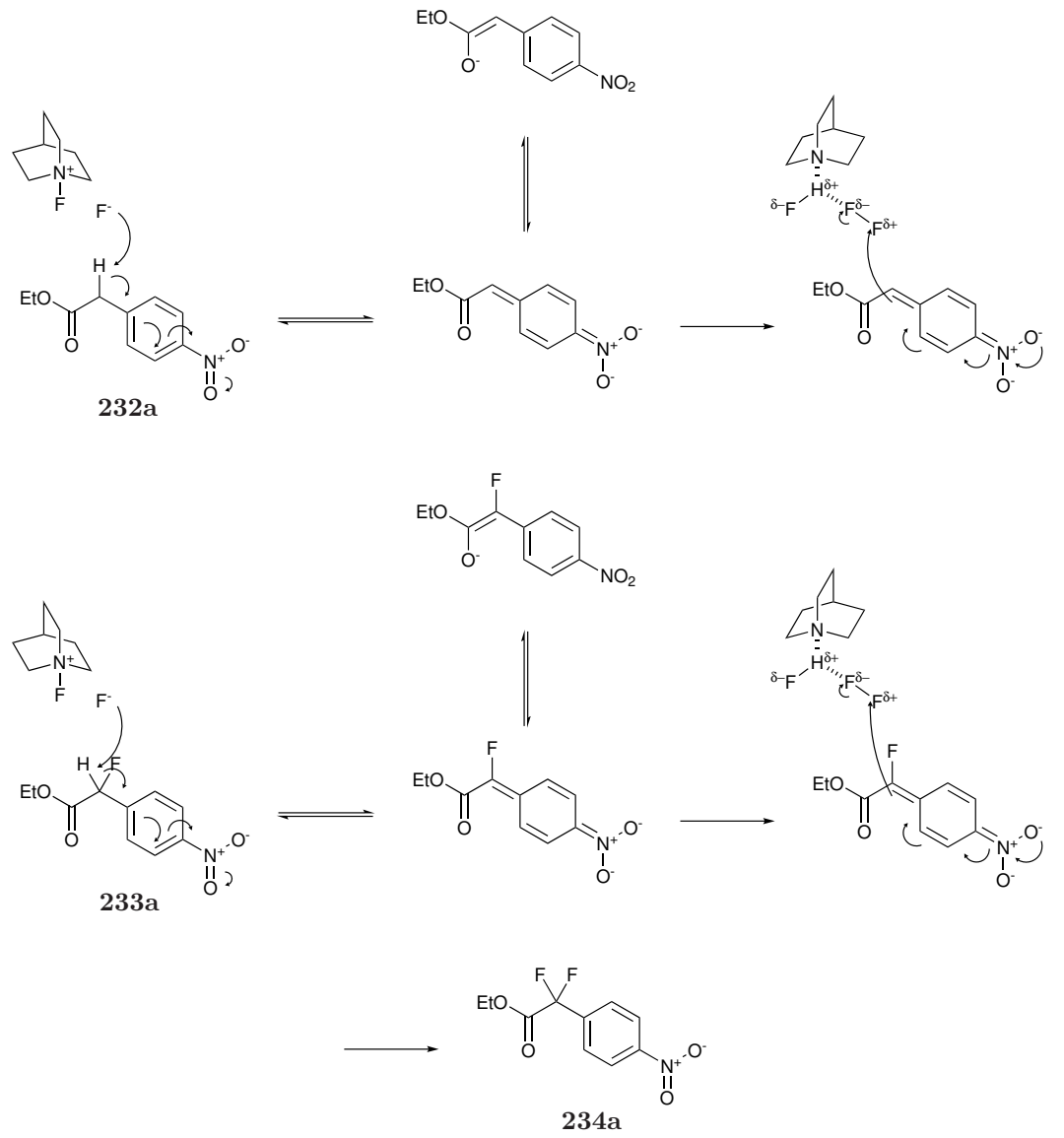

Scheme 4.13: Proposed mechanism of the quinuclidine mediated fluorination of ethyl 2-(4-nitrophenyl)acetate

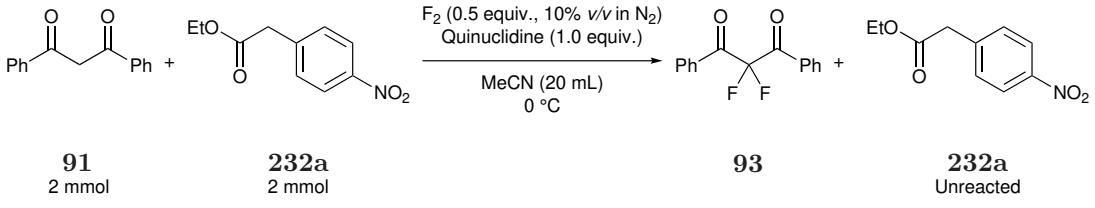

Scheme 4.14: Competition reaction between DBM and ethyl 2-(4-nitrophenyl)acetate

Analysis by NMR spectroscopy indicated that selective difluorination of **91** was observed to give **93** (Figure 4.12). No fluorination of **232a** was detected confirming the lower reactivity of the monocarbonyl substrates to direct fluorination with F_2.

Figure 4.12: ^{19}F NMR spectra of the crude product post aqueous workup up (top) and reference spectra of ethyl 2,2-difluoro-2-(4-nitrophenyl)acetate (middle) and 2,2-difluoro-1,3-diphenylpropane-1,3-dione (bottom)

4.6 Reactions of Ethyl 2,2-Difluoro-2-(4-nitrophenyl)acetate

Amii *et al.* developed conditions to hydrolyse a range of ethyl 2,2-difluoro-2-phenylacetate derivatives to the corresponding difluoro acid, and subsequently decarboxylate to give the corresponding ArCF$_2$H derivative.[164] This hydrolysis reaction proved successful for **234a**, giving 2,2-difluoro-2-(4-nitrophenyl)acetic acid **223a** as a pale yellow solid, isolated in near quantitive yields (Scheme 4.15).

The difluoroacid **223a** was then decarboxylated using the same literature procedure to give the ArCF$_2$H containing compound 1-(difluoromethyl)-4-nitrobenzene **238a** as a dark yellow oil (Scheme 4.16).

These reactions allow a ArCF$_2$H containing compound **238a** to be isolated in good overall yield (59%) after three steps from the readily commercially available starting material **232a** (Scheme 4.17). This is a significant improvement on the current literature synthetic route that this work adapts (16%, 5 steps).[164]

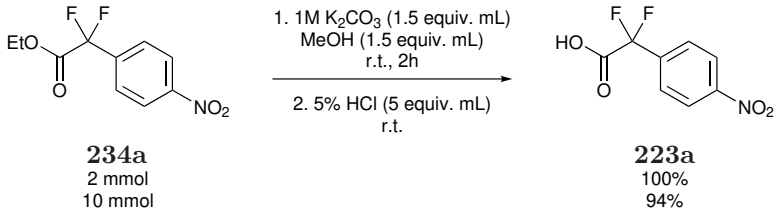

234a
2 mmol
10 mmol

223a
100%
94%

Scheme 4.15: Hydrolysis of ethyl 2,2-difluoro-2-(4-nitrophenyl)acetate following a literature procedure[164]

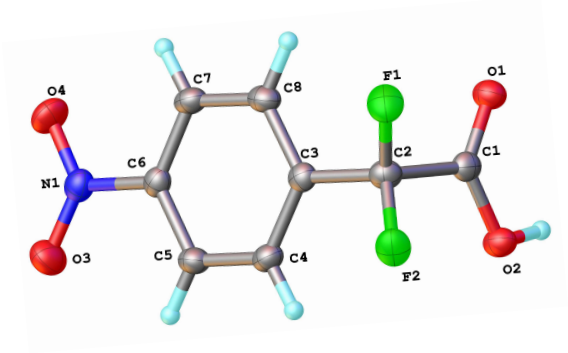

Figure 4.13: Molecular structure of 2,2-difluoro-2-(4-nitrophenyl)acetic acid as confirmed by X-ray crystallography

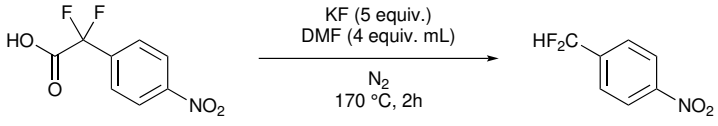

223a
2 mmol
7.3 mmol

238a
93%
94%

Scheme 4.16: Decarboxylation of 2,2-difluoro-2-(4-nitrophenyl)acetic acid following a literature procedure[164]

However, unfortunately this new direct fluorination synthetic strategy only appears to be successful with **232a**. Other ethyl phenylacetates do not appear to undergo a selective difluorination at the CH_2 position α- to the carbonyl and are usually not commercially available. A possible method of expanding the range of $ArCF_2H$ compounds made using F_2 would be to hydrogenate the $-NO_2$ group in **238a** to produce the amine **239**, and subsequently perform diazotisation reactions to produce the diazonium salt **240** (Scheme 4.18). This diazonium salt could undergo many substitution reactions to expand the range of $ArCF_2H$ derivatives available using our potentially lower cost methodology.

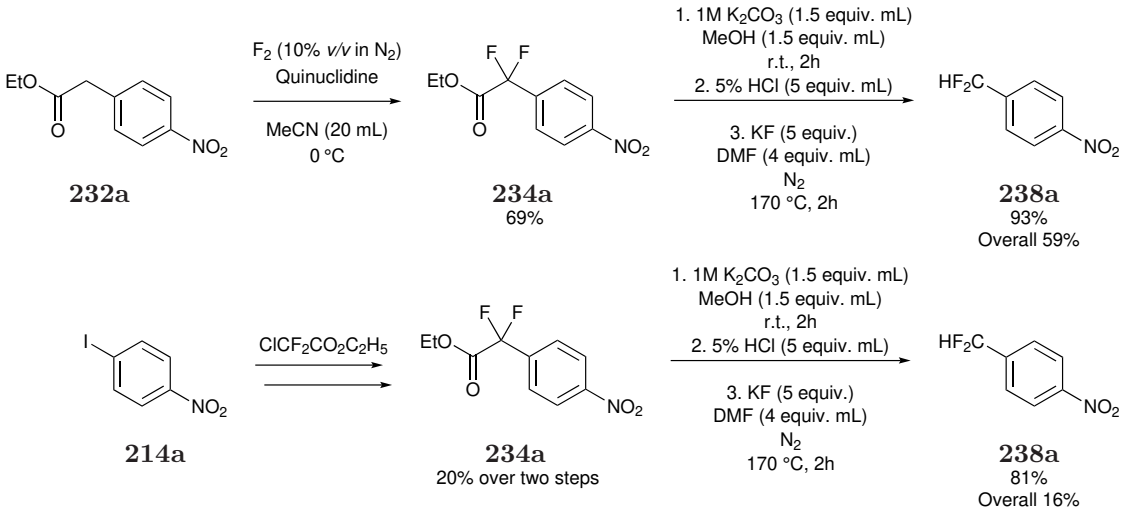

Scheme 4.17: Comparison of the 3 step route to 1-(difluoromethyl)-4-nitrobenzene using F_2 with an existing 5 step literature method[164]

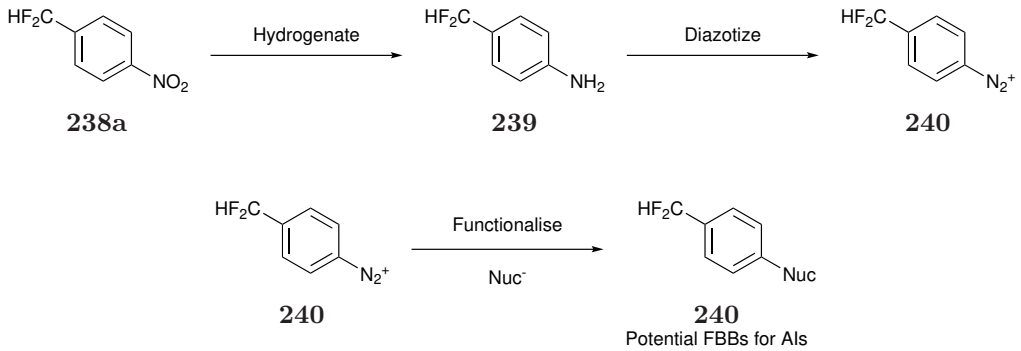

Scheme 4.18: Proposed hydrogenation and subsequent diazotisation of **238a** to produce a reactive diazonium salt

4.6.1 Hydrogentations of $ArCF_2X$ Compounds

There are two possible synthetic routes to the target **239** from the difluoroester **234a** as either of the two functionalities of **234a** could be transformed first (Scheme 4.19). There is a literature example of the hydrogenation of **234a** to give ethyl 2,2-difluoro-2-(4-aniline)acetate **241**, but not of **238a**.[175] No details were provided on the reaction conditions other than the reaction occured in EtOAc with a palladium on carbon (Pd/C) catalyst.

The following work in this chapter was undertaken during a placement at Syngenta's Jealotts Hill site under the supervision of Martin Bowden.

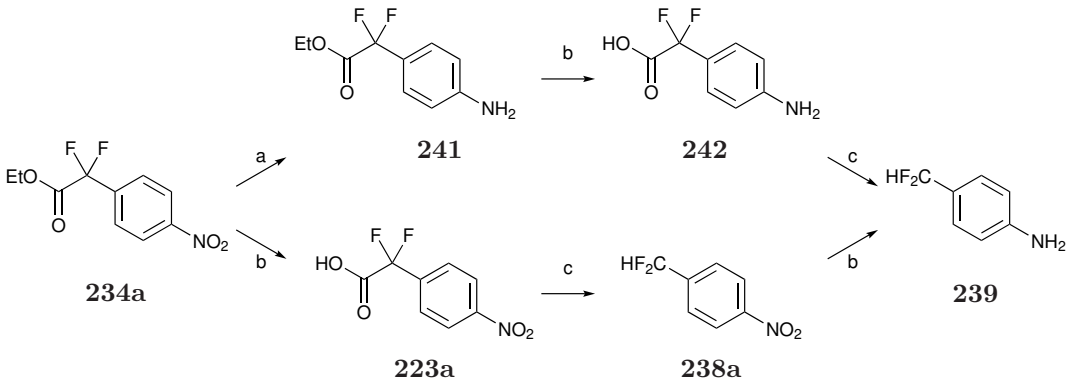

Scheme 4.19: Possible routes to 1-(difluoromethyl)-4-nitrobenzene. a) hydrogenation, b) hydrolysis, c)decarboxylation

A catalyst screening for the hydrogenation of **234a** was performed on a 0.1 mmol scale using a Cat24 hydrogenation reactor and pressurised with H_2 to 5 bar (Scheme 4.20). The screening involved trialling 10% w/mol of either a 5% Pd on C, 10% Pd on C, 5% Pt on C or 5% Rh on C in either MeOH or EtOAc (Scheme 4.20).

After the reaction, the vessel was purged of H_2 and left under an atmosphere of nitrogen for 62 h. Analysis by ^{19}F NMR spectroscopy showed no conversion to the desired product in either solvent. However, significant amount (∼30%) of the unreacted **234a** in the samples with MeOH as the solvent underwent transesterification to form methyl 2,2-difluoro-2-(4-nitrophenyl)acetate **243** when the reaction was left before workup (Scheme 4.21).

After hydrogenation, the desired amine **241** would need to be hydolysed to **242** as an intermediate step of the synthesis of **239**. Analysis of the pK_a of **242** suggests that extraction of the product into the organic layer may be difficult due to zwitterion formation. **241** can exist as one of four different forms depending on the pH, with extraction into an organic phase likely only occuring when **241** exists in a non-charged isomer. A computer simulation of the ratios of these possible products predicts that the highest distribution of the desired non charged form is 7.4% at pH 3.4 (Figure 4.14, Compound 1), and this narrow distribution range is likely to prevent a simple extraction of the **241** to be used as an intermediate step in the synthesis of **239**.

Given the potential issues in isolating **242** and the difficulty in reducing the $-NO_2$ to $-NH_2$ in **234a**, it was decided to investigate hydrogenation of **238a**. Several changes were made to the experimental setup to try and increase the conversion in each trial so a better comparison of the catalyst efficiency could be made. The

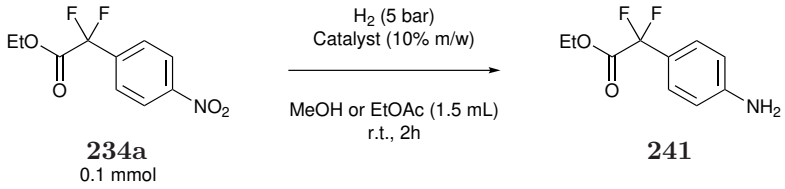

234a
0.1 mmol

241

Scheme 4.20: Catalyst screening for the hydrogenation of ethyl 2,2-difluoro-2-(4-nitrophenyl)acetate using a Cat24 hydrogenation reactor

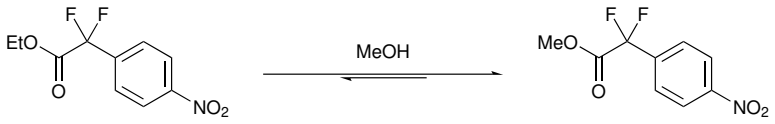

234a **243**

Scheme 4.21: Transesterification of ethyl 2,2-difluoro-2-(4-nitrophenyl)acetate

amount of catalyst added as part of the screening was increased to 10% w/w of **238a**. The hydrogenation reactor was charged with the relevant catalyst before 1.5 mL of a 0.067 M solution of **238a** was added. MeOH was replaced by EtOH as a solvent to trial hydrogenation in an protic solvent that could not cause an unwanted transesterification.

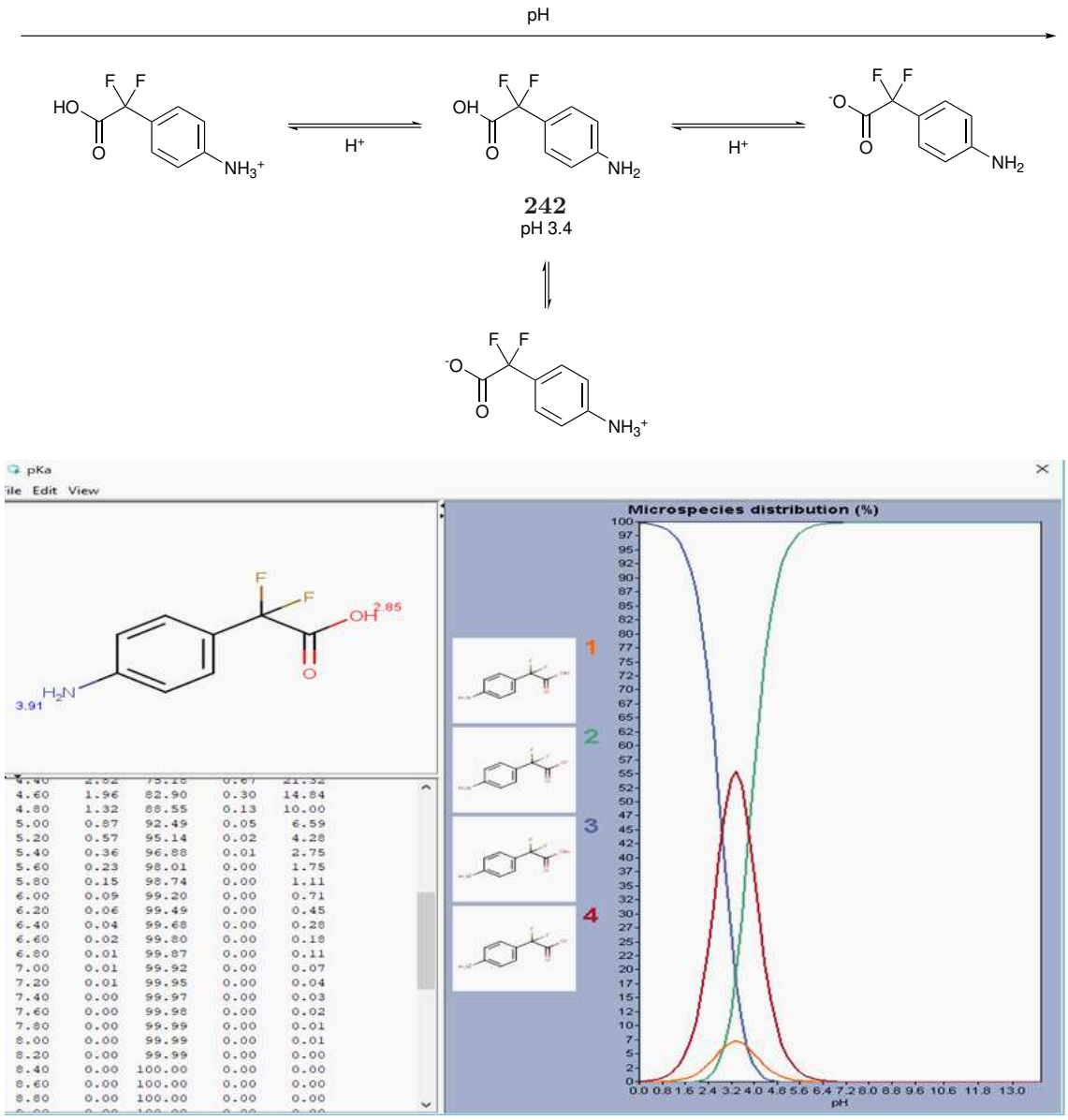

Figure 4.14: Various forms of 2,2-difluoro-2-(4-nitrophenyl)acetic acid across a range of pHs

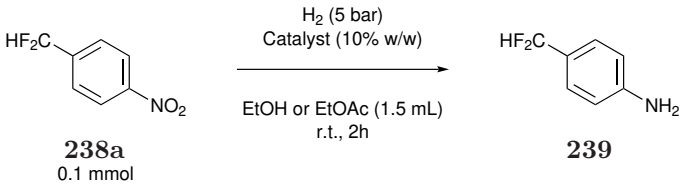

Scheme 4.22: Catalyst screening for the hydrogenation of 1-(difluoromethyl)-4-nitrobenzene

Reaction conversions were monitored by following the shift of signals in the ^{1}H and ^{19}F NMR spectra corresponding to the CF_2H moiety. In EtOH, there was no noticeable difference in the NMR spectra of the reaction mixture after hydrogenation and the starting material regardless of which catalyst was used. It appears that no noticeable conversion had taken place. By contrast, the NMR spectra of the reactions in EtOAc showed noticeable conversion of the starting material (Figure 4.15). An additional triplet was detected in the ^{1}H NMR spectra of the reaction mixture at 6.34 ppm, as were two new doublets at approximately 7.1 and 6.8 ppm.

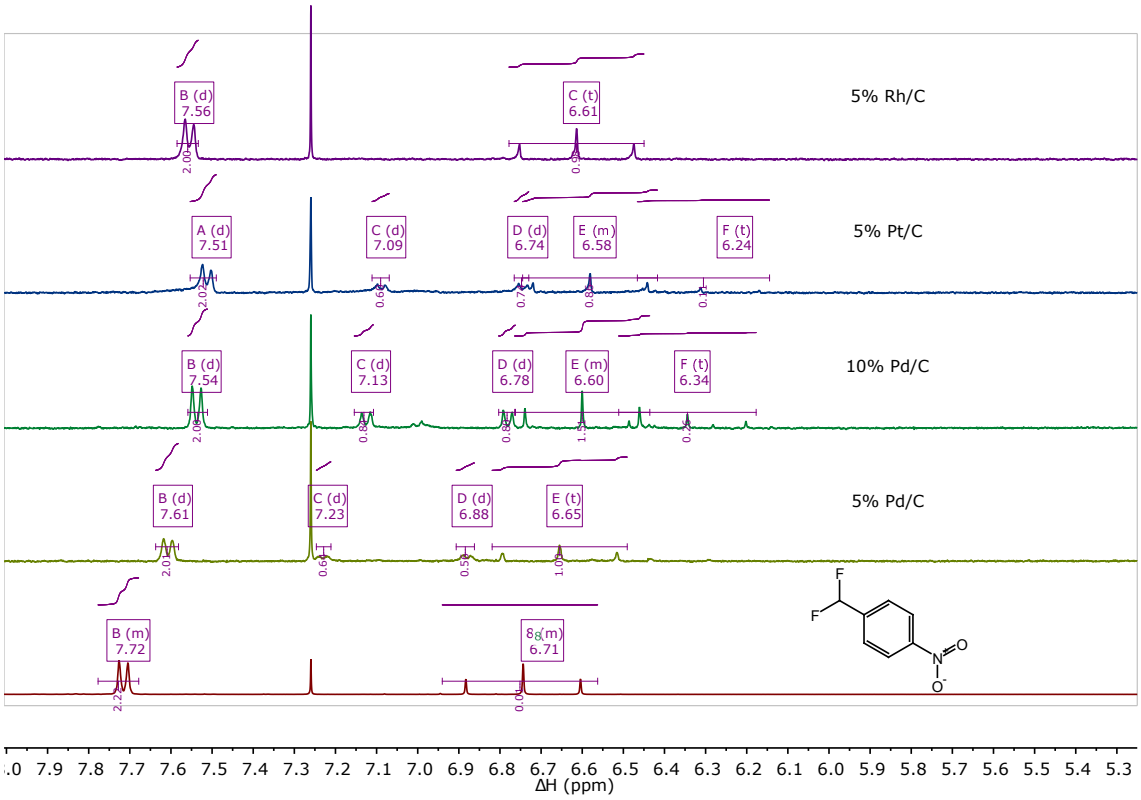

Figure 4.15: ^{1}H NMR spectra of the screens in EtOAc after hydrogenation and a 1-(difluoromethyl)-4-nitrobenzene reference

Several new doublets corresponding to various $-CF_2H$ intermediates were present in the ^{19}F NMR spectra. There are two possible reaction pathways that **238a** can undertake during hydrogenation to produce **244**, one of which involves a coupling to produce an azo intermediate (Scheme 4.23). All of these intermediates contain a $-CF_2H$ group in a slightly different chemical environment. These can be detected independently by ^{19}F NMR spectroscopy due to the sensitivity of the fluorine nucleus.

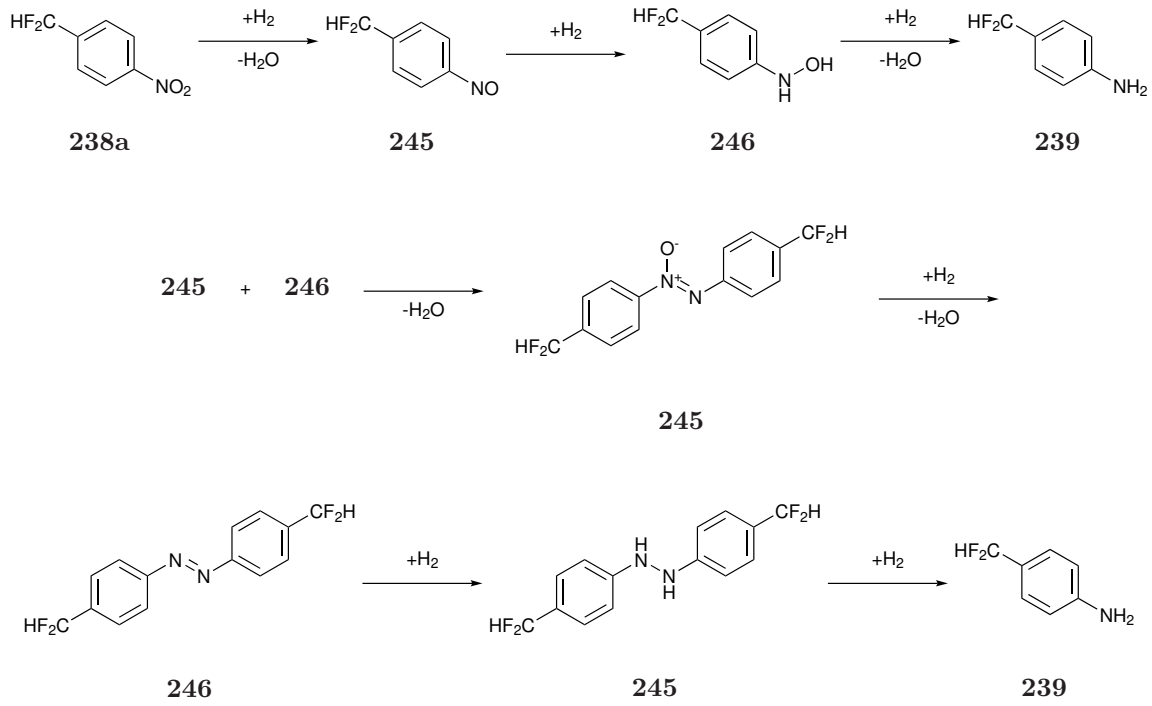

Scheme 4.23: Mechanism of the hydrogenation of 1-(difluoromethyl)-4-nitrobenzene

While the specific intermediates could not be identified by analysis of the ^{19}F NMR spectra, the conversion of **238a** could be calculated by comparing the integrals of each signal. Conversion was highest when 10% Pd/C was used as the catalyst with EtOAc as the solvent giving a 35% conversion of **238a**.

This reaction was repeated on a larger scale using an EasyMax reactor using the optimised catalyst conditions (Figure 4.16). This reactor has a significantly higher mass transfer ratio which should help increase conversion by increasing the contact between substrate, catalyst and H_2. It also allows for samples to be taken during the reaction and *in situ* monitoring using infrared (IR) spectroscopy.

Samples were periodically taken throughout the reaction and analysed by ^{19}F NMR spectroscopy. Conversion was monitored by the gradual disappearance of the doublet at −113.0 ppm indicative of **238a** and the appearance of new doublets (Figure 4.17). After 5 h 30 min there appeared to be nearly full conversion to a $-CF_2H$ containing product with a doublet at −107.5 ppm arising from the product.

The reaction vessel was purged with N_2 before samples were filtered to remove the catalyst then concentrated under reduced pressure using a rotary evaporator. During this process the product appeared to decompose, going from a clear yellow solution to a dark tar that was sparingly soluble in organic solvents. Analysis by ^{19}F NMR

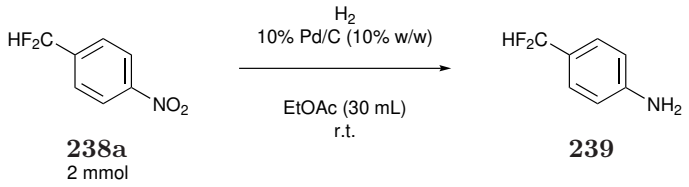

238a
2 mmol

239

Figure 4.16: Hydrogenation of 1-(difluoromethyl)-4-nitrobenzene using an EasyMax reactor

of this tar confirmed that the integral of the peak at −107.5 ppm had significantly decreased while signals at −111.4 and −112.0 ppm increased (Figure 4.18).

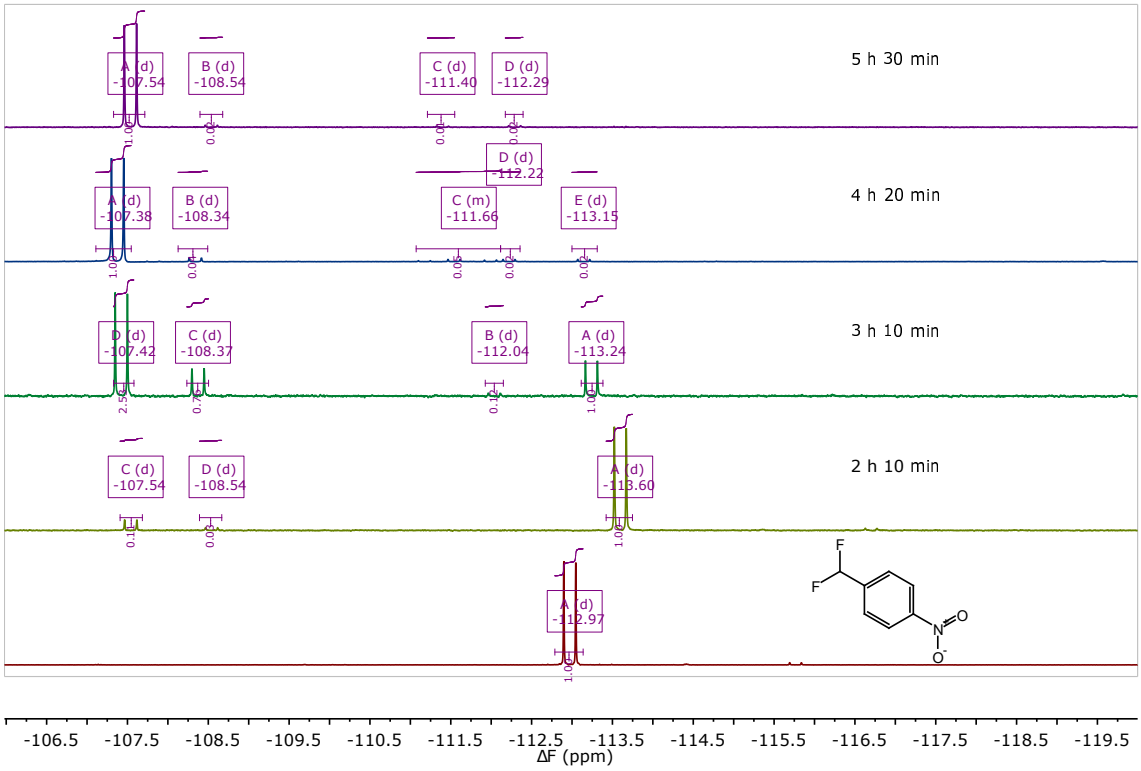

Figure 4.17: ^{19}F NMR spectra of samples taken at increasing time intervals

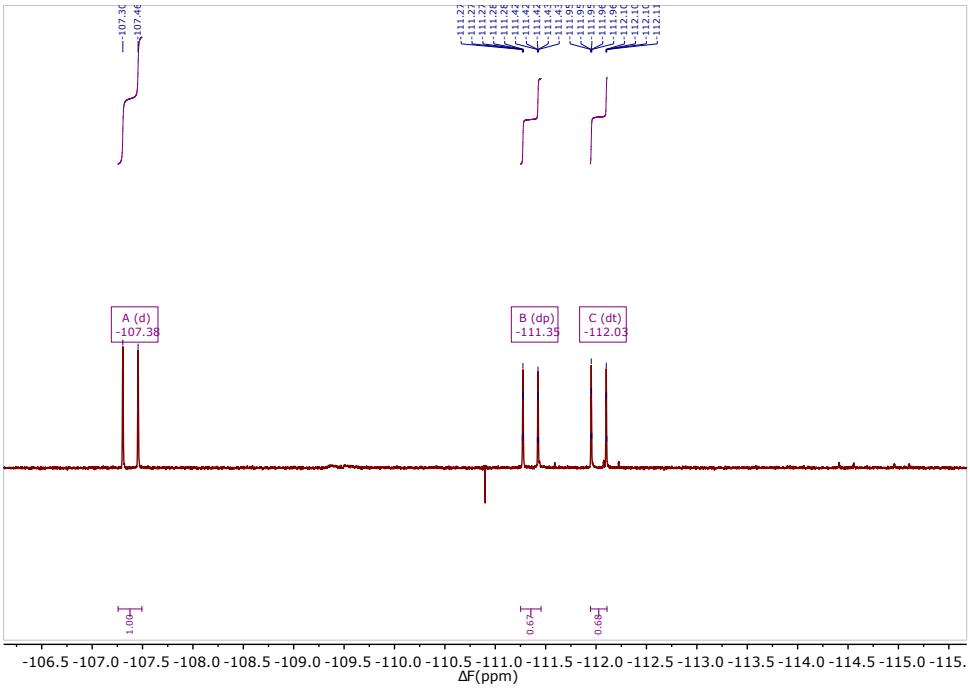

Figure 4.18: ^{19}F NMR spectra of the orange tar

Any azo intermediates present are likely to be unstable when the solvent is removed. Additionally the target product **239** may also be unstable in air due to the pres-

ence of an amine and $-CF_2H$ moiety *para* to each other (Scheme 4.24). There is no reported literature on the synthesis or properties of **239** which may be due to difficulties in its isolation.

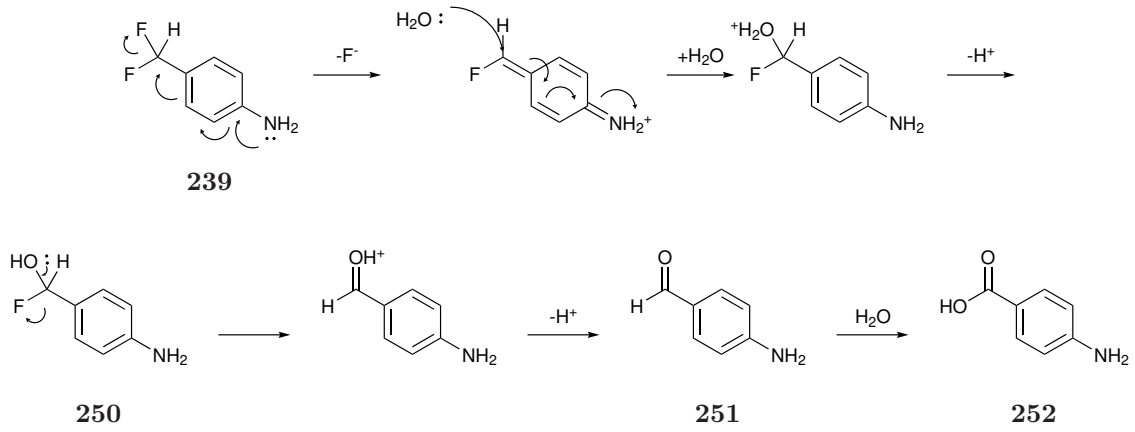

Scheme 4.24: Possible hydrolysis of 4-(difluoromethyl)aniline

The reaction was repeated with the substrate under hydrogenation conditions for 6 h to try and push conversion completely to the desired product **253**. After filtering off the catalyst, the product was concentrated by rotary evaporation to yield a dark brown solid that was also sparingly soluble in $CDCl_3$. Analysis of the ^{19}F NMR spectrum showed the presence of similar doublets indicating that a similar decomposition has occurred. No further attempts at isolating **253** from the tarry mixtures were attempted.

4.7 Further Reactions of Ethyl 2,2-Difluoro-2-(4-nitrophenyl)acetate

Unfortunately, reduction of the $-NO_2$ group in both **234a** and **238a**, and isolation of the amine products proved unsuccessful. Other reactions of **234a** were carried out in collaboration with Jonathan Hill, a 4th year MChem student at Durham University, and the rest of this chapter is a brief summary of the results of his Masters thesis, included here for completeness.[176]

Reduction to the alcohol using sodium borohydride ($NaBH_4$) following a literature procedure was achieved with complete conversion at r.t. highlighting how incorporation of fluorine α- to a carbonyl increases its electrophilicity.[177] The desired product 2,2-difluoro-2-(4-nitrophenyl)ethanol **254** was isolated in 90% yield after tituration with hexane and filtration through celite (Scheme 4.25).

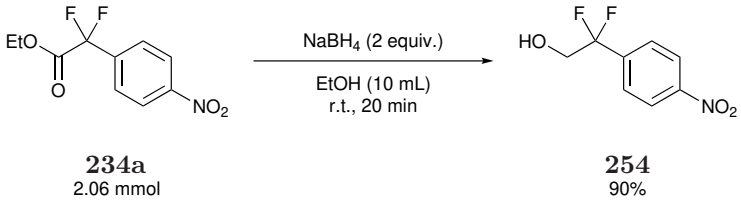

Scheme 4.25: Reduction of ethyl 2,2-difluoro-2-(4-nitrophenyl)acetate using $NaBH_4$[176]

A sample was dissolved in $CHCl_3$ and gave crystals by slow evaporation of the solvent which were analysed by single crystal XRC. Investigation of the F−C−C=O torsion angles shows that the C−OH bond bisects the F−C−F moiety.

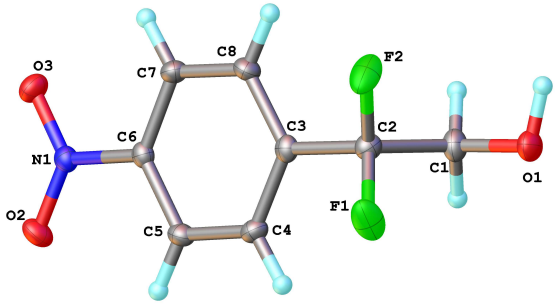

Figure 4.19: Molecular structure of 2,2-difluro-2-(4-nitrophenyl)ethanol as confirmed by X-ray crystallography

The tosylation reaction of the non-fluorinated derivative of **254** has previously been reported in the literature.[178] This methodology was followed to tosylate **254** to give 2,2-difluoro-2-(4-nitrophenyl)ethyl tosylate **255** in good isolated yields of 68% (Scheme 4.26).

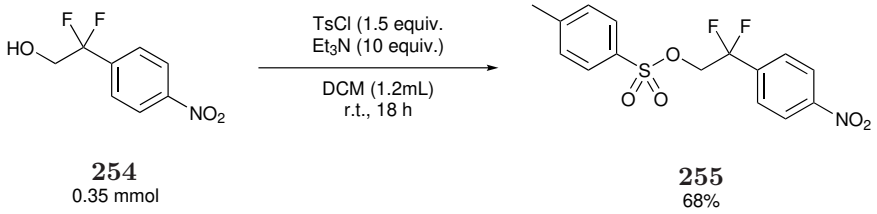

Scheme 4.26: Tosylation of 2,2-difluro-2-(4-nitrophenyl)ethanol[176]

Amidation reactions were performed between **234a** and a range of amines similarly to previous aminations using **211** (Table 3.7). Conversions and isolated yields were significantly higher when **234a** is used highlighting the increased reactivity of the *gem*-difluoro ester compared to the 2,2-difluoro BKE.

Table 4.3: Amidation reactions of ethyl 2,2-difluoro-2-(4-nitrophenyl)acetate[176]

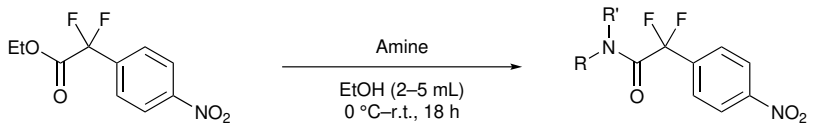

234a **256**

Entry	Base	Product	Structure	Isolated Yield/%
1	Benzylamine	**256a**	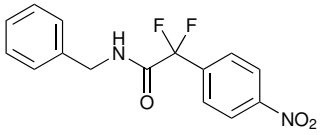	94
2	Allylamine	**256b**	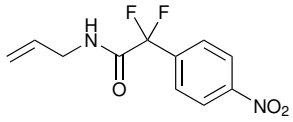	99[a]
3	Propargylamine	**256c**	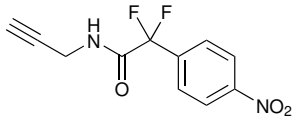	95
4	Morpholine	**256d**	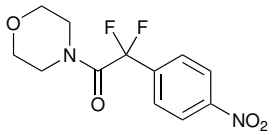	97
5	Methylamine	**256e**	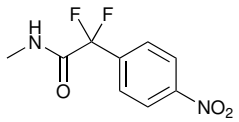	95[a]
6	*t*-Butylamine	**256f**	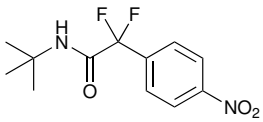	90

[a] Reaction was carried out using an excess of the amine and no solvent.

With the exception of **256e**, the desired products were isolated as solids. Crystals were grown by slow evaporation of $CHCl_3$ and analysed by XRC. These single crystals exist as a mix of monoclinic or orthorhombic crystal systems, and usually adopt conformations in which the two fluorine atoms are paired *gauche-anti* to the C=O moiety. This geometry minimises unfavourable dipole-dipole interactions between the C=O and the two C−F groups and also maximises possible intramolecular H-bonding between the amide proton and a fluorine atom. An *eclipsed-eclipsed* conformation is seen in **256d** due to the lack of proton on the amide produced by the secondary amine morpholine which prevents stabilisation from an intramolecular H-bond. Without this stabilisation, the fluorine atoms would not appear *anti* to

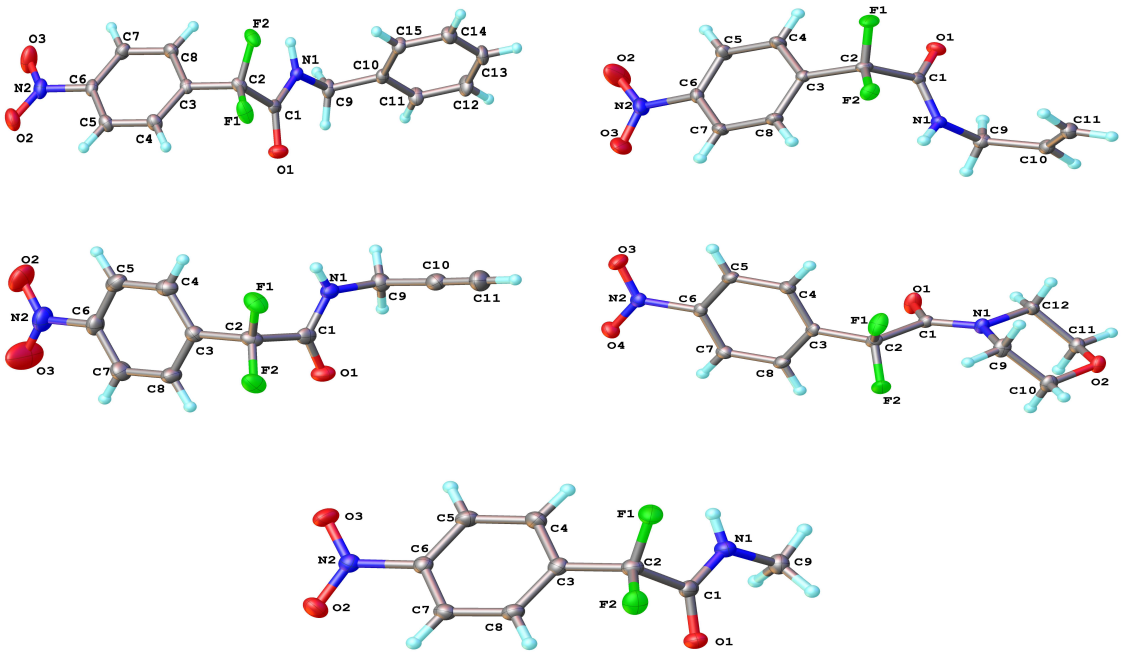

Figure 4.20: Molecular structure of difluoroamides **256a**–**d**,**f** as determined by XRC[176]

the C=O, and instead are both *eclipsed* in order to maximise distance between the three EWGs.

4.8 Conclusion

Several nitrogen bases were trialled to increase the selectivity of fluorination of nitrophenylesters with F_2 to give desired ethyl 2,2-difluoro-2-phenyl esters. Similarly to the fluorination of 1,3-diketones and BKEs, quinuclidine was found to most effectively mediate fluorination to give the desired *gem*-difluoro product. The 4-nitrophenyl derivative **232a** was successfully difluorinated to give a product that could be isolated. This was successfully hydrolysed and decarboxylated following a literature procedure to the corresponding $ArCF_2H$ derivative, but attempts at subsequent hydrogenations were unsuccessful. The difluoroesters appear more reactive than their related non-fluorinated analogues, and were successfully reacted with several amines, with their structures confirmed by XRC.

Chapter 5

Attempted Direct Fluorination of Aromatic Systems Using Mediating Agents

Previous chapters of this thesis have focused on the use of F_2 as a selective fluorination reagent to synthesise potential difluorinated FBBs. One of the most widely used class of FBB are the fluoroaromatics and this Chapter will focus on the ongoing development of synthesising fluoroaromatics with high selectivity using F_2 as the source of fluorine.

5.1 Introduction to Fluoroaromatics

HF is often used on an industrial scale to synthesise fluorobenzene derivatives using halex reactions with other haloaromatics, or by using well established Balz-Schiemann chemistry. In this case, a reactive diazonium salt is allowed to thermally decompose in the presence of an HF source to generate the desired fluoroaromatic (Scheme 5.1). While care is needed with the unstable diazonium intermediate, the reaction does not require the presence of an EWG, on the aromatic ring as would be needed for a standard nucleophilic aromatic substitution (S_NAr) processes.

Previous work at Durham has shown that direct fluorination of aromatic substrates using F_2 can proceed with some selectively using acidic conditions. Mono- and difluorination of 1,4-disubstituted aromatic compounds occurs *ortho* to EDGs and *meta* to EWGs as would be expected of an electrophilic aromatic substitution (S_EAr)

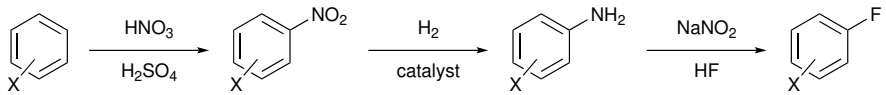

257 **258** **259** **260**

Scheme 5.1: Multistep synthesis of fluoroaromatics using Balz-Schiemann chemistry

process (Scheme 5.2).[99,179] The presence of a single strong EWG such as $-NO_2$ or $-CN$ affords good conversion of starting material, but substrates bearing two EWGs prevents fluorination indicating that highly electron deficient aromatics do not react well with F_2. Fluorinations of electron rich aromatics containing two or more alkoxy groups leads to a complicated mixture of fluorinated products.[127]

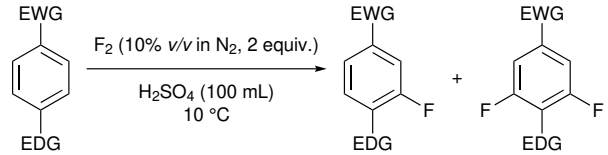

261 25 mmol **262** **263**

Scheme 5.2: Fluorination of 1,4-disubstituted aromatics[99]

Fluorinating aromatics with an EWG *para* to an EDG allows for good regioselectivity of fluorination *ortho* to the EDG as would be expected for an S_EAr process. For example, full conversion of 4-nitroanisole **264** can be achieved if fluorinated in HCOOH (Scheme 5.3).[99,102]

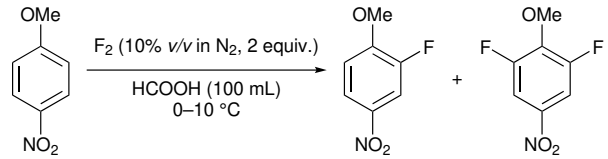

264 25 mmol **265** 50% **266** 20%

Scheme 5.3: Fluorination of 4-nitroanisole in HCOOH[99]

5.2 Fluorination of Aromatics

Similar attempts at fluorinating simple aromatics using F_2 were trialled under basic conditions to try and increase the selectivity of aromatic fluorination for more electron rich substrates. Quinuclidine was trialled as a mediating agent due to its success

at improving the selectivity of fluorinations with F_2 α- to carbonyls as described in previous chapters.

5.2.1 Anisole

Anisole was fluorinated with an equivalent of quinuclidine at a flow rate of 15 cm^3 min^{-1} (Scheme 5.4). After the reaction had proceeded for approximately 5 minutes small amounts of a white gas, presumably HF, evolves.

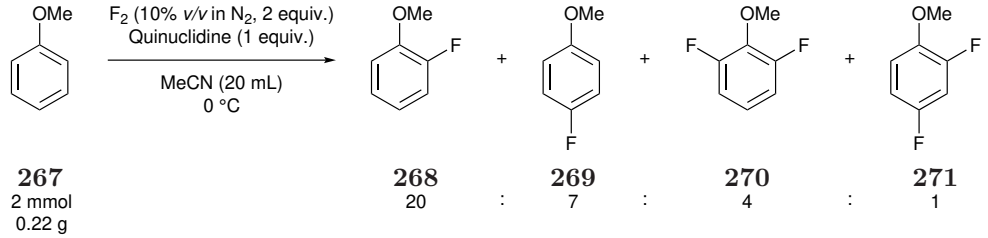

Scheme 5.4: Quincuclidine mediated fluorination of anisole

An aqueous workup was performed and yielded 0.244 g of a mixture of a brown oil with small amounts of tar. This tar was not soluble in $CDCl_3$. Analysis of soluble organics by ^{19}F NMR spectra showed several fluorinated products as well as some unidentifiable peaks. Fluorinated analogues were identified by comparing chemical shifts in the ^{19}F NMR spectra to reference samples. Comparison of the intensities of the 5 signals due to $-OMe$ moieties in the ^1H NMR spectrum indicated that 60% of the oily tar consisted of unreacted **267**. Ratios of the identified fluorinated products were calculated, and showed that **267** was preferentially converted to **268**.

The two difluoro products **270** and **271** have boiling points of 78 °C and 85 °C. It is, therefore, possible that some of these products were lost on the rotary evaporator when the MeCN and EtOAc used in the reaction and purification steps were removed. The 3-fluoro product **272** was not detected to have been made by ^{19}F NMR spectroscopy. Fluorinated products could not be isolated by Kugelröhr distillation and this non-selective reaction was not studied further.

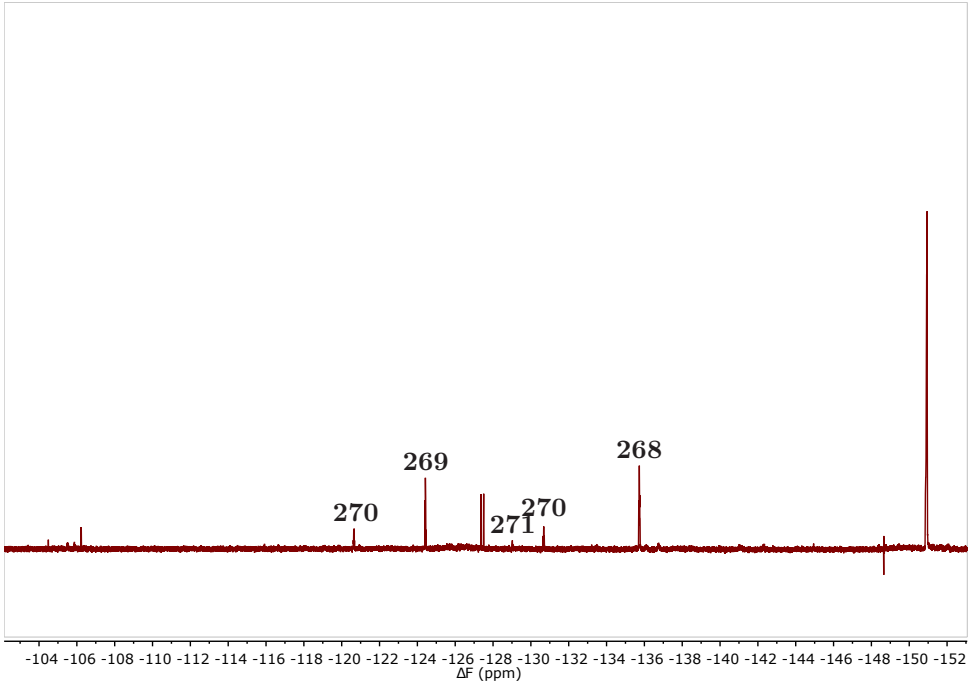

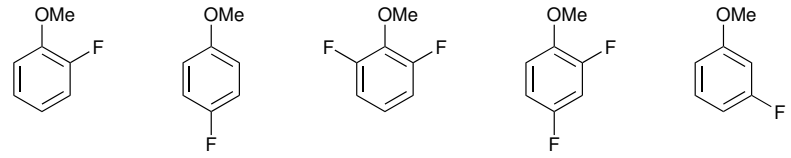

268	**269**	**270**	**271**	**272**
		Literature values:		
−135	−125		−121, −131	−113

Figure 5.1: ^{19}F NMR spectrum of product from fluorination of anisole[180–182]

5.2.2 Aniline

A similar reaction was performed using aniline as a starting material (Scheme 5.5). After 5 minutes, large volumes of HF were produced as seen by the evolution of large amounts of white gas. During this time the reaction solvent rapidly changed from a very pale yellow to a clear orange colour. At this point, the flow rate was reduced from 15 to 5 mL min^{-1} for the remainder of the experiment. After workup, a black polyfluorinated tar was produced containing numerous signals in the ^{19}F and ^{1}H NMR spectra. The reaction was not pursued further.

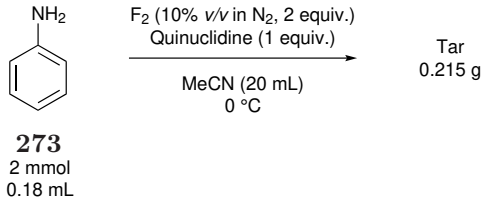

Scheme 5.5: Quincuclidine mediated fluorination of aniline

5.2.3 4-Nitroaniline

4-Nitroaniline was then trialed as a less activated aniline system due to the incorporation of a $-NO_2$ group (Scheme 5.6).

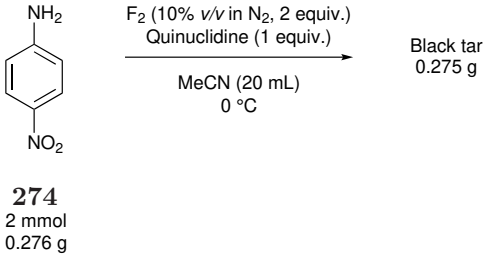

Scheme 5.6: Quincuclidine mediated fluorination of 4-nitroaniline

Significantly fewer fluorinated signals were detected in the ^{19}F NMR spectrum of the crude product. Purification by Kugelröhr distillation was attempted to try and identify these products but proved unsuccessful. After this result, no further investigations of anline based systems were investigated.

5.2.4 4-Nitroanisole

Given the synthetic problems using anisole and aniline as starting materials, a less activated substrate was used to assess the effect of quinuclidine on fluorination reactions. 4-Nitroanisole **264** was trialled. Unlike anisole, it is a solid, and so it is unlikely that there will be volatility issues caused by the addition of fluorine atoms to the aromatic ring. The introduction of a $-NO_2$ group in the 4-position should also limit the number of fluorinated products produced by blocking the *para* position. The $-$OMe group will activate the ring *ortho* to its position while the $-NO_2$ group will deactivate the ring, but also direct electrophilic substitution at the same position.

A sample of **264** was fluorinated using our previous methodology (Scheme 5.7). The reaction solvent was removed under reduced pressure, and an aqueous workup

performed yielding a large amount of orange tar that was only partially soluble in $CDCl_3$. This tarry mixture was then filtered through a small scale silica plug with $CHCl_3$ as the eluent to remove the tar and yield 0.158 g of yellow crystals.

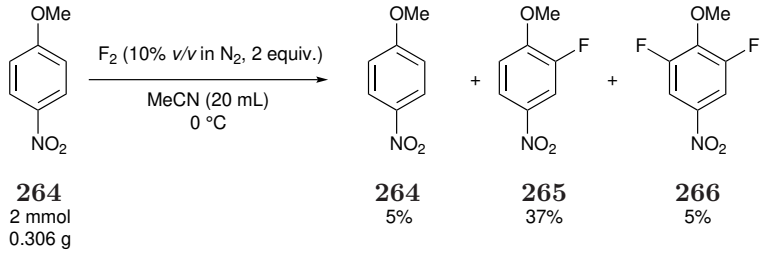

Scheme 5.7: Fluorination of 4-nitroanisole

Analysis of the crude product by NMR spectroscopy and GC-MS indicated the presence of significant amounts of tar, as well as products with a m/z of 171 and 189 corresponding to the formation of a monofluoro and difluoro product. Two peaks were present in the ^{19}F NMR spectra at shifts consistent with **265** and **266** (Figure 5.2). Yields of each product were estimated by calculating the relative product distribution of these crystals. Trace amounts of an additional unidentified product (X) was detected in the ^{19}F NMR spectra (Figure 5.2).

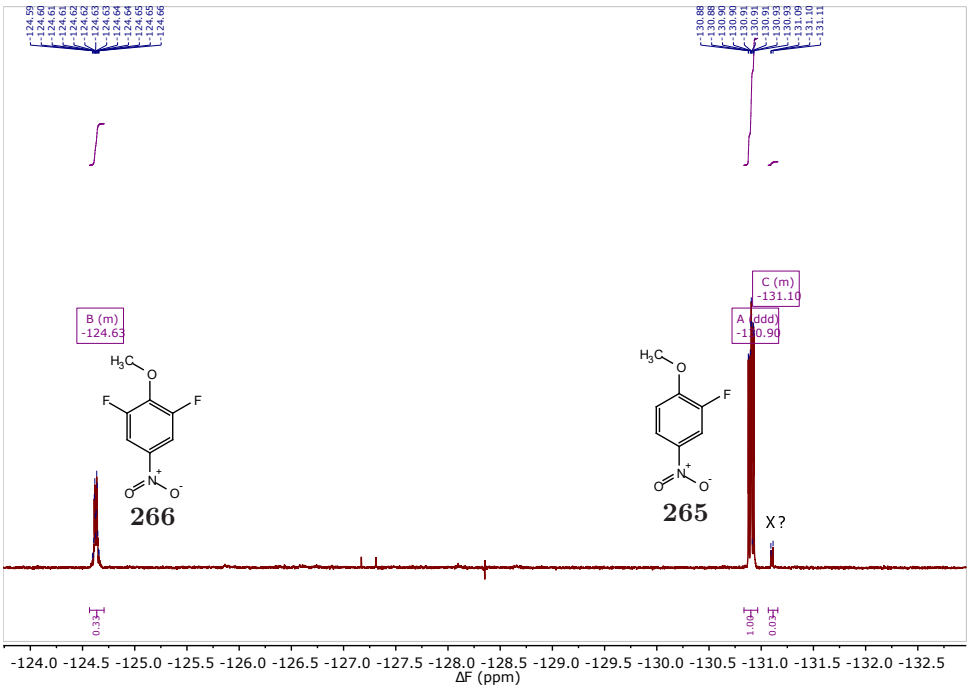

Figure 5.2: ^{19}F NMR spectrum of product mixture from the fluorination of 4-nitroanisole **264**

The fluorination was repeated with the addition of an equivalent of quinuclidine (Scheme 5.8) and, after purging, the reaction was filtered through a small scale silica plug (Figure 3.2) with MeCN as the eluent to remove unwanted tarry by-products. Removal of solvent under reduced pressure gave 0.323 g of an orange solid.

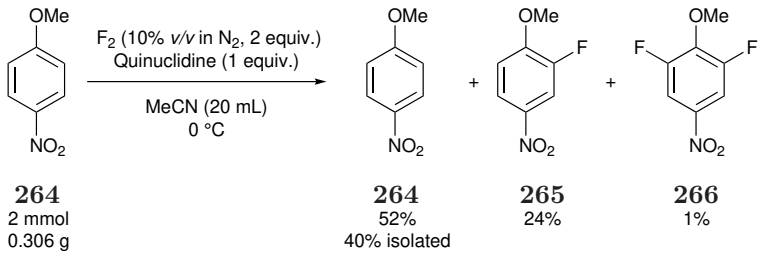

Scheme 5.8: Quincuclidine mediated fluorination of 4-nitroanisole

Purification of the crude product was performed by column chromatography on silica gel with a gradient of 0–15% EtOAc *v/v* in hexane solvent mixture as the eluent. Unreacted **264** was isolated in a 40% yield while other fractions contained mixtures of two compounds. By comparing the relative integrals and coupling constants (J) of signals in the NMR spectra with product masses from GC-MS results taken of each fraction, it was possible to identify the identity of each peak in the ^{1}H NMR spectra of the crude products of both reactions (Figure 5.3).

While the conversion of **264** is higher when no base is added, a significant amount of tar was produced. The addition of quinuclidine as a mediating agent lowered the overall conversion, but also limited the formation of unwanted tar.

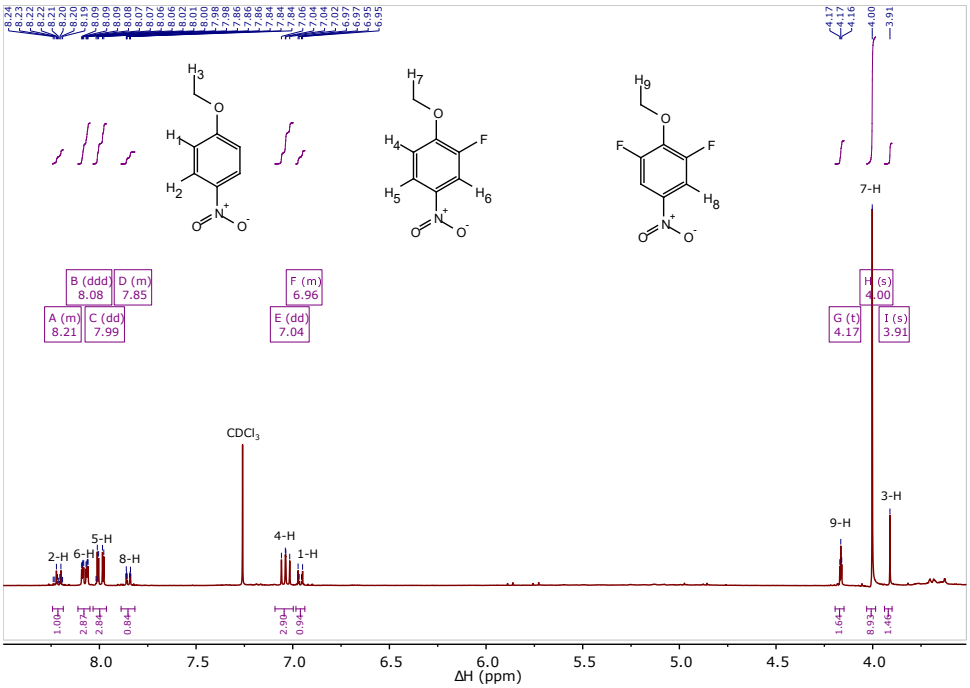

Figure 5.3: ^{1}H NMR spectrum from the quinuclidine mediated fluorination of 4-nitroanisole

5.2.4.1 Base Screening

Quinuclidine appears to lower the reactivity of F_2 when 4-nitroanisole **264** is the substrate as shown by the lower conversion and lack of other fluorinated products or tar. Other nitrogen bases were trialled in order to compare their effect at mediating the selectivity of fluorination to the desired products **265** and **266** (Table 5.1).

Previous attempts at workup involved an aqeuous workup. While this is an efficient method of removing HF, it does not appear to remove unwanted tarry products. During base screening reactions, the reaction mixture was concentrated under reduced pressure after fluorination. This mixture was then filtered through a small scale silica plug with $CHCl_3$ as the eluent to remove unwanted HF and tarry products. Yields of the desired products were then calculated by comparing the product distributions of the samples after removal of all unwanted tarry by-products.

Table 5.1: Screening conditions for the base mediated fluorination of 4-nitroanisole **264**

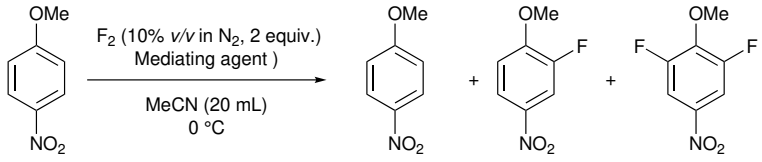

264 2 mmol | **264** | **265** | **266**

Entry	Base	Equiv. of base	NMR yield/%			Recovered mass/%
			264	**265**	**266**	
1	-	-	5	37	5	47[a]
2	Quinuclidine	1	52	24	1	77[a]
3	-	-	11	65	9	86
4	Quinuclidine	1	67	20	3	90
5	Quinuclidine	2	90	3	0	93
6	DABCO	1	94	5	0	99
7	DABCO	2	95	2	0	97
8	DBU	1	76	19	2	97
9	DBU	2	92	4	1	96
10	Et_3N	1	49	25	3	77
11	Et_3N	2	91	3	1	95
12	Pyridine	1	74	11	2	87
13	Pyridine	2	94	3	0	97
14	DABCO	1[b]	23	51	5	79
15	DBU	1[b]	Polyfluorinated tar			
16	Et_3N	1[b]	Polyfluorinated tar			

[a] Aqueous workup performed prior to washing the product mixture through a small silica plug with $CHCl_3$ as the eluent

[b] 5.0 equiv. of F_2 used

Repeating the previous fluorinations of **264** without performing an aqueous workup significantly improved the recovered yield (Table 5.1, Entries 1–4). Increasing the equiv. of quinuclidine (Table 5.1, Entry 5) lowered the conversion of **264** to desired fluorinated products, but increased the recovered mass. It appears that an excess of base interacts with either F_2 or **264** and significantly limits the overall amount of fluorination that occurs. A similar trend was observed for allmost all of

the nitrogen bases when the equivalents were increased from one to two. In each case, the recovered yield increased, but the proportion of unreacted starting material increased to ∼90% of the recovered material. Exceptions were when DABCO or DBU were used (Table 5.1, Entries 6–9). There was very little change in the product distribution when the equivalents were increased from one to two and these bases prevent almost any tar from being formed. Unfortunately DABCO almost completely stopped fluorination of **264** from occurring.

The highest conversion to the fluorinated products **265** and **266** was achieved when Et_3N was used as the mediating agent (Table 5.1, Entry 10). Unfortunately, the conversion of **264** to desired fluorinated products was significantly lower than previously reported using no base or HCOOH as the solvent (Scheme 5.3).[99]

In an attempt to push conversion, mediations using DABCO, Et_3N and DBU were trialled using a large excess (5 equiv.) of F_2 (Table 5.1, Entries 14–16). When Et_3N and DBU were trialled the excess of fluorine caused large amounts of unselective fluorination to occur producing large amounts of tarry products that could not be removed by the small scale silica plug purification method.

Conversion to **265** reached 51% when DABCO was used, significantly higher than other attempts (Table 5.1, Entry 14). It appears that while DABCO lowers the reactivity of F_2 with **264**, it appears to promote selective fluorination as seen by the relatively high recovered yield of 79% and minimal formation of tar compared to Entries 15–16.

It is possible that there is some form of interaction between F_2 and DABCO that occurs preferentially to a reaction between F_2 and **264** which accounts for the low conversion of **264** when 2 equiv. of DABCO were added (Table 5.1, Entry 7). This might involved forming small amounts of an *N*-fluoro compound which performs the fluorination, and then is remade *in situ* by the addition of F_2 (Scheme 5.9).

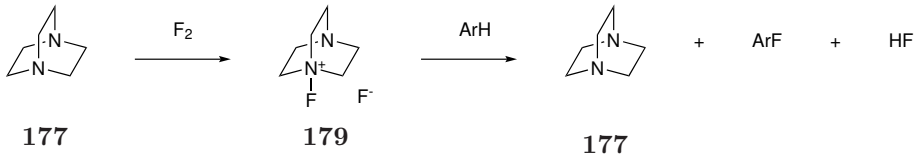

177 **179** **177**

Scheme 5.9: Possible fluorination by an *in situ* N-F reagent

To test this hypothesis, fluorination of **264** was attempted with the commonly available electrophilic fluorinating agent Selectfluor™ **66** (Scheme 5.10). This fluorinat-

ing agent has a similar structure to any possible N-F compound produced between DABCO and F_2 (Scheme 2.2).

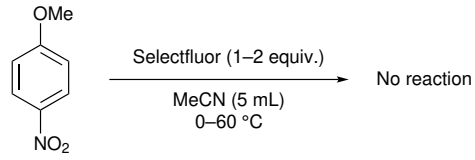

264
0.5 mmol

Scheme 5.10: Selectfluor™ fluorination of 4-nitroanisoleane

After stirring overnight at r.t., no reaction appeared to have occurred by NMR spectroscopy. The reaction mixture was then left to react for 72 h at 60 °C, but again no conversion was detected by NMR spectroscopy. The reaction was repeated with 2 equiv. of **66** but again no reaction with **264** was detected by NMR spectroscopy. This indicated that an *N*-F compound made *in situ* between DABCO and F_2 is unlikely to be a fully formed *N*-fluoro salt and may have a loose interaction between the base and F_2.

5.3 Conclusion

New industrially viable routes to fluoroaromatics are desired to increase the range of available FBBs at lower costs. Several fluorinations of a mixture of electron rich and electron poor aromatics in MeCN were performed, and various nitrogen bases were trialled as mediating agents. Electron rich aromatics were fluorinated in multiple different positions which prevented simple determination of products and their isolation.

The presence of an EWG *para* to an EDG in the case of 4-nitroanisole allowed for regioselective fluorination to form one of two fluorinated products. The additions of nitrogen bases increased the recovered mass by limiting the formation of polyfluorinated tar, but also tended to limit the overall rate of fluorination. Conversions are currently lower than related fluorinations in acidic systems, but by increasing the amount of F_2 added and further base screening, it may be possible to achieve regioselective fluorinations of *para*-substituted aromatics with full conversion of starting material by this base mediated approach.

Chapter 6

Conclusions

In this thesis we have presented the advantages of organofluorine chemistry, in particular the beneficial impact of introducing a $>CF_2$ functionalitiy into potential active ingredients. While methods of selectively introducing a $>CF_2$ group into an organic molecule is an active area of research, there are limited industrially viable routes available. In this thesis, selective difluorination α- to carbonyls was investigated using fluorine gas as a potentially cheaper route to this class of compounds for large scale synthesis.

Selective difluorination of 1,3-diketones was investigated using F_2 (Scheme 6.1). We discovered that the addition of various nitrogen bases had a noticeable effect on the efficiency of the fluorination reaction and, in particular, the addition of quinuclidine afforded high conversion to desired 2,2-difluoro products.

This synthetic methodolgy was successfully applied to related 1,3-ketoester compounds. Further base screening was investigated, though quinuclidine again provided the highest conversion to the desired 2,2-difluoro products. Reactions with various amines were established to generate difluoro amides by utilising the increased reactivity of 2,2-difluoro-1,3-ketoesters towards nucleophiles (Scheme 6.2).

Highly desired fluorinated systems are $ArCF_2H$ containing compounds. Methods for the synthesis of $ArCF_2H$ compounds was expanded to include the one-step synthesis using F_2 highlighting the application of base mediated direct fluorinations of sufficiently reactive monocarbonyl compounds (Scheme 6.1, **232a**). Further attempts to expand the substrate scope by developing hydrogenation conditions were investigated at Syngenta's Jealotts Hill site with limited success.

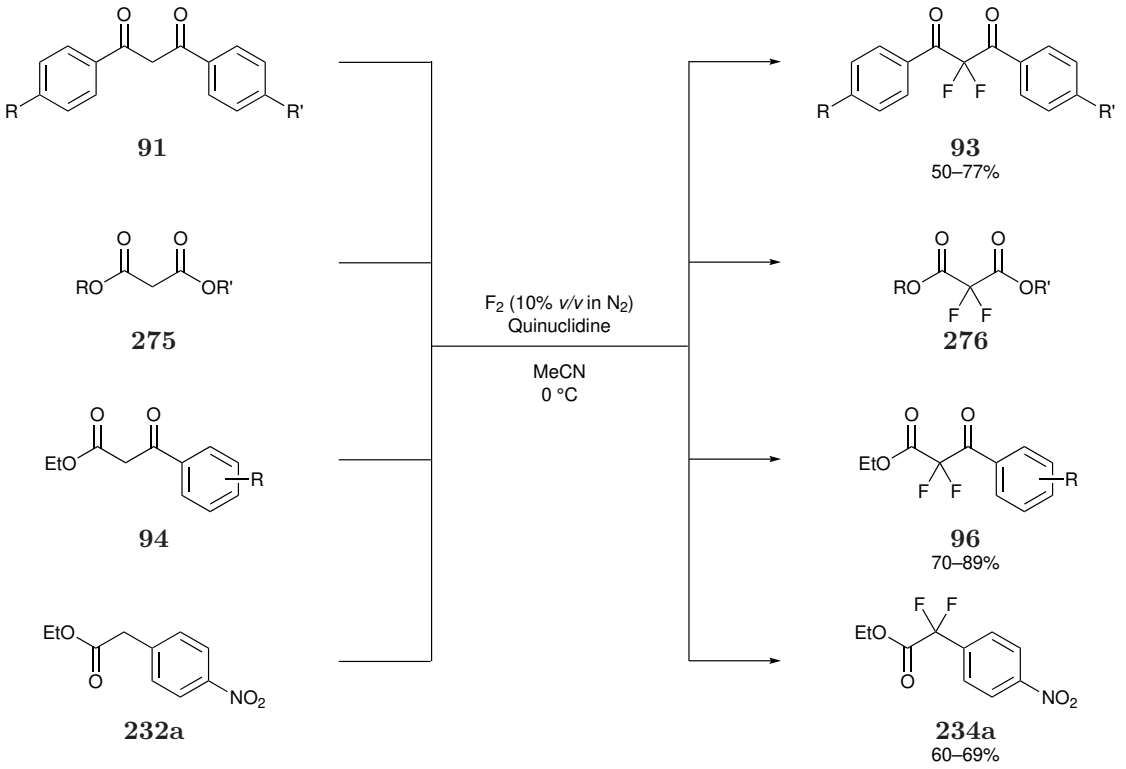

Scheme 6.1: Summary of selective difluorinations performed using F_2 in this thesis

Amidation reactions of difluoro-amide **232a** were undertaken in collaboration with MChem student Jonathan Hill. X-ray analysis of these products provides further insight into the effect of intramolecular H–F interactions on the conformation around the amide bond.

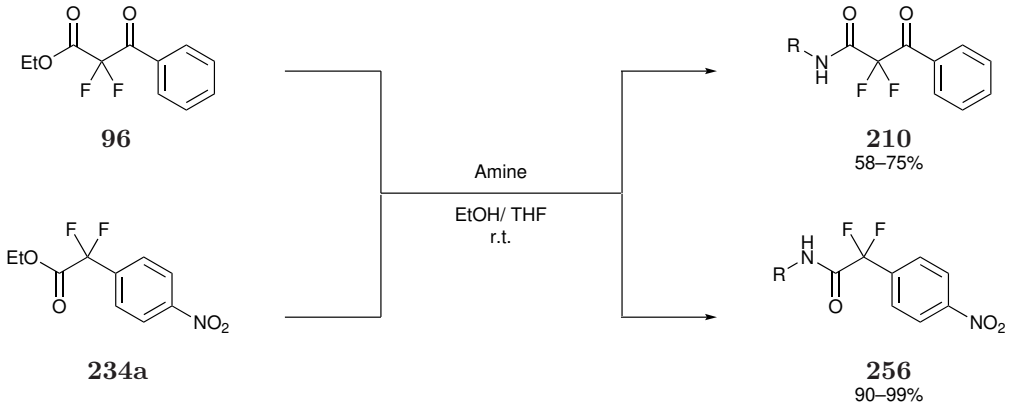

Scheme 6.2: Summary of amidation reactions performed on difluoroesters

The final chapter involved further development on direct fluorinations of aromatic systems. It appears that the addition of nitrogen bases lower the overall conver-

sion and prevent the formation of unwanted tar-like by-products but conversions to desired products remained low.

Out of all the mediating agents tested, quinuclidine was the most successful mediating agent at increasing conversion to the desired difluoro- products. While some mechanistic experiments were undertaken in Chapter 2 to try and identify the roles of quinuclidine in the fluorination, the specific reasoning behind quinuclidines superior results remains elusive. Comparing the conversion to desired products against the pK_a of the nitrogen bases gives no evidence as to why quinuclidine affords such a selective difluorination (Figure 6.1).

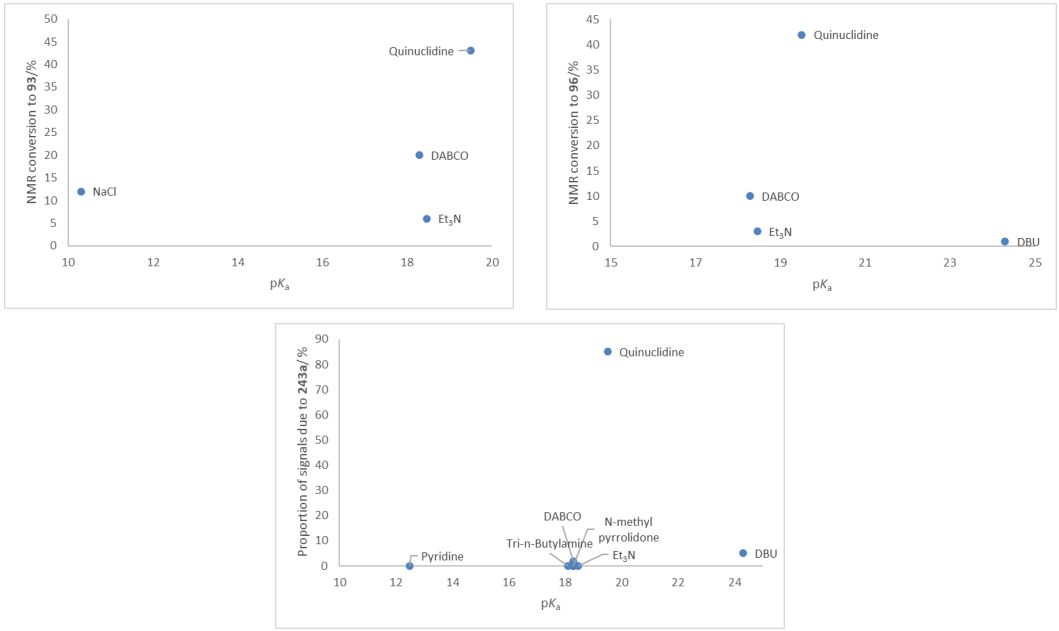

Figure 6.1: Comparisons of the NMR conversions to **93** (top-left), **96** (top-right) and selectivity for **234a** compared to other signals in the ^{19}F NMR spectrum (bottom) for various mediating agents

Many of the substrates fluorinated in this thesis undergo monofluorination or no reaction with the commonly used electrophilic fluorinating agents Selectfluor™. It appears that a quinuclidine-HF adduct forms an *in situ* fluorinating agent with F_2. This appears to be more reactive than commercially available solid, electrophilic fluorinating agents, while less reactive than F_2 as shown by the selective formation of *gem*-difluoro products (Scheme 6.3).

Overall, new methodology for the synthesis of various $>CF_2$ containing derivatives from F_2 mediated by quinuclidine provides the potential for inexpensive large-scale synthesis of many CF_2 derivatives.

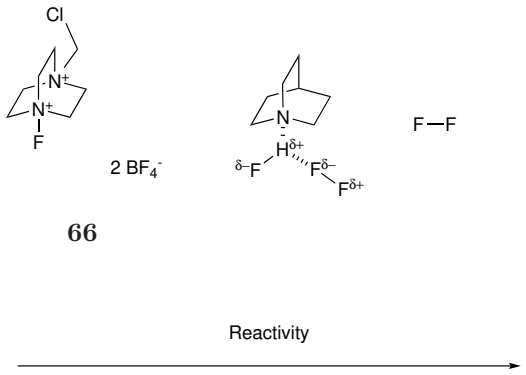

Scheme 6.3: Comparison of the reactivity of possible fluorinating agents

Chapter 7

Future Work

While quinuclidine has excelled at mediating the selectivity towards desired difluoro-products, its toxicity and cost may limit its use on an industrial scale. For this work to be applied on an industrial scale, an alternative mediating agent is needed. While small nitrogen bases gave inferior results, it is possible that a mediating agent based on cinchona alkaloids such as quinine may prove successful (Figure 7.1). These readily available alkaloids are either made synthetically or extracted from the bark of Rubiaceae *Cinchona* genus of flowering plants, and notably all contain a quinuclidine-like bicyclic amine.

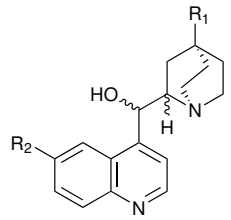

277

Figure 7.1: General structure of a cinchona alkalkoid

Selective difluorinations using F_2 were most effective for 1,3-dicarbonyl substrates as these have relatively acidic $>CH_2$ protons. Fluorinations using the methodologies developed in this thesis could be performed on a range of other 1,3-dicarbonyl derivatives to expand the range of available $>CF_2$ containing compounds as potential fluorinated building blocks.

Amidation reactions were successfully performed with high conversion on some of the difluoroesters synthesised in this thesis. This work could be readily expan-

ded to include other amines or difluoroesters, possibly as a route to the synthesis of tetrafluoro compounds (Figure 7.2). Conformations of these difluoro and tetrafluoro amides could be determined by single crystal X-ray crystallography and could provide useful insight for designing new active ingredients incorporating new di- or tetra- fluorinated subunits.

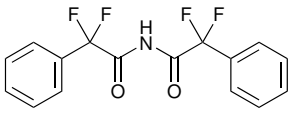

278

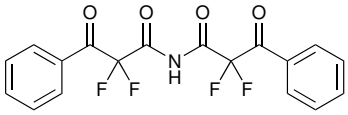

279

Figure 7.2: Possible tetrafluoro amides that could be synthesised using synthetic strategies investigated in this thesis

While selective difluorination of 1,3-diesters was achieved, these products were not successfully isolated due to their tendency to hydrolyse and decarboxylate. Future studies may determine non-aqueous purification conditions to successfully isolate these compounds.

The selective fluorination of aromatics using fluorine gas remains an industrially important reaction. Work in this thesis has determined that the addition of nitrogen bases significantly lowers the degree of conversion, and prevents unwanted tar formation. Mediation of activated aromatics may lead to an increased conversion to desired fluorinated products upon developing appropriate conditions

Chapter 8

General Experimental and Instrumentation

Chemicals were purchased from Fisher Scientific, Apollo Scientific, Fluorochem or Sigma Aldrich and, unless otherwise stated, were used without any further purification. All column chromatography was carried out using Silicagel LC60A (40 63 micron) purchased from Fluorochem. Proton, carbon and fluorine nuclear magnetic resonance spectra (^{1}H NMR, ^{13}C NMR and ^{19}F NMR)were recorded on a Bruker 400 Ultrashield (^{1}H NMR at 400 MHz; ^{13}C NMR at 101 MHz; ^{19}F NMR at 376 MHz) spectrometer, Varian DD2-500 (^{1}H NMR at 500 MHz; ^{13}C NMR at 126 MHz) spectrometer, Varian VNMR-600 Ultrashield (^{1}H NMR at 600 MHz; ^{13}C NMR at 151 MHz) spectrometer or a Varian VNMRS-700 (^{1}H NMR at 700 MHz; ^{13}C NMR at 176 MHz) spectrometer with residual solvent peaks as the internal standard. ^{1}H NMR, ^{13}C NMR and ^{19}F NMR spectroscopic data are reported as follows: chemical shift (ppm), integration, multiplicity (s = singlet, d = doublet, t = triplet, q = quartet, p = pentet, m = multiplet), coupling constant (Hz). Accurate mass analysis was achieved with a QtoF Premier mass spectrometer (Waters Ltd, UK) or an LCT Premier XE mass spectrometer (Waters Ltd, UK) equipped with an accurate solids analysis probe (ASAP). Infra-red (IR) spectra were recorded on a Perkin Elmer FTIR Spectrum Two™ fitted with an ATR probe. Melting points were measured with a Gallenkamp apparatus at atmospheric pressure and are uncorrected.

Fluorinations were carried out in a borosilicate glass fluorination reactor (100 mL, 250 mL or 500 mL) unless otherwise stated. The reactor was built from a standard glass bottle with GL 45 thread joint and a PTFE screw crap equipped with a gas

inlet/outlet head built of stainless steel, PTFE and FEP Swagelok components. The flow rates were controlled with a Brooks instruments gas mass flow controller.

Figure 8.1: Small scale ($\leq$ 10 mmol) fluorination set-up

Figure 8.2: Large scale ($\leq$ 20 mmol) fluorination set-up

Chapter 9

Experimental to Chapter 2

9.1 General Procedure 1 (GP1)—Synthesis of compounds 91a–91g

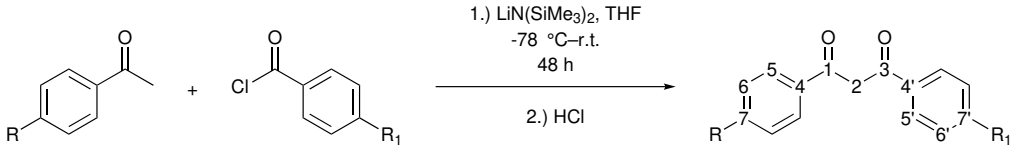

The acetophenone derivative (10 mmol) and $LiN(SiMe_3)_2$ (1 M in THF, 20 mmol, 20 mL) in anhydrous THF (20 mL) were stirred at −78 °C for 30 min under N_2. The corresponding acid chloride (10 mmol) was added slowly and the reaction mixture allowed to warm to room temperature overnight and stirred for 48 hours. Where the acid chloride was a solid, the amount was added to a round bottom flask, purged with argon, and dissolved in anhydrous tetrahydrofuran (10 mL) before being transferred to the reaction mixture via cannula. The reaction mixture was quenched with 36% hydrochloric acid (3 mL), before being partitioned between water (10 mL) and ethyl acetate (30 mL). The aqueous layer was extracted with ethyl acetate (2×30 mL) and the combined organic phases washed with saturated sodium bicarbonate solution (30 mL) and water (30 mL). The organic layer was dried over magnesium sulfate and the solvent removed under reduced pressure to yield the crude product. This was further purified by recrystallisation or column chromatography on silica gel if required to give the pure product.

1-(4-Methylphenyl)-3-phenylpropane-1,3-dione (91a)

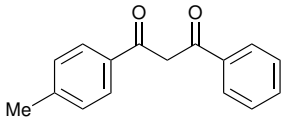

Prepared according to **GP1**, 4-methylacetophenone (1.34 mL, 10.03 mmol) and benzoyl chloride (1.16 mL, 9.99 mmol) after purification by column chromatography on silica gel with ethyl acetate 15% *v/v* in hexane solvent mixture as the eluent gave *1-(4- methylphenyl)-3-phenyl-1,3-propanedione* (2.408 g, 95%) as a white solid; Mp 85–86 °C [lit. Mp 84–85 °C[183]]. *Enol product* (92%) ^{1}H NMR (700 MHz, $CDCl_3$) δ 2.44 (3 H, s, C**8**H$_3$), 6.84 (1 H, s, C**2**H), 7.28–7.31 (2 H, m, C**6**H), 7.47–7.51 (2 H, m, C**6'**H), 7.53–7.57 (1 H, m, C**7'**H), 7.88–7.92 (2 H, m, C**5**H), 7.97–7.99 (2 H, m, C**5'**H); ^{13}C NMR (176 MHz, $CDCl_3$) δ 21.8 (C**8**), 93.0 (C**2**), 127.2 (C**5'**), 127.4 (C**5**), 128.8 (C**6'**), 129.6 (C**6**), 132.4 (C**7'**), 133.0 (C**4**), 135.8 (C**4'**), 143.4 (C**7**), 185.3 (C**3**), 186.2 (C**1**); *ketone product* (8%) ^{1}H NMR (700 MHz, $CDCl_3$) δ 4.61 (2H, s, C**2**H), 2.42 (3 H, s, C**8**H); *m/z* (EI$^+$) 238.2 ([M]$^+$, 92%), 223.1 ([$C_{15}H_{11}O_2$]$^+$, 11%), 161.1 ([$C_{10}H_9O_2$]$^+$, 22%), 147.1 ([$C_9H_7O_2$]$^+$, 16%), 119.1 ([C_8H_7O]$^+$, 87%), 105.1 ([C_7H_5O]$^+$, 44%), 91.1 ([C_7H_7]$^+$, 43%), 77.1 ([C_6H_5]$^+$, 39%), 69.0 ([C_5H_9]$^+$, 59%). HRMS (ASAP) *m/z* calculated for [M+H]$^+$ $C_{16}H_{15}O_2$ 239.1072; found 239.1067. IR (neat, cm^{-1}) 2923, 1459, 1185, 1018, 767, 687, 582. Crystals suitable for x-ray diffraction were grown by slow evaporation from hexane. Data consistent with that previously reported in the literature.[184]

1-(4-Methoxyphenyl)-3-phenylpropane-1,3-dione (91b)

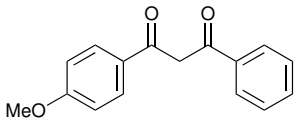

Prepared according to **GP1**, acetophenone (1.17 mL, 10.03 mmol) and 4-methoxybenzoyl chloride (1.35 mL, 9.97 mmol) after recrystallisation from ethyl acetate gave *1-(4-methoxyphenyl)-3-phenyl-1,3-propanedione* (2.399 g, 95%) as colourless crystals; Mp 127–128 °C [lit. Mp 127–128 °C[185]]. *Enol product* (90%) ^{1}H NMR (700 MHz, $CDCl_3$) δ 3.89 (3 H, s, C**8**H), 6.80 (1 H, s, C**2**H), 6.97–7.00 (2 H, m, C**6**H), 7.47– 7.50 (2 H, m, C**6'**H), 7.53–7.56 (1 H, m, C**7'**H), 7.96–7.98 (2 H, m, C**5'**H), 7.97–7.99 (2 H, m, C**5**H); ^{13}C NMR (176 MHz, $CDCl_3$) δ 55.6 (C**8**), 92.5 (C**2**), 114.1 (C**6**), 127.1 (C**5'**), 128.4 (C**4**), 129.5 (C**5**), 132.3 (C**7'**), 135.7 (C**4'**), 163.4 (C**7**), 163.4 (C**7**), 184.2 (C**3**), 186.3 (C**1**); *ketone product* (10%) ^{1}H NMR (700 MHz, $CDCl_3$) δ 4.59

(2H, s, C**2**H), 3.87 (3 H, s, C**8**H); *m/z* (EI$^+$) 254.1 ([M]$^+$, 100%), 177.1 ([$C_{10}H_{19}O_3$]$^+$, 19%), 135.1 ([$C_8H_7O_2$]$^+$, 95%), 108.1 ([C_7H_8O]$^+$, 60%), 105.1 ([C_7H_5O]$^+$, 30%), 77.1 ([C_6H_5]$^+$, 56%), 69.0 ([C_5H_9]$^+$, 31%), 51.1 ([C_4H_3]$^+$, 9%). HRMS (ASAP) *m/z* calculated for [M+H]$^+$ $C_{16}H_{15}O_3$ 255.1021; found 255.1024. IR (neat, cm^{-1}) 2923, 1459, 1185, 1018, 767, 687, 582. Crystals suitable for x-ray diffraction were grown by slow evaporation from hexane. Data consistent with that previously reported in the literature.[186]

1-(4-Chlorophenyl)-3-phenylpropane-1,3-dione (91c)

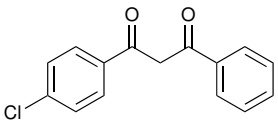

Prepared according to **GP1**, acetophenone (1.17 mL, 10.03 mmol) and 4-chlorobenzoyl chloride (1.28 mL, 9.98 mmol) after recrystallisation from hexane afforded *1-(4-chlorophenyl)-3-phenyl-1,3-propanedione* (2.314 g, 90%) as a pale yellow solid; Mp 85–87 °C [lit. Mp 86–88 °C[187]]. *Enol product* (94%) ^{1}H NMR (600 MHz, $CDCl_3$) δ 6.81 (1 H, s, C**2**H), 7.47 (2 H, dt, $^3J_{HH}$ 8.7, $^4J_{HH}$ 2.4, C**6**H), 7.48–7.51 (2 H, m, C**5'**H), 7.57 (1 H, tt, $^3J_{HH}$ 7.4, $^4J_{HH}$ 1.4, C**7'**H), 7.93 (2 H, dt, $^3J_{HH}$ 8.7, $^4J_{HH}$ 2.4, C**5**H), 7.97–8.00 (2 H, m, C**6'**H); ^{13}C NMR (151 MHz, $CDCl_3$) δ 93.2 (C**2**), 127.3 (C**6'**), 128.7 (C**5**), 128.9 (C**5'**), 129.1 (C**6**), 132.8 (C**7'**), 134.1 (C**4**), 135.5 (C**4'**), 138.9 (C**7**), 184.7 (C**1**), 185.9 (C**3**); *ketone product* (6%) ^{1}H NMR (600 MHz, $CDCl_3$) δ 4.61 (2H, s, C**2**H); *m/z* (EI$^+$) 258.1 ([M]$^+$, 79%), 181.0 ([$C_9H_6ClO_2$]$^+$, 22%), 147.1 ([$C_9H_7O_2$]$^+$, 21%), 139.1 ([C_7H_4ClO]$^+$, 43%), 111.1 ([C_6H_4Cl]$^+$, 20%), 105.1 ([C_7H_5O]$^+$, 56.7%), 77.1 ([C_6H_5]$^+$, 96%). HRMS (ASAP) *m/z* calculated for [M+H]$^+$ $C_{15}H_{12}ClO_2$ 259.0526; found 259.0531. IR (neat, cm^{-1}) 2924, 1516, 1282, 1093, 1012, 843, 757, 682. Data consistent with that previously reported in the literature.[186]

1-(4-Fluorophenyl)-3-phenylpropane-1,3-dione (91d)

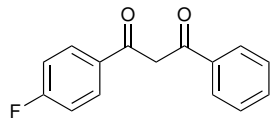

Prepared according to **GP1**, 4-fluoroacetophenone (1.16mL, 9.99 mmol) and benzoyl chloride (1.28 mL, 9.98 mmol) after recrystallisation from hexane afforded *1-(4-fluorophenyl)-3-phenyl-1,3-propanedione* (2.417 g, 100%) as a beige solid; Mp 78–79 °C [lit. Mp 88 °C[188]]. *Enol product* (93%) ^{1}H NMR (700 MHz, $CDCl_3$) δ 6.81

(1 H, s, C**2**H), 7.14–7.20 (2 H, m, C**6**H), 7.47–7.52 (2 H, m, C**5'**H) 7.56 (1H, tt, $^{3}J_{HH}$ 7.4, $^{4}J_{HH}$ 1.2, C**7'**H), 7.97–7.99 (2 H, m, C**6'**H), 8.00–8.02 (2 H, m, C**5**H); ^{19}F NMR (376 MHz, $CDCl_3$) δ −106.22 (tt, $^{3}J_{HF}$ 8.4, $^{4}J_{HF}$ 5.4); ^{13}C NMR (176 MHz, $CDCl_3$) δ 93.0 (C**2**), 116.0 (d, $^{2}J_{CF}$ 21.9, **6**), 127.3 (C**6'**), 128.9 (C**5'**), 129.8 (d, d, $^{3}J_{CF}$, C**5**), 132.6 (C**7'**), 135.4 (C**4'**), 165.6 (d, $^{1}J_{CF}$ 253.9, C**7**), 185.26 (C**1**), 185.27 (C**3**); *ketone product* (7%) ^{1}H NMR (700 MHz, CD Cl_3) δ 4.61 (2H, s, C**2**H); ^{19}F NMR (376 MHz, $CDCl_3$) δ −103.90 (tt, $^{3}J_{HF}$ 8.3, $^{3}J_{HF}$ 5.3); *m/z* (EI^+) 242.0 ($[M]^+$, 19%), 223.1 ($[C_{15}H_{11}O_2]^+$, 3%), 147.1 ($[C_9H_7O_2]^+$, 10%), 123.1 ($[C_7H_4FO]^+$, 10%), 119.1 ($[C_8H_7O]^+$, 4%), 105.1 ($[C_7H_5O]^+$, 20%), 77.0 ($[C_6H_5]^+$, 29%), 69.0 ($[C_5H_9]^+$, 19%), 51.0 ($[C_4H_3]^+$, 12%). HRMS (ASAP) *m/z* calculated for $[M+H]^+$ $C_{15}H_{12}FO_2$ 243.0821; found 243.0826. IR (neat, cm^{-1}) 3112, 1729, 1520, 1348, 1284, 1108, 955, 764, 688, 562. Data consistent with that previously reported in the literature.[189]

1-(4-Nitrophenyl)-3-phenylpropane-1,3-dione (91e)

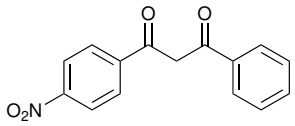

Prepared according to GP1, acetophenone (1.17 mL, 10.03 mmol) and 4-nitrobenzoyl chloride (1.860 g, 10.02 mmol) without further purification gave *1-(4 nitrophenyl)-3-phenyl-1,3-propanedione* (2.677 g, 99%) as a yellow solid Mp 145–146 °C [lit. Mp 160–161 °C[183]]. *Enol product* (95%) ^{1}H NMR (700 MHz, $CDCl_3$) δ 6.90 (1 H, s, C**2**H), 7.51–7.54 (2 H, m, C**5'**H), 7.59–7.62 (1 H, C**5**H), 8.00–8.03 (2 H, m, C**6'**H), 8.14 (2 H, dt, $^{3}J_{HH}$ 9.0, $^{4}J_{HH}$ 2.3, C**6**H), 8.34 (2 H, dt, $^{3}J_{HH}$ 9.0, $^{4}J_{HH}$ 2.3, C**5**H); ^{13}C NMR (176 MHz, $CDCl_3$) δ 94.4 (C**2**), 124.0 (C**2**), 127.6 (C**6'**), 128.2 (C**6**), 129.0 (C**5'**), 133.3 (C**7'**), 135.3 (C**4'**), 141.1 (C**2**), 150.1 (C**7**), 181.8 (C**1**), 188.0 (C**3**); *ketone product* (5%) ^{1}H NMR (700 MHz, $CDCl_3$) δ 4.69 (2 H, s, C**2**H); *m/z* (EI^+) 269.1 ($[M]^+$, 77%), 222.1 ($[C_{15}H_{10}O_2]^+$, 15%), 192.0 ($[C_9H_6NO_4]^+$, 17%), 147.1 ($[C_9H_7O_2]^+$, 24%), 120.1 ($[C_8H_8O]^+$, 7%), 105.1 ($[C_7H_5O]^+$, 76%), 91.1 ($[C_7H_7]^+$, 4%), 77.1 ($[C_6H_5]^+$, 49%), 69.0 ($[C_5H_9$, 51%), 51.0 ($[C_4H_3]^+$, 11%). HRMS (ASAP) *m/z* calculated for $[M+H]^+$ $C_{15}H_{12}NO_4$ 270.0766; found 270.0757. Crystals suitable for x-ray diffraction were grown by slow evaporation from hexane. IR (neat, cm^{-1}) 3121, 2981, 1692, 1513, 1343, 1103, 855, 744. Data consistent with that previously reported in the literature.[190]

1,3-Bis(4-chlorophenyl)-propane-1,3-dione (91f)

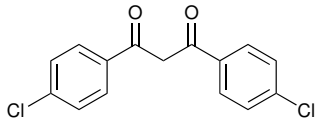

Prepared according to GP1, 4-chloroacetophenone (1.30 mL, 10.03 mmol) and 4-chlorobenzoyl chloride (1.28 mL, 9.98 mmol) after recrystallisation from hexane and ethyl acetate afforded *1,3-bis(4 chlorophenyl)propane-1,3-dione* (2.882 g, 99%) as a very pale yellow solid; Mp 151–153 °C [lit. Mp 159 °C[191]]. *Enol product* (94%) ^{1}H NMR (700 MHz, $CDCl_3$) δ 6.77 (1 H, s, C**2**H), 7.46–7.48 (4 H, m, C**4**H), 7.91–7.93 (4 H, m, C**5**H); ^{13})C NMR (176 MHz, $CDCl_3$) δ 93.0 (C**2**), 128.7 (C**4**), 129.2 (C**5**), 133.9 (C**6**), 139.1 (C**3**), 184.8 (C**1**); *ketone product* (6%) ^{1}H NMR (700 MHz, $CDCl_3$) δ 4.58 (2 H, s, C**2**H); *m/z* (EI$^+$) 292.1 ([M]$^+$, 68%), 223.1 ([$C_{15}H_{11}O_2$]$^+$, 11%), 181.0 ([$C_9H_6ClO_2$]$^+$, 40%), 139.1 ([C_7H_4ClO]$^+$, 100%), 111.1 ([C_6H_4Cl]$^+$, 54%), 69.0 ([C_5H_9]$^+$, 54%). HRMS (ASAP) *m/z* calculated for [M+H]$^+$ ([$C_{15}H_{11}Cl_2O_2$]$^+$ 293.0136; found 293.0147. Crystals suitable for x-ray diffraction were grown by slow evaporation from hexane. IR (neat, cm^{-1}) 2981, 1582, 1503, 1397, 1279, 1177, 970, 775. Data consistent with that previously reported in the literature.[192]

1,3-Bis(4-fluorophenyl)-propane-1,3-dione (91g)

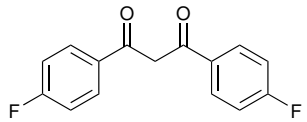

Prepared according to GP1, 4-fluoroacetophenone (1.21 mL, 9.97 mmol) and 4-fluorobenzoyl chloride (1.18 mL, 9.99 mmol) after recrystallisation from hexane and ethyl acetate afforded *1,3-bis(4-fluorophenyl)-propane-1,3-dione* (2.099 g, 81%) as a beige solid; Mp 107–108 °C [lit. Mp 109 °C[193]]. *Enol product* (92%) ^{1}H NMR (700 MHz, $CDCl_3$) δ 6.74 (1 H, s, C**2**H), 7.14–7.20 (4 H, m, C**5**H), 7.98–8.02 (4 H, m, C**4**H); ^{19}F NMR (376 MHz, $CDCl_3$) δ −106.1 (tt, $^{3}J_{HF}$ 8.4, $^{4}J_{HF}$ 5.4); ^{13})C NMR (176 MHz, $CDCl_3$) 92.6 (C**2**), 116.0 (d, $^{2}J_{CF}$ 21.9, C**5**), 129.7 (d, $^{3}J_{CF}$ 9.2, C**4**), 131.8 (d, $^{4}J_{CF}$ 3.1, C**3**), 165.6 (d, $^{1}J_{CF}$ 254.1, C**6**), 184.6 (s, C**1**); *ketone product* (8%) ^{1}H NMR (700 MHz, $CDCl_3$) δ 4.58 (2 H, s, C**4**H); ^{19}F NMR (376 MHz, $CDCl_3$) δ −103.6 (tt, $^{3}J_{HF}$ 8.3, $^{3}J_{HF}$ 5.3); *m/z* (EI$^+$) 260.1 ([M]$^+$, 58%), 223.1 ([$C_{15}H_{11}O_2$]$^+$, 11%), 165.1 ([$C_9H_6FO_2$]$^+$, 30%), 123.1 ([C_7H_4FO]$^+$, 100%), 95.1 ([C_6H_4F]$^+$, 47%), 69.0 ([C_5H_9]$^+$, 32%). HRMS (ASAP) *m/z* calculated for [M+H]$^+$. $C_{15}H_{11}F_2O_2$] 293.0727; found 261.0718. IR (neat, cm^{-1}) 3082, 1596, 1467, 1301, 1221, 1012, 859, 856, 784, 505. Data consistent with that previously reported in the literature.[192]

1,3-Bis(4-nitrophenyl)-propane-1,3-dione (91h)

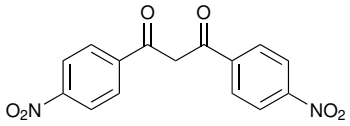

4-Nitroacetophenone (1.648 g, 9.97 mmol) and $LiN(SiMe_3)_2$ (1M in tetrahydrofuran, 20 mmol, 20 mL, 2 equiv.) in anhydrous tetrahydrofuran (20 mL) were stirred at −78 °C for 30 min under N_2. 4-Nitrobenzoyl chloride (1.856 g, 10.0 mmol) was dissolved in anhydrous tetrahydrofuran (10 mL) and added to the reaction mixture which was left to stir for 48 hours. The reaction mixture was quenched with 36% hydrochloric acid (3 mL) before partitioned between water (10 mL) and dichloromethane (500 mL). The aqueous layer was extracted with dichloromethane (2×50 mL) and the combined organic phases washed with sodium bicarbonate (30 mL) and water (20 mL). The organic layer was dried over magnesium sulfate and the solvent removed under reduced pressure to yield the crude product. Recrystallisation from acetone gave *1,3-(4-nitrophenyl)propane-1,3-dione* (3.098 g, 99%) as a yellow solid; Mp 240–242 °C [lit. Mp 241-242 °C[191]]. *Enol product* (100%) ^{1}H NMR (700 MHz, $CDCl_3$) δ 6.93 (1 H, s, C**2**H), 8.15–8.18 (4 H, m, C**5**H), 8.35–8.38 (4 H, m, C**4**H); ^{13}C NMR (176 MHz, $CDCl_3$) δ 95.2 (C**2**), 124.2 (C**4**), 128.5 (C**5**), 140.5 (C**3**), 150.4 (C**6**), 184.1 (C**1**); *m/z* (ES^-) 313.2 ($[M\text{-}H]^-$, 100%. HRMS (ASAP) m/z calculated for $[M\text{-}H]^+$. $C_{15}H_9N_2O_4$ 313.0461; found 313.0434. IR (neat, cm^{-1}) 3095, 1511, 1344, 1224, 1093, 1009, 855, 747, 450. Data consistent with that previously reported in the literature.[192]

9.2 General Procedure 2 (GP2)—Synthesis of 93–93g

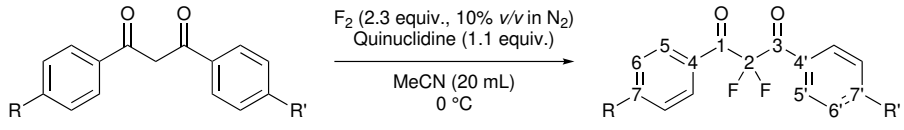

The corresponding 1,3-diketone (2.0 mmol, 1 equiv.) and quinuclidine (0.245 g, 2.2 mmol, 1.1 equiv.) were added to a SIMAX glass bottle and dissolved in acetonitrile (20 mL). The reaction vessel was cooled to 0 °C, stirred rapidly and purged with nitrogen for 10 minutes before fluorine, as a 10% mixture in nitrogen (*v/v*), was passed through the reaction mixture at a prescribed flow rate, (4.6 mmol, 2.3 equiv.,

15 mL min^{-1}) that was controlled by a mass flow controller for 75 min. After purging with nitrogen for 20 minutes, the reaction vessel was removed and the solvent diluted with water (20 mL) and dichloromethane (90 mL). The two layers were separated and the aqueous layers were washed with dichloromethane (3×30 mL). The organic fractions were combined, washed with saturated sodium bicarbonate solution (20 mL) and dried over magnesium sulfate. The solvent was removed under reduced pressure to yield the crude product which was purified by column chromatography on silica gel or recrystallisation to yield the pure product.

2,2-Difluoro-1,3-diphenylpropane-1,3-dione (93)

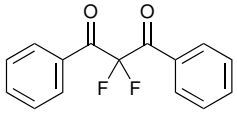

Prepared according to **GP2**, 1,3-diphenyl-1,3-propanedione (0.448 g, 2.00 mmol) after column chromatography on silica gel with hexane and DCM (1:1) as the eluent yielded *2,2-difluroro-1,3-diphenyl-1,3-propanedione* (0.338 g, 57%) as a white solid; Mp 56–57 °C [lit. Mp 56–57 °C[194]]. ^{1}H NMR (600 MHz, $CDCl_3$) δ 7.50 (4 H, td, $^{3}J_{HH}$ 7.4, $^{4}J_{HH}$ 2.0, C**6**H), 7.62–7.68 (2 H, m, C**7**H), 8.09 (4 H, d, $^{3}J_{HH}$ 7.4, C**5**H); ^{19}F NMR (376 MHz, $CDCl_3$) δ −102.7 (s); ^{13}C NMR (151 MHz, $CDCl_3$) δ 112.8 (t, $^{1}J_{CF}$ 265.8, C**2**), 129.1 (C**6**), 130.4 (t, $^{4}J_{CF}$ 2.7, C**5**), 135.2 (C**7**), 187.5 (t, $^{2}J_{CF}$ 27.0, C**1**); *m/z* (EI^+) 105.2 ($[C_7H_5F_2O_2]^+$, 87%), 77.1 $[C_6H_5]^+$, 43%). HRMS (ASAP) *m/z* calculated for $[M+H]^+$ $C_{15}H_{11}F_2O_2$ 261.0727; found 261.0723. Crystals suitable for x-ray diffraction were grown by slow evaporation from hexane. IR (neat, cm^{-1}) 3073, 1694, 1594, 1449, 1251, 1135, 887, 679, 523. Data consistent with that previously reported in the literature.[129]

2,2-Difluoro-1-(4-methylphenyl)-3-phenylpropane-1,3-dione (93a)

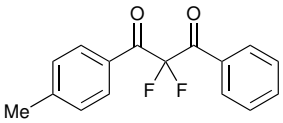

Prepared according to GP2, 1-(4-methylphenyl)-3-phenyl-1,3-propanedione (0.477 g, 2.00 mmol) after column chromatography on silica gel with hexane and DCM (1:1) as the eluent yielded 0.397 g of a yellow oil that contained a mixture of fluorinated products; ^{19}F NMR (376 MHz, $CDCl_3$) −187.4-–−186.2 (m, monofluoro product), −168.7 (d, *J* 4.6), −116.3 (d, *J* 11.9), −115.3 (ddd, *J* 9.9, *J* 7.6, *J* 2.3), −114.9 (ddq, *J* 9.9, *J* 7.6, *J* 2.4), −105.5-–−105.2 (m), −102.6 (s, difluoro product).

2,2-Difluoro-1-(4-methoxyphenyl)-3-phenylpropane-1,3-dione (93b)

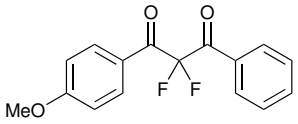

Prepared according to GP2, 1-(4-methoxyphenyl)-3-phenyl-1,3-propanedione (0.509 g, 2.00 mmol) after column chromatography on silica gel with hexane and DCM (1:1) as the eluent yielded 0.270 g of a yellow oil that contained a mixture of fluorinated products; ^{19}F NMR (376 MHz, $CDCl_3$) −186.4 (dt, $^2J_{HF}$ 49.3, $^5J_{HF}$ 1.0, monofluoro product), −133.4 (ddd, *J* 11.8, *J* 8.1, *J* 1.2), −132.9 (ddd, *J* 11.7, *J* 8.0, *J* 1.2), −126.4 (dq, *J* 9.8, *J*2.1), −107.3 (s), −102.5 (s, difluoro product), −102.5 (t, *J* 1.0), −102.4 (t, *J* 1.0).

2,2-Difluoro-1-(4-chlorophenyl)-3-phenylpropane-1,3-dione (93c)

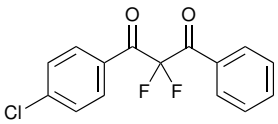

Prepared according to GP2, 1-(4-chlorophenyl)-3-phenyl-1,3-propanedione (0.514 g, 2.01 mmol) after column chromatography on silica gel with hexane and DCM (1:1) as the eluent yielded *2,2-difluroro-1-(4-chlorophenyl)-3-phenyl-1,3-propanedione* (0.352 g, 59%) as a white solid; Mp 63–64 °C. ^{1}H NMR (700 MHz, $CDCl_3$) δ 7.44–7.49 (2 H, m, C**6**H), 7.50–7.53 (2 H, m, C**6'**H), 7.67 (1 H, tt, $^3J_{HH}$ 7.5, $^4J_{HH}$ 1.2, C**7'**H), 8.03 (2 H, d, $^3J_{HH}$ 8.8, C**5**H), 8.08 (2 H, dd, $^3J_{HH}$ 8.5, $^4J_{HH}$ 1.0, C**5'**H); ^{19}F NMR (376 MHz, $CDCl_3$) δ −102.7 (p, $^5J_{HF}$ 0.9); ^{13}C NMR (176 MHz, $CDCl_3$) δ 112.8 (t, $^1J_{CF}$ 266.0, C**2**), 129.1 (C**6'**), 129.5 (C6), 130.1 (C**4**), 130.4 (t, $^4J_{CF}$ 2.7, C**5'**), 131.6 (C**4'**), 131.8 (t, $^4J_{CF}$ 2.8, C**5**), 135.3 (C**7'**), 142.0 (C**7**), 186.5 (t, $^2J_{CF}$ 27.1, C**1**), 187.4 (t, $^2J_{CF}$ 26.9, C**3**); *m/z* (EI$^+$) 294.1 ([M]$^+$, 1%), 139.1 ([C_7H_4ClO]$^+$, 62%), 77.1 ([C_6H_5]$^+$, 96%), 51.1 ([C_3H_4]$^+$, 12%). HRMS (ASAP) *m/z* calculated for [M+H]$^+$ $C_{15}H_{10}ClF_2O_2$ 295.0337; found 295.0335. Crystals suitable for x-ray diffraction were grown by slow evaporation from hexane. IR (neat, cm^{-1} 1692, 1588, 1449, 1250, 1138, 884, 682, 561.

2,2-Difluoro-1-(4-fluorophenyl)-3-phenylpropane-1,3-dione (93d)

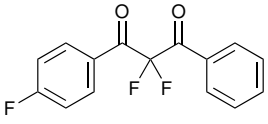

Prepared according to **GP2**, 1-(4-fluorophenyl)-3-diphenyl-1,3-propanedione (0.484 g, 2.00 mmol)) after column chromatography on silica gel with hexane and DCM (1:1) as the eluent yielded *2,2-difluroro-1-(4-fluorophenyl)-3-diphenyl-1,3-propanedione* (0.327 g, 59%) as a white solid; Mp 36–37 °C. ^{1}H NMR (700 MHz, $CDCl_3$) δ 7.1–7.2 (2 H, m, C**6**H), 7.5–7.5 (2 H, m, C**6'**H), 7.7 (1 H, tt, $^{3}J_{HH}$ 7.3, $^{4}J_{HH}$ 1.3, C**7'**H), 8.1 (2 H, ddd, $^{3}J_{HH}$ 7.7, $^{4}J_{HH}$ 2.2, $^{5}J_{HH}$ 1.1, C**5'**H), 8.1–8.2 (2 H, m, C**5**H); ^{19}F NMR (376 MHz, $CDCl_3$) δ −102.6 (s, CF2, C**2**F), −100.6 (tt, $^{3}J_{HF}$ 8.2, $^{4}J_{HF}$ 5.3, C**7**F); ^{13}C NMR (176 MHz, $CDCl_3$) δ 112.8 (t, $^{1}J_{CF}$ 265.8, C**2**), 116.5 (d, $^{2}J_{CF}$ 22.1, C**6**), 128.2 (d, $^{3}J_{CF}$ 2.9, C**4**), 129.1 (s, C**6'**), 130.4 (t, $^{4}J_{CF}$ 2.6, C**5'**), 131.7 (C**4'**), 133.4 (dt, $^{3}J_{CF}$ 9.9, $^{4}J_{CF}$ 2.8, C**5**), 135.3 (C**7**), 167.0 (d, $^{1}J_{CF}$ 259.2, C**2**), 186.0 (t, $^{2}J_{CF}$ 27.1, C**1**), 187.5 (t, $^{2}J_{CF}$ 26.8 C**3**); *m/z* (EI$^+$) 278.1 ([M]$^+$, 2%), 123.2 ([C_7H_4FO]$^+$, 100%), 105.2 ([C_7H_5O]$^+$, 100%), 95.1 ([C_6H_4F]$^+$, 58%), 77.1 ([C_6H_5]$^+$, 90%), 51.1 ([C_3H_4]$^+$, 26%). HRMS (ASAP) *m/z* calculated for [M+H]$^+$ $C_{15}H_{10}F_3O_2$ 279.0633; found 279.0642. IR (neat, cm$^-$1) 3080, 1693, 1597, 1450, 1241, 1108, 885, 683, 572.

2,2-Difluoro-1-(4-nitrophenyl)-3-phenylpropane-1,3-dione (93e)

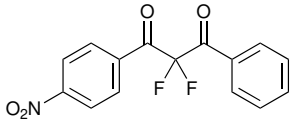

Prepared according to **GP2**, 1-(4-nitrophenyl)-3-phenylpropane-1,3-dione (0.535 g, 1.99 mmol) in MeCN (60 mL) after column chromatography on silica gel with hexane and DCM (1:1) as the eluent yielded *2,2-difluoro-1-(4-nitrophenyl)-3-diphenylpropane-1,3-dione* (304 g, 50%) as a pale yellow solid; Mp 54–56 °C. ^{1}H NMR (700 MHz, $CDCl_3$) δ 7.52–7.58 (2 H, m), 7.71 (1 H, tt, $^{3}J_{HH}$ 7.5, $^{4}J_{HH}$ 1.2), 8.09–8.12 (2 H, m), 8.22–8.25 (2 H, m), 8.33–8.35 (2 H, m); ^{19}F NMR (376 MHz, $CDCl_3$) δ −102.7 (pent, $^{5}J_{HF}$ 0.8); ^{13}C NMR (176 MHz, $CDCl_3$) δ 112.5 (t, $^{1}J_{CF}$ 266.9, C**2**), 124.1 (C**6**), 129.3 (C**6'**), 130.5 (t, $^{5}J_{CF}$ 2.7, C**5'**), 131.3 (C**4'**), 131.5 (t, $^{5}J_{CF}$ 2.8, C**4**), 135.7 (C**7'**), 136.3 (C**4**), 151.2 (C**7**), 186.6 (t, $^{2}J_{CF}$ 27.7, C**1**), 187.4 (t, $^{2}J_{CF}$ 27.1, C**3**); *m/z* (EI$^+$) 150.1 ([$C_7H_4NO_3$]$^+$, 32%), 105.2 ([C_7H_5O]$^+$, 100%), 77.1 ([C_6H_5]$^+$, 54%), 51.1 ([C_3H_4]$^+$, 10%). HRMS (ASAP) *m/z* calculated for [M+H]$^+$ $C_{15}H_{10}F_2NO_4$ 306.0567; found 306.0578. Crystals suitable for x-ray diffraction were grown by slow evaporation from hexane. IR (neat, cm$^-$1) 3111, 1698, 1525, 1290, 1101, 954, 841, 711, 522.

2,2-Difluoro-1,3-bis(4-chlorophenyl)propane-1,3-dione (93f)

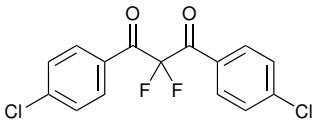

Prepared according to **GP2**, 1,3-bis(4 chlorophenyl)-propane-1,3-dione (0.590 g, 2.01 mmol) in MeCN (60 mL) after column chromatography on silica gel with hexane and DCM (1:1) as the eluent yielded *1,3-bis(4-chlorophenyl)-2,2-difluoropropane-1,3-dione* (0.475 g, 72%) as a white solid; Mp 93–94 °C. ^{1}H NMR (700 MHz, $CDCl_3$) δ 7.48–7.50 (4 H, m, C**5**H), 8.02 (4 H, d, $^{3}J_{HH}$ 8.4, C**4**H); ^{19}F NMR (376 MHz, $CDCl_3$) δ −102.8 (s); ^{13}C NMR (176 MHz, $CDCl_3$) δ 112.7 (t, $^{1}J_{CF}$ 266.3, C**2**), 129.6 (C**5**), 129.9 (t, $^{3}J_{CF}$ 1.5, C**3**), 131.8 (t, $^{4}J_{CF}$ 2.8, C**4**), 142.2 (C**6**), 186.4 (t, $^{2}J_{CF}$ 27.1, C**1**); *m/z* (EI)$^{+}$ 328.0 ([M]$^{+}$, 1%), 139.1 ([C_7H_4ClO]$^{+}$, 100%), 111.0 ([C_6H_4Cl]$^{+}$, 41%), 50.0 ([C_4H_2]$^{+}$, 4%). HRMS (ASAP) *m/z* calculated for [M+H]$^{+}$ $C_{15}HCl_{29}F_2O_2$328.9948; found 328.9937. Crystals suitable for x-ray diffraction were grown by slow evaporation from hexane. IR (neat, cm^{-}1) 1698, 1588, 1488, 1405, 1251, 1139, 1013, 884, 773, 542.

2,2-Difluoro-1,3-bis(4-fluorophenyl)propane-1,3-dione (93g)

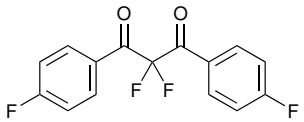

Prepared according to **GP2**, 1,3-bis(4-fluorophenyl)-propane 1,3 dione (0.522 g, 2.01 mmol) in MeCN (60 mL) after recrystallisation from hexane and chloroform yielded *2,2-difluoro-1,3-bis(4-fluorophenyl)propane-1,3-dione* (0.451 g, 76%) as a pale yellow solid; Mp 79–81 °C. ^{1}H NMR (700 MHz, $CDCl_3$) δ 7.16–7.20 (4 H, m, C**5**H), 8.12–8.16 (4 H, m, C**4**H); ^{19}F NMR (376 MHz, $CDCl_3$) δ −102.6 (s, C**2**F_2), −100.3 (tt, $^{3}J_{HF}$ 8.2, $^{4}J_{HF}$ 5.3, C**6**F); ^{13}C NMR (126 MHz, $CDCl_3$) δ 112.9 (t, $^{1}J_{CF}$ 265.9, C**2**), 116.5 (d, $^{2}J_{CF}$ 22.2, C**5**), 128.1 (dt, $^{3}J_{CF}$ 3.1, $^{4}J_{CF}$ 1.6, C**3**), 133.5 (dt, $^{4}J_{CF}$ 9.9, $^{5}J_{CF}$ 2.9, C**4**), 167.0 (d, $^{1}J_{CF}$ 259.4, C**6**), 186.0 (t, $^{2}J_{CF}$ 27.0, C**1**); *m/z* (EI)$^{+}$ 296 ([M]$^{+}$, 1%), 123.1 ([C_7H_4FO]$^{+}$, 100%), 95.1 ([C_6H_4F]$^{+}$, 78%), 50.0 ([C_4H_2]$^{+}$, 3%). HRMS (ASAP) *m/z* calculated for [M+H]$^{+}$ $C_{15}H_9F_4O_2$ 297.0539; found 297.0537. Crystals suitable for x-ray diffraction were grown by slow evaporation from hexane. IR (neat, cm^{-}1) 1695, 1596, 1504, 1413, 1235, 1134, 867, 780, 600.

2,2-Difluoro-1,3-bis(4-nitrophenyl)propane-1,3-dione (93h)

Prepared according to **GP2**, 1,3-bis(4-nitrophenyl)-propane 1,3 dione (0.630 g, 2.00 mmol) in MeCN (60 mL) after recrystallisation from hexane and chloroform yielded

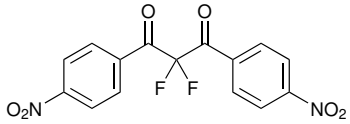

1,3-bis(4-nitrophenyl)-2,2-difluoropropane-1,3-dione (0.542 g, 77%) as a pale yellow solid; Mp 117–119 °C. ^{1}H NMR (700 MHz, $CDCl_3$) δ 8.25–8.28 (4 H, m, C**4**H), 8.37–8.40 (4 H, m, C**5**H); ^{19}F NMR (376 MHz, $CDCl_3$) δ −102.9 (s); ^{13}C NMR (176 MHz, $CDCl_3$) δ 112.2 (t, $^{1}J_{CF}$ 267.7, C**2**), 124.3 (C**5**), 131.5 (t, $^{4}J_{CF}$ 2.9, C**4**), 135.8 (C**6**), 151.5 (C**2**), 186.3 (t, $^{2}J_{CF}$ 27.9, C**1**). *m/z* (EI)$^{+}$ 150.1 ($[C_7H_4NO_3]^{+}$, 100%), 76.1 ($[C_6H_4]^{+}$, 22%). HRMS (ASAP) *m/z* calculated for $[M+H]^{+}$ $_{15}H_9F_2N_2O_4$ 351.0430; found 351.0429. Crystals suitable for x-ray diffraction were grown by slow evaporation from hexane. IR (neat, cm^{-}1) 3112, 1729, 1520, 1349, 1126, 955, 827, 715, 562.

N-Fluoroquinuclidinium triflate (192)

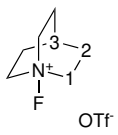

Quinuclidine (0.556 g, 5.0 mmol, 1 equiv.) and sodium triflate (1.032 g, 6.0 mmol, 1.2 equiv.) were added to a SIMAX glass bottle and dissolved in acetonitrile (40 mL). The reaction vessel was cooled to −40 °C, stirred rapidly and purged with nitrogen for 10 minutes before fluorine, as a 10% mixture in nitrogen (*v/v*), was added at a prescribed flow rate, (6.0 mmol, 1.2 equiv., 15 mL min^{-1}) that was controlled by a mass flow controller for 98 min. After purging with nitrogen for 20 minutes, the reaction vessel was removed and the reaction mixture filtered, and the solvent removed under reduced pressure. The crude product was dissolved in hot acetone, and triturated with cold ethyl acetate to yield *N-fluoroquinuclidinium triflate* (1.241 g, 89%) as a white solid. ^{1}H NMR (400 MHz, D_2O) δ 2.26 (1 H, dp, $^{3}J_{HH}$ 9.5, $^{4}J_{HH}$ 3.1, C**3**H), 2.32—2.40 (6 H, m, C**2**H), 4.19 (6 H, q, $^{3}J_{HF}$ 8.4, C**1**H); ^{19}F NMR (376 MHz, D_2O) δ −78.9 (3F, s, C**4**F_3), 56.6 (1F, s, NF); ^{13}C NMR (101 MHz, D_2O) δ 18.9 (d, $^{4}J_{CF}$ 4.8, C**3**), 27.3 (d, $^{3}J_{CF}$ 4.0, C**2**), 60.8 (d, $^{2}J_{CF}$ 9.2, C**1**), 119.6 (q, $^{1}J_{CF}$ 317.2, C**4**). Data consistent with that previously reported in the literature.[144,147]

9.3 Screening Conditions for Base Mediated Direct Fluorination of DBM

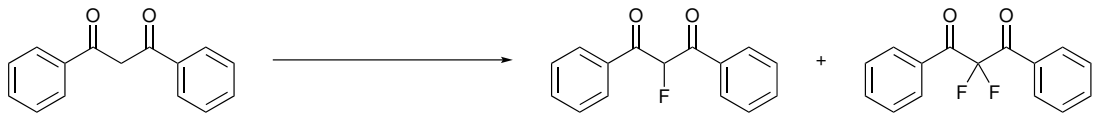

Dibenzoylmethane (0.449 g, 2.00 mmol) and the mediating agent were added to a SIMAX glass bottle and dissolved in acetonitrile (20 mL). The reaction vessel was cooled to 0 °C, stirred rapidly and purged with nitrogen for 10 minutes before fluorine gas, as a 10% mixture in nitrogen (*v/v*), was passed through the reaction mixture at a prescribed flow rate, (15 mL min^{-1}) that was controlled by a mass flow controller. After purging with nitrogen for 10 minutes, the reaction vessel was disconnected and the solvent removed under reduced pressure. A known mass of α,α,α,-trifluorotoluene was added as a reference standard, and the organic products were analysed by NMR spectroscopy.

Entry	Base	Equiv of base	Equiv of F_2	Yield by NMR/%		
				91	**92**	**93**
1	-	-	1	100	0	0
2	-	-	20	Polyfluorinated tar		
3	DABCO	1	1	32	4	20(7)[a]
4	DABCO	1	1[b]	30	3	19
5	DABCO	1	2	1	1	37
6	DABCO	1	3	Polyfluorinated tar		
7	DABCO	2	2	Many fluorinated products		
8	DABCO	0.1	1	22	28	8
9	Quinuclidine	1	1	42(41)[a]	10(8)[a]	43(33)[*]
10	Quinuclidine	1.2	1[b]	54	1	43
11	Et_3N	1	1	56	25	6
12	Cs_2CO_3	1	1	0	4	14
13	NaCl	1	1	0	33	12(6)[a]
14	NaCl, DBU	1	1	7	19	16

[a] Isolated yield

b F_2 (20% v/ v in N_2) used

9.4 Screening Conditions for the Quinuclidine Mediated Direct Fluorination of DBM

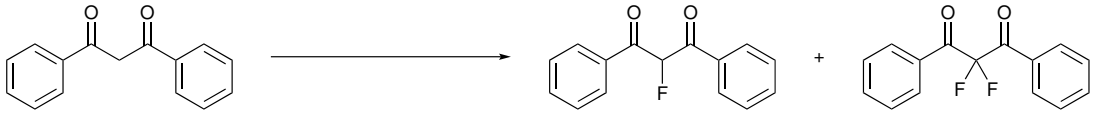

Dibenzoylmethane (0.449 g, 2.00 mmol) and quinuclidine were added to a SIMAX glass bottle and dissolved in acetonitrile (20 mL). The reaction vessel was cooled to 0 °C, stirred rapidly and purged with nitrogen for 10 minutes before fluorine gas, as a 10% mixture in nitrogen (*v/v*), was passed through the reaction mixture at a prescribed flow rate, (15 mL min^{-1}) that was controlled by a mass flow controller. After purging with nitrogen for 10 minutes, the reaction vessel was disconnected and the solvent removed under reduced pressure. The organic products were analysed by NMR spectroscopy as described above.

Entry	Equiv of quinuclidine	Equiv of F_2	Ratio of products by NMR		
			91	**92**	**93**
1	1	1	3	2	4
2	1.1	2.1	1	5	47
3	1.1	2.3	1	16	120

Chapter 10

Experimental to Chapter 3

10.1 General Procedure 3 (GP3)—Synthesis of compounds 94a–94f

Based on a literature procedure,[153] ethyl potassium malonate (2.383 g, 14 mmol) in ethyl acetate (40 mL) was cooled to 0 °C. Triethylamine (4.9 mL, 35 mmol) and magnesium chloride (1.619 g, 17 mmol) were added and the resulting slurry stirred at 30 °C for 6 h before the mixture was cooled to 0 °C and the corresponding benzoyl chloride (10 mmol) was added dropwise over 5 min. The mixture was stirred overnight at r.t. before being cooled to 0 °C and quenched with 13% hydrochloric acid (30 mL). The aqueous phase was removed and extracted with toluene (20 mL), then the combined organic phases were washed with 13% hydrochloric acid (2×10 mL) and water (2×10 mL),dried over magnesium sulfate and the sovlent removed under reduced pressure. The crude product was filtered through a silica plug with chloroform as the eluent to give the desired product which did not need any further purification.

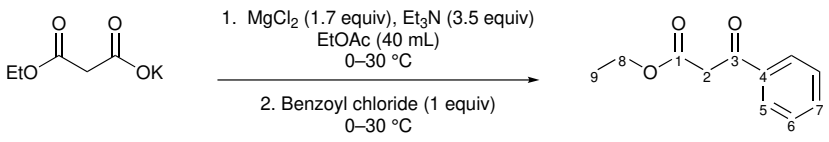

Ethyl (4-methoxy)benzoylacetate (94a)

4-(Methoxy)benzoyl chloride (1.354 mL, 2.00 mmol) gave *ethyl (4-methoxy)benzoylacetate* (1.658 g, 75%) as a pale orange oil. *Ketone product* (75%) ^{1}H NMR (700 MHz,

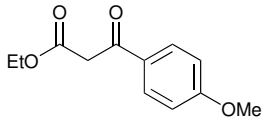

$CDCl_3$) δ 1.26 (3 H, t, $^3J_{HH}$ 7.1, C**9**H), 3.88 (3 H, s, C**10**H), 3.94 (2 H, s, C**2**H), 4.21 (2 H, q, $^3J_{HH}$ 7.1, C**8**H), 6.93–6.96 (2 H, m, C**6**H), 7.91–7.94 (2 H, m, C**5**H); ^{13}C NMR (176 MHz, $CDCl_3$) δ 14.2 (C**9**), 46.0 (C**2**), 55.7 (C**10**), 61.6 (C**8**), 114.1 (C**6**), 129.3 (C**4**), 131.1 (C**5**), 164.1 (C**7**), 167.9 (C**1**), 191.1. (C**3**); *enol product* (17%) ^{1}H NMR (700 MHz, $CDCl_3$) δ 5.58 (1 H, s, C**2**H), 3.85 (3H, s, C**10**H); *enol product* (8%) ^{1}H NMR (700 MHz, $CDCl_3$) δ 6.06 (1 H, s, C**2**H), 3.86 (3H, s, C**10**H); *m/z* (EI^+) 222.1 ($[M]^+$, 7%), 150.1 ($[C_9H_{10}O_2]^+$, 14%), 135.1 ($[C_8H_7O_2]^+$, 100%), 107.1 ($[C_7H_7O]^+$, 15%), 77.1 (($[C_6H_5]^+$, 18%). HRMS (ASAP) *m/z* calculated for $[M+H]^+$ = $C_{12}H_{15}O_4$ 223.0970, found 223.0968. IR (neat, cm^{-1}) 2982, 1675, 1599, 1511, 1422, 1257, 1170, 1024, 843, 566. Data consistent with that previously reported in the literature.[149]

Ethyl (4-chloro)benzoylacetate (94b)

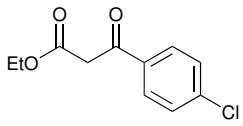

4-(Chloro)benzoyl chloride (1.282 mL, 2.00 mmol) gave *ethyl (4-chloro)benzoylacetate* (2.053 g, 91%) as a low-melting yellow solid. *Ketone product* (73%) ^{1}H NMR (700 MHz, $CDCl_3$) δ 1.25 (3 H, t, 3JHH 7.1, C**9**H), 3.95 (2 H, s, C**2**H), 4.20 (2 H, q, 3JHH 7.2, C**8**H), 7.43–7.46 (2 H, m, C**6**H), 7.87–7.90 (2 H, m, C**5**H); ^{13}C NMR (176 MHz, $CDCl_3$) δ 14.19 (s, C**9**), 46.06 (s, C**2**), 61.74 (s, C**8**), 129.25 (s, C**6**), 130.06 (s, C**5**), 140.42 (s, C**7**), 167.32 (s, C**1**), 191.42 (s, C**3**); *enol product* (20%) ^{1}H NMR (700 MHz, $CDCl_3$) δ 5.63 (1 H, s, C**2**H), 12.57 (1H, s, C**2**OH); *enol product* (7%) ^{1}H NMR (700 MHz, $CDCl_3$) δ 6.04 (1 H, s, C**2**H), 13.48 (1H, s, C**2**OH); *m/z* (EI^+) 226.0, ([M]m/z, 5%), 154.1 ($[C_8H_7ClO]^+$]+, 9%), 139.1 ($[C_7H_4ClO]^+$]$^+$, 100%), 111.0 ($[C_6H_4Cl]^+$]$^+$, 29%). HRMS (ASAP) *m/z* calculated for $[M+H]^+$ = $C_{11}H_{12}ClO_3$ 227.0475, found 227.0471. IR (neat, cm^{-1}) 2980, 2160, 1722, 1624, 1426, 1258, 1177, 1073, 796. Data consistent with that previously reported in the literature.[150]

Ethyl (4-trifluoromethyl)benzoylacetate (94c)

4-(Trifluoromethyl)benzoyl chloride (1.486 mL, 2.00 mmol) gave *ethyl (4-trifluoro methyl)benzoylacetate* (2.463 g, 95%) as a pale orange oil. *Ketone product* (60%) ^{1}H

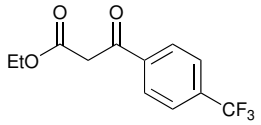

NMR (700 MHz, $CDCl_3$) δ 1.26 (3 H, t, $^3J_{HH}$ 7.1, C**9**H), 4.01 (2 H, s, C**2**H), 4.22 (2 H, q, $^3J_{HH}$ 7.1, C**8**H), 7.76 (2 H, d, $^3J_{HH}$ 8.2, C**6**H), 8.04–8.07 (2 H, m, C**5**H); ^{19}F NMR (376 MHz, $CDCl_3$) δ −63.2 (s, C**10**F_3), ^{13}C NMR (176 MHz, $CDCl_3$) δ 14.2 (C**9**), 46.3 (C**2**), 61.9 (C**8**), 122.8 (q, $^1J_{CF}$ 273.0, C**10**), 126.0 (q, $^4J_{CF}$ 3.7, C**6**), 129.0 (C**5**), 135.1 (q, $^2J_{CF}$ 32.8, C**7**), 138.8 (C**4**), 167.1 (C**1**), 191.7 (C**3**); *enol product* (40%) ^{1}H NMR (700 MHz, $CDCl_3$) δ 1.35 (3 H, t, $^3J_{HH}$ 7.1, C**9**H), 4.29 (2 H, q, $^3J_{HH}$ 7.1, C**8**H), 5.71 (1 H, s, C**2**H), 7.68 (2 H, d, $^3J_{HH}$ 8.3, C**6**H), 7.87–7.89 (2 H, m, C**5**H), 12.56 (1 H, s, C**3**OH); ^{19}F NMR (376 MHz, $CDCl_3$) δ −63.0 (s, C**10**F_3); ^{13}C NMR (176 MHz, $CDCl_3$) δ 14.4 (C**9**), 60.8 (C**8**), 89.2 (C**2**), 124.7 (q, $^1J_{CF}$ 272.9, C**10**), 125.7 (q, $^4J_{CF}$ 3.8, C**6**), 126.5 (C**5**), 132.9 (q, $^2J_{CF}$ 32.6, C**7**), 137.0 (s, C**4**), 169.6 (C**1**), 173.0 (C**3**); *m/z* (EI^+) 260.1, ($[M]^+$, 6%), 173.1 ($[C_8H_4F_3O]^+$, 100%), 145.1 ($[C_7H_4F_3]^+$, 39%), 69.0 ($[CF_3]^+$, 3%), 45.0 ($[C_2H_5O]^+$, 3%). HRMS (ASAP) *m/z* calculated for $[M+H]^+ = C_{12}H_{12}F_3O$ 261.0739, found 261.0743. IR (neat, cm^{-1}) 2980, 2160, 1722, 1624, 1426, 1258, 1177, 1073, 796. Data consistent with that previously reported in the literature.[195]

Ethyl (4-nitro)benzoylacetate (94d)

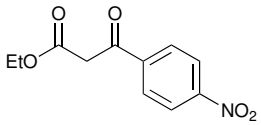

4-(Nitro)benzoyl chloride (1.856 g, 2.00 mmol) was dissolved in 5 mL EtOAc and gave *ethyl (4-nitro)benzoylacetate* (2.336 g, 99%) as a peach coloured solid; Mp 62–63 °C [lit. Mp. 63–67 °C[150]]. *Enol product* (74%) ^{1}H NMR (700 MHz, $CDCl_3$) δ 1.35 (3 H, t, $^3J_{HH}$ 7.2, C**9**H), 4.30 (2 H, q, $^3J_{HH}$ 7.1, C**8**H), 5.76 (1 H, s, C**2**H), 7.92–7.95 (2 H, m, C**5**H), 8.26–8.29 (2 H, m, C**6**H), 12.57 (1 H, s, C**2**OH); ^{13}C NMR (176 MHz, $CDCl_3$) δ 14.4 (C**9**), 61.0 (C**8**), 90.4 (C**2**), 123.9 (C**6**), 127.1 (C**5**), 139.5 (C**4**), 149.4 (C**7**), 168.4 (C**1**), 172.8 (C**3**); *ketone product* (26%) ^{1}H NMR (700 MHz, $CDCl_3$) δ 1.26 (3 H, t, $^3J_{HH}$ 7.1, C**9**H), 4.03 (2 H, s, C**2**H), 4.22 (2 H, q, $^3J_{HH}$ 7.1, C**9**H), 8.10–8.13 (2 H, m, C**5**H), (8.32–8.35 (2 H, m, C**6**H), ^{13}C NMR (176 MHz, $CDCl_3$) δ 14.2 (C**9**), 46.4 (C**2**), 62.0 (C**8**), 124.1 (C**6**), 129.7 (C**5**), 140.5 (C**4**), 150.8 (C**7**), 166.8 (C**1**), 191.2 (C**3**); *m/z* (EI^+) 165.0 ($[_8H_7NO_3]^+$, 20%), 150.1 ($[_7H_4NO_3]^+$, 100%). HRMS (ASAP) *m/z* calculated for $[M+H]^+ = C_{11}H_{11}NO_5$ 238.0715, found

238.0715. IR (neat, cm^{-1}) 3114, 2910, 2160, 1619, 1519, 1428, 1339, 1215, 1032, 797. Data consistent with that previously reported in the literature.[150]

Ethyl (4-cyano)benzoylacetate (94e)

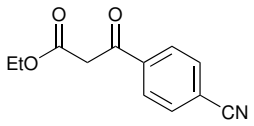

4-(Cyano)benzoyl chloride (1.656 g, 2.00 mmol) was dissolved in 5 mL of ETOAc and gave *ethyl (4-cyano)benzoylacetate* (2.060 g, 95%) as a white solid after recrystallisation from EtOH; Mp 60–62 °C [lit. Mp. 62–63 °C[196]]. *Enol product* (88%) ^{1}H NMR (400 MHz, $CDCl_3$) δ 1.34 (3 H, t, $^3J_{HH}$ 7.1, C**9**H), 4.30 (2 H, q, $^3J_{HH}$ 7.1, C**8**H), 5.72 (1 H, s, C**2**H), 7.71 (2 H, d, $^3J_{HH}$ 7.6, C**6**H), 7.86 (2 H, d, $^3J_{HH}$ 7.6, C**5**H), 12.57 (1 H, s, C**2**OH); ^{13}C NMR (101 MHz, $CDCl_3$) δ 14.4 (C**9**), 60.9 (C**8**), 89.9 (C**2**), 123.9 (C**6**), 137.7 (C**4**), 118.4 (C**10**), 126.7 (C**5**), 132.5 (C**6**), 149.4 (C**7**), 168.7 (C**1**), 172.8 (C**3**); *ketone product* (12%) ^{1}H NMR (400 MHz, $CDCl_3$) δ 1.25 (3 H, t, $^3J_{HH}$ 7.0, C**9**H), 4.00 (2 H, s, C**2**H), 4.22 (2 H, q, $^3J_{HH}$ 7.0, C**8**H), 7.79 (2 H, d, $^3J_{HH}$ 7.7, C**6**H), 8.04 (2 H, d, $^3J_{HH}$ 7.7, C**5**H); ^{13}C NMR (101 MHz, $CDCl_3$) δ 14.2 (C**9**), 46.2 (C**2**), 62.0 (C**8**), 117.1 (C**7**), 117.9 (C**10**), 129.1 (C**5**), 132.8 (C**6**), 139.0 (C**4**), 166.9 (C**1**), 191.4 (C**3**); *m/z* (EI^+) 145.1 ($[C_9H_7NO]^+$, 34%), 130.1 ($[C_8H_4NO]^+$, 100%), 102.1 ($[C_7H_4N]^+$, 70%), 75.1 ($[C_3H_7O_2]^+$, 16%), 63.1 ($[C_2H_5O_2]^+$, 2%), 51.1 ($[C_4H_3]^+$, 9%), 43.1 ($[C_2H_3O]^+$, 19%). HRMS (ASAP) *m/z* calculated for $[M+H]^+$ = $C_{12}H_{12}NO_3$ 218.0817, found 218.0836. IR (neat, cm^{-1}) 2999, 2233, 2159, 1977, 1739, 1621, 1422, 1356, 1253, 1192, 1029, 800, 715, 543, 433. Data consistent with that previously reported in the literature.[197]

Ethyl (3-nitro)benzoylacetate (94f)

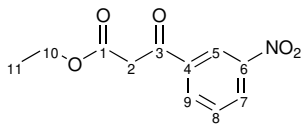

3-(Nitro)benzoyl chloride (1.856 g, 2.00 mmol) was dissolved in 5 mL EtOAc and reacted according to the general procedure to yield *ethyl (3-nitro)benzoylacetate* (1.777 g, 75%) as a peach coloured solid; Mp 70–71 °C [lit. Mp. 66–67 °C[198]]. *Ketone product* (58%) ^{1}H NMR (700 MHz, $CDCl_3$) δ 1.27 (3 H, t, $^3J_{HH}$ 7.1, C**11**H), 4.05 (2 H, s, C**2**H), 4.23 (2 H, q, $^3J_{HH}$ 7.1, C**10**H), 7.71 (1 H, t, $^3J_{HH}$ 7.9, C**8**H), 8.29 (1 H, dt, $^3J_{HH}$ 7.9, $^4J_{HH}$ 1.2, C**9**H), 8.46 (1 H, ddd, $^3J_{HH}$ 8.2, $^4J_{HH}$ 2.1, $^4J_{HH}$ 1.2, C**7**H), 8.77 (1 H, t, $^4J_{HH}$ 2.1, C**5**H); ^{13}C NMR (176 MHz, $CDCl_3$) δ 14.2 (C**11**), 46.1

(C**2**), 62.0 (C**10**), 123.6 (C**5**), 128.1 (C**7**), 130.3 (C**8**), 134.1 (C**9**), 137.4 (C**4**), 148.7 (C**6**), 166.8 (C**1**), 190.6 (C**3**); *enol product* (42%) ^{1}H NMR (700 MHz, $CDCl_3$) δ 1.35 (3 H, t, $^{3}J_{HH}$ 7.1, C**11**H), 4.30 (1 H, q, $^{3}J_{HH}$ 7.1, C**10**H), 5.77 (1 H, s, C**2**H), 7.62 (1 H, t, $^{3}J_{HH}$ 7.9, C**8**H), 8.10 (1 H, ddd, $^{3}J_{HH}$ 7.9, $^{4}J_{HH}$ 1.7, $^{4}J_{HH}$ 1.0, C**9**H), 8.31 (1 H, ddd, $^{3}J_{HH}$ 8.2, $^{4}J_{HH}$ 2.2, $^{4}J_{HH}$ 1.0, C**7**H), 8.62 (1 H, t, $^{4}J_{HH}$ 2.2, C**5**H), 12.62 (1 H, s, C**3**OH); ^{13}C NMR (176 MHz, $CDCl_3$) δ 14.4 (C**11**), 61.0 (C**10**), 89.4 (C**2**), 121.2 (C**5**), 125.7 (C**7**), 129.8 (C**8**), 131.8 (C**9**), 135.4 (C**4**), 128.1 (C**9**), 148.6 (C**6**), 168.4 (C**1**), 172.9 (C**3**); *m/z* (ESI$^+$) 238.3 ($[C_{11}H_{11}NO_5]^+$, 100%), 115.1 ($[C_7H_5NO_3]^+$, 29%), *m/z* (EI$^+$) 165.0 ($[C_8H_7NO_3]^+$, 17%), 150.1 ($[C_7H_4NO_3]^+$, 100%). HRMS (ASAP) *m/z* calculated for $[M+H]^+ = C_{11}H_{11}NO_5$ 238.0715, found 238.0722. Data consistent with that previously reported in the literature.[199]

Ethyl 3-oxo-3-(pyridin-4-yl)propanoate (94g)

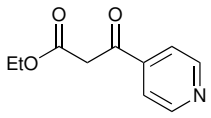

Based on a literature procedure,[154] ethyl isonicotinate (1.498 mL, 10 mmol) was dissolved in ethyl acetate (30 mL) and cooled to -50 °C before $LiN(SiMe_3)_2$ (1 M in THF, 30 mL, 30 mmol) was added and the mixture was stirred for 20 min. The reaction was quenched with acetic acid (50 mmol), basified with saturated sodium bicarbonate solution and extracted with ethyl acetate (2×100 mL). The organic phases were combined, washed with water (20 mL), saturated sodium chloride solution (20 mL) before drying over magnesium sulfate and the solvents removed under reduced pressure. Recrystallisation from ethanol gave the desired *ethyl 3-oxo-(pyridin-4-yl)propanoate* (1.377 g, 71%) as a white solid; Mp 52–54 °C [lit. Mp. 55–57 °C[200]]. *Ketone product* (42%) ^{1}H NMR (600 MHz, $CDCl_3$) δ 1.25 (3 H, t, $^{3}J_{HH}$ 7.1, C**8**H), 3.98 (2 H, s, C**2**H), 4.21 (2 H, q, $^{3}J_{HH}$ 7.1, C**7**H), 7.71 (2 H, dt, $^{3}J_{HH}$ 4.3, $^{4}J_{HH}$ 1.3 C**5**H), 8.83 (2 H, dt, $^{3}J_{HH}$ 4.4, $^{4}J_{HH}$ 1.3, C**6**H); ^{13}C NMR (151 MHz, $CDCl_3$) δ 14.2 (C**8**), 46.1 (C**2**), 62.0 (C**7**), 121.4 (C**5**), 141.9 (C**4**), 151.3 (C**6**), 166.8 (C**1**), 192.2 (C**3**); *enol product* (58%) ^{1}H NMR (600 MHz, $CDCl_3$) δ 1.34 (3 H, t, $^{3}J_{HH}$ 7.1, C**8**H), 4.28 (2 H, q, $^{3}J_{HH}$ 7.2, C**7**H), 5.76 (1 H, s, C**2**H), 7.60 (2 H, dt, $^{3}J_{HH}$ 4.5, $^{4}J_{HH}$1.3, C**5**H), 8.70 (2 H, dt, $^{3}J_{HH}$ 4.4, $^{4}J_{HH}$ 1.3, C**6**H), 12.43 (1 H, s,); ^{13}C NMR (151 MHz, $CDCl_3$) δ 14.4 (C**8**), 61.0 (C**7**), 90.1 (C**2**), 119.8 (C**5**), 140.9 (C**4**), 150.6 (C**6**), 168.4 (C**3**), 172.8 (C**1**); *m/z* (ESI$^+$) 194.1 ($[C_{10}H_{11}NO_3]^+$, 100%), 148.1 ($[C_8H_6NO_2]^+$, 69%), 120.1 (($[C_7H_6NO]^+$, 3%), 106.0 ($[C_6H_4NO]^+$, 1%). HRMS (ASAP) *(m/z)* calculated for $[M+H]^+$ $C_{10}H_{12}NO_3$ 194.0817; found 194.0810. Data consistent with that previously reported in the literature.[154]

10.2 General Procedure 4 (GP4)—Synthesis of compounds 96–96g

Quinuclidine (0.334 g, 3.00 mmol, 1.5 equiv.) and the relevant ethyl benzoylacetate (2.00 mmol, 1.0 equiv.) were added to a SIMAX glass bottle and dissolved in acetonitrile (20 mL). The reaction vessel was cooled to 0 °C, stirred rapidly and purged with nitrogen for 10 minutes before fluorine, as a 10% mixture in nitrogen (*v/v*), was passed through the reaction mixture at a prescribed flow rate, (6.00 mmol, 3.0 equiv., 30 mL min^{-1}) that was controlled by a mass flow controller for 49 min. After purging with nitrogen for 10 min., the reaction vessel was disconnected and the solvent removed *in vacuo*. The crude residue was filtered through a silica plug with chloroform as the eluent to give the desired product.

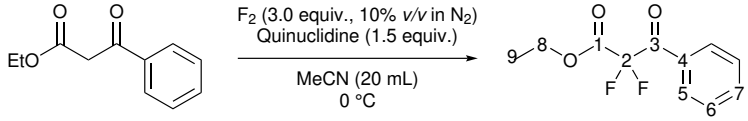

Ethyl 2,2-difluoro-3-oxo-3-phenylpropanoate (96)

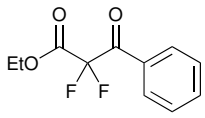

Following **GP4**, ethyl benzoylacetate (0.35 mL, 2.02 mmol, 1.0 equiv.) afforded *ethyl 2,2-difluoro-3-oxo-3-phenylpropanoate* (0.393 g, 85%) as a pale yellow oil; ^{1}H NMR (700 MHz, $CDCl_3$) δ 1.32 (3 H, t, $^{3}J_{HH}$ 7.1, C**9**H), 4.39 (2 H, q, $^{3}J_{HH}$ 7.1, C**8**H), 7.51–7.54 (2 H, m, C**6**H), 7.66–7.69 (1 H, m, C**7**H), 8.08 (2 H, ddt, $^{3}J_{HH}$ 7.8, $^{4}J_{HH}$ 2.2, $^{5}J_{HH}$ 1.1, C**5**H); ^{19}F NMR (376 MHz, $CDCl_3$) δ −107.6 (s); ^{13}C NMR (176 MHz, $CDCl_3$) δ 14.0 (C**9**), 63.9 (C**8**), 109.9 (t, $^{1}J_{CF}$ 264.6, C**2**), 129.1 (C**4**), 130.1 (t, $^{4}J_{CF}$ 2.7, C**5**), 131.2 (t, $^{5}J_{CF}$ 2.0, C**6**), 135.2 (C**7**), 161.9 (t, $^{2}J_{CF}$ 30.5, C**1**), 185.6 (t, $^{2}J_{CF}$ 27.6, C**3**); *m/z* (EI)$^{+}$ 183.0 ($[C_9H_5F_2O_2]^{+}$, 2%), 155.1 ($[C_8H_5F_2O]^{+}$, 3%), 105.1 ($[C_7H_5O]^{+}$, 100%), 77.1 ($[C_6H_5]^{+}$, 76%), 51.0 ($[C_4H_3]^{+}$, 17%). HRMS (ASAP) *m/z* calculated for $[M+H]^{+}$ $C_{11}H_{11}F_2O_3$ 229.0676; found 229.0682. IR (neat, cm^{-1}) 2988, 1772, 1599, 1451, 1311, 1098, 922, 832, 685, 584. Data consistent with that previously reported in the literature.[155]

Ethyl 2,2-difluoro-3-(4-methoxyphenyl)-3-oxopropanoate (96a)

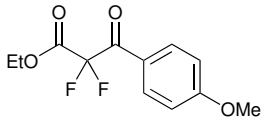

Following **GP4**, ethyl (4-methoxy)benzoylacetate (0.444 g, 2.00 mmol, 1.0 equiv.) after washing through a silica plug with $CHCl_3$ as the eluent gave 0.424 g of a yellow oil that contained a mixture of products; ^{19}F NMR (376 MHz, $CDCl_3$) δ −132.9 (ddd, *J* 11.7, *J* 8.1, *J* 1.2), −126.7–−126.1 (m), −107.3 (s), −107.3 (s, difluoro product), −107.3 (s).

Ethyl 2,2-difluoro-3-(4-chlorophenyl)-3-oxopropanoate (96b)

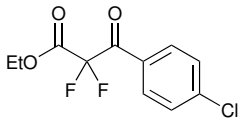

Following **GP4**, ethyl (4-chloro)benzoylacetate (0.453 g, 2.00 mmol, 1.0 equiv.) afforded *ethyl 2,2-difluoro-3-(4-chlorophenyl)-3-oxopropanoate* (0.466 g, 89%) as a pale yellow oil; ^{1}H NMR (600 MHz, $CDCl_3$) δ 1.33 (3H, t, $^3J_{HH}$ 7.1, C**9**H), 4.39 (2H, q, $^3J_{HH}$ 7.1, C**8**H), 7.49–7.52 (2H, m, C**6**H), 8.03 (2H, d, $^3J_{HH}$ 8.8, C**5**H); ^{19}F NMR (376 MHz, $CDCl_3$) δ −107.6 (s, C**2**F_2); ^{13}C NMR (151 MHz, $CDCl_3$) δ 14.0 (s, C**9**), 64.0 (s, C**9**), 109.9 (t, $^1J_{CF}$ 264.8, C**2**), 129.5 (t, $^3J_{CF}$ 2.1, C**4**), 129.6 (s, C**6**), 134.5 (t, $^4J_{CF}$ 2.9, C**5**), 142.1 (s, C**7**), 161.7 (t, $^2J_{CF}$ 30.4, C**1**), 184.6 (t, $^2J_{CF}$ 28.0, C**3**); *m/z* (EI)$^+$ 217.0 ($[C_9H_4ClF_2O_2]^+$, 3%), 189.0 ($[C_8H_4CLF_2O]^+$, 3%), 139.1 ($[C_7H_4ClO]^+$, 100%), 111.0 ($[C_6H_4Cl]^+$, 83%), 85.0 ($[C_6H_{13}]^+$, 3%), 75.0 ($[C_3H_7O_2]^+$, 35%), 50.0 ($[C_4H_2]^+$, 9%). HRMS (ASAP) *m/z* calculated for $[C_{11}H_{10}ClF_2O_3]^+$ 263.0287; found 263.0287. IR (neat, cm^{-1}) 2988, 1773, 1702, 1589, 1491, 1373, 1406, 1310, 1254, 1158, 1088, 1014, 922, 847, 759, 549.

Ethyl 2,2-difluoro-3-(4-(trifluoromethyl)phenyl)-3-oxopropanoate (96c)

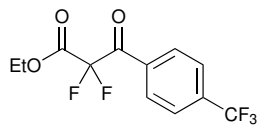

Following **GP4**, ethyl (4-trifluoromethyl)benzoylacetate (0.520 g, 2.00 mmol, 1.0 equiv.) afforded *ethyl 2,2-difluoro-3-(4-trifluoromethylphenyl)-3-oxopropanoate* (0.516 g, 87%) as a pale yellow oil; ^{1}H NMR (700 MHz, $CDCl_3$) δ 1.34 (3H, t, $^3J_{HH}$ 7.1, C**9**H), 4.41 (2H, q, $^3J_{HH}$ 7.1, C**8**H), 7.79–7.81 (2H, m, C**6**H), 8.19–8.21 (2H, m, C**5**H); ^{19}F NMR (376 MHz, $CDCl_3$) δ −107.9 (2F, s, C**2**F_2), −63.5 (3F, s, C**10**F_3);

^{13}C NMR (176 MHz, $CDCl_3$) δ 14.0 (s, C**9**), 64.2 (s, C**9**), 109.7 (t, $^1J_{CF}$ 264.9, C**2**), 123.4 (q, $^1J_{CF}$ 273.0, C**10**), 126.2 (q, $^3J_{CF}$ 3.8, C**6**), 130.5 (t, $^4J_{CF}$ 2.8, C**5**), 133.9 (s, C**4**), 136.3 (q, $^2J_{CF}$ 33.1, C**7**), 161.5 (t, $^2J_{CF}$ 30.3, C**1**), 185.1 (t, $^2J_{CF}$ 28.4, C**3**); *m/z* (EI)$^+$) 297.1 ($[C_{12}H_{10}F_5O_3]^+$, 34%), 269.0 ($[C_{10}H_6F_5O_3]^+$, 6%), 232.1 ($[C_{10}H_4F_4O_2{}^+$, 3%), 173.0 ($[C_8H_4F_3O]^+$, 16%), 145 ($[C_7H_4F_3]^+$, 4%). HRMS (ASAP) *m/z* calculated for $[C_{12}H_{10}F_5O_3]^+$ 297.0539; found 297.0538. IR (neat, cm^{-1}) 1775, 1713, 1514, 1414, 1375, 1327, 1315, 1254, 1128, 1117, 1064, 1017, 925, 857, 832, 708, 595. Data consistent with that previously reported in the literature.[201]

Ethyl 2,2-difluoro-3-(4-nitrophenyl)-3-oxopropanoate (96d)

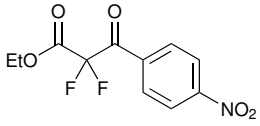

Following **GP4**, ethyl (4-nitro)benzoylacetate (0.474 g, 2.00 mmol, 1 equiv.) afforded *ethyl 2,2-difluoro-3-(4-nitrophenyl)-oxo-3-phenylpropanoate* (0.455 g, 77%) as a white solid; Mp 66–68 °C. ^{1}H NMR (700 MHz, $CDCl_3$) δ 1.34 (3 H, t, $^3J_{HH}$ 7.1, C**9**H), 4.41 (2 H, q, $^3J_{HH}$ 7.1, C**9**H), 8.24–8.27 (2 H, m, C**6**H), 8.35–8.38 (2 H, m, C**5**H); ^{19}F NMR (376 MHz, $CDCl_3$) δ −107.8 (s); ^{13}C NMR (176 MHz, $CDCl_3$) δ 14.0 (C**9**), 64.4 (C**8**), 109.6 (t, $^1J_{CF}$ 265.1, C**2**), 124.2 (s, C**6**), 131.3 (t, $^4J_{CF}$ 2.9, C**5**), 135.6 (s, $^3J_{CF}$ 2.0, C**4**), 151.4 (s, C**7**), 161.2 (t, $^2J_{CF}$ 30.2, C**1**), 184.7 (t, $^2J_{CF}$ 28.8, C**3**) ;*m/z* (EI)$^+$ 228.0 ($[C_{11}H_{10}F_2O_3]^+$, 2%), 200.0 ($[C_8H_4F_2NO_3]^+$, 4%), 150.1 ($[C_7H_4NO_3]^+$, 100%), 76.1 ($[C_6H_4]^+$, 55%), 50.0 ($[C_4H_2]^+$, 13%). HRMS (ASAP) *m/z* calculated for $[M+H]^+$ $C_{11}H_{10}F_2NO_5$ 274.0527; found 274.0526. IR (neat, cm^{-1}) 3539, 3411, 2991, 1773, 1748, 1724, 1606, 1527, 1349, 1312, 1165, 1137, 1100, 1082, 1043, 1012, 1001, 926, 854, 827, 782, 733, 710, 671, 567. Data consistent with that previously reported in the literature.[129]

Ethyl 2,2-difluoro-3-(4-cyano)-3-oxopropanoate (96e)

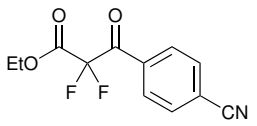

Following **GP4**, ethyl (4-cyano)benzoylacetate (0.4346 g, 2.00 mmol, 1.0 equiv.) afforded *ethyl 2,2-difluoro-3-(4-cyanophenyl)-3-oxopropanoate* (0.339 g, 67%) as a pale yellow oil; ^{1}H NMR (400 MHz, $CDCl_3$) δ 1.33 (3H, t, $^3J_{HH}$ 7.1, C**9**H), 4.40 (2H, q, $^3J_{HH}$ 7.1, C**8**H), 7.80–7.86 (2H, m, C**6**H), 8.18 (2H, d, $^3J_{HH}$ 8.1, C**5**H); ^{19}F NMR (376 MHz, $CDCl_3$) δ −107.8 (s); ^{13}C NMR (101 MHz, $CDCl_3$) δ 14.0 (s, C**9**),

64.3 (s, C**9**), 109.6 (t, $^{1}J_{CF}$ 265.0, C**2**), 117.5 (s, C**10**), 118.4 (s, C**7**), 130.4 (t, $^{5}J_{CF}$ 2.9, C**5**), 132.8 (s, C**6**), 134.1 (t, $^{3}J_{CF}$ 2.1, C**4**), 161.3 (t, $^{2}J_{CF}$ 30.2, C**1**), 184.8 (t, $^{2}J_{CF}$ 28.7, C**3**); *m/z* (ESI^{+}) 208.0 ($[C_{10}H_4F_2N_{02}]^{+}$, 2%), 180.0 ($[C_9H_4F_2NO]^{+}$, 4%), 130.2 ($[[C_8H_4NO]^{+}$, 100%), 102.1 ($[C_7H_4N]^{+}$, 76%), 75.1 ($[C_3H_7O_2]^{+}$, 17%), 51.0 ($[C_4H_3]^{+}$, 9%). HRMS (ASAP) *m/z* calculated for $[C_{12}H_{10}F_2NO_3]^{+}$ 254.0629; found 254.0635. IR (neat, cm^{-1}) 2986, 2235, 1772, 1718, 1608, 1471, 1448, 1410, 1374, 1312, 1294, 1253, 1156, 1128, 1098, 1077, 1007, 924, 855, 765, 544. Data consistent with that previously reported in the literature.[201]

Ethyl 2,2-difluoro-3-(3-nitrophenyl)-oxo-3-phenylpropanoate (96f)

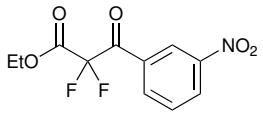

Following **GP4**, ethyl (3-nitro)benzoylacetate (0.474 g, 2.00 mmol, 1 equiv.) afforded *ethyl 2,2-difluoro-3-(3-nitrophenyl)-oxo-3-phenylpropanoate* (0.460 g, 78%) as a pale yellow oil. ^{1}H NMR (700 MHz, $CDCl_3$) δ 1.35 (3 H, t, $^{3}J_{HH}$ 7.2, C**11**H), 4.42 (2 H, q, $^{3}J_{HH}$ 7.1, C**10**H), 7.77–7.79 (1 H, m, C**9**H), 8.40 (1 H, ddq, $^{3}J_{HH}$ 8.1, $^{4}J_{HH}$ 1.9, $^{5}J_{HH}$ 0.8, C**8**H), 8.53 (1 H, ddd, $^{3}J_{HH}$ 8.1, $^{4}J_{HH}$ 2.3, $^{4}J_{HH}$ 1.1, C**7**H), 8.91 (1 H, ddd, $^{4}J_{HH}$ 2.3, $^{4}J_{HH}$ 1.6, $^{5}J_{HH}$ 0.8, C**5**H); ^{19}F NMR (376 MHz, $CDCl_3$) δ −107.7 (s); ^{13}C NMR (176 MHz, $CDCl_3$) δ 14.0 (C**11**), 64.4 (C**10**), 109.6 (t, $^{1}J_{CF}$ 265.2, C**2**), 125.0 (t, $^{4}J_{CF}$ 2.9, C**5**), 129.3 (C**7**), 130.5 (C**9**), 132.4 (t, $^{3}J_{CF}$ 2.2, C**4**), 135.4 (t, $^{5}J_{CF}$ 2.9, C**8**), 148.7 (C**6**), 161.2 (t, $^{2}J_{CF}$ 30.1, C**1**), 184.2 (t, $^{2}J_{CF}$ 28.8, C**3**); *m/z* (EI)$^{+}$ 228.0 ($[C_{11}H_{10}F_2O_3]^{+}$, 1%), 200.0 ($[C_8H_4F_2NO_3]^{+}$, 4%), 150.1 ($[C_7H_4NO_3]^{+}$, 100%), 76.1 ($[C_6H_4]^{+}$, 55%). HRMS (ASAP) *m/z* calculated for $[M+H]^{+}$ $C_{11}H_{10}F_2NO_5$ 274.0527; found 274.0525. IR (neat, cm^{-1}) 2990, 1773, 1714, 1615, 1534, 1350, 1316, 1250, 1163, 1126, 1078, 1003, 968, 949, 929, 857, 829, 719, 691, 585.

Ethyl 2,2-difluoro-3-(pyridin-4-yl)-3-oxopropanoate (96g)

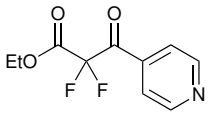

Following **GP4**, ethyl 3-oxo-3-(pyridin-4-yl)propanoate (0.193 g, 1.00 mmol, 1.0 equiv.) and quinuclidine (0.167 g, 1.5 mmol, 1.5 equiv.) were reacted with F_2 (3.0 mmol, 3.0 equiv., 24 min). Washing the product mixture through a silica plug with $CHCl_3$ as the eluent gave 0.023 g of a yellow oil that contained several products by

NMR spectroscopy; ^{19}F NMR (376 MHz, $CDCl_3$) δ −229.1, −225.0–−222.0 (m), −208.3–−207.6 (m), −191.3 (dt, *J* 48.8, 1.1) (s), −150.0 (s), −144.9 (s), −127.3 (d, J 53.4), −126.7–−125.2 (m), −118.5 (s), −117.7 (s), −117.3 (s), −112.6 (s), −112.2 (s), −110.9 (d, *J* 48.2) (s), −108.5 (s), −106.5 (s), −105.5 (s), −86.2–−85.2 (m), −76.0 (s), −67.8 (s), −66.8 (s), −65.9 (s), −65.2 (s), −64.6 (s).

10.3 General Procedure 5 (GP5)—Synthesis of compounds 210b–210e

Ethyl 2,2-difluoro-3-oxo-3-phenylpropanoate (0.114 g, 0.5 mmol, 1 equiv.) and the corresponding amine (5 mmol, 10 equiv.) were dissolved in THF (5 mL) and stirred at r.t. for 3 d. The reaction mixture was partitioned between DCM (20 mL) and 13% HCl (25 mL), and the aqueous phase washed with DCM (2×10 mL). The organic phases were combined, dried over magnesium sulfate before removal of the solvent under reduced pressure. The crude product was filtered through a silica plug with ethyl acetate 15% *v/v* in hexane solvent mixture as the eluent to give the desired product.

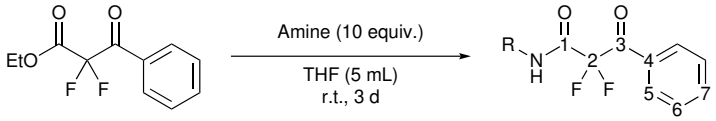

2,2-Difluoro-3-oxo-3-phenylpropanamide (210b)

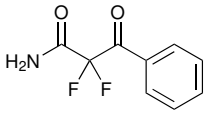

Following **GP5**, ammonia (1.25 mL of 4M NH_3 in MeOH, 5 mol, 10 equiv.) afforded *2,2-difluoro-3-oxo-3-phenylpropanamide* (0.058g, 58%) as a white solid; Mp 92–94 °C. ^{1}H NMR (400 MHz, $CDCl_3$) δ 6.56 (2 H, s, NH_2), 7.48–7.54 (2 H, C**5**H), 7.67, (1 H, t, $^3J_{HH}$ 7.4, C**7**H), 8.13 (2 H, d, $^3J_{HH}$ 7.8, C**5**H); ^{19}F NMR (376 MHz, $CDCl_3$) δ −108.1 (q, $^5J_{CF}$ 1.2); ^{13}C NMR (101 MHz, $CDCl_3$) δ 110.8 (t, $^1J_{CF}$ 266, C**2**), 129.0 (s, C**6**), 130.5 (t, $^4J_{CF}$ 2.9, C**5**), 131.5 (t, $^3J_{CF}$ 1.4, C**4**), 135.2 (s, C**7**), 163.8 (t, $^2J_{CF}$ 28.1, C**1**), 187.1 (t, $^2J_{CF}$ 27.1, C**3**); *m/z* (EI)$^+$ 199.3 ($[C_9H_7F_2NO_2]^+$, 1%), 156.0 ($[C_8H_6F_2O]^+$, 1%), 105.1 ($[C_7H_5O]^+$, 100%), 77.1 ($[C_6H_5]^+$, 83%), 51.0 ($[C_4H_3]^+$, 25%). HRMS (ASAP) calculated for $[M+H]^+$ $C_9H_8F_2NO_2$ 200.0523; found 200.0524.

IR (neat, cm^{-1}) 3383, 3184, 2922, 2537, 2159, 2027, 1977, 1721, 1689, 1622, 1597, 1451, 1402, 1312, 1271, 1145, 1061, 911, 891, 818, 788, 744, 681, 619, 602, 569, 552. Data consistent with that previously reported in the literature.[202]

N-Benzyl-2,2-difluoro-3-oxo-3-phenylpropanamide (210c)

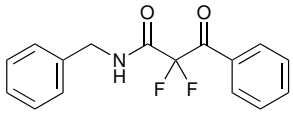

Following **GP5**, benzylamine (0.109g mL, 1 mmol, 2 equiv.) afforded *N-benzyl-2,2-difluoro-3-oxo-3-phenylpropanamide* (0.109 g, 75%) as a yellow solid; Mp 91–93 °C. ^{1}H NMR (600 MHz, $CDCl_3$) δ 4.54 (2H, d, $^3J_{HH}$ 5.9, C**8**H), 6.76, (1H, s, NH), 7.27–7.30 (2H, m, C**10**H), 7.30–7.33 (1H, m, C**12**H), 7.34–7.37 (2H, m, C**H**), 7.49–7.53 (2H, m, C**6**H), 7.64–7.68 (2H, m, C**7**H), 8.13–8.16 (2H, m, C**5**H); ^{19}F NMR (376 MHz, $CDCl_3$) δ −108.1 (s); ^{13}C NMR (151 MHz, $CDCl_3$) δ 44.0 (s, C**8**), 111.1 (t, $^1J_{CF}$ 265.7, C**2**), 128.0 (s, C**10**), 128.3 (s, C**12**), 128.9 (s, C**6**), 129.1 (s, C**11**), 130.5 (t, $^4J_{CF}$ 2.9, C**5**), 131.8 (s, C**4**), 135.1 (s, C**7**), 136.4 (s, C**9**); *m/z* $(EI)^+$ 289.1 ($[C_{16}H_{13}F_2NO_2]^+$, 14%), 164.1 (10%), 105.1 ($[C_7H_5O]^+$, 100%), 91.1 ($[C_7H_7]^+$, 36%), 77.1 ($[C_6H_5]^+$, 43%), 65.0 (7%), 51.1 ($[C_4H_3]^+$, 8%). HRMS (ASAP) calculated for $[M+H]^+$ $C_{16}H_{14}F_2NO_2$ 290.0993; found 290.0982. IR (neat, cm^{-1}) 3313, 2547, 2159, 2030, 1977, 1708, 1681, 1596, 1544, 1495, 1450, 1324, 1274, 1239, 1154, 1134, 1102, 1011, 922, 903, 806, 754, 706, 684, 667, 607, 581, 526. Data consistent with that previously reported in the literature.[203]

2,2-Difluoro-3-oxo-3-phenyl-*N*-(prop-2-en-1-yl)propanamide (210d)

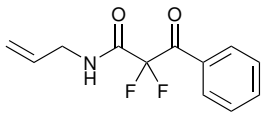

Following **GP5**, allylamine (0.375 mL, 5.00 mol, 10 equiv.) afforded *2,2-difluoro-3-oxo-3-phenyl-N-(prop-2-en-1-yl)propanamide* (0.084 g, 70%) as a colourless oil. ^{1}H NMR (600 MHz, $CDCl_3$) δ 3.99 (2 H, t, $^3J_{HH}$ 5.9, C**8**H), 5.18– 5.30 (2 H, m, C**10**H), 5.77–5.90 (1 H, m, C**9**H), 6.59 (1 H, s, NH), 7.51 (2 H, t, $^3J_{HH}$ 7.7, C**6**H), 7.6 (1 H, t, $^3J_{HH}$ 7.4, C**7**H), 8.15 (2 H, d, $^3J_{HH}$ 7.9, C**5**H); ^{19}F NMR (376 MHz, $CDCl_3$) δ −108.2 (s); ^{13}C NMR (101 MHz, $CDCl_3$) δ 42.2 (s, C**8**), 111.1 (t, $^1J_{CF}$ 265.5, C**2**), 118.0 (s, C**10**), 128.9 (s, C**6**), 130.6 (t, $^4J_{CF}$ 2.9, C**5**), 131.7 (t, $^3J_{CF}$ 1.6, C**4**), 132.3 (s, C**9**), 135.1 (s, C**7**), 161.5 (t, $^2J_{CF}$ 27.4, C**1**), 187.6 (t, $^2J_{CF}$ 27.2, C**3**); *m/z* $(EI)^+$ 239.1 ($[C_{12}H_{11}F_2NO_2]^+$, 4%), 156.1 ($[C_8H_6F_2O]^+$, 12%), 105.1 ($[C_7H_5O]^+$, 100%),

77.1 ($[C_6H_5]^+$, 80%), 56.1 ($[C_3H_6N]^+$, 5%), 51.0 ($[C_4H_3]^+$, 18%). HRMS (ASAP) calculated for $[M+H]^+$ $C_{12}H_{12}F_2NO_2$ 240.0836; found 240.0840. IR (neat, cm^{-1}) 3313, 3075, 1686, 1647, 1598, 1581, 1450, 1432, 1267, 1160, 1100, 1028, 992, 915, 805, 746, 710, 684, 575.

2,2-Difluoro-3-oxo-3-phenyl-N-(prop-2-yn-1-yl)propanamide (210e)

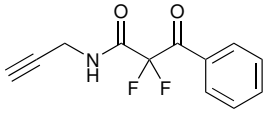

Following **GP5**, propargylamine (0.320 mL, 5 mmol, 10 equiv.) afforded *2,2-difluoro-3-oxo-3-phenyl-N-(prop-2-yn-1-yl)propanamide* (0.074g, 62%) as a colourless oil. ^{1}H NMR (600 MHz, $CDCl_3$) δ 2.30 (1 H, t, $^4J_{HH}$ 2.6, C**10**H), 4.15 (2 H, dd, $^3J_{HH}$ 5.4, $^4J_{HH}$ 2.6, C**8**H), 6.86 (1 H, s, NH), 7.50 (2 H, t, $^3J_{HH}$ 7.9, C**6**H), 7.63–7.67 (1 H, m, C**7**H), 8.12 (2 H, dd, $^3J_{HH}$ 8.1, $^4J_{HH}$ 1.7, C**5**H); ^{19}F NMR (376 MHz, $CDCl_3$) δ −108.2 (s); ^{13}C NMR (151 MHz, $CDCl_3$) δ 29.8 (s, C**8**), 73.1 (s, C**10**), 77.6 (s, C**9**), 110.8 (t, $^1J_{CF}$ 265.8, C**2**), 128.9 (s, C**6**), 130.5 (t, $^4J_{CF}$ 2.9, C**5**), 131.6 (s, C**4**), 135.1 (s, C**7**), 161.3 (t, $^2J_{CF}$ 27.9, C**1**), 187.1 (t, $^2J_{CF}$ 27.1, C**3**); *m/z* $(EI)^+$ 237.0 ($[C_{12}H_9F_2NO_2]^+$, 1%), 156.1 ($[C_8H_6F_2O]^+$, 4%), 106.1 ($[C_7H_6O]^+$, 41%), 105.1 ($[C_7HO]^+$, 100%), 77.1 ($[C_6H_5]^+$, 82%), 51.0 ($[C_4H_3]^+$, 20%), 39.1 ($[C_3H_3]^+$, 13%). HRMS (ASAP) calculated for $[M+H]^+$ $C_{12}H_{10}F_2NO_2$ 238.0680; found 238.0692.

10.4 Screening Conditions for the Base Mediated Direct Fluorination of Ethyl Benzoylacetate

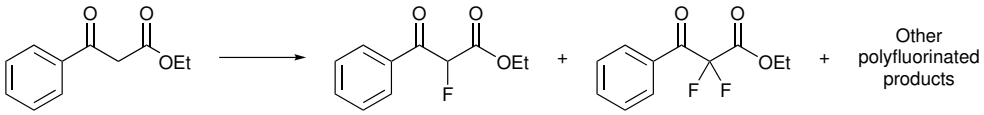

Ethyl benzoylacetate (0.346 mL, 2.0 mmol) and the mediating agent were added to a SIMAX glass bottle and dissolved in acetonitrile (20 mL). The reaction vessel was cooled to 0 °C, stirred rapidly and purged with nitrogen for 10 min. before fluorine gas, (4.6 mmol, 2.3 equiv.) as a 10% mixture in nitrogen (*v/v*), was passed through the reaction mixture at a prescribed flow rate, (15 mL min^{-1}) that was controlled by a mass flow controller for 75 min. After purging with nitrogen for 10 minutes, the reaction vessel was disconnected and the solvent removed under reduced pressure. The organic products were washed through a silica plug with $CHCl_3$ (100 mL) and

concentrated under reduced pressure to give the crude product which was analysed by NMR spectroscopy.

Entry	Base	Equiv of Base	Equiv of F_2	NMR yield/%	
				95	**96**
1	None	-	2.3	8	2
2	DABCO	1.1	2.3	16	10
3	DABCO[a]	1.1	2.3	1	1
4	DABCO[b]	1.1	2.3	0	0
5	DABCO	1.5	2.3	0	3
6	DABCO	1.5	4.0	0	1
7	DBU	0.5	2.3	12	6
8	DBU	1.5	2.3	18	3
9	Et_3N	1.1	2.3	11	1
10	3-Quinuclidinol[a]	1.1	2.3	0	1
11	Quinuclidine	1.1	2.3	0	42
12	Quinuclidine	1.1	3.5	6	41
13	Quinuclidine	1.1	3.0[c]	6	51
14	Quinuclidine	1.5	3.0[c]	0	73
15	Quinuclidine	1.5	3.0[c]	0	85[d]

[a] 40 mL MeCN used

[b] 40 mL MeCN, 4.0 mmol **94**, 2.3 equiv. F_2 and 1.1 equiv. DABCO used

[c] 30 mL min^{-1} flow rate of 10% *v/v* F_2 in N_2 used

[d] Isolated yield after 20 mL column

Chapter 11

Experimental to Chapter 4

11.1 Screening Conditions for the Base Mediated Direct Fluorination of Ethyl 2-(4-nitrophenyl)-acetate

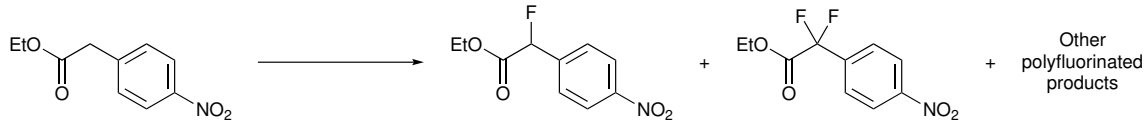

Ethyl 2-(4-nitrophenyl)acetate (0.418 g, 2.0 mmol) and the mediating agent were added to a SIMAX glass bottle and dissolved in acetonitrile (20 mL). The reaction vessel was cooled to 0 °C, stirred rapidly and purged with nitrogen for 10 minutes before fluorine gas, (4.6 mmol, 2.3 equiv.) as a 10% mixture in nitrogen (v/v), was added at a prescribed flow rate, (15 mL min^{-1}) that was controlled by a mass flow controller. After purging with nitrogen for 10 minutes, the reaction vessel was disconnected and the solvent removed under reduced pressure. The organic products were washed through a silica plug with chloroform (100 mL) and concentrated under reduced pressure to give the crude product which was analysed by NMR spectroscopy.

Entry	Base	Equiv. of base	Proportion of signals in the ^{19}F NMR spectrum/%	
			233a	**234a**
1	None	-	14	0
2	KF	2.0	8	0
3	KF 18-crown-6	2.0 2.0	6	1
4	KF 18-crown-6	2.0 0.1	8	0
5	Urea	1.0	0	0
6	Tetramethylurea	1.0	0	0
7	DABCO	2.0	27	2
8	Et_3N	2.0	0	0
9	Quinuclidine	1.1	7	85
10	DBU	0.1	9	0
11	DBU	2.0	22	5
12	Tri-*n*-butylamine	1.0	0	0
13	Pyridine	1.0	0	0
14	*N*-methyl pyrrolidone	0.5	4	0

11.2 General Procedure 6 (GP6)—Direct fluorination of Ethyl Phenylacetates

Quinuclidine and the relevant ethyl benzoylacetate (2.00 mmol, 1.0 equiv.) were added to a SIMAX glass bottle and dissolved in acetonitrile (10 mL equiv.). The reaction vessel was cooled to 0 °C, stirred rapidly and purged with nitrogen for 10 min. before fluorine gas, as a 10% mixture in nitrogen (*v/v*), was passed through the reaction mixture at a prescribed flow rate, (15 mL min^{-1}) that was controlled by a mass flow controller. After purging with nitrogen for 10 min., the reaction vessel was disconnected and the solvent removed *in vacuo*.

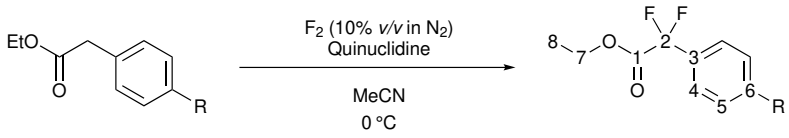

2,2-Difluoro-2-(4-nitrophenyl)acetate (234a)

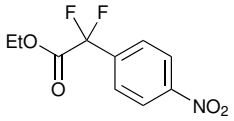

Ethyl 2-(4-nitrophenyl)acetate (1.675 g, 8.0 mmol) and quinuclidine (0.865 g, 7.8 mmol, 1.0 equiv.) in acetonitrile (80 mL) were directly fluorinated with fluorine gas (5.6 mmol, 2.3 equiv.) for 5 h. The reaction mixture was partitioned between water (30 mL) and dichloromethane (120 mL), and the aqueous phase washed with dichloromethane (3×30 mL). The combined organic phases were dried over magnesium sulfate and concentrated under reduced pressure. The crude product was purified by column chromatography on silica gel with ethyl acetate 15% *v/v* in hexane solvent mixture as the eluent to yield *2,2-difluoro-2-(4-nitrophenyl)acetate* (0.637 g, 32%) as a while solid. ^{1}H NMR (599 MHz, $CDCl_3$) δ 1.32 (3 H, t, $^{3}J_{HH}$, 7.1, C**8**H), 4.32 (2 H, q, $^{3}J_{HH}$ 7.1, C**7**H), 7.80–7.83 (2 H, m, C**4**H), 8.31–8.34 (2 H, m, C**5**H); ^{19}F NMR (376 MHz, $CDCl_3$) δ −104.5 (s, C**2**F_2); ^{13}C NMR (151 MHz, $CDCl_3$) δ 14.0 (C**8**), 63.9 (C**7**), 112.5 (t, $^{1}J_{CF}$ 253.8, C**2**), 124.0 (C**5**), 127.2 (t, $^{3}J_{CF}$ 6.0, C**4**), 139.0 (t, $^{1}J_{CF}$ 25.9, C**3**), 149.7 (C**6**), 163.3 (t, $^{2}J_{CF}$ 34.4, C**1**); *m/z* (EI)$^+$ 245.1 ([$CH_9F_2NO_4$]$^+$, 1%), 172.1 ([$C_7H_4F_2NO_2$]$^+$, 100%), 156.1 ([$C_6H_4NO_2Na$]$^+$, 20%), 142.1 (29%), 126.1 (57%), 114.1 (35%), 107.1 (9%), 95.1 (6%), 75.1 (11%), 57.1 (3%). HRMS (ASAP) calculated for [M+H]$^+$ $C_{10}H_{10}F_2NO_4$ 246.0578, found 246.0569. Crystals suitable for x-ray diffraction were grown by slow evaporation from hexane. Data consistent with reported literature.[164]

The reaction was repeated on a 2 mmol and 20 mmol scale to give the desired *2,2-difluoro-2-(4-nitrophenyl)acetate* in yields of 60% and 69% respectively. Spectroscopic data consistent with that reported above.

Ethyl 2,2-difluoro-2-(4-fluorophenyl)acetate (234b)

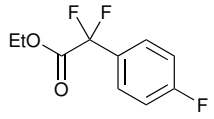

Ethyl 2-(4-fluorophenyl)acetate (0.364 g, 2.0 mmol) and quinuclidine (0.334 g, 3 mmol, 1.5 equiv.) in acetonitrile (20 mL) were directly fluorinated with fluorine gas (8.0 mmol, 4.0 equiv.) for 98 min. Removal of the reaction solvent under reduced pressure gave a tarry mixture which consisted of many products by NMR; ^{19}F NMR (376 MHz, $CDCl_3$) δ −167.4 (d, J 217.0), −115.9 (ddd, J 14.0, J 8.9, J 5.4), 57.6 (s), 58.6 (s).

Ethyl 2,2-difluoro-2-(4-(trifluoromethyl)phenyl)acetate (234c)

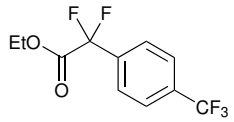

Ethyl 2-(4-(trifluoromethyl)phenyl)acetate (0.464 g, 2.0 mmol) and quinuclidine (0.334 g, 3 mmol, 1.5 equiv.) in acetonitrile (20 mL) were directly fluorinated with fluorine gas (12.0 mmol, 6.0 equiv.) for 3 h and 13 min. After removal of the reaction solvent under reduced pressure the organic products were partitioned between water (30 mL) and ethyl acetate (30 mL), and the aqueous phase washed with ethyl acetate (2×30 mL). The combined organic phases were washed with saturated sodium bicarbonate solution (20 mL), dried over magnesium sulfate and concentrated under reduced pressure to give 0.583 g of a yellow oil. Purification of this crude product was attempted by column chromatography on silica gel with ethyl acetate 5% *v/v* in hexane solvent mixture as the eluent, but the desired product could not be isolated; ^{19}F NMR (376 MHz, $CDCl_3$) δ −184.4 (d, $^2J_{HF}$ 49.1, monofluoro product), −115.7–−114.0 (m), −66.5 (s), −66.3 (s), −63.2 (s), −63.0–−62.8 (m), −62.7 (d, J 5.3), −62.3 (s), −61.8 (d, J 12.8), −61.7 (d, J 13.1), −61.4 (d, J 13.9), −61.2 (d, J 11.2).

Ethyl 2,2-difluoro-2-(4-cyanophenyl)acetate (234d)

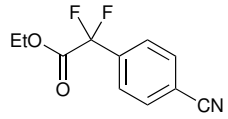

Ethyl 2-(4-cyanophenyl)acetate (0.378 g, 2.0 mmol) and quinuclidine (0.334 g, 3 mmol, 1.5 equiv.) in acetonitrile (20 mL) were directly fluorinated with fluorine gas (12.0 mmol, 6.0 equiv.) for 3 h and 13 min. After removal of the reaction solvent under reduced pressure the organic products were partitioned between water (30 mL) and ethyl acetate (30 mL), and the aqueous phase washed with ethyl acetate (2×30 mL). The combined organic phases were washed with saturated sodium bicarbonate solution (20 mL), dried over magnesium sulfate and concentrated under reduced pressure to give 0.536 g of a brown oil. Purification of this crude product was attempted by column chromatography on silica gel with ethyl acetate 5% *v/v* in hexane solvent mixture as the eluent, but the desired product was not isolated; ^{19}F NMR (376 MHz, $CDCl_3$) δ −186.0 (d, *J* 46.6, monofluoro product), −119.4 (dddt, *J* 16.8, *J* 8.4, *J* 5.7, *J* 1.5), J113.6 (dd, *J* 9.2, *J* 6.9), −111.7 (ddd, *J* 16.6, *J* 8.6, *J* 5.1), −104.9 (s, difluoro product).

Ethyl 2,2-difluoro-2-(2-nitrophenyl)acetate (234e)

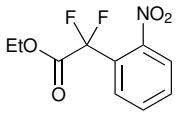

Ethyl 2-(2-nitrophenyl)acetate (0.418 g, 2.0 mmol) and quinuclidine (0.334 g, 3.0 mmol, 1.5 equiv.) in acetonitrile (20 mL) were directly fluorinated with fluorine gas (9.0 mmol, 4.5 equiv.) for, 2 h and 15 min. After removal of the reaction solvent under reduced pressure the organic products were partitioned between water (15 mL) and ethyl acetate (15 mL), and the aqueous phase washed with ethyl acetate (2×30 mL). The combined organic phases were washed with saturated sodium bicarbonate solution (10 mL), dried over magneisum sulfate and concentrated under reduced pressure give 0.498 g of an orange oil containing many fluorinated products by NMR spectroscopy. Purification of this crude product was attempted by column chromatography on silica gel with ethyl acetate 5% *v/v* in hexane solvent mixture as the eluent, but the desired product was not isolated; ^{19}F NMR (376 MHz, $CDCl_3$) δ −188.3–−187.8 (m), −187.5 (d, *J* 46.6), −185.0 (d, *J* 45.2), −113.3–112.3 (m), −111.4–−111.0 (m), −110.8 (t, *J* 7.0), −108.7–−107.9 (m), −107.4 (d, *J* 7.9),

−103.7–−103.1 (m), −100.0 (s); ^{19}F NMR (376 MHz, $CDCl_3$) δ −185.9 (d, J 47.0), −184.6 (d, J 46.4), −184.4 (d, J 47.2, monofluoro product), −184.0 (d, J 46.1), −129.2 (dt, J 20.2, J 6.1), −126.5 (d, J 16.9), −122.4 (t, J 6.5), −122.0–−121.7 (m), −120.0–−119.8 (m), −114.6–−114.4 (m), −109.0 (t, J 8.4), −107.0 (t, J 8.1), −106.0 (ddd, J 8.7, J 6.0, 4.4), −105.9–−105.6 (m), −103.9 (s, difluoro product).

Ethyl 2,2-difluoro-2-(3-nitrophenyl)acetate (234f)

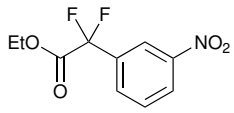

Ethyl 2-(3-nitrophenyl)acetate (0.418 g, 2.0 mmol) and quinuclidine (0.334 g, 3.0 mmol, 1.5 equiv.) in acetonitrile (20 mL) were directly fluorinated with fluorine gas (9.0 mmol, 4.5 equiv.) for 2 h and 15 min. After removal of the reaction solvent under reduced pressure the organic products were partitioned between water (15 mL) and ethyl acetate (15 mL), and the aqueous phase washed with ethyl acetate (2×30 mL). The combined organic phases were washed with saturated sodium bicarbonate solution (10 mL), dried over magnesium sulfate and concentrated under reduced pressure give 0.524 g of an orange oil containing many fluorinated products by NMR spectroscopy. Purification of this crude product was attempted by column chromatography on silica gel with ethyl acetate 5% *v/v* in hexane solvent mixture as the eluent, but the desired product was not isolated.

2,2-Difluoro-2-(4-nitrophenyl)acetic acid (223a)

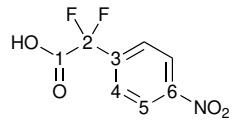

Ethyl 2,2-difluoro-2-(4-nitrophenyl)acetate (0.245 g, 1.00 mmol) was dissolved in methanol (3 mL) and stirred with 1 M potassium carbonate solution (3 mL) for 2 h at r.t. before being poured into 5% hydrochloric acid (20 mL) to quench the reaction. The mixture was extracted with ethyl acetate (3×30 mL), and the organic fractions combined, washed with saturated sodium bicarbonate solution (20 mL) then dried over magnesium sulfate. The solvent was removed under reduced pressure to yield without further purification *2,2-difluoro-2-(4-nitrophenyl)acetic acid* (0.218 g, 100%) as an off white solid. ^{1}H NMR (500 MHz, $(CD_3)_2CO$) δ 8.0 (2H, d, $^3J_{HH}$ 8.9, C**4**H), 8.4 (2H, d, $^3J_{HH}$ 8.6, C **5**H); ^{19}F NMR (376 MHz, $(CD_3)_2CO$) δ −104.9 (s); ^{13}C NMR (126 MHz, $(CD_3)_2CO$) δ 113.7 (t, $^1J_{CF}$ 251.8, C**2**), 124.7 (C**5**), 127.8

(t, $^{3}J_{CF}$ 6.1, C**4**), 139.7 (t, $^{2}J_{CF}$ 25.7, C**3**), 150.5 (C**6**), 164.2 (t, $^{2}J_{CF}$ 33.8, C**1**); *m/z* (ESI)$^{-}$ 433.2 ([2M]$^{-}$, 100%), 216.1 ([M]$^{-}$, 22%), 172.1 ([$C_7H_4F_2NO_2$]$^{-}$, 79%). Data consistent with reported literature.[164]

The reaction was repeated on a 10 mmol scale to give the desired *2,2-difluoro-2-(4-nitrophenyl)acetic acid* in yield of 95%. Spectroscopic data consistent with that reported above.

1-(Difluoromethyl)-4-nitrobenzene (238a)

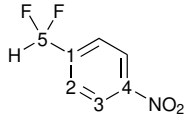

2,2-Difluoro-2-(4-nitrophenyl)acetic acid (1.592 g, 7.33 mmol) was dissolved in dimethylformamide (64 mL) and stirred with potassium fluoride (2.3 g, 39.6 mmol, 5.4 equiv.) at 170 °C for 2 h under an atmosphere of nitrogen gas before being allowed to cool to r.t. The reaction mixture was partitioned between water (50 mL) and ethyl acetate (50 mL), and the aqueous phase extracted with ethyl acetate (2×30 mL). The organic phases were combined, washed with water (10×20 mL) then dried over magnesium sulfate. The solvent was removed under reduced pressure to yield without further purification *1-(difluoromethyl)-4-nitrobenzene* (1.191 g, 94%) as a dark yellow oil. ^{1}H NMR (400 MHz, $CDCl_3$) δ 6.74 (1 H, t, $^{2}J_{HF}$ 55.6, C**5**H), 7.72 (2 H, d, $^{3}J_{HH}$ 8.7,C**2**H), 8.33 (2 H, d, $^{3}J_{HH}$ 8.7, C**3**H); ^{19}F NMR (376 MHz, $CDCl_3$) δ −113.0 (d, $^{2}J_{HF}$ 55.6, C**5**F_2); ^{13}C NMR (101 MHz, $CDCl_3$) δ 113.3 (t, $^{2}J_{CF}$ 241.0, C**5**), 124.2 (C**3**), 127.0 (t, $^{3}J_{CF}$ 6.1, C**2**), 140.3 (t, $^{2}J_{CF}$ 22.9, C**1**), 149.5 (C**4**) *m/z* (EI)$^{+}$ 173.1 ([M]$^{+}$, 83%), 143.1 (14%), 127.1 ([$C_7H_5F_2$]$^{+}$, 100%), 115.1 (22%), 107.1 (26%), 101.1 (36%), 95.1 (13%), 77.1 (35%), 63.0 (5%), 51.0 (12%). Data consistent with reported literature.[164]

The reaction was repeated on a 2 mmol scale to give the desired *1-(difluoromethyl)-4-nitrobenzene* in yield of 93%. Spectroscopic data consistent with that reported above.

11.3 Screening Conditions for the Quinuclidine Mediated Direct Fluorination of Ethyl 2-(4-nitrophenyl)-acetate

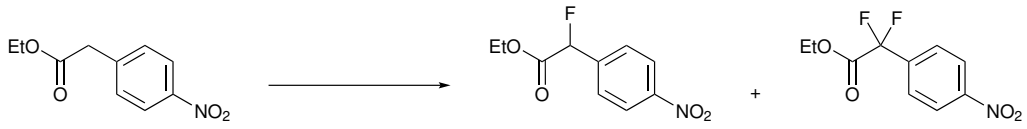

Ethyl 2-(4-nitrophenyl)acetate (0.418 g, 2.0 mmol) and quinuclidine were added to a SIMAX glass bottle and dissolved in acetonitrile (20 mL). The reaction vessel was cooled to 0 °C, stirred rapidly and purged with nitrogen for 10 minutes before fluorine gas, (4.6 mmol, 2.3 equiv.) as a 10% mixture in nitrogen (*v/v*), was added at a prescribed flow rate, (15 mL min^{-1}) that was controlled by a mass flow controller for 75 min. After purging with nitrogen for 10 minutes, the reaction vessel was disconnected and the solvent removed under reduced pressure. The organic products were washed through a silica plug with chloroform (100 mL) and concentrated under reduced pressure to give the crude product which was analysed by NMR spectroscopy.

Entry	Equiv. of quinuclidine	Equiv. of F_2	Ratio of products by NMR		
			232a	**233a**	**234a**
1	0.1	2.3[a]	50	4	1
2	1.0	2.3	3	1	5
3	1.1	2.3	3	1	5
4	1.5	2.3	2	1	7
5	1.1	3.0	1	1	7
6	1.5	2.5	3	1	10
7	1.5	3.0	2	11	11
8	1.5	3.5	1	Trace	7
9	1.5	4.0	1	Trace	6
10	1.5	4.5	1	Trace	11
11[b]	1.5	4.1	2	1	12
12[b]	1.5	4.5	1	1	13
13[b]	1.3	4.6	1	1	11

[a] 5 mmol **232a**, 5 ml min^{-1} flow rate of 10% *v/v* F_2 in N_2 and 50 mL acetonitrile used

[b] 20 mmol of **232a** and 200 mL acetonitrile used

11.4 Hydrogenation Screening of Ethyl 2,2-difluoro-2-(4-nitrophenyl)acetate

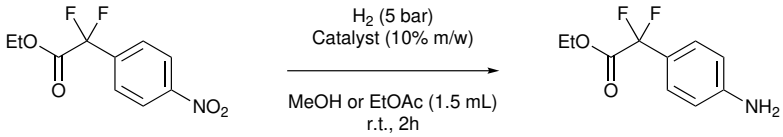

Ethyl 2,2-difluoro-2-(4-nitrophenyl)acetate (0.025 g, 0.1 mmol) and the desired solvent (ethyl acetate or methanol, 1.5 mL) were loaded into 3 mL glass vials in a HEL CAT24 reactor with 10% m/w of the catalyst to be screened (5% Pd/C, 10% Pd/C, 5% Pt/C or 5% Rh/C). After performing a leak test, the reactor was purged 3× with nitrogen gas then 3× with hydrogen gas and agitation started. The reactor was left under an atmosphere of hydrogen (5 bar) for 2 h before venting and purging 3× with nitrogen. The catalysts were filtered off and the reaction mixtures analysed by NMR spectroscopy as discussed in the text.

11.5 Hydrogenation Screening of 1-(Difluoromethyl)-4-nitrobenzene

Stock solutions were made by dissolving 1-(difluoromethyl)-4-nitrobenzene (0.087 g, 0.5 mmol) in 7.5 mL of ethyl acetate and ethanol. Aliquots (1.5 mL) of each solution were loaded into 3 mL glass vials in a HEL CAT24 reactor with 10% w/w of the catalyst to be screened (5% Pd/C, 10% Pd/C, 5% Pt/C or 5% Rh/C). After performing a leak test, the reactor was purged 3× with nitrogen gas then 3× with hydrogen gas and agitation started. The reactor was left under an atmosphere of hydrogen (5 bar) for 2 h before venting and purging 3× with nitrogen. The catalysts were filtered off and the reaction mixtures analysed by NMR spectroscopy as discussed in the text.

11.5.1 Hydrogenation of 1-(Difluoromethyl)-4-nitrobenzene Using an EasyMax Reactor

An EasyMax hydrogenator was charged with 1-(difluoromethyl)-4-nitrobenzene (0.346 g, 2.0 mmol), 10% Pd/C (0.035 g, 10% w/w) and ethyl acetate (30 mL). After per-

forming a leak test, the reactor was purged 3× with nitrogen gas then 3× with hydrogen gas and agitation started. The reactor was left under an atmosphere of hydrogen (5 bar) for 5 h 30 min before venting and purging 3× with nitrogen. The catalyst was filtered off, and the reaction solvent removed under reduced pressure to give a brown tar that was sparingly soluble in organic solvents.

11.6 Further Reactions of Ethyl 2,2-Difluoro-2-(4-nitrophenyl)acetate

The following reactions were carried out by Durham University MChem student Jonathan Hill as part of his 4th year work, and included here for completeness.[176]

2,2-Difluoro-2-(4-nitrophenyl)ethanol (254)

This product was characterised by Jonathan Hill.[176]

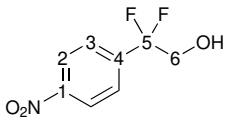

Ethyl 2,2-difluoro-2-(4-nitrophenyl)acetate (0.505 g, 2.06 mmol) was dissolved in EtOH (10.0 ml) and NaBH4 (0.158 g, 4.18 mmol) was slowly added. The reaction was stirred at r.t. for 20 mins before being quenched with 2 M HCl (20 ml). Diethyl ether (30 ml) was added and the organic solution was washed with 2 M HCl (3×20 ml), NaHCO3 soln (3×20 ml) and finally with brine (3×20 ml). The organic fraction was then dried ($MgSO_4$) and concentrated in vacuo to give the title compound as a pale yellow solid (0.378 g, 90%). Mp 78–79 °C; IR (neat, cm^{-1} 3524, 3123, 3087, 2936, 2161, 1728, 1607, 1517, 1354; ^1H NMR (400 MHz; $CDCl_3$) δ 8.27 (2H, d, $^3J_{HH}$ 8.4, C**2**H) 7.71 (2H, d, $^3J_{HH}$ 8.6, C**3**H) 4.00 (2H, t, $^3J_{HF}$ 12.9, C**6**H) 2.69 (1H, s, -OH); ^{19}F NMR (176 MHz; $CDCl_3$) δ −107.18 (t, $^3J_{FH}$ 12.9); ^{13}C NMR (101 MHz; $CDCl_3$) δ 149.24 (s, C**1**) 140.90 (t, $^2J_{CF}$ 26.1, C**4**) 127.18 (t, $^3J_{CF}$ 6.1, C**3**) 123.86 (s, C**2**) 119.80 (t, $^1J_{CF}$ 244.9, C**5**) 65.72 (t, $^2J_{CF}$ 32.8, C**6**); MS (ASAP) *m/z* 204 ($[M+H]^+$, 100%); HRMS (ASAP) *m/z* calculated for $C_8H_8F_2NO_3$ $[M+H]^+$ 246.0472, found 246.0473.

2,2-Difluoro-2-(4-nitrophenyl)ethyl tosylate (255)

This product was characterised by Jonathan Hill.[176]

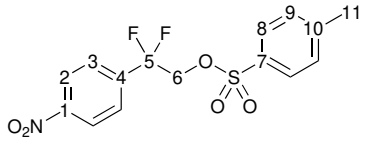

2,2-Difluoro-2-(4-nitrophenyl)ethanol (0.071 g, 0.350 mmol) and NEt3 (0.5 ml, 3.6 mmol) were dissolved in DCM (1.2 ml), followed by addition of TsCl (0.099 g, 0.519 mmol). The reaction was then stirred at r.t. overnight, after which, further NEt3 (5 ml, 36 mmol) was added and a white precipitate formed. Dil. HCl (10 ml) was added, and the mixture was extracted with DCM (2×10 ml). The combined organic fractions were washed with dil. HCl (5×20 ml), brine (3 × 10 ml) and then dried (MgSO4). Solvents were removed under reduced pressure yielding the crude product as a yellow oil. The oil was triturated with ice-cold hexane (3×20 ml) which precipitated 2,2-difluoro-2-(4-nitrophenyl)ethyl tosylate as a yellow solid (0.085 g, 68%). Mp 110–111 °C; IR (neat, cm^{-1} 3124, 2925, 1940, 1612, 1597, 1523, 1363, 1350, 1319; ^{1}H NMR (400 MHz, $CDCl_3$) δ 8.23 (2H, d, $^3J_{HH}$ 9.0, C**2**H) 7.65 (2H, d, $^3J_{HH}$ 8.3, C**8**H) 7.60 (2H, d, $^3J_{HH}$ 9.0, C**3**H) 7.30 (2H, d, $^3J_{HH}$ 8.4, C**9**H) 4.40 (2H, t, J 11.2, C**6**H) 2.44 (3H, s, **11**H); ^{19}F NMR (176 MHz; $CDCl_3$) δ −104.30 (t, J 11.3); ^{13}C NMR (101 MHz; $CDCl_3$) δ 149.45 (s, C**1**) 145.88 (s, C**10**) 139.27 (t, $^2J_{CF}$ 25.7, C**4**) 132.10 (s, C**7**) 130.15 (s, C**8**) 128.01 (s, C**9**) 127.16 (t, $^3J_{CF}$ 6.2, C**3**) 123,90 (s, C**2**) 117.63 (t, $^1J_{CF}$ 246.6, C**5**) 69.16 (t, $^2J_{CF}$ 37.4, C**6**) 21.79 (s, C**11**); MS (ASAP) *m/z* 356 ([M-H]$^+$, 9%) 338 ([M-F]$^+$, 82%); HRMS (ASAP) *m/z* calculated for $C_{15}H_{12}F_2NO_5S$[M-H]$^+$ 356.0404, found 356.0419.

11.6.1 General Synthesis of α,α-Difluoroamides

Ethyl 2,2-difluoro-2-(4-nitrophenyl)acetate (1 eq.) and an excess of the amine were dissolved in EtOH (2–5 ml) at 0 °C and the reaction was then stirred at r.t. for 18–24 h. Volatile materials were then removed under reduced pressure, followed by addition of DCM (20 ml). The organic solution was then washed with dil. HCl (5×30 ml), followed by NaHCO3 soln (3×20 ml) and brine (3×20 ml) before being dried ($MgSO_4$). Solvents were then removed in vacuo to yield the crude amide which was then purified by Celite or silica plug. Single crystals suitable for X-ray diffraction analysis were grown from $CHCl_3$.

***N*-benzyl-2,2-difluoro-2-(4-nitrophenyl)acetamide (256a)**

This product was characterised by Jonathan Hill.[176]

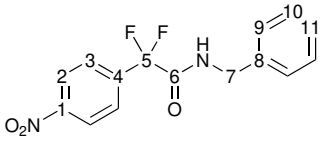

Ethyl 2,2-difluoro-2-(4-nitrophenyl)acetate (0.042 g, 0.17 mmol) was dissolved in EtOH (2 ml) at 0 °C and benzylamine (0.02 ml, 0.17 mmol) was added with stirring. The reaction mixture was then stirred at r.t. for 19 h. The solvent was then removed under reduced pressure followed by addition of DCM (c. 20 ml). The organic solution was then washed according to the general procedure. The crude product was purified by flash silica column chromatography and *N-benzyl-2,2-difluoro-2-(4-nitrophenyl)acetamide* was isolated as a pale yellow crystalline solid (0.050 g, 94%). Mp 154–156 °C; IR (neat, cm^{-1} 3284, 2917, 1717, 1688, 1525; ^1H NMR (700 MHz, $CDCl_3$) δ 8.31 (2H, d, $^3J_{HH}$ 9.0, C**2**H) 7.83 (2H, d, $^3J_{HH}$ 9.0, C**3**H) 7.39–7.25 (5H, m, C**9**H–C**11**H) 6.81 (1H, s, R_2NH) 4.52 (2H, d, J 5.8, C**7**H); ^{19}F NMR (376 MHz, $CDCl_3$) δ −104.24 (s) −104.29 (s); $13^{13}C$ NMR (176 MHz, $CDCl_3$) δ 163.01 (t, $^2J_{CF}$ 30.1, C**6**) 149.66 (s, C**1**) 139.04 (t, $^2J_{CF}$ 25.8, C**4**) 136.47 (s, C**2**) 129.19 (s, C**8**) 128.40 (s, C**10**) 128.06 (s, C**9**) 127.30 (t, $^3J_{CF}$ 6.1, C**3**) 123.91 (s, C**11**) 114.00 (t, $^1J_{CF}$ 256.2, C**5**) 44.06 (s, C**7**); MS (ESI) *m/z* 307 ($[M+H]^+$, 25%) 348 ($[M+HMeCN]^+$, 100); HRMS (ESI) *m/z* calculated for $C_{15}H_{11}F_2N_2O_3$ $[M+H]^+$ 305.0738, found 305.0747.

N-allyl-2,2-difluoro-2-(4-nitrophenyl)acetamide (256b)

This product was characterised by Jonathan Hill.[176]

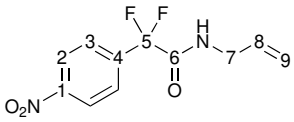

Ethyl 2,2-difluoro-2-(4-nitrophenyl)acetate (0.060 g, 0.24 mmol) was dissolved in allylamine (15.0 ml, 201 mmol) and stirred at r.t. for 24 h. The reaction was worked up according to the general procedure to yield *N-allyl-2,2-difluoro-2-(4-nitrophenyl)acetamide* as pale yellow crystals (0.062 g, 99%). Mp 109–111 °C; IR (neat, cm^{-1} 3292, 3085, 2924, 2854, 1687, 1553, 1520; ^1H NMR (400 MHz, $CDCl_3$) δ 8.31 (2H, d, $^3J_{HH}$ 9.0, C**2**H) 7.83 (2H, d, $^3J_{HH}$ 8.9, C**3**H) 6.68 (1H, s, R_2NH) 5.84 (1H, m, C**8**H) 5.23 (2H, m, C**9**H) 3.96 (2H, t, $^3J_{HH}$ C**7**H); ^{19}F NMR (376 MHz; $CDCl_3$) δ −103.55 (s); ^{13}C NMR (101 MHz; $CDCl_3$) δ 162.95 (t, $^2J_{CF}$ 30.2, C**6**) 149.59 (s, C**1**) 139.05 (t, $^2J_{CF}$ 25.7, C**4**) 132.43 (s, C**2**) 127.26 (t, $^3J_{CF}$ 6.1, C**3**) 123.88 (s, C**8**) 118.07 (s, C**9**) 113.94 (t, $^1J_{CF}$ 255.0, C**5**) 42.21 (s, C**7**); MS (ASAP)

m/z 257 ([M+H]$^+$, 100%) 209 ([M−HNO$_2$]$^+$, 20%); HRMS (ASAP) *m/z* calculated for $C_{11}H_{11}F_2N_2O_3$ [M+H]$^+$ 257.0738, found 257.0739.

2,2-difluoro-2-(4-nitrophenyl)-*N*-(prop-2-ynyl)acetamide (256c)

This product was characterised by Jonathan Hill.[176]

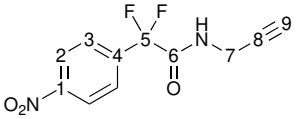

Ethyl 2,2-difluoro-2-(4-nitrophenyl)acetate (0.088 g, 0.360 mmol) and propargylamine (0.5 ml, 7.8 mmol) were dissolved in EtOH (2 ml) and stirred at r.t. for 24 h. The reaction was worked up according to the general procedure to yield *2,2-difluoro-2-(4-nitrophenyl)-N-(prop-2-ynyl)acetamide* as a yellow solid. (0.087 g, 95%). Mp 171–172 °C; IR (neat, cm^{-1} 3266, 3086, 2925, 1687, 1608, 1519; ^{1}H NMR (400 MHz, CD_3CN) δ 8.32 (2H, d, $^3J_{HH}$ 9.2, C**2**H) 7.84 (2H, d, $^3J_{HH}$9.0, C**3**H) 4.01 (2H, dd, $^3J_{HH}$ 5.8, $^4J_{HH}$ 2.6, C**7**H) 2.49 (1H, t, $^3J_{HH}$ 2.6, C**9**H); ^{19}F NMR (376 MHz; CD_3CN) δ −104.46 (s); ^{13}C NMR (101 MHz; CD_3CN) δ 163.69 (t, $^2J_{CF}$ 30.7, C**6**) 150.73 (s, C**1**) 139.87 (t, $^2J_{CF}$ 25.9, C**4**) 127.99 (t, $^3J_{CF}$ 6.2, C**3**) 124.94 (s, C**2**) 114.91 (t, $^1J_{CF}$253.3, C**5**) 79.73 (s, C**8**) 72.61 (s, C**9**) 29.59 (s, C**7**); MS (EI) *m/z* 254 (M+, 1%) 173 ([M-CONHR]$^+$, 100%) 126 ($C_7H_4NO^+$, 41%) 82 ($C_4H_4NO^+$, 76%) 39 ($C_3H_3^+$, 82%); HRMS (ASAP) *m/z* calculated for $C_{11}H_9F_2N_2O_3$ [M+H]$^+$ 255.0581, found 255.0587.

2,2-difluoro-1-morpholino-2-(4-nitrophenyl)ethenone (256d)

This product was characterised by Jonathan Hill.[176]

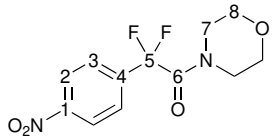

Ethyl 2,2-difluoro-2-(4-nitrophenyl)acetate (0.052 g, 0.212 mmol) was dissolved in ^{t}Bu-NH2 (3.0 ml, 29 mmol) and stirred at r.t. for 21 h. The reaction was worked up according to the general procedure to yield *N-(tert-butyl)-2,2-difluoro-2-(4-nitrophenyl)acetamide* as a pale yellow oil. (0.055 g, 95%); IR (neat, cm^{-1} 3385, 2973, 1705, 1530, 1353, 1264, 1130; ^{1}H NMR (400 MHz; $CDCl_3$) δ8.30 (2H, d, $^3J_{HH}$ 8.9, C**2**H) 7.80 (2H, d, $^3J_{HH}$ 9.1, C**3**H) 6.34 (1H, s, R_2NH); ^{19}F NMR (376 MHz; $CDCl_3$) δ −102.74 (m); ^{13}C NMR (101 MHz; $CDCl_3$) δ 127.25 (t, $^3J_{CF}$ 6.0, C**3**)

123.84 (s, C**2**) 52.62 (s, C**7**) 28.53 (s, C**8**); MS (EI) *m/z* 273 ([M+H]$^+$, 1%) 173 ([M-CONH^{t}Bu]$^+$, 72) 57 (^{t}Bu$^+$, 100); HRMS (ASAP) *m/z* calculated for $C_{12}H_{15}F_2N_2O_3$ [M+H]$^+$ 273.1051, found 273.1048.

,2-difluoro-2-(4'-nitrophenyl)acetamide (256e)

This product was characterised by Jonathan Hill.[176]

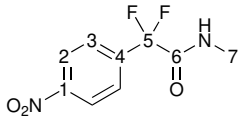

Ethyl 2,2-difluoro-2-(4-nitrophenyl)acetate (0.085 g, 0.347 mmol) and 33% $MeNH_2$ in EtOH (5.0 ml, 40 mmol) were dissolved in EtOH (2 ml) and stirred at r.t. for 24 h. The reaction was worked up according to the general procedure to yield *2,2-difluoro-2-(4'-nitrophenyl)acetamide* as a yellow solid (0.072 g, 90%). Mp 146–148 °C; IR (neat, cm^{-1} 3317, 3092, 2960, 1682, 1527, 1350, 1145; ^{1}H NMR (400 MHz, $CDCl_3$) δ 8.29 (2H, d, $^3J_{HH}$ 8.9, C**2**H) 7.82 (2H, d, $^3J_{HH}$ 8.9, C**3**H) 6.69 (1H, s, R_2NH) 2.93 (3H, d, $^3J_{HH}$ 5.0, C**7**H); ^{19}F NMR (376 MHz; $CDCl_3$) δ −103.58 (m); ^{13}C NMR (101 MHz; $CDCl_3$) δ 163.72 (t, $^2J_{CF}$ 30.0, C**6**) 149.55 (s, C**1**) 139.12 (t, $^2J_{CF}$ 25.9, C**4**) 127.25 (t, $^3J_{CF}$ 6.1, C**3**) 123.83 (s, C**2**) 113.95 (t, $^1J_{CF}$ 254.8, C**5**) 26.56 (s, C**7**); MS (ASAP) *m/z* 231 ([M+H]$^+$, 100%) 183 ([M−HNO_2]$^+$, 95%); HRMS (ASAP) *m/z* calculated for $C_9H_9F_2N_2O_3$ [M+H]$^+$ 231.0581, found 231.0580.

Chapter 12

Experimental to Chapter 5

12.1 Fluorination of Aromatics

Anisole

Anisole (0.217 mL, 2.00 mmol, 1.0 equiv.) and quinuclidine (0.222 g, 2.0 mmol, 1.0 equiv.) were added to a SIMAX glass bottle and dissolved in acetonitrile (20 mL). The reaction vessel was cooled to 0 °C, stirred rapidly and purged with nitrogen for 10 minutes before fluorine gas, as a 10% mixture in nitrogen (*v/v*), was added at a prescribed flow rate, (4.0 mmol, 2.0 equiv., 15 mL min^{-1}) that was controlled by a mass flow controller for 65 min. After purging with nitrogen for 10 minutes, the reaction vessel was disconnected and the reaction mixture was partitioned between ethyl acetate (50 mL), water (20 mL) and saturated sodium chloride solution (10 mL), and the aqueous phase washed with ethyl acetate (2×30 mL). The combined organic phases were dried over magnesium sulfate and concentrated under reduced pressure to yield 0.244 g of a vicous brown oil that was analysed by NMR spectroscopy as discussed in the text.

Aniline

Aniline (0.182 mL, 2.00 mmol, 1.0 equiv.) and quinuclidine (0.222 g, 2.0 mmol, 1.0 equiv.) were added to a SIMAX glass bottle and dissolved in acetonitrile (20 mL). The reaction vessel was cooled to 0 °C, stirred rapidly and purged with nitrogen for 10 minutes before fluorine gas, as a 10% mixture in nitrogen (*v/v*), was added at a prescribed flow rate, (4.0 mmol, 2.0 equiv., 15 mL min^{-1}) that was controlled by a mass flow controller for 65 min. After purging with nitrogen for 10 minutes, the reaction vessel was disconnected and the solvent removed under reduced pressure.

The crude product was partitioned between ethyl acetate (30 mL), water (30 mL) and saturated sodium chloride solution (10 mL), and the aqueous phase washed with ethyl acetate (2×30 mL). The combined organic phases were washed with saturated sodium bicarbonate solution (20 mL), dried over magnesium sulfate and concentrated under reduced pressure to yield 0.215 g of a black tar. Analysis by NMR spectroscopy showed the presence of many polyfluorinated products and not pursued further.

4-Nitroaniline

4-Nitroaniline (0.276 g, 2.00 mmol, 1.0 equiv.) and quinuclidine (0.222 g, 2.0 mmol, 1.0 equiv.) were added to a SIMAX glass bottle and dissolved in acetonitrile (20 mL). The reaction vessel was cooled to 0 °C, stirred rapidly and purged with nitrogen for 10 minutes before fluorine gas, as a 10% mixture in nitrogen (*v/v*), was added at a prescribed flow rate, (4.0 mmol, 2.0 equiv., 15 mL min^{-1}) that was controlled by a mass flow controller for 65 min. After purging with nitrogen for 10 minutes, the reaction vessel was disconnected and the solvent removed under reduced pressure. The crude product was partitioned between ethyl acetate (30 mL) and water (30 mL), and the aqueous phase washed with ethyl acetate (2×20 mL). The combined organic phases were washed with saturated sodium bicarbonate solution (20 mL), dried over magnesium sulfate and concentrated under reduced pressure to yield 0.275 g of a black tar. Purification by kugelrohr distillation was attempted but unsuccessful.

4-Nitroanisole

4-Nitroanisole (0.306 g, 2.00 mmol, 1.0 equiv.) was added to a SIMAX glass bottle and dissolved in acetonitrile (20 mL). The reaction vessel was cooled to 0 °C, stirred rapidly and purged with nitrogen for 10 minutes before fluorine gas, as a 10% mixture in nitrogen (*v/v*), was added at a prescribed flow rate, (4.0 mmol, 2.0 equiv., 15 mL min^{-1}) that was controlled by a mass flow controller for 65 min. After purging with nitrogen for 10 minutes, the reaction vessel was disconnected and the solvent removed under reduced pressure. The crude product was partitioned between ethyl acetate (30 mL) and water (30 mL), and the aqueous phase washed with ethyl acetate (2×20 mL). The combined organic phases were washed with saturated sodium bicarbonate solution (20 mL), dried over magnesium sulfate and concentrated under reduced pressure to yield 0.389 g of an orange tar. The crude residue was filtered through a silica plug with chloroform as the eluent to yield 0.158 g of yellow crystals. Analysis by NMR spectroscopy identified this a mixture of unreacted 4-nitroanisole

(5%, ^{1}H NMR (400 MHz, $CDCl_3$ δ) 3.91 (3H, s, $-OCH_3$), 6.93-–6.98 (2 H, m, Ar-H), 8.17—8.23 (2 H, m, Ar-H)), 2-fluoro-4-nitroanisole (37%, ^{1}H NMR (400 MHz, $CDCl_3$ δ) 4.00 (3 H, s, $-OCH_3$), 7.04 (1 H, dd, $^{3}J_{HH}$ 9.1, $^{4}J_{HF}$ 8.1, Ar-H), 7.98 (1 H, dd, $^{3}J_{HF}$ 10.8, $^{4}J_{HH}$ 2.8, Ar-H), 8.07 (1 H, ddd, $^{3}J_{HH}$ 9.1, $^{4}J_{HH}$ 2.8, $^{5}J_{HF}$ 1.6, Ar-H); ^{19}F NMR (376 MHz, $CDCl_3$) -131.0 (ddd, $^{3}J_{HF}$ 10.2, $^{4}J_{HF}$ 8.1, $^{5}J_{HF}$ 1.6)), 2,6-difluoro-4-nitroanisole (5%, ^{1}H NMR (400 MHz, $CDCl_3$ δ) 4.16 (3 H, t, $^{5}J_{HF}$ 2.0, $-OCH_3$), 7.81—7.86 (2 H, m, Ar-H); ^{19}F NMR (376 MHz, $CDCl_3$) -124.7 (dq, $^{3}J_{HF}$ 8.6, $^{5}J_{HF}$ 2.0)).

4-Nitroanisole

4-Nitroanisole (0.306 g, 2.00 mmol, 1.0 equiv.) and quinuclidine (0.222 g, 2.0 mmol, 1.0 equiv.) were added to a SIMAX glass bottle and dissolved in acetonitrile (20 mL). The reaction vessel was cooled to 0 °C, stirred rapidly and purged with nitrogen for 10 minutes before fluorine gas, as a 10% mixture in nitrogen (*v/v*), was added at a prescribed flow rate, (4.0 mmol, 2.0 equiv., 15 mL min^{-1}) that was controlled by a mass flow controller for 65 min. After purging with nitrogen for 10 minutes, the reaction vessel was disconnected and the solvent removed under reduced pressure. The crude product was partitioned between ethyl acetate (30 mL) and water (30 mL), and the aqueous phase washed with ethyl acetate (2×20 mL). The combined organic phases were washed with saturated sodium bicarbonate solution (20 mL), dried over magnesium sulfate and concentrated under reduced pressure to yield 0.323 g of an orange solid. (52%, ^{1}H NMR (400 MHz, $CDCl_3$ δ) 3.91 (3H, s, $-OCH_3$), 6.93-–6.98 (2 H, m, Ar-H), 8.18—8.23 (2 H, m, Ar-H)), 2-fluoro-4-nitroanisole (24%, ^{1}H NMR (400 MHz, $CDCl_3$ δ) 4.00 (3 H, s, $-OCH_3$), 7.04 (1 H, dd, $^{3}J_{HH}$ 9.1, $^{4}J_{HF}$ 8.1, Ar-H), 7.99 (1 H, dd, $^{3}J_{HF}$ 10.7, $^{4}J_{HH}$ 2.7, Ar-H), 8.07 (1 H, ddd, $^{3}J_{HH}$ 9.1, $^{4}J_{HH}$ 2.7, $^{5}J_{HF}$ 1.6, Ar-H); ^{19}F NMR (376 MHz, $CDCl_3$ δ) -131.0 (ddd, $^{3}J_{HF}$ 10.2, $^{4}J_{HF}$ 8.1, $^{5}J_{HF}$ 1.6)), 2,6-difluoro-4-nitroanisole (1%, ^{1}H NMR (400 MHz, $CDCl_3$ δ) 4.17 (3 H, t, $^{5}J_{HF}$ 2.0, $-OCH_3$), 7.83—7.86 (2 H, m, Ar-H); ^{19}F NMR (376 MHz, $CDCl_3$ δ) -124.7 (dq, $^{3}J_{HF}$ 8.6, $^{5}J_{HF}$ 2.0)). Purification of this crude product by column chromatography on silica gel with ethyl acetate 15% *v/v* in hexane solvent mixture as the eluent afforded any recovered 4-nitroanisole (40% isolated).

12.1.1 Fluorinations Using Selectfluor™

4-Nitroanisole (0.077 g, 0.50 mmol, 1.0 equiv.) and Selectfluor™(0.177 g, 0.50 mmol, 1.0 equiv.) were dissolved in MeCN (5 mL) and stirred at r.t. overnight, then at 60

°C for 72 h. The reaction solvent was removed under reduced pressure. Analysis by NMR spectroscopy indicated that no reaction had occured.

4-Nitroanisole (0.077 g, 0.50 mmol, 1.0 equiv.) and Selectfluor™(0.354 g, 1.0 mmol, 2.0 equiv.) were dissolved in MeCN (5 mL) and stirred at r.t. overnight, then at 60 °C for 72 h. The reaction solvent was removed under reduced pressure. Analysis by NMR spectroscopy indicated that no reaction had occured.

12.2 Screening Conditions for the Base Mediated Direct Fluorination of 4-nitroanisole

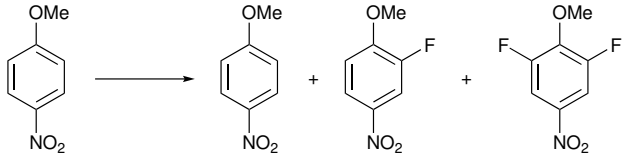

4-Nitroanisole (0.306 g, 2.00 mmol, 1.0 equiv.) and the mediating agent were added to a SIMAX glass bottle and dissolved in acetonitrile (20 mL). The reaction vessel was cooled to 0 °C, stirred rapidly and purged with nitrogen for 10 minutes before fluorine gas, as a 10% mixture in nitrogen (v/v), was added at a prescribed flow rate, (4.0 mmol, 2.0 equiv., 15 mL min^{-1}) that was controlled by a mass flow controller for 65 min. After purging with nitrogen for 10 minutes, the reaction vessel was disconnected and the solvent removed under reduced pressure. The crude product was filtered through a silica plug with chloroform as the eluent to remove unwanted tarry by-products. NMR yields of the desired products were then calculated by comparing the product distributions in the crystalline product.

Entry	Base	Equiv of base	NMR yield/%			Recovered yield/%
			264	**265**	**266**	
1	-	-	5	37	5	47[a]
2	Quinuclidine	1	52	24	1	77[a]
3	-	-	11	65	9	86
4	Quinuclidine	1	67	20	3	90
5	Quinuclidine	2	90	3	0	93
6	DABCO	1	94	5	0	99
7	DABCO	2	95	2	0	97
8	DBU	1	76	19	2	97
9	DBU	2	92	4	1	96
10	Et_3N	1	49	25	3	77
11	Et_3N	2	91	3	1	95
12	Pyridine	1	74	11	2	87
13	Pyridine	2	94	3	0	97
14	DABCO	1[b]	23	51	5	79
15	DBU	1[b]	Polyfluorinated tar			
16	Et_3N	1[b]	Polyfluorinated tar			

[a] Aqueous workup performed prior to washing the product mixture through a small silica plug with $CHCl_3$ as the eluent

[b] 5.0 equiv. of F_2 used

References

(1) *Department of Social and Economic Affairs, Population Division (2019). World Population Prospects 2019: Ten Key Findings*, tech. rep., United Nations, 2019.

(2) D. Pimentel and M. Pimentel, *Am. J. Clin. Nutr.*, 2003, **78**, 660S–663S.

(3) K. Müller, C. Faeh and F. Diederich, *Fluorine in pharmaceuticals: Looking beyond intuition*, 2007.

(4) S. Purser, P. R. Moore, S. Swallow and V. Gouverneur, *Chem Soc Rev*, 2008, **37**, 237–432.

(5) T. Liang, C. N. Neumann and T. Ritter, *Angew. Chemie, Int. Ed.*, 2013, **52**, 8214–8264.

(6) B. G. de la Torre and F. Albericio, *The pharmaceutical industry in 2018. An analysis of FDA drug approvals from the perspective of molecules*, 2019.

(7) J. Marais and Du Toi PJ, *J. Vet. Sci. Anim. Ind.*, 1943, **18**, 203–206.

(8) J. Marais, *Onderstepoort J. Vet. Sci. Anim. Ind.*, 1944, **20**, 67–73.

(9) O. Thomas, S., L. Singleton, V., A. Lowery, J., W. Sharpe, R., M. Pruess, L., N. Porter, J., H. Mowat, J. and N. Bohonos, *Antibiot. Annu.*, 1956, 716–721.

(10) M. Sanada, T. Miyano, S. Iwadare, J. M. Williamson, B. H. Arison, J. L. Smith, A. W. Douglas, J. M. Liesch and E. Inamine, *J. Antibiot.*, 1986, **39**, 259–265.

(11) D. O'Hagan and D. B. Harper, *J. Fluorine. Chem.*, 1999, **100**, 127–133.

(12) M. F. Carvalho and R. S. Oliveira, *Crit. Rev. Biotechnol.*, 2017, **37**, 880–897.

(13) L. Ma, A. Bartholome, M. H. Tong, Z. Qin, Y. Yu, T. Shepherd, K. Kyeremeh, H. Deng and D. O'Hagan, *Chem. Sci.*, 2015, **6**, 1414–1419.

(14) G. W. Gribble, *Acc. Chem. Res.*, 1998, **31**, 141–152.

(15) A. Bondi, *J. Phys. Chem.*, 1964, **68**.

(16) D. O'Hagan, *Chem. Soc. Rev.*, 2008, **37**, 308–319.

(17) N. A. Meanwell, *J. Med. Chem.*, 2018, **61**, 5822–5880.

(18) P. Jeschke, *ChemBioChem*, 2004, **5**, 570–589.

(19) V. P. Reddy, *Organofluor. Compd. Biol. Med.*, 2015, 1–27.

(20) W. R. Dolbier and K. W. Palmer, *J. Am. Chem. Soc.*, 1993, **115**, 9349–9350.

(21) M. Morgenthaler, E. Schweizer, A. Hoffmann-Röder, F. Benini, R. E. Martin, G. Jaeschke, B. Wagner, H. Fischer, S. Bendels, D. Zimmerli, J. Schneider, F. Diederich, M. Kansy and K. Müller, *Predicting and tuning physicochemical properties in lead optimization: Amine basicities*, 2007.

(22) M. B. Van Niel, I. Collins, M. S. Beer, H. B. Broughton, S. K. Cheng, S. C. Goodacre, A. Heald, K. L. Locker, A. M. MacLeod, D. Morrison, C. R. Moyes, D. O'Connor, A. Pike, M. Rowley, M. G. Russell, B. Sohal, J. A. Stanton, S. Thomas, H. Verrier, A. P. Watt and J. L. Castro, *J. Med. Chem.*, 1999, **42**, 2087–2104.

(23) J. M. Luteijn and J. Tipker, *Pestic. Sci.*, 1986, **17**, 456–458.

(24) R. H. Bromilow, K. Chamberlain and A. A. Evans, *Weed Sci.*, 1990, **38**, 305–314.

(25) B. E. Smart, J. Fluorine. Chem. Elsevier, 2001, vol. 109, pp. 3–11.

(26) M. Tohnishi, T. Nishimatsu, K. Motoba, T. Hirooka and A. Seo, *J. Pestic. Sci.*, 2010, **35**, 508–515.

(27) W. B. Nimmo, P. C. de Wilde and A. Verloop, *Pestic. Sci.*, 1984, **15**, 574.

(28) A. S. Hampton, L. Mikulski, W. Palmer-Brown, C. D. Murphy and G. Sandford, *Bioorg. Med. Chem. Lett.*, 2016, **26**, 2255–2258.

(29) S. B. Rosenblum, T. Huynh, A. Afonso, H. R. Davis, N. Yumibe, J. W. Clader and D. A. Burnett, *J. Med. Chem.*, 1998, **41**, 973–980.

(30) M. Van Heek, C. F. France, D. S. Compton, R. L. McLeod, N. P. Yumibe, K. B. Alton, E. J. Sybertz and H. R. Davis, *J. Pharmacol. Exp. Ther.*, 1997, **283**, 157–163.

(31) J. A. Olsen, D. W. Banner, P. Seiler, B. Wagner, T. Tschopp, U. Obst-Sander, M. Kansy, K. Müller and F. Diederich, *ChemBioChem*, 2004, **5**, 666–675.

(32) H. Yamamoto, *Organofluorine Compounds: Chemistry and Applications*, Springer, 2000.

(33) M. G. Campbell and T. Ritter, *Modern carbon-fluorine bond forming reactions for aryl fluoride synthesis*, 2015.

(34) P. A. Champagne, J. Desroches, J. D. Hamel, M. Vandamme and J. F. Paquin, *Chem. Rev.*, 2015, **115**, 9073–9174.

(35) X. Liu, C. Xu, M. Wang and Q. Liu, *Trifluoromethyltrimethylsilane: Nucleophilic trifluoromethylation and beyond*, 2015.

(36) X. Yang, T. Wu, R. J. Phipps and F. D. Toste, *Advances in catalytic enantioselective fluorination, mono-, di-, and trifluoromethylation, and trifluoromethylthiolation reactions*, 2015.

(37) G. Pattison, *Methods for the Synthesis of α,α-Difluoroketones*, 2018.

(38) P. Adler, C. J. Teskey, D. Kaiser, M. Holy, H. H. Sitte and N. Maulide, *Nat. Chem.*, 2019, **11**, 329–334.

(39) B. Imperiali and R. H. Abeles, *Biochemistry*, 1986, **25**, 3760–3767.

(40) H. L. Sham, N. E. Wideburg, S. G. Spanton, W. E. Kohlbrenner, D. A. Betebenner, D. J. Kempf, D. W. Norbeck, J. J. Plattner and J. W. Erickson, *J. Chem. Soc. Chem. Commun.*, 1991, 110–112.

(41) J. A. Erickson and J. I. McLoughlin, *J. Org. Chem.*, 1995, **60**, 1626–1631.

(42) N. A. Meanwell, *J. Med. Chem.*, 2011, **54**, 2529–2591.

(43) M. J. Graneto and W. G. Phillips, *3-difluoromethylpyrazolecarboxamide fungicides, compositions and use*, 1992.

(44) T. Fujiwara and D. O'Hagan, 2014, **167**, 16–29.

(45) A. J. Bloodworth, K. J. Bowyer and J. C. Mitchell, *Tetrahedron Lett.*, 1987, **28**, 5347–5350.

(46) J. P. Praly and G. Descotes, *Tetrahedron Lett.*, 1987, **28**, 1405–1408.

(47) L. N. Markovskij, V. E. Pashinnik and A. V. Kirsanov, *Synthesis*, 1973, **1973**, 787–789.

(48) C. Fäh, R. Mathys, L. A. Hardegger, S. Meyer, D. Bur and F. Diederich, *European J. Org. Chem.*, 2010, 4617–4629.

(49) A. Lheureux, F. Beaulieu, C. Bennett, D. R. Bill, S. Clayton, F. Laflamme, M. Mirmehrabi, S. Tadayon, D. Tovell and M. Couturier, *J. Org. Chem.*, 2010, **75**, 3401–3411.

(50) B. Modarai and E. Khoshdel, *J. Org. Chem.*, 1977, **42**, 3527–3531.

(51) W. J. Middleton and E. M. Bingham, *J. Org. Chem.*, 1980, **45**, 2883–2887.

(52) R. P. Singh, U. Majumder and J. M. Shreeve, *J. Org. Chem.*, 2001, **66**, 6263–6267.

(53) R. P. Singh and J. M. Shreeve, *Org. Lett.*, 2001, **3**, 2713–2714.

(54) K. Orito, Y. Seki, H. Suginome and T. Iwadare, *Bull. Chem. Soc. Jpn.*, 1989, **62**, 2013–2017.

(55) M. Kuroboshi, S. Furuta and T. Hiyama, *Tetrahedron Lett.*, 1995, **36**, 6121–6122.

(56) R. E. Banks, N. J. Lawrence and A. L. Popplewell, *J. Chem. Soc. Chem. Commun.*, 1994, **92**, 343–344.

(57) G. Stavber, M. Zupan, M. Jereb and S. Stavber, *Org. Lett.*, 2004, **6**, 4973–4976.

(58) W. Ying, D. D. DesMarteau and Y. Gotoh, *Tetrahedron*, 1996, **52**, 15–22.

(59) R. E. Banks, M. K. Besheesh and R. G. Pritchard, *Acta Crystallogr. Sect. C Cryst. Struct. Commun.*, 2003, **59**, m141–m143.

(60) J. A. Ma and D. Cahard, *J. Fluorine. Chem.*, 2004, **125**, 1357–1361.

(61) X. Yang, T. Wu, R. J. Phipps and F. D. Toste, *Advances in catalytic enantioselective fluorination, mono-, di-, and trifluoromethylation, and trifluoromethylthiolation reactions*, 2015.

(62) J. Zhou, C. Jin and W. Su, *Org. Process Res. Dev.*, 2014, **18**, 928–933.

(63) G. S. Lai, W. Pastore and R. Pesaresi, *J. Org. Chem.*, 1995, **60**, 7340–7342.

(64) G. W. Visser, R. E. Herder, F. J. De Kanter and J. D. Herscheid, *J. Chem. Soc., Perkin Trans. 1*, 1988, 1203–1207.

(65) F. A. Davis, W. Han and C. K. Murphy, *J. Org. Chem.*, 1995, **60**, 4730–4737.

(66) J. C. Xiao and J. M. J. M. Shreeve, *J. Fluorine. Chem.*, 2005, **126**, 473–476.

(67) G. Stavber, M. Zupan and S. Stavber, *Tetrahedron Lett.*, 2007, **48**, 2671–2673.

(68) G. Stavber and S. Stavber, *Adv. Synth. Catal.*, 2010, **3521 G. St**, 2838–2846.

(69) E. Differding, G. M. Rüegg and R. W. Lang, *Tetrahedron Lett.*, 1991, **32**, 1779–1782.

(70) I. Pravst, M. Zupan and S. Stavber, *Synthesis*, 2005, 3140–3146.

(71) S. Stavber and M. Zupan, *J. Org. Chem.*, 1987, **52**, 5022–5025.

(72) M. Zupan, J. Iskra and S. Stavber, *J. Org. Chem.*, 1995, **60**, 259–260.

(73) S. Stavber and M. Zupan, *Synlett*, 1996, **1996**, 693–694.

(74) J. L. Howard, Y. Sagatov, L. Repusseau, C. Schotten and D. L. Browne, *Green Chem.*, 2017, **19**, 2798–2802.

(75) J. L. Howard, Y. Sagatov and D. L. Browne, *Tetrahedron*, 2018, **74**, 3118–3123.

(76) J. A. Codelli, J. M. Baskin, N. J. Agard and C. R. Bertozzi, *J. Am. Chem. Soc.*, 2008, **130**, 11486–11493.

(77) C. E. Iacono, T. C. Stephens, T. S. Rajan and G. Pattison, *J. Am. Chem. Soc.*, 2018, **140**, 2036–2040.

(78) T. Hagiwara and T. Fuchikami, *Synlett*, 1995, **1995**, 717–718.

(79) Y. Zhao, W. Huang, J. Zheng and J. Hu, *Org. Lett.*, 2011, **13**, 5342–5345.

(80) G. K. Prakash, J. Hu, Y. Wang and G. A. Olah, *Org. Lett.*, 2004, **6**, 4315–4317.

(81) L. Zhu, Y. Li, C. Ni, J. Hu, P. Beier, Y. Wang, G. K. Surya Prakash and G. A. Olah, *J. Fluorine. Chem.*, 2007, **128**, 1241–1247.

(82) S. Furuta, M. Kuroboshi and T. Hiyama, *Bull. Chem. Soc. Jpn.*, 1998, **71**, 1939–1951.

(83) E. A. Hallinan and J. Fried, *Tetrahedron Lett.*, 1984, **25**, 2301–2302.

(84) T. T. Curran, *J. Org. Chem.*, 1993, **58**, 6360–6363.

(85) K. Iseki, Y. Kuroki, D. Asada and Y. Kobayashi, *Tetrahedron Lett.*, 1997, **38**, 1447–1448.

(86) K. Sato, A. Tarui, T. Kita, Y. Ishida, H. Tamura, M. Omote, A. Ando and I. Kumadaki, *Tetrahedron Lett.*, 2004, **45**, 5735–5737.

(87) K. Sato, M. Omote, A. Ando and I. Kumadaki, *J. Fluorine. Chem.*, 2004, **125**, 509–515.

(88) Y. Ohtsuka and T. Yamakawa, *Tetrahedron*, 2011, **67**, 2323–2331.

(89) K. Araki and M. Inoue, *Tetrahedron*, 2013, **69**, 3913–3918.

(90) Q. Lin, L. Chu and F. L. Qing, *Chinese J. Chem.*, 2013, **31**, 885–891.

(91) M. C. Belhomme, T. Poisson and X. Pannecoucke, *J. Org. Chem.*, 2014, **79**, 7205–7211.

(92) Y. Gu, X. Leng and Q. Shen, *Nat. Commun.*, 2014, **5**, 5405.

(93) Z. Feng, Q. Q. Min and X. Zhang, *Org. Lett.*, 2016, **18**, 44–47.

(94) H. Ito, T. Ishizuka, J. I. Tateiwa and A. Hosomi, *Tetrahedron Lett.*, 1998, **39**, 6295–6298.

(95) Y. Kuroki, D. Asada and K. Iseki, *Tetrahedron Lett.*, 2000, **41**, 9853–9858.

(96) K. Uneyama, H. Tanaka, S. Kobayashi, M. Shioyama and H. Amii, *Org. Lett.*, 2004, **6**, 2733–2736.

(97) R. E. Banks, *J. Fluorine. Chem.*, 1986, **33**, 3–26.

(98) R. D. Chambers, J. Hutchinson and G. Sandford, *J. Fluorine. Chem.*, 1999, **100**, 63–73.

(99) R. D. Chambers, J. Hutchinson, M. E. Sparrowhawk, G. Sandford, J. S. Moilliet and J. Thomson, *J. Fluorine. Chem.*, 2000, **102**, 169–173.

(100) R. D. Chambers, A. M. Kenwright, M. Parsons, G. Sandford and J. S. Moilliet, *J. Chem. Soc., Perkin Trans. 1*, 2002, **2**, 2190–2197.

(101) R. D. Chambers, D. Holling, G. Sandford, H. Puschmann and J. A. Howard, *J. Fluorine. Chem.*, 2002, **117**, 99–101.

(102) G. Sandford, *Elemental fluorine in organic chemistry (1997-2006)*, 2007.

(103) H. G. Adolph, R. E. Oesterling and M. E. Sitzmann, *J. Org. Chem.*, 1968, **33**, 4296–4299.

(104) S. T. Purrington, N. V. Lazaridis and C. L. Bumgardner, *Tetrahedron Lett.*, 1986, **27**, 2715–2716.

(105) S. T. Purrington, C. L. Bumgardner, N. V. Lazaridis and P. Singh, *J. Org. Chem.*, 1987, **52**, 4307–4310.

(106) R. D. Chambers, M. P. Greenhall and J. Hutchinson, *J. Chem. Soc. Chem. Commun.*, 1995, **52**, 21–22.

(107) R. D. Chambers and J. Hutchinson, *J. Fluorine. Chem.*, 1998, **89**, 229–232.

(108) H. Weintritt, U. Stelzer, H. Gayer and W. Hubsch, *US 20030092723A1.* 2003.

(109) M. O. Polla, L. Tottie, C. Nordén, M. Linschoten, D. Müsil, S. Trumpp-Kallmeyer, I. R. Aukrust, R. Ringom, K. H. Holm, S. M. Neset, M. Sandberg, J. Thurmond, P. Yu, G. Hategan and H. Anderson, *Bioorg. Med. Chem.*, 2004, **12**, 1151–1175.

(110) Y. Zhao, L. Zhu, D. P. Provencal, T. A. Miller, C. O'Bryan, M. Langston, M. Shen, D. Bailey, D. Sha, T. Palmer, T. Ho and M. Li, *Org. Process Res. Dev.*, 2012, **16**, 1652–1659.

(111) C. A. Fisher, A. Harsanyi, G. Sandford, D. S. Yufit and J. A. K. Howard, *CHIMIA*, 2014, **68**, 425–429.

(112) A. Harsanyi, G. Sandford, D. S. Yufit and J. A. Howard, *Beilstein J. Org. Chem.*, 2014, **10**, 1213–1219.

(113) A. Harsanyi and G. Sandford, *2-Fluoromalonate esters: Fluoroaliphatic building blocks for the life sciences*, 2014.

(114) R. D. Chambers, J. Hutchinson and J. Thomson, *J. Fluorine. Chem.*, 1996, **78**, 165–166.

(115) R. D. Chambers and J. Hutchinson, *J. Fluorine. Chem.*, 1998, **92**, 45–52.

(116) A. Harsanyi and G. Sandford, *Green Chem.*, 2015, **17**, 3000–3009.

(117) M. Butters, *J. Heterocycl. Chem.*, 1992, **29**, 1369–1370.

(118) M. Butters, J. Ebbs, S. P. Green, J. MacRae, M. C. Morland, C. W. Murtiashaw and A. J. Pettman, *Org. Process Res. Dev.*, 2001, **5**, 28–36.

(119) J. Leroy and C. Wakselman, *J. Chem. Soc., Perkin Trans. 1*, 1978, 1224–1227.

(120) T. B. Patrick, J. J. Scheibel and G. L. Cantrell, *J. Org. Chem.*, 1981, **46**, 3917–3918.

(121) R. D. Chambers, J. Hutchinson, A. S. Batsanov, C. W. Lehmann and D. Y. Naumov, *J. Chem. Soc., Perkin Trans. 1*, 1996, 2271–2275.

(122) K. O. Christe, *J. Fluorine. Chem.*, 1987, **35**, 621–626.

(123) N. Rozatian, I. W. Ashworth, G. Sandford and D. R. Hodgson, *Chem. Sci.*, 2018, **9**, 8692–8702.

(124) N. Rozatian, A. Beeby, I. W. Ashworth, G. Sandford and D. R. W. Hodgson, *Chem. Sci.*, 2019, **Advance Ar**, DOI: 10.1039/C9SC04185K.

(125) S. H. Wood, S. Etridge, A. R. Kennedy, J. M. Percy and D. J. Nelson, *Chem. - Eur. J.*, 2019, **25**, 5574–5585.

(126) R. E. Banks, S. N. Mohialdin-Khaffaf, G. S. Lal, Sharif Iqbal; and R. G. Syvret, *J. Chem. Soc. Chem. Commun.*, 1992, 595–596.

(127) J. Breen, Ph.D. Thesis, Durham University, 2012.

(128) N. Y. Yang, Z. L. Li, L. Ye, B. Tan and X. Y. Liu, *Chem. Commun.*, 2016, **52**, 9052–9055.

(129) T. J. Nash and G. Pattison, *European J. Org. Chem.*, 2015, **2015**, 3779–3786.

(130) Y. M. Lin, W. B. Yi, W. Z. Shen and G. P. Lu, *Org. Lett.*, 2016, **18**, 592–595.

(131) J. D. Calfee and L. A. Bigelow, *J. Am. Chem. Soc.*, 1937, **59**, 2072–2073.

(132) J. L. Adcock and R. J. Lagow, *J. Am. Chem. Soc.*, 1974, **96**, 7588–7589.

(133) R. J. Lagow and J. L. Margrave, in, John Wiley & Sons, Ltd, 2007, pp. 161–210.

(134) W. T. Miller and S. D. Koch, *J. Am. Chem. Soc.*, 1957, **79**, 3084–3089.

(135) M. Moriyasu, A. Kato and Y. Hashimoto, *J. Chem. Soc., Perkin Trans. 2*, 1986, 515–520.

(136) W. R. Dolbier, K. S. Medinger, A. Greenberg and J. F. Liebman, *Tetrahedron*, 1982, **38**, 2415–2420.

(137) J. F. Coetzee and G. R. Padmanabhan, *J. Am. Chem. Soc.*, 1965, **87**, 5005–5010.

(138) B. G. Cox, *Acids and Bases: Solvent Effects on Acid-Base Strength*, Oxford University Press, 1st edn., 2013, p. 137.

(139) W. N. Olmstead and F. G. Bordwell, *J. Org. Chem.*, 1980, **45**, 3299–3305.

(140) R. E. Banks and I. Sharif, *J. Fluorine. Chem.*, 1991, **55**, 207–214.

(141) R. E. Banks, R. A. Du Boisson, W. D. Morton and E. Tsiliopoulos, *J. Chem. Soc., Perkin Trans. 1*, 1988, 2805–2811.

(142) R. E. Banks and I. Sharif, *J. Fluorine. Chem.*, 1988, **41**, 297–300.

(143) R. E. Banks and I. Sharif, *J. Fluorine. Chem.*, 1988, **41**, 297–300.

(144) R. E. Banks, R. G. Pritchard and I. Sharif, *Acta Crystallogr. Sect. C Cryst. Struct. Commun.*, 1993, **49**, 1806–1807.

(145) M. Abdul-Ghani, E. R. Banks, M. K. Besheesh, I. Sharif and R. G. Syvret, *J. Fluorine. Chem.*, 1995, **73**, 255–257.

(146) R. E. Banks, I. Si-Iarif and R. G. Pritchard, *Acta Crystallogr. Sect. C Cryst. Struct. Commun.*, 1993, **49**, 492–495.

(147) R. E. Banks and I. Sharif, *J. Fluorine. Chem.*, 1991, **55**, 207–214.

(148) N. Sampathkumar, A. Murugesh and S. P. Rajendran, *J. Heterocycl. Chem.*, 2016, **53**, 924–928.

(149) S. Kumar, W. Namkung, A. S. Verkman and P. K. Sharma, *Bioorg. Med. Chem.*, 2012, **20**, 4237–4244.

(150) U. Košak, A. Kovač and S. Gobec, *Synlett*, 2012, **23**, 1609–1612.

(151) Y. Zhu, X. Zou, F. Hu, C. Yao, B. Liu and H. Yang, *J. Agric. Food Chem.*, 2005, **53**, 9566–9570.

(152) Y. Fu, X. L. Zhao, H. Hügel, D. Huang, Z. Du, K. Wang and Y. Hu, *Org. Biomol. Chem.*, 2016, **14**, 9720–9724.

(153) R. J. Clay, T. A. Collom, G. L. Karrick and J. Wemple, *Synthesis*, 1993, **1993**, 290–292.

(154) R. Venkat Ragavan, V. Vijayakumar, K. Rajesh, B. Palakshi Reddy, S. Karthikeyan and N. Suchetha Kumari, *Bioorg. Med. Chem. Lett.*, 2012, **22**, 4193–4197.

(155) G. Stavber and S. Stavber, *Adv. Synth. Catal.*, 2010, **352**, 2838–2846.

(156) T. L. Andersen, M. W. Frederiksen, K. Domino and T. Skrydstrup, *Angew. Chemie, Int. Ed.*, 2016, **55**, 10396–10400.

(157) K. Sato, R. Kawata, F. Ama, M. Omote, A. Ando and I. Kumadaki, *Chem. Pharm. Bull.*, 1999, **47**, 1013–1016.

(158) S. Murakami, S. Kim, H. Ishii and T. Fuchigami, *Synlett*, 2004, 0815–0818.

(159) Z. Feng, Q. Q. Min, Y. L. Xiao, B. Zhang and X. Zhang, *Angew. Chemie, Int. Ed.*, 2014, **53**, 1669–1673.

(160) R. Beniazza, B. Abadie, L. Remisse, D. Jardel, D. Lastécouères and J. M. Vincent, *Chem. Commun.*, 2017, **53**, 12708–12711.

(161) S. I. Arlow and J. F. Hartwig, *Angew. Chemie, Int. Ed.*, 2016, **55**, 4567–4572.

(162) X. L. Jiang, Z. H. Chen, X. H. Xu and F. L. Qing, *Org. Chem. Front.*, 2014, **1**, 774–776.

(163) S. B. Munoz, C. Ni, Z. Zhang, F. Wang, N. Shao, T. Mathew, G. A. Olah and G. K. Prakash, *European J. Org. Chem.*, 2017, **2017**, 2322–2326.

(164) K. Fujikawa, Y. Fujioka, A. Kobayashi and H. Amii, *Org. Lett.*, 2011, **13**, 5560–5563.

(165) S. Utsumi, T. Katagiri and K. Uneyama, *Tetrahedron*, 2012, **68**, 580–583.

(166) J. N. Desrosiers, C. B. Kelly, D. R. Fandrick, L. Nummy, S. J. Campbell, X. Wei, M. Sarvestani, H. Lee, A. Sienkiewicz, S. Sanyal, X. Zeng, N. Grinberg, S. Ma, J. J. Song and C. H. Senanayake, *Org. Lett.*, 2014, **16**, 1724–1727.

(167) O. René, A. Souverneva, S. R. Magnuson and B. P. Fauber, *Tetrahedron Lett.*, 2013, **54**, 201–204.

(168) B. Yang, X. H. Xu and F. L. Qing, *Org. Lett.*, 2016, **18**, 5956–5959.

(169) F. Chen and A. S. K. Hashmi, *Org. Lett.*, 2016, **18**, 2880–2882.

(170) X. Li, S. Li, S. Sun, F. Yang, W. Zhu, Y. Zhu, Y. Wu and Y. Wu, *Adv. Synth. Catal.*, 2016, **358**, 1699–1704.

(171) F. G. Bordwell and H. E. Fried, *J. Org. Chem.*, 1981, **46**, 4327–4331.

(172) R. Beniazza, B. Abadie, L. Remisse, D. Jardel, D. Lastécouères and J. M. Vincent, *Chem. Commun.*, 2017, **53**, 12708–12711.

(173) M. Baidya, S. Kobayashi, F. Brotzel, U. Schmidhammer, E. Riedle and H. Mayr, *Angew. Chemie, Int. Ed.*, 2007, **46**, 6176–6179.

(174) J. Ammer, M. Baidya, S. Kobayashi and H. Mayr, *J. Phys. Org. Chem.*, 2010, **23**, 1029–1035.

(175) L. Willard, B. Subramanian, O. Johan D. and Y. Joshua C., *United States Patent Application: 0060035908*, 2005.

(176) J. Hill, MA thesis, 2019.

(177) T. Hirayama, J. Fujimoto, D. R. Cary and Y. Hirata, *US20170044132 (A1)*, 2017.

(178) S. S. Y. Cho, *WO2004041793 (A1)*, 2004.

(179) M. E. Sparrowhawk, Ph.D. Thesis, 1998, pp. 1–236.

(180) S. Stavber and M. Zupan, *Fluorination with cesium fluoroxysulfate. Room-temperature fluorination of benzene and naphthalene derivatives*, 1985.

(181) S. D. Schimler, R. D. Froese, D. C. Bland and M. S. Sanford, *J. Org. Chem.*, 2018, **83**, 11178–11190.

(182) K. K. Laali and G. I. Borodkin, *J. Chem. Soc., Perkin Trans. 2*, 2002, 953–957.

(183) I. Urasaki and Y. Ogata, *J. Chem. Soc., Perkin Trans. 1*, 1975, 1285–1287.

(184) S. Nakaiida, S. Kato, O. Niyomura, M. Ishida, F. Ando and J. Koketsu, *Phosphorus, Sulfur Silicon Relat. Elem.*, 2010, **185**, 930–946.

(185) E. Hasegawa, K. Ishiyama, T. Horaguchi and T. Shimizu, *J. Org. Chem.*, 1991, **56**, 5236.

(186) H. S. P. Rao and N. Muthanna, *European J. Org. Chem.*, 2015, **2015**, 1525–1532.

(187) H. Ishihara and Y. Hirabayashi, *Chem. Lett.*, 1978, **7**, 1007–1010.

(188) J. C. Hubaud, I. Bombarda, L. Decome, J. C. Wallet and E. M. Gaydou, *J. Photochem. Photobiol. B Biol.*, 2008, **92**, 103–109.

(189) S. Saito, T. Tanaka, T. Koizumi, N. Tsuboya, H. Itagaki, T. Kawasaki, S. Endo and Y. Yamamoto, *J. Am. Chem. Soc.*, 2000, **122**, 1810–1811.

(190) Z. He, X. Qi, S. Li, Y. Zhao, G. Gao, Y. Lan, Y. Wu, J. Lan and J. You, *Angew. Chemie, Int. Ed.*, 2015, **54**, 855–859.

(191) A. Sieglitz and O. Horn, *Chem. Ber.*, 1951, **84**, 607–618.

(192) J. Zawadiak and M. Mrzyczek, *Spectrochim. Acta, Part A Mol. Biomol. Spectrosc.*, 2012, **96**, 815–819.

(193) M. Lipp, F. Dallacker and S. Munnes, *Justus Liebigs Ann. Chem.*, 1958, **618**, 110–117.

(194) S. Stavber, B. Šket, B. Zajc and M. Zupan, *Tetrahedron*, 1989, **45**, 6003–6010.

(195) M. Gao, Y. Zhao, C. Zhong, S. Liu, P. Liu, Q. Yin and L. Hu, *Org. Lett.*, 2019, **21**, 5679–5684.

(196) G. Wagner, C. Garbe and P. Richter, *Pharmazie*, 1975, **30**, 271–276.

(197) W. Wendell and I. S. Harvey, *J. Org. Chem.*, 1979, **44**, 310–311.

(198) C. A. Maggiuli, *FR 1318368*, 1963.

(199) H.-S. Wang and J.-E. Zeng, *Chem. Res. Chin. Univ.*, 2009, **25**, 343–346.

(200) A. R. Katritzky, Z. Wang, M. Wang, C. R. Wilkerson, C. D. Hall and N. G. Akhmedov, *J. Org. Chem.*, 2004, **69**, 6617–6622.

(201) H. Y. Zhao, Z. Feng, Z. Luo and X. Zhang, *Angew. Chemie, Int. Ed.*, 2016, **55**, 10401–10405.

(202) Z. Zhang, D. Zheng, Y. Wan, G. Zhang, J. Bi, Q. Liu, T. Liu and L. Shi, *J. Org. Chem.*, 2018, **83**, 1369–1376.

(203) A. P. Häring, P. Biallas and S. F. Kirsch, *European J. Org. Chem.*, 2017, **2017**, 1526–1539.

Appendix: Crystallographic Data

1-(4-Methylphenyl)-3-phenylpropane-1,3-dione 91a

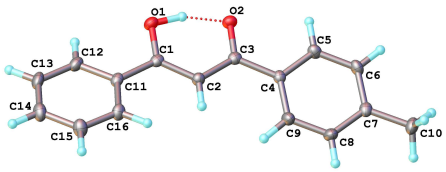

Table 12.1: Crystal data and structure refinement for **91a**

Identification code	17srv259
Empirical formula	$C_{16}H_{14}O_2$
Formula weight	238.27
Temperature/K	120.0
Crystal system	orthorhombic
Space group	Pbca
a/Å	8.7320(40)
b/Å	10.2647(5)
c/Å	27.3442(13)
α/°	90
β/°	90
γ/°	90
Volume/Å^3	2450.9(2)
Z	8
ρ_{calc}g/cm^3	1.291
μ/mm^{-1}	0.084
F(000)	1008.0
Crystal size/mm^3	$0.27 \times 0.23 \times 0.06$
Radiation	MoKα ($\lambda = 0.71073$)
2Θ range for data collection/°	5.536 to 57.994
Index ranges	$-11 \leq h \leq 11$, $-14 \leq k \leq 14$, $-37 \leq l \leq 37$
Reflections collected	34007
Independent reflections	3254 [$R_{int} = 0.0495$, $R_{sigma} = 0.0269$]
Data/restraints/parameters	3254/0/219
Goodness-of-fit on F^2	1.055
Final R indexes [I>=2σ (I)]	$R_1 = 0.0469$, $wR_2 = 0.1268$
Final R indexes [all data]	$R_1 = 0.0690$, $wR_2 = 0.1268$
Largest diff. peak/hole / e Å^{-3}	0.46/−0.23

1-(4-Methoxyphenyl)-3-phenylpropane-1,3-dione 91b

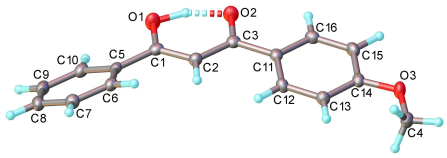

Table 12.2: Crystal data and structure refinement for **91b**

Identification code	17srv227
Empirical formula	$C_{16}H_{14}O_3$
Formula weight	254.27
Temperature/K	120.0
Crystal system	orthorhombic
Space group	Pbca
a/Å	7.5562(6)
b/Å	10.7325(8)
c/Å	30.169(2)
α/°	90
β/°	90
γ/°	90
Volume/Å^3	2446.6(3)
Z	8
ρ_{calc}g/cm^3	1.381
μ/mm^{-1}	0.095
F(000)	1072.0
Crystal size/mm^3	0.225 × 0.191 × 0.041
Radiation	MoKα (λ = 0.71073)
2Θ range for data collection/°	5.402 to 54.984
Index ranges	$-9 \leq h \leq 9$, $-13 \leq k \leq 13$, $-39 \leq l \leq 39$
Reflections collected	37412
Independent reflections	2791 [R_{int} = 0.0452, R_{sigma} = 0.0209]
Data/restraints/parameters	2791/0/228
Goodness-of-fit on F^2	1.049
Final R indexes [I>=2σ (I)]	R_1 = 0.0373, wR_2 = 0.0862
Final R indexes [all data]	R_1 = 0.0506, wR_2 = 0.0932
Largest diff. peak/hole / e Å^{-3}	0.28/−0.21

1-(4-Fluorophenyl)-3-phenylpropane-1,3-dione 91d

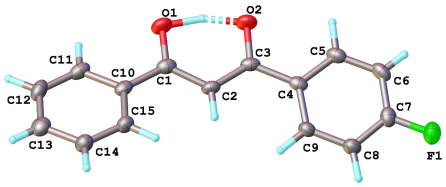

Table 12.3: Crystal data and structure refinement for **91d**

Identification code	17srv287
Empirical formula	$C_{15}H_{11}FO_2$
Formula weight	242.24
Temperature/K	120.0
Crystal system	monoclinic
Space group	$P2_1/c$
a/Å	11.5084(10)
b/Å	11.5599(9)
c/Å	9.3184(8)
$\alpha/°$	90
$\beta/°$	112.899(3)
$\gamma/°$	90
Volume/Å^3	1141.98(17)
Z	4
ρ_{calc}g/cm^3	1.409
μ/mm^{-1}	0.104
F(000)	504.0
Crystal size/mm^3	$0.43 \times 0.06 \times 0.03$
Radiation	MoKα ($\lambda = 0.71073$)
2Θ range for data collection/°	5.214 to 54.998
Index ranges	$-14 \leq h \leq 14$, $-15 \leq k \leq 15$, $-12 \leq l \leq 12$
Reflections collected	15666
Independent reflections	2618 [$R_{int} = 0.0595$, $R_{sigma} = 0.0513$]
Data/restraints/parameters	2618/0/203
Goodness-of-fit on F^2	1.020
Final R indexes [I>=2σ (I)]	$R_1 = 0.0582$, $wR_2 = 0.1454$
Final R indexes [all data]	$R_1 = 0.0980$, $wR_2 = 0.1663$
Largest diff. peak/hole / e Å^{-3}	0.96/−0.32

1-(4-Nitrophenyl)-3-phenylpropane-1,3-dione 91e

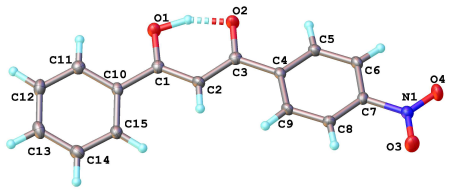

Table 12.4: Crystal data and structure refinement for **91e**

Identification code	17srv289
Empirical formula	$C_{15}H_{11}NO_4$
Formula weight	269.25
Temperature/K	120.0
Crystal system	monoclinic
Space group	$P2_1/c$
a/Å	8.1666(6)
b/Å	6.7088(5)
c/Å	22.0382(15)
α/°	90
β/°	94.322(3)
γ/°	90
Volume/Å^3	1204.00(15)
Z	4
ρ_{calc}g/cm^3	1.485
μ/mm^{-1}	0.109
F(000)	560.0
Crystal size/mm^3	$0.22 \times 0.04 \times 0.02$
Radiation	MoKα ($\lambda = 0.71073$)
2Θ range for data collection/°	5.002 to 54.996
Index ranges	$-10 \leq h \leq 10$, $-8 \leq k \leq 8$, $-28 \leq l \leq 28$
Reflections collected	21883
Independent reflections	2769 [$R_{int} = 0.0739$, $R_{sigma} = 0.0621$]
Data/restraints/parameters	2769/0/225
Goodness-of-fit on F^2	1.034
Final R indexes [I>=2σ (I)]	$R_1 = 0.0463$, $wR_2 = 0.1019$
Final R indexes [all data]	$R_1 = 0.0867$, $wR_2 = 0.1174$
Largest diff. peak/hole / e Å^{-3}	0.30/−0.24

1,3-Bis(4-chlorophenyl)-3-phenylpropane-1,3-dione 91g

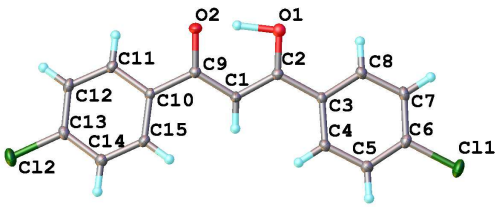

Table 12.5: Crystal data and structure refinement for **91g**

Identification code	Ah81
Empirical formula	$C_{15}H_{10}O_2Cl_2$
Formula weight	273.135
Temperature/K	273.15
Crystal system	orthorhombic
Space group	Pnma
a/Å	6.0742(2)
b/Å	30.4413(12)
c/Å	6.9268(3)
α/°	90
β/°	90
γ/°	90
Volume/Å^3	1280.81(9)
Z	4
ρ_{calc}g/cm^3	1.520
μ/mm^{-1}	0.500
F(000)	600.0
Crystal size/mm^3	$0.224 \times 0.520 \times 0.626$
Radiation	MoKα ($\lambda = 0.71073$)
2Θ range for data collection/°	5.352 to 63.208
Index ranges	$-8 \leq h \leq 8$, $-44 \leq k \leq 44$, $-10 \leq l \leq 9$
Reflections collected	23769
Independent reflections	21731 [$R_{int} = 0.0634$, $R_{sigma} = 0.0329$]
Data/restraints/parameters	2173/0/92
Goodness-of-fit on F^2	1.234
Final R indexes [I>=2σ (I)]	$R_1 = 0.0508$, $wR_2 = 0.1159$
Final R indexes [all data]	$R_1 = 0.0570$, $wR_2 = 0.1178$
Largest diff. peak/hole / e Å^{-3}	0.39/−0.40

1,3-Bis(4-fluorophenyl)-3-phenylpropane-1,3-dione 91h

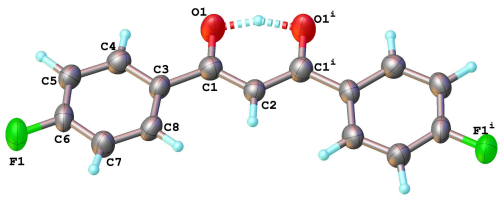

Table 12.6: Crystal data and structure refinement for **91h**

Identification code	19srv262
Empirical formula	$C_{15}H_{10}F_2O_2$
Formula weight	260.23
Temperature/K	120.0
Crystal system	monoclinic
Space group	C2/c
a/Å	3.8574(15)
b/Å	11.914(5)
c/Å	25.388(10)
α/°	90
β/°	94.36
γ/°	90
Volume/Å^3	1163.4(8)
Z	4
ρ_{calc}g/cm^3	1.486
μ/mm^{-1}	0.119
F(000)	536.0
Crystal size/mm^3	$0.28 \times 0.24 \times 0.01$
Radiation	MoKα ($\lambda = 0.71073$)
2Θ range for data collection/°	4.828 to 53.952
Index ranges	$-4 \leq h \leq 4$, $-14 \leq k \leq 14$, $-32 \leq l \leq 32$
Reflections collected	7253
Independent reflections	1257 [$R_{int} = 0.1021$, $R_{sigma} = 0.0998$]
Data/restraints/parameters	1257/0/108
Goodness-of-fit on F^2	0.951
Final R indexes [I>=2σ (I)]	$R_1 = 0.0553$, $wR_2 = 0.1169$
Final R indexes [all data]	$R_1 = 0.1410$, $wR_2 = 0.1505$
Largest diff. peak/hole / e Å^{-3}	0.16/−0.27

2-Fluoro-1,3-diphenylpropane-1,3-dione 92

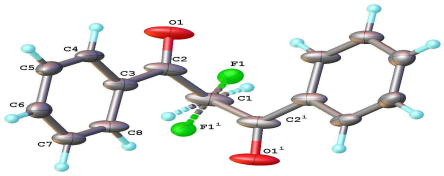

Table 12.7: Crystal data and structure refinement for **92**

Identification code	17srv039
Empirical formula	$C_{15}H_{11}FO_2$
Formula weight	242.24
Temperature/K	120.0
Crystal system	monoclinic
Space group	C2/c
a/Å	19.951(3)
b/Å	5.1203(7)
c/Å	13.2495(18)
α/°	90
β/°	123.559(5)
γ/°	90
Volume/Å^3	1127.9(3)
Z	4
ρ_{calc}g/cm^3	1.427
μ/mm^{-1}	0.105
F(000)	540.0
Crystal size/mm^3	$0.11 \times 0.07 \times 0.06$
Radiation	MoKα ($\lambda = 0.71073$)
2Θ range for data collection/°	4.9 to 54.976
Index ranges	$-25 \leq h \leq 25$, $-6 \leq k \leq 6$, $-17 \leq l \leq 17$
Reflections collected	9993
Independent reflections	1302 [$R_{int} = 0.0547$, $R_{sigma} = 0.0364$]
Data/restraints/parameters	1302/0/90
Goodness-of-fit on F^2	1.024
Final R indexes [I>=2σ (I)]	$R_1 = 0.0502$, $wR_2 = 0.1138$
Final R indexes [all data]	$R_1 = 0.0847$, $wR_2 = 0.1288$
Largest diff. peak/hole / e Å^{-3}	0.16/−0.23

2,2-Difluoro-1,3-diphenylpropane-1,3-dione 93

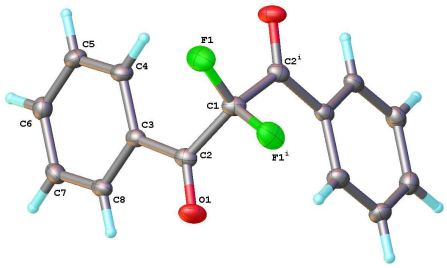

Table 12.8: Crystal data and structure refinement for **93**

Identification code	17srv034
Empirical formula	$C_{15}H_{10}F_2O_2$
Formula weight	260.23
Temperature/K	120.0
Crystal system	monoclinic
Space group	C2/c
a/Å	19.9091(14)
b/Å	5.3345(4)
c/Å	13.0943(9)
α/°	90
β/°	123.898(2)
γ/°	90
Volume/Å^3	1154.31(15)
Z	4
ρ_{calc}g/cm^3	1.497
μ/mm^{-1}	0.120
F(000)	536.0
Crystal size/mm^3	0.31 × 0.3 × 0.18
Radiation	MoKα (λ = 0.71073)
2Θ range for data collection/°	4.93 to 57.924
Index ranges	$-26 \leq h \leq 26$, $-7 \leq k \leq 7$, $-17 \leq l \leq 17$
Reflections collected	11191
Independent reflections	1531 [R_{int} = 0.0338, R_{sigma} = 0.0206]
Data/restraints/parameters	1531/0/87
Goodness-of-fit on F^2	1.086
Final R indexes [I>=2σ (I)]	R_1 = 0.0480, wR_2 = 0.1373
Final R indexes [all data]	R_1 = 0.0597, wR_2 = 0.1480
Largest diff. peak/hole / e Å^{-3}	0.45/−0.39

2,2-Difluoro-1-(4-chlorophenyl)-3-phenylpropane-1,3-dione 93c

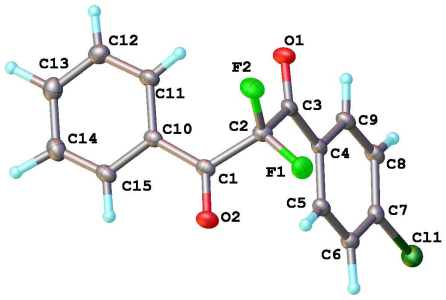

Table 12.9: Crystal data and structure refinement for **93c**

Identification code	ASH85
Empirical formula	$C_{15}H_9ClF_2O_2$
Formula weight	294.68
Temperature/K	120.0
Crystal system	triclinic
Space group	P-1
a/Å	7.719(2)
b/Å	7.814(2)
c/Å	11.659(3)
α/°	102.016(20)
β/°	92.78(2)
γ/°	112.898(13)
Volume/Å^3	627.0(5)
Z	2
ρ_{calc}g/cm^3	1.5611
μ/mm^{-1}	0.327
F(000)	300.5
Crystal size/mm^3	$0.210 \times 0.262 \times 0.377$
Radiation	MoKα ($\lambda = 0.71073$)
2Θ range for data collection/°	5.78 to 63.14
Index ranges	$-11 \leq h \leq 11$, $-11 \leq k \leq 11$, $-17 \leq l \leq 17$
Reflections collected	14755
Independent reflections	4185 [$R_{int} = 0.0259$, $R_{sigma} = 0.0277$]
Data/restraints/parameters	4185/0/218
Goodness-of-fit on F^2	1.066
Final R indexes [I>=2σ (I)]	$R_1 = 0.0415$, $wR_2 = 0.1150$
Final R indexes [all data]	$R_1 = 0.0553$, $wR_2 = 0.1225$
Largest diff. peak/hole / e Å^{-3}	0.91/−0.37

2,2-Difluoro-1-(4-nitrophenyl)-3-phenylpropane-1,3-dione 93e

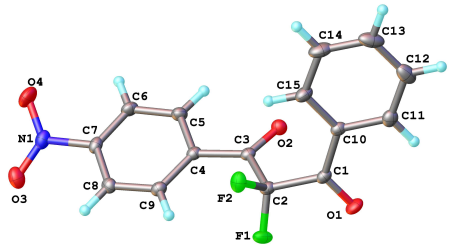

Table 12.10: Crystal data and structure refinement for **93e**

Identification code	19srv123
Empirical formula	$C_{15}H_9F_2NO_4$
Formula weight	305.23
Temperature/K	120.0
Crystal system	triclinic
Space group	P-1
a/Å	7.1508(3)
b/Å	8.0322(3)
c/Å	12.1238(5)
α/°	77.7835(16)
β/°	76.0100(16)
γ/°	77.3328(17)
Volume/Å^3	649.93(5)
Z	2
ρ_{calc}g/cm^3	1.560
μ/mm^{-1}	0.133
F(000)	312.0
Crystal size/mm^3	$0.35 \times 0.17 \times 0.06$
Radiation	MoKα ($\lambda = 0.71073$)
2Θ range for data collection/°	5.272 to 55.996
Index ranges	$-9 \leq h \leq 9$, $-10 \leq k \leq 10$, $-16 \leq l \leq 15$
Reflections collected	12595
Independent reflections	3138 [$R_{int} = 0.0521$, $R_{sigma} = 0.0453$]
Data/restraints/parameters	3138/0/199
Goodness-of-fit on F^2	1.033
Final R indexes [I>=2σ (I)]	$R_1 = 0.0415$, $wR_2 = 0.1082$
Final R indexes [all data]	$R_1 = 0.0518$, $wR_2 = 0.1138$
Largest diff. peak/hole / e Å^{-3}	0.58/−0.25

2,2-Difluoro-1,3-bis(4-chlorophenyl)-propane-1,3-dione 93f

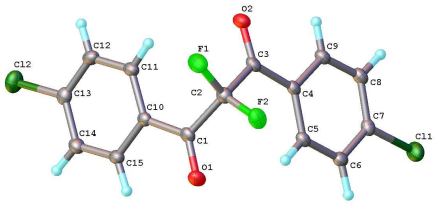

Table 12.11: Crystal data and structure refinement for **93f**

Identification code	ASH88
Empirical formula	$C_{15}H_8Cl_2F_2O_2$
Formula weight	329.11
Temperature/K	120.0
Crystal system	triclinic
Space group	P-1
a/Å	8.0050(5)
b/Å	8.0563(5)
c/Å	11.9916(8)
α/°	96.853(2)
β/°	96.648(2)
γ/°	115.655(2)
Volume/Å^3	679.91(8)
Z	2
ρ_{calc}g/cm^3	1.608
μ/mm^{-1}	0.501
F(000)	332.0
Crystal size/mm^3	$0.150 \times 0.242 \times 0.0397$
Radiation	MoKα ($\lambda = 0.71073$)
2Θ range for data collection/°	5.714 to 63.184
Index ranges	$-11 \leq h \leq 11$, $-11 \leq k \leq 11$, $-17 \leq l \leq 17$
Reflections collected	16351
Independent reflections	4544 [$R_{int} = 0.0298$, $R_{sigma} = 0.0296$]
Data/restraints/parameters	4544/0/223
Goodness-of-fit on F^2	1.058
Final R indexes [I>=2σ (I)]	$R_1 = 0.0312$, $wR_2 = 0.0809$
Final R indexes [all data]	$R_1 = 0.0436$, $wR_2 = 0.0856$
Largest diff. peak/hole / e Å^{-3}	0.41/−0.30

2,2-Difluoro-1,3-bis(4-fluorophenyl)-propane-1,3-dione 93g

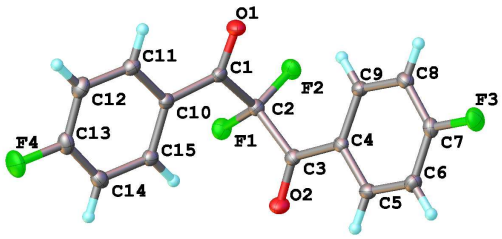

Table 12.12: Crystal data and structure refinement for **93g**

Identification code	ASH88
Empirical formula	$C_{15}H_8F_4O_2$
Formula weight	296.22
Temperature/K	120.0
Crystal system	triclinic
Space group	P-1
a/Å	7.5207(19)
b/Å	7.775(2)
c/Å	11.654(3)
α/°	97.358(16)
β/°	97.935(14)
γ/°	112.458(12)
Volume/Å^3	611.4(4)
Z	2
Crystal size/mm^3	$0.253 \times 0.369 \times 0.480$
Radiation	MoKα ($\lambda = 0.71073$)
2Θ range for data collection/°	5.938 to 60.02
Reflections collected	25651

2,2-Difluoro-1,3-bis(4-nitrophenyl)-propane-1,3-dione 93h

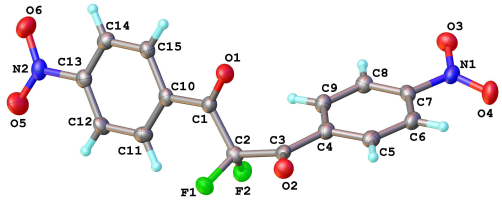

Table 12.13: Crystal data and structure refinement for **93h**

Identification code	19srv022
Empirical formula	$C_{15}H_8F_2N_2O_6$
Formula weight	350.23
Temperature/K	120.0
Crystal system	monoclinic
Space group	$P2_1/c$
a/Å	13.4814(12)
b/Å	6.9481(5)
c/Å	15.0112(11)
α/°	90
β/°	96.591(7)
γ/°	90
Volume/Å^3	1396.82(19)
Z	4
ρ_{calc}g/cm^3	1.665
μ/mm^{-1}	0.147
F(000)	712.0
Crystal size/mm^3	$0.34 \times 0.3 \times 0.02$
Radiation	MoKα ($\lambda = 0.71073$)
2Θ range for data collection/°	5.464 to 55
Index ranges	$-17 \leq h \leq 17$, $-9 \leq k \leq 8$, $-19 \leq l \leq 19$
Reflections collected	17018
Independent reflections	3204 [$R_{int} = 0.0904$, $R_{sigma} = 0.0730$]
Data/restraints/parameters	3204/0/226
Goodness-of-fit on F^2	1.018
Final R indexes [I>=2σ (I)]	$R_1 = 0.0841$, $wR_2 = 0.2604$
Final R indexes [all data]	$R_1 = 0.1276$, $wR_2 = 0.2511$
Largest diff. peak/hole / e Å^{-3}	0.87/−0.34

Ethyl (4-chloro)benzoylacetate 94b

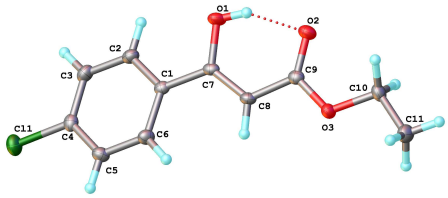

Table 12.14: Crystal data and structure refinement for **94b**

Identification code	19srv294
Empirical formula	$C_{11}H_{11}ClO_3$
Formula weight	226.65
Temperature/K	120.0
Crystal system	monoclinic
Space group	$P2_1/c$
a/Å	5.5336(3)
b/Å	26.5949(14)
c/Å	7.2914(4)
$\alpha/°$	90
$\beta/°$	102.921(2)
$\gamma/°$	90
Volume/Å^3	1045.87(10)
Z	4
ρ_{calc}g/cm^3	1.439
μ/mm^{-1}	0.348
F(000)	472.0
Crystal size/mm^3	$0.23 \times 0.17 \times 0.03$
Radiation	MoKα ($\lambda = 0.71073$)
2Θ range for data collection/°	5.934 to 58.998
Index ranges	$-7 \leq h \leq 7$, $-36 \leq k \leq 36$, $-10 \leq l \leq 9$
Reflections collected	21815
Independent reflections	2903 [$R_{int} = 0.0410$, $R_{sigma} = 0.0280$]
Data/restraints/parameters	2903/0/180
Goodness-of-fit on F^2	1.056
Final R indexes [I>=2σ (I)]	$R_1 = 0.0394$, $wR_2 = 0.0878$
Final R indexes [all data]	$R_1 = 0.0532$, $wR_2 = 0.0927$
Largest diff. peak/hole / e Å^{-3}	0.38/−0.24

Ethyl (4-nitro)benzoylacetate 94c

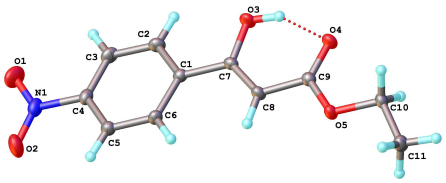

Table 12.15: Crystal data and structure refinement for **94d**

Identification code	19srv295
Empirical formula	$C_{11}H_{11}NO_5$
Formula weight	237.21
Temperature/K	120.0
Crystal system	monoclinic
Space group	$P2_1/c$
a/Å	13.0608(12)
b/Å	10.8129(10)
c/Å	7.6147(7)
α/°	90
β/°	91.584(4)
γ/°	90
Volume/Å^3	1074.98(17)
Z	4
ρ_{calc}g/cm^3	1.466
μ/mm^{-1}	0.117
F(000)	496.0
Crystal size/mm^3	$0.46 \times 0.21 \times 0.08$
Radiation	MoKα ($\lambda = 0.71073$)
2Θ range for data collection/°	4.892 to 57.996
Index ranges	$-17 \leq h \leq 17$, $-14 \leq k \leq 14$, $-10 \leq l \leq 10$
Reflections collected	20718
Independent reflections	2854 [$R_{int} = 0.0646$, $R_{sigma} = 0.0475$]
Data/restraints/parameters	2854/0/198
Goodness-of-fit on F^2	1.053
Final R indexes [I>=2σ (I)]	$R_1 = 0.0409$, $wR_2 = 0.1097$
Final R indexes [all data]	$R_1 = 0.0546$, $wR_2 = 0.1203$
Largest diff. peak/hole / e Å^{-3}	0.38/−0.30

Ethyl (4-cyano)benzoylacetate 94e

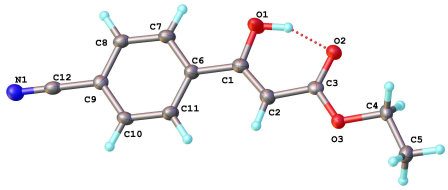

Table 12.16: Crystal data and structure refinement for **94e**

Identification code	19srv260
Empirical formula	$C_{12}H_{11}NO_3$
Formula weight	217.22
Temperature/K	120.0
Crystal system	monoclinic
Space group	$P2_1/n$
a/Å	7.3255(6)
b/Å	14.0134(11)
c/Å	11.1405(9)
$\alpha/°$	90
$\beta/°$	108.533(3)
$\gamma/°$	90
Volume/Å^3	1084.32(15)
Z	4
ρ_{calc}g/cm^3	1.331
μ/mm^{-1}	0.097
F(000)	456.0
Crystal size/mm^3	$0.4 \times 0.07 \times 0.06$
Radiation	MoKα ($\lambda = 0.71073$)
2Θ range for data collection/°	4.83 to 53.996
Index ranges	$-9 \leq h \leq 9$, $-17 \leq k \leq 17$, $-14 \leq l \leq 14$
Reflections collected	18915
Independent reflections	2374 [$R_{int} = 0.0948$, $R_{sigma} = 0.0778$]
Data/restraints/parameters	2374/0/189
Goodness-of-fit on F^2	1.031
Final R indexes [I>=2σ (I)]	$R_1 = 0.0532$, $wR_2 = 0.1255$
Final R indexes [all data]	$R_1 = 0.0845$, $wR_2 = 0.1408$
Largest diff. peak/hole / e Å^{-3}	0.56/−0.26

Ethyl (3-nitro)benzoylacetate 94f

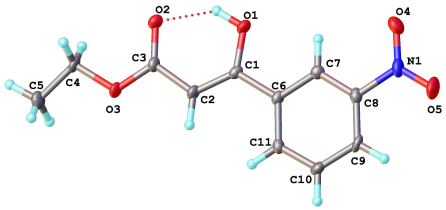

Table 12.17: Crystal data and structure refinement for **94f**

Identification code	19srv235
Empirical formula	$C_{11}H_{11}NO_5$
Formula weight	237.21
Temperature/K	120.0
Crystal system	triclinic
Space group	P-1
a/Å	8.6967(10)
b/Å	8.7824(10)
c/Å	15.0932(17)
α/°	76.146(4)
β/°	76.070(4)
γ/°	76.820(5)
Volume/Å^3	1068.4(2)
Z	4
ρ_{calc}g/cm^3	1.475
μ/mm^{-1}	0.118
F(000)	496.0
Crystal size/mm^3	$0.34 \times 0.17 \times 0.08$
Radiation	MoKα ($\lambda = 0.71073$)
2Θ range for data collection/°	4.858 to 56.998
Index ranges	$-11 \leq h \leq 11$, $-11 \leq k \leq 11$, $-20 \leq l \leq 20$
Reflections collected	19986
Independent reflections	5398 [$R_{int} = 0.0527$, $R_{sigma} = 0.0661$]
Data/restraints/parameters	5398/0/318
Goodness-of-fit on F^2	1.030
Final R indexes [I>=2σ (I)]	$R_1 = 0.0630$, $wR_2 = 0.1624$
Final R indexes [all data]	$R_1 = 0.0940$, $wR_2 = 0.1859$
Largest diff. peak/hole / e Å^{-3}	0.68/−0.41

Ethyl 3-oxo-(pyridn-4-yl)propanoate 94g

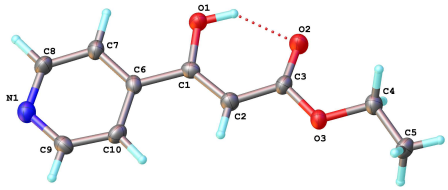

Table 12.18: Crystal data and structure refinement for **94g**

Identification code	19srv259
Empirical formula	$C_{10}H_{11}NO_3$
Formula weight	193.20
Temperature/K	120.0
Crystal system	monoclinic
Space group	$P2_1/c$
a/Å	10.0076(14)
b/Å	11.2997(16)
c/Å	9.2450(14)
$\alpha/°$	90
$\beta/°$	115.701(6)
$\gamma/°$	90
Volume/Å^3	942.0(2)
Z	4
ρ_{calc}g/cm^3	1.362
μ/mm^{-1}	0.101
F(000)	408.0
Crystal size/mm^3	$0.37 \times 0.06 \times 0.05$
Radiation	MoKα ($\lambda = 0.71073$)
2Θ range for data collection/°	4.518 to 53.982
Index ranges	$-12 \leq h \leq 12$, $-14 \leq k \leq 14$, $-11 \leq l \leq 11$
Reflections collected	11759
Independent reflections	2056 [$R_{int} = 0.1129$, $R_{sigma} = 0.1038$]
Data/restraints/parameters	2056/0/171
Goodness-of-fit on F^2	1.019
Final R indexes [I>=2σ (I)]	$R_1 = 0.0582$, $wR_2 = 0.1074$
Final R indexes [all data]	$R_1 = 0.1049$, $wR_2 = 0.1304$
Largest diff. peak/hole / e Å^{-3}	0.28/−0.22

Ethyl 2,2-difluoro-3-(4-nitrophenyl)3-oxopropanoate 211a

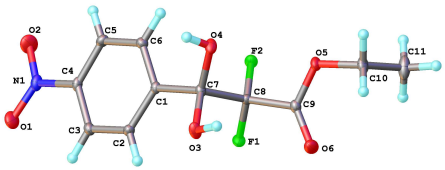

Table 12.19: Crystal data and structure refinement for **211a**

Identification code	18srv057
Empirical formula	$C_{11}H_{11}F_2NO_6$
Formula weight	291.21
Temperature/K	120.0
Crystal system	triclinic
Space group	P-1
a/Å	7.0838(5)
b/Å	9.1649(7)
c/Å	9.4064(7)
α/°	92.399(3)
β/°	97.285(3)
γ/°	106.626(3)
Volume/Å^3	578.46(7)
Z	2
ρ_{calc}g/cm^3	1.672
μ/mm^{-1}	0.156
F(000)	300.0
Crystal size/mm^3	$0.43 \times 0.21 \times 0.1$
Radiation	MoKα ($\lambda = 0.71073$)
2Θ range for data collection/°	4.38 to 58
Index ranges	$-9 \leq h \leq 9$, $-12 \leq k \leq 12$, $-12 \leq l \leq 12$
Reflections collected	11966
Independent reflections	3062 [$R_{int} = 0.0380$, $R_{sigma} = 0.0318$]
Data/restraints/parameters	3062/0/225
Goodness-of-fit on F^2	1.062
Final R indexes [I>=2σ (I)]	$R_1 = 0.0333$, $wR_2 = 0.0896$
Final R indexes [all data]	$R_1 = 0.0407$, $wR_2 = 0.0940$
Largest diff. peak/hole / e Å^{-3}	0.44/−0.24

Ethyl 2,2-difluoro-2-(4-nitrophenyl)acetate 234a

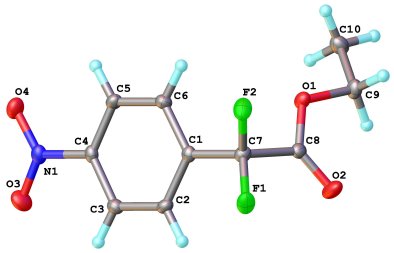

Table 12.20: Crystal data and structure refinement for **234a**

Identification code	18srv057
Empirical formula	$C_{10}H_9F_2NO_4$
Formula weight	245.18
Temperature/K	120.0
Crystal system	monoclinic
Space group	$P2_1/c$
a/Å	7.7025(5)
b/Å	17.7810(10)
c/Å	7.6053(5)
$\alpha/°$	90
$\beta/°$	93.423(2)
$\gamma/°$	90
Volume/Å^3	1039.75(11)
Z	4
ρ_{calc}g/cm^3	1.566
μ/mm^{-1}	0.144
F(000)	504.0
Crystal size/mm^3	$0.28 \times 0.15 \times 0.03$
Radiation	MoKα ($\lambda = 0.71073$)
2Θ range for data collection/°	5.298 to 58.986
Index ranges	$-10 \leq h \leq 10$, $-24 \leq k \leq 24$, $-10 \leq l \leq 10$
Reflections collected	21973
Independent reflections	2903 [$R_{int} = 0.0383$, $R_{sigma} = 0.0246$]
Data/restraints/parameters	2903/0/190
Goodness-of-fit on F^2	1.068
Final R indexes [I>=2σ (I)]	$R_1 = 0.0347$, $wR_2 = 0.0845$
Final R indexes [all data]	$R_1 = 0.0496$, $wR_2 = 0.0906$
Largest diff. peak/hole / e Å^{-3}	0.42/−0.28

2,2-Difluoro-2-(4-nitrophenyl)acetic acid 223a

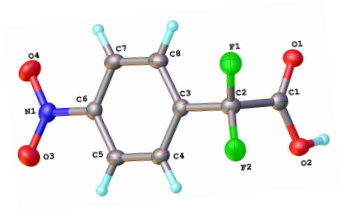

Table 12.21: Crystal data and structure refinement for **223a**

Identification code	19srv021
Empirical formula	$C_8H_5F_2NO_4$
Formula weight	217.13
Temperature/K	120.0
Crystal system	monoclinic
Space group	$P2_1/n$
a/Å	10.4392(4)
b/Å	7.3807(3)
c/Å	7.6053(5)
$\alpha/°$	90
$\beta/°$	91.051(4)
$\gamma/°$	90
Volume/Å^3	847.85(6)
Z	4
ρ_{calc}g/cm^3	1.701
μ/mm^{-1}	0.164
F(000)	440.0
Crystal size/mm^3	$0.41 \times 0.22 \times 0.06$
Radiation	MoKα ($\lambda = 0.71073$)
2Θ range for data collection/°	5.33 to 57.998
Index ranges	$-14 \leq h \leq 14$, $-10 \leq k \leq 10$, $-15 \leq l \leq 15$
Reflections collected	10311
Independent reflections	2255 [$R_{int} = 0.0471$, $R_{sigma} = 0.0401$]
Data/restraints/parameters	2255/0/156
Goodness-of-fit on F^2	1.052
Final R indexes [I>=2σ (I)]	$R_1 = 0.0428$, $wR_2 = 0.0984$
Final R indexes [all data]	$R_1 = 0.06446$, $wR_2 = 0.0118$
Largest diff. peak/hole / e Å^{-3}	0.33/−0.23